NATIONAL ENERGY TECHNOLOGY LABORATORY
OIL & GAS

DOE Award No.: DE-FE0022898

Final Technical Report

Alaska Natural Gas Hydrate Production Testing, Test Site Selection, Characterization, and Testing Operations

Project Period (09/01/2014 – 01/15/2021)

Submitted by:
Timothy S. Collett

United States Geological Survey
DUNS #: 137781949
DFC, MS-939, Box 25046
Denver, CO 80225
Email: tcollett@usgs.gov
Phone number: (303) 236-5731

Prepared for:
United States Department of Energy
National Energy Technology Laboratory

August 23, 2021

U.S. DEPARTMENT OF ENERGY | NATIONAL ENERGY TECHNOLOGY LABORATORY

Office of Fossil Energy

DISCLAIMER

ACKNOWLEDGMENTS

This work was funded by the U.S. Department of Energy (Award Number: DE-FE0022898) and the Energy Resources Program of the U.S. Geological Survey.

ABSTRACT

Alaska Natural Gas Hydrate Production Testing, Test Site Selection, Characterization and Testing Operations

DOE Award Number: DE-FE0022898

The objective of this Department of Energy (DOE) - United States Geological Survey (USGS) Interagency Agreement (IA) was to provide geologic and geophysical technical support to identify and characterize gas hydrate production test sites on the Alaska North Slope. This effort was designed to address critical issues associated with production of gas hydrates and has contributed to our understanding of the geologic nature of the gas hydrate accumulations, the geophysical characteristics of in situ natural gas hydrates, and it has led to the development of plans for an extended gas hydrate production test in northern Alaska. This project was designed as a cooperative research effort, with the USGS providing technical geoscience support in a partnership that included the DOE, the Alaska Department of Natural Resources, the Japan Oil Gas and Metals National Corporation (JOGMEC), and Petrotechnical Resources Alaska (PRA).

TABLE OF CONTENTS

Disclaimer 2
Abstract 4
Table of Contents 5
1. Executive Summary 6
 1.A. Introduction 6
 1.B. Project Objectives 9
 1.C. Project Scope 9
2. Project Background 13
 2.A. Gas Hydrate Technical Review 13
 2.B. Alaska North Slope Gas Hydrate Petroleum Systems 13
  2.B.1. Gas Hydrate Stability Conditions 14
  2.B.2. Reservoir Rocks 23
  2.B.3. Gas Source and Migration 33
  2.B.4. Eileen Gas Hydrate Trend Petroleum System - Summary 36
3. Test Sites Review and Selection 37
 3.A. Site Selection in Support of the Iġnik Sikumi Test Well 43
  3.A.1. Evaluation of Locations in the Milne Point Unit (MPU) 43
  3.A.2. Evaluation of Locations in the Prudhoe Bay Unit (PBU) 44
  3.A.3. Evaluation of Locations in the Kuparuk River Unit (KRU) 46
  3.A.4. Evaluation of Downdip Locations in the Prudhoe Bay Unit (PBU) 47
  3.A.5. Gas Hydrate Production Modeling in Support Test Site Selection 47
  3.A.6. Prudhoe Bay Unit L-Pad Test Site 49
  3.A.7. Iġnik Sikumi CO2/CH4 Exchange Field Trial 55
 3.B. Site Selection in Support of the PBU 7-11-12 Test Site 57
  3.B.1. Reservoir Controls on Gas Hydrate in the Eileen Gas Hydrate Trend 58
  3.B.2. Reevaluation of Test Site Locations in the Eileen Gas Hydrate Trend 95
4. PBU 7-11-12 Test Site Planning, Operations, and Technical Findings 114
 4.A. Planning and Operations of the Site 7-11-12 (Hydrate-01) Strat Test Well 117
  4.A.1. Hydrate-01 Pre-Drill Project and Operational Planning 117
  4.A.2. Hydrate-01 Drilling Operations 121
  4.A.3. Hydrate-01 Logging Operations 124
  4.A.4. Hydrate-01 Acquisition of Sidewall Pressure Cores 124
  4.A.5. Hydrate-01 Well Completion and Monitoring Systems 126
  4.A.6. Hydrate-01 Operational Lessons Learned 126
  4.A.7. Hydrate-01 Operational Summary 127
 4.B. Hydrate-01 Stratigraphic Test Well Technical Findings 128
  4.B.1. Hydrate-01 Gas Hydrate Reservoir Conditions 128
  4.B.2. Hydrate-01 Gas Hydrate Reservoir Petrophysical Properties 130
  4.B.3. Hydrate-01 Gas Hydrate Reservoir Production Modeling 132
5. PBU 7-11-12 Test Site Production Testing Planning 135
6. Accomplishments of the Alaska Gas Hydrate Interagency Agreement 138
Cited References 142
List of Abbreviations and Symbols 154
Appendix: Project Publications 157

1. EXECUTIVE SUMMARY

1.A. Introduction

Work conducted under this Interagency Agreement (IA) was intended to provide support to the Department of Energy (DOE) and its research partners in understanding, predicting, and testing the recoverability and potential production characteristics of onshore natural gas hydrate in the greater Prudhoe Bay area on the Alaska North Slope (ANS) and other areas deemed suitable for potential long-term production testing of gas hydrate. To do so, this project was designed to evaluate the occurrence and resource potential of the known gas hydrate accumulations in the Eileen Gas Hydrate Trend in northern Alaska (Figure 1a, b). This project consisted of one task that included two subtasks. The first subtask involved the geologic and engineering assessment of gas hydrate accumulations in the Eileen Gas Hydrate Trend. The second subtask supported DOE and their industry partners with evaluation, planning, and preparations for drilling and testing of gas hydrate research wells in northern Alaska.

The cooperative research conducted under this IA by the U.S. Geological Survey (USGS) was built on the strengths of a well-established applied research program and information obtained from a long history of highly successful field research projects in Alaska and other areas. The overall objectives of the research conducted under this IA were to understand the ultimate energy resource potential of gas hydrates and to evaluate the technologies required to safely produce gas hydrate. These objectives were addressed through a highly integrated research program structure, which contributed directly to the development of gas hydrate field characterization techniques that provided the information and data needed to identify and characterize the occurrence of gas hydrate accumulations suitable for gas hydrate production testing and analysis. The gas hydrate production test design part of this IA was established to provide input into the methods and procedures for safely testing gas hydrates in Alaska and other settings.

This report is the "*Final Technical Report*" in support of the DOE-USGS IA titled "*Alaska Natural Gas Hydrate Production Testing, Test Site Selection, Characterization, and Testing Operations*" under DOE Award Number DE-FE0022898. This report provides a comprehensive review of all aspects of the cooperative research and project planning efforts conducted under this agreement between the DOE and the USGS. This report begins with a systematic review of the primary objectives and goals of the research and project organizational efforts conducted under the IA. The project background section of this report includes a comprehensive review of the geologic controls on the occurrence of gas hydrate in northern Alaska with a focus on the known gas hydrate accumulations in the greater Prudhoe Bay area. The main body of the report describes the geologic criteria and other considerations used to identify and characterize potential gas hydrate production test sites within this cooperative effort. This section is followed by details of two test site review efforts that led to the selection of a site in the western portion of the Prudhoe Bay Unit (PBU) that was determined to possess all the geologic and operational requirements needed for the successful completion of a long-term gas hydrate production field test. As described in this report, the test site review effort included the drilling of a stratigraphic test well in 2018 at the location

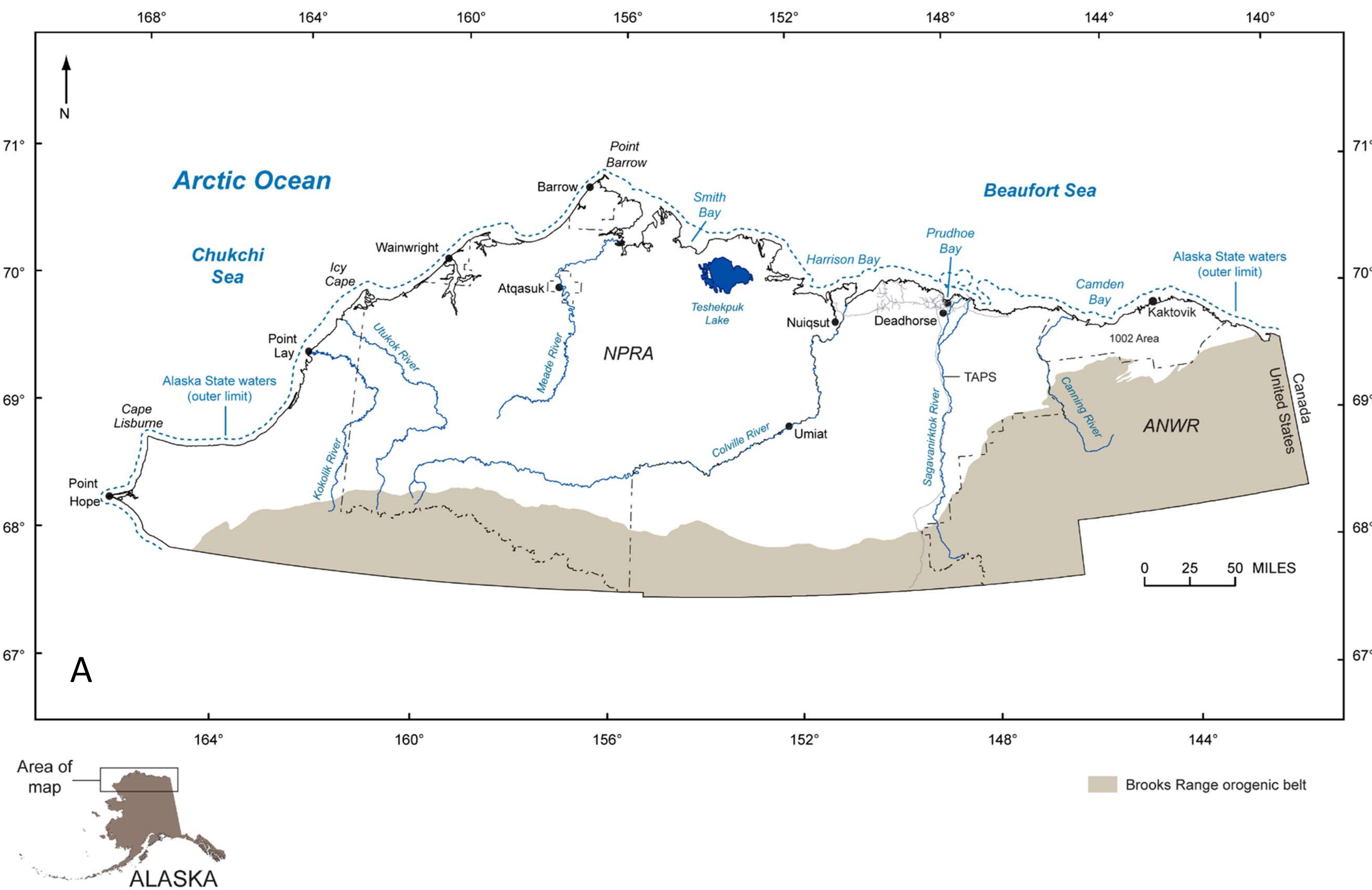

Figure 1. (A) Generalized geographic map of the Alaska North Slope showing the location of coastline, rivers, lakes, major political boundaries, villages, pipelines, and other features (modified from Collett, 1993, 2002). NPRA = National Petroleum Reserve in Alaska, ANWR = Arctic National Wildlife refuge, TAPS = Trans Alaska Pipeline System

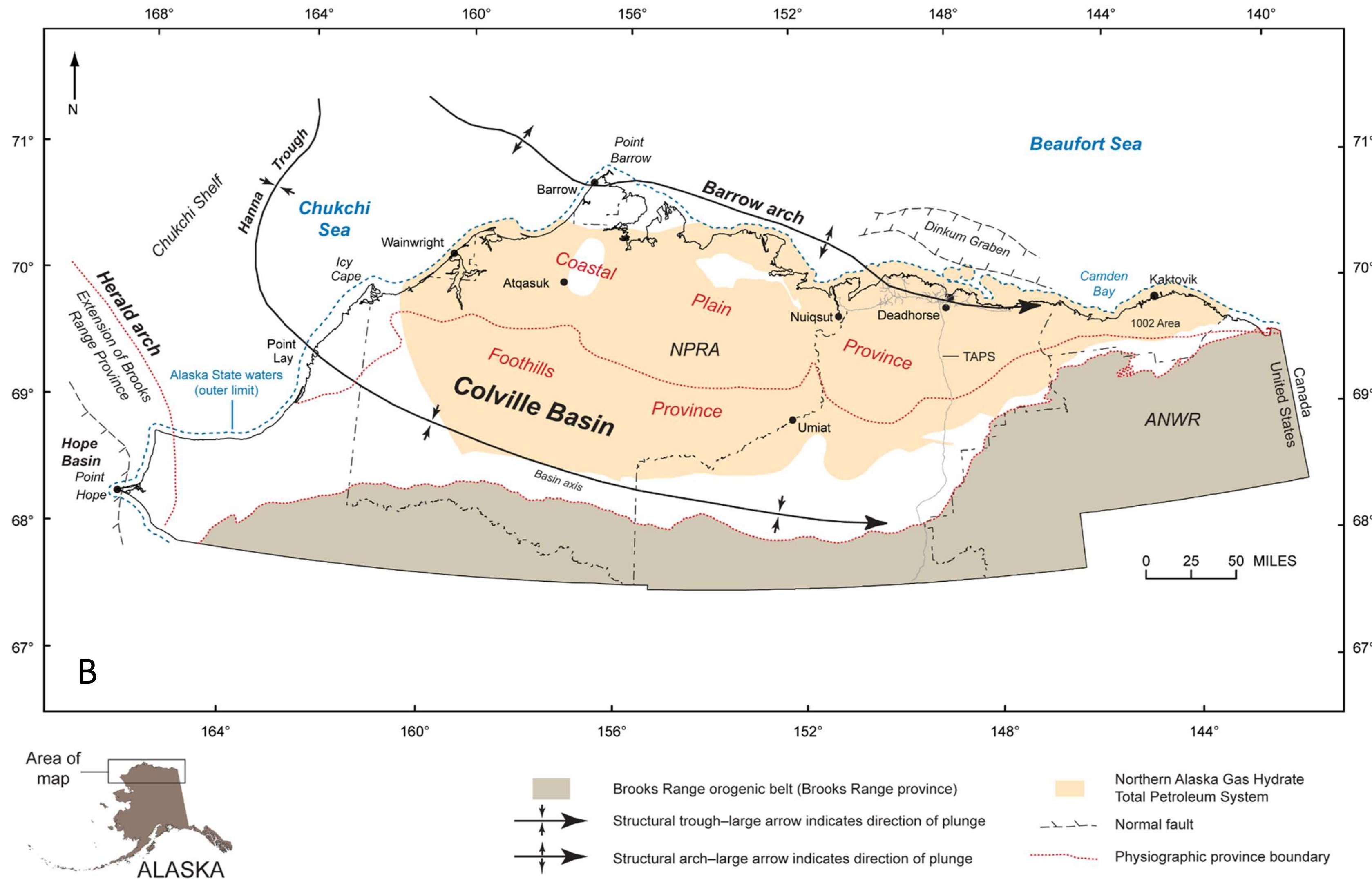

Figure 1. (B) Map of the physiographic provinces and major tectonic features of the Alaska North Slope (modified from Collett, 1993, 2002). NPRA = National Petroleum Reserve in Alaska, ANWR = Arctic National Wildlife refuge, TAPS = Trans Alaska Pipeline System

selected for production testing. The *Hydrate-01 Stratigraphic Test Well* met all the project objectives and confirmed the occurrence of highly saturated gas hydrate-bearing reservoirs suitable for long-term production testing. With the success of the *Hydrate-01 Stratigraphic Test Well,* the project leadership groups turned their attention to the development of a comprehensive plan for the proposed production tests. As reviewed at the end of this report, the USGS coordinated the effort to develop and maintain the project "*Science and Operational Plan*" that was designed to capture the entire scope of the "*Alaska Gas Hydrate Production Field Experiment.*"

1.B. Project Objectives

The objective of this DOE-USGS IA was to provide geologic and geophysical technical support to identify and characterize gas hydrate production test sites in the ANS as specified in the goals of the 2005 Energy Act for National Methane Hydrates R&D, the 2013 DOE-led U.S. interagency roadmap for gas hydrates research, and elements of the USGS mission related to energy resources.

Under this IA, the USGS led the geologic research effort in support of the test site characterization. The USGS also provided technical information and reviews of specific components of the future drilling and production testing program, including, but not limited to, drilling operations, analysis of physical properties of pressure cores, planning for post-field testing of cores, core flow, and downhole logging and coring plans. In general, the goals of the task and subtasks under this IA remained the same over the duration of this project (09/01/2014 – 01/15/2021) with the USGS leading the geoscience aspects of the DOE-sponsored effort to conduct an extended (12–24 months) gas hydrate production test on the ANS. The USGS played a key role in the planning and operation of the DOE-JOGMEC-USGS sponsored gas hydrate production test on the Alaska North Slope, focusing on the identification and characterization of the PBU Kuparuk 7-11-12 gas hydrate test site and contributing to the design of the test well program.

1.C. Project Scope

The primary overall goal of the DOE-sponsored gas hydrate research efforts in Alaska is to conduct a scientific field production test in northern Alaska from one or more gas hydrate-bearing sand reservoirs using "depressurization" technology. The project was originally envisioned to include the drilling and evaluation of a stratigraphic test well (which was completed in December 2018), followed by the establishment of a production test site (including a geoscience data well, two production test wells, deployment of well-monitoring systems, and surface monitoring), and the testing of reservoir response to pressure reduction over a period of about 12 months or for whatever period the parties find operations at the site to be valuable. The next drilling and production testing phase for this project is anticipated to start sometime in 2022.

Within the scope of the DOE-sponsored gas hydrate research efforts in Alaska, the DOE-USGS research partnership is intended to provide support to the DOE and its research partners in understanding, predicting, and testing the recoverability and potential production characteristics of onshore natural gas hydrate in the greater Prudhoe Bay area on the ANS (including but not limited to Prudhoe Bay, Kuparuk River, and Milne Point areas) or other areas deemed suitable for potential long-term production testing of gas hydrate. To do so, this project was designed to evaluate the occurrence and resource potential of the known gas hydrate accumulations in the Eileen trend. Geologic, geochemical, and geophysical (two-dimensional, 2D, and three-dimensional, 3D, seismic surveys) data and other related data sources, including wireline and mud log surveys of wells of opportunity, were used to assess the occurrence and nature of the known gas hydrate accumulations in northern Alaska.

This cooperative project consisted of one task and two subtasks in each of the project phases. The first subtask in each phase of the project involved the geologic and engineering assessment of the Eileen related gas-hydrate accumulations in the greater Prudhoe Bay area. The second subtask supported DOE and their industry partners with the evaluation, planning, and preparations for drilling and testing of gas hydrate research wells in northern Alaska. Eventually, this project evolved to include four distinct phases (Phases 1–4) with each phase established through formal contractual "modifications" to the original IA as listed and reviewed below in this section of this IA Final Report.

Phase 1
Original Award (09/01/2014 – 12/31/2015)
Task 1: Gas Hydrate Production Testing Support

Subtask 1.1: Geologic occurrences of gas hydrate, analyzing available Eileen geologic and geophysical data
The USGS shall refine current interpretations of the regional Alaska North Slope gas hydrate stability field as well as the distribution and properties of previously identified gas hydrate accumulations in the Eileen Gas Hydrate Trend through the collection and incorporation of new well log and seismic data.

Subtask 1.2: Gas hydrate field test technical and operational support
The objectives of this subtask are to (1) provide technical and scientific leadership and advice for formulation of a research drilling and production testing program designed to assess the nature and production potential of gas hydrate on the Alaska North Slope; (2) provide personnel and resources to enhance field and laboratory analyses of material recovered (under separate DOE projects) by conventional and pressure core systems; and (3) partner in the synthesis of data from logging, direct sampling, and geophysical and geologic characterization studies conducted under separate DOE projects.

Phase 2
Mod-1 (09/01/2014 – 12/31/2016)
Mod-2 (09/01/2014 – 12/31/2017)
Task 2: Gas Hydrate Production Testing Support (continued)

Subtask 2.1: Geologic occurrences of gas hydrate, analyzing available Eileen geologic and geophysical data
The general goals of this subtask under Phase 2 are the same as those identified in Subtask 1.1 with the USGS leading the geoscience aspects of the DOE-sponsored effort to conduct an extended gas hydrate production test on the Alaska North Slope. The specific focus of USGS geologic studies shall expand to further characterize two additional high-priority potential gas hydrate test sites for consideration of testing: The Milne Point Unit Cascade site and Prudhoe Bay Unit Kuparuk 7-11-12 site. The USGS shall work closely with the Alaska Department of Natural Resources geoscientists and shall access critical confidential industry 3D seismic data volumes from the area of the Milne Point and Prudhoe Bay units.

Subtask 2.2 Gas hydrate field test technical and operational support
The USGS shall work with DOE, who will coordinate with JOGMEC, and Petrotechnical Resources of Alaska (PRA), to generate a preliminary plan for the long-term gas hydrate production test in northern Alaska with a specific emphasis on identifying and designing the data acquisition requirements for the proposed test well program. The USGS shall provide DOE the reservoir data needed to model the production response of the gas hydrate accumulations being considered for testing.

Phase 3
Mod-3 (09/01/2014 – 12/31/2018)
Task 3: Gas Hydrate Production Testing Support (continued)

Subtask 3.1: Geologic occurrences of gas hydrate, analyzing available Eileen geologic and geophysical data
The general goals of this subtask are the same as those identified in Subtasks 1.1 and 2.1. During the DOE planned site review and appraisal project stage, the USGS shall work with DOE and appropriate project interest groups to conduct a detailed geologic and geophysical analysis of the Prudhoe Bay Unit Kuparuk 7-11-12 site.

Subtask 3.2 Gas hydrate field test technical and operational support
The USGS shall work with DOE to develop a plan for the long-term gas hydrate production test in northern Alaska with a specific emphasis on identifying and designing the data acquisition requirements for the proposed test well program. The USGS shall contribute to the development of an integrated project "Statement of Requirements" (SOR) for the proposed test well program. The USGS shall work with providers to develop both distributed and gauge-based wellbore monitoring systems to evaluate the potential contribution of these systems to the Alaska North Slope gas hydrate test program.

Phase 4
Mod-4 (09/01/2014 – 8/31/2019)
Mod-5 (09/01/2014 – 6/1/2020)
Mod-6 (09/01/2014 – 1/15/2021)
Task 4: Gas Hydrate Production Testing Support (continued)

Subtask 4.1: Geologic occurrences of gas hydrate, analyzing available Eileen geologic and geophysical data
The general goals of this subtask are the same as those identified in Subtasks 1.1, 2.1, and 3.1. During this performance period, the field phase of this project is expected to start with the drilling of the stratigraphic test well to verify the viability of the PBU Kuparuk 7-11-12 production test site. The USGS shall contribute to the acquisition, processing, and analysis of well log data sets and sidewall cores.

Subtask 4.2 Gas hydrate field test planning technical and operational support
The USGS shall work as a member of the newly formed project "R&D Committee" to review and modify the existing operational plan in support of the "Alaska Gas Hydrate Production Field Experiment" well test plan, and incorporate results of the recently completed Hydrate-01 Stratigraphic Test Well and other international gas hydrate production testing projects.

2. PROJECT BACKGROUND

2.A. Gas Hydrate Technical Review

Gas hydrates are naturally occurring "ice-like" combinations of natural gas and water that have the potential to provide an immense resource of natural gas from the world's oceans and polar regions. Gas hydrates are known to be widespread in permafrost regions and beneath the sea in sediments of outer continental margins. It is generally accepted that the volume of natural gas contained in the world's gas hydrate accumulations exceeds that of known gas reserves (Makogon, 1981; Collett, 2002). It is also generally accepted that gas hydrate in sand-rich reservoirs (with high intrinsic porosities and permeabilities) are conducive to production (Moridis and Sloan, 2007; Moridis et al., 2009). In addition, gas hydrate production tests in Arctic terrestrial settings (Dallimore and Collett, 2005; Anderson et al., 2011a, 2011b; Boswell and Collett, 2011; Hunter et al., 2011; Ashford et al., 2012; Schoderbek et al., 2012; Boswell et al., 2014, 2017) and deep-marine environments offshore Japan (Yamamoto et al., 2014) have confirmed that the depressurization of hydrate-bearing sand-rich reservoir systems, the same process used to produce conventional natural gas, is the most promising technical approach for the production of gas hydrate.

Gas hydrates are crystalline compounds that result from the 3D stacking of "cages" of hydrogen-bonded water molecules. Generally, each cage can hold a single gas molecule. The empty cagework is unstable and requires the presence of encapsulated gas molecules to stabilize the clathrate crystal. The compact nature of the hydrate structure makes for highly effective packing of gas. A volume of gas hydrate expands between 150- and 180-fold when released in gaseous form at standard pressure and temperature (14.696 pounds per square inch (psi), 68°F).

Clathrate hydrates can form in the presence of gas molecules that are in the size range of 4.8 to 9.0 angstroms. Three distinct structural types can form depending on the size of the largest guest molecules that can be included in the clathrate cage of water molecules. There are considerable complexities in the structure-size relation; however, methane and ethane individually form Structure I (sI) hydrate, but in certain combinations also form Structure II (sII) hydrate. Propane and isobutane form sII hydrate, either individually or in combination with ethane and methane. Normal-butane and neopentane form sII hydrate only when methane is present as well, and larger hydrocarbon molecules form Structure H (sH) hydrate, again where methane is present. On a macroscopic level, many of the physical properties of gas hydrates resemble those of ice because hydrates contain about 85 percent water on a molar basis. For a complete description of the structure and physical properties of gas hydrates, see the summary by Sloan and Koh (2008).

2.B. Alaska North Slope Gas Hydrate Petroleum Systems

The long history of conventional oil and gas exploration and oil production in northern Alaska along with dedicated gas hydrate test well projects (as reviewed below in this section of the IA Final Report) have yielded the geologic and reservoir engineering data needed to study and assess the occurrence of gas hydrate within the Eileen Gas

Hydrate Trend on the Alaska North Slope (ANS). Gas hydrate research projects on the ANS have identified exploration targets and confirmed the presence of definable gas hydrate accumulations through drilling. The Eileen Gas Hydrate Trend has emerged as one of the best-defined areas of gas hydrate occurrence in the world and will continue to be a focal point for gas hydrate research studies into the future. Also in this section of the report, industry-acquired well and seismic data along with the results of dedicated gas hydrate research drilling projects will be used to examine the geologic controls on the occurrence of gas hydrate in order to provide the analytical tools with which to effectively identify and evaluate candidate gas hydrate production test sites.

In recent years, the concept of a gas hydrate petroleum system, similar to the concept that guides conventional oil and gas exploration, has gained acceptance (Collett et al., 2009). In a gas hydrate petroleum system, the individual factors that contribute to the formation of gas hydrate can be identified and assessed; the most important include (1) gas hydrate pressure-temperature stability conditions, (2) suitable host sediment or "reservoir," (3) gas source, and (4) gas migration. In the following discussion, these geologic controls on the stability and formation of gas hydrate deposits in northern Alaska are reviewed and evaluated.

2.B.1. Gas Hydrate Stability Conditions

Gas hydrates exist under a limited range of temperature and pressure conditions such that the depth and thickness of the zone of potential gas hydrate stability can be calculated given information on formation temperatures, pore-pressure gradients, and gas and formation water chemistry. Depicted in the temperature/depth plot in Figure 2 are a series of subsurface temperature profiles from an onshore permafrost area and two laboratory-derived gas hydrate stability curves for different natural gases (modified from Holder et al., 1987). This gas hydrate phase diagram (Fig. 2) illustrates how variations in formation temperature, pore pressure, and gas composition can affect the thickness of the gas hydrate stability zone. In this example, the mean annual surface temperature is assumed to be 14°F (-10°C), and the depth to the base of permafrost (32°F; 0°C isotherm) is varied for three example temperature profiles, at permafrost depths of 1000 feet (ft) (305 meters (m), 2000 ft (610 m), and 3000 ft (914 m). Below permafrost, three different example geothermal gradients of 2.19°F/100 ft (4.0°C/100 m), 1.76°F/100 ft (3.2°C/100 m), and 1.10°F/100 ft (2.0°C/100 m) are used to project the sub-permafrost temperature profiles. The two gas hydrate stability curves represent gas hydrates with different gas chemistries: one with 100 percent methane, and the other with 98 percent methane, 1.5 percent ethane, and 0.5 percent propane. This phase diagram (Fig. 2) is constructed assuming a hydrostatic pore-pressure gradient of 0.433 pounds per square inch per foot (psi/ft) (9.795 kilopascals per meter (kPa/m)).

The zone of potential gas hydrate stability in the phase diagram (Fig. 2) lies between the depths of the two intersections of the geothermal gradient and the gas hydrate stability curve. For example, in Figure 2, the temperature profile projected to an assumed permafrost base of 2000 ft (610 m) intersects the 100-percent methane-hydrate stability curve at about 656 ft (200 m), thus marking the upper boundary of the methane-hydrate stability zone. A geothermal gradient of 2.19°F/100 ft (4.0°C/100 m) projected from the base of permafrost at 2000 ft (610 m) intersects the 100-percent

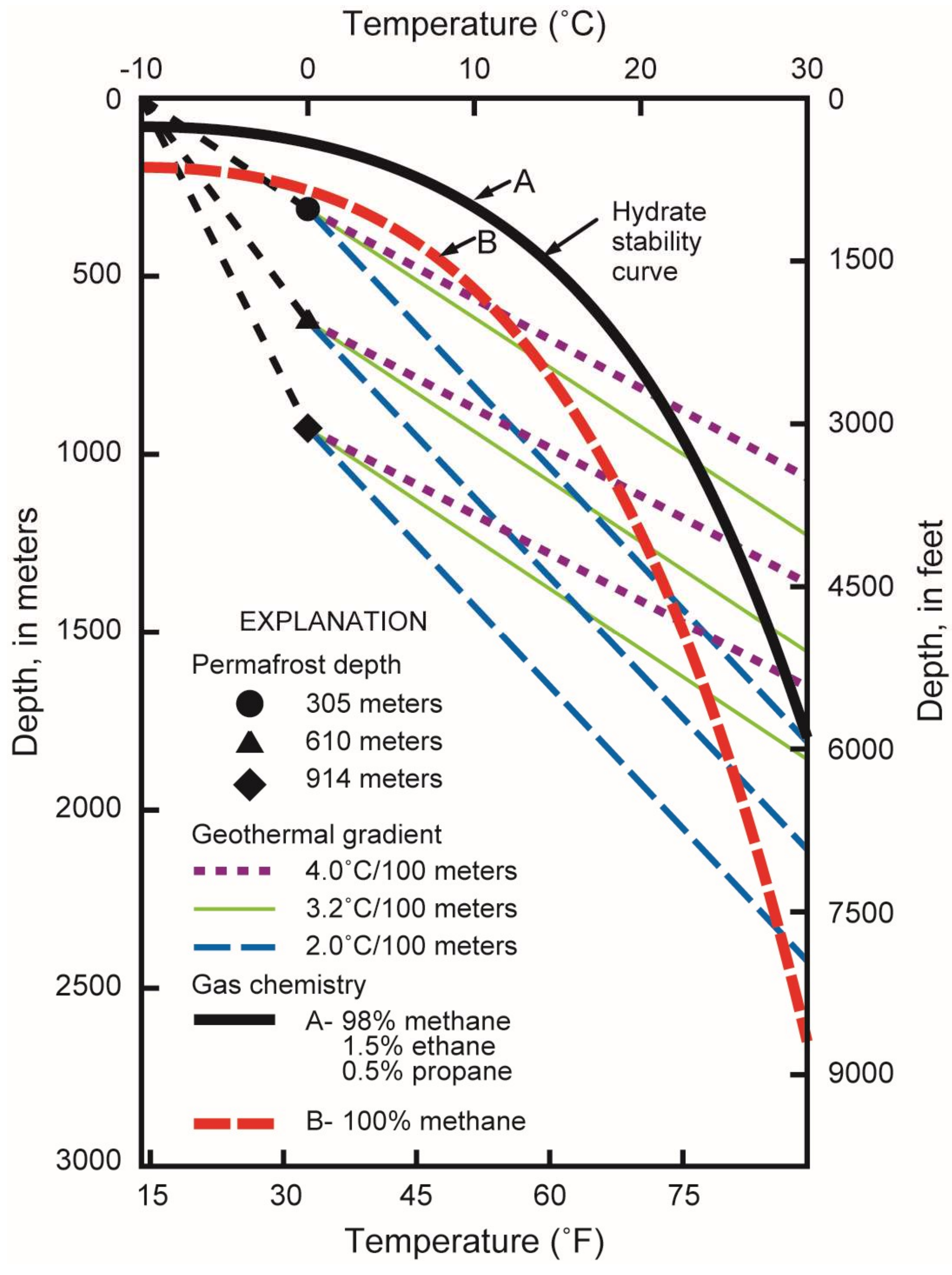

Figure 2. Gas hydrate phase diagram showing the depth and temperature conditions suitable for the formation of gas hydrate under various conditions of permafrost depth, geothermal gradient, gas chemistry, and a pore-pressure gradient of 0.433 psi/ft (9.795 kPa/m). Modified from Holder et al. (1987). psi/ft = pounds per square inch per feet, kPa/m = kilopascals per meter

methane-hydrate stability curve at about 3609 ft (1100 m); thus, the zone of potential methane-hydrate stability is approximately 2953 ft (900 m) thick. However, if permafrost is extended to a depth of 3000 ft (914 m) and if the geothermal gradient below permafrost is 1.10°F/100 ft (2.0°C/100 m), the zone of potential methane-hydrate stability would be approximately 6890 ft (2100 m) thick.

Most gas hydrate stability studies assume a hydrostatic pore-pressure gradient (see Collett, 2002). Pore-pressure gradients greater than hydrostatic conditions correspond to higher pore pressures with depth and a thicker gas hydrate stability zone, whereas a pore-pressure gradient less than hydrostatic corresponds to a thinner gas hydrate stability zone. The gas hydrate stability curves in Figure 2 were obtained from laboratory data published by Holder et al. (1987). The addition of 1.5 percent ethane and 0.5 percent propane to the pure methane gas system shifts the stability curve up and to the right, thus deepening the base of the zone of potential gas-hydrate stability. It is well known that dissolved salt can depress the freezing-point of water. Where present in a gas hydrate system, salt (such as NaCl) also lowers the temperature at which gas hydrates form.

Collett et al. (1988) and Collett (1993) included extensive analyses of gas hydrate stability conditions in northern Alaska. In support of this test site review project, Lee et al. (2008) also used log data from wells drilled since these earlier studies for updating the permafrost (Fig. 3) and methane hydrate stability maps (Fig. 4A–C; Table 1) in northern Alaska as reviewed below.

On the North Slope, the subsurface temperature data needed to assess the distribution of the gas hydrate stability zone are provided by high-resolution, equilibrated well-bore surveys in 46 wells (Table 1) and from well log estimates of the base of ice-bearing permafrost in 102 other wells (Collett, 1993). Beginning in 1958, a series of 46 North Slope wells, considered to be in or near thermal equilibrium, have been surveyed with high-resolution temperature devices (Lachenbruch et al., 1987a, 1987b; Lee et al., 2008). Geothermal gradients, which are needed to predict the depth and thickness of the gas-hydrate stability zone, can be interpreted directly from these equilibrated temperature profiles. However, specific evaluation of subsurface temperatures at any one particular site on the North Slope is subject to error because of the vastness of the region and the limited number of equilibrated well-bore temperature surveys. To augment the limited North Slope temperature database, Collett et al. (1993) developed a new method to evaluate local geothermal gradients.

In this method, well-log picks for the base of the ice-bearing permafrost from 102 wells (Fig. 3) were combined with regional temperature constants derived from the high-resolution surveys (Table 1) to extrapolate temperature data. The comparison of geothermal gradients calculated from the high-resolution temperature surveys and projected from known ice-bearing permafrost depths are similar over most of the North Slope, with gradient values in the ice-bearing sequence ranging from about 0.82°F/100 ft (1.5°C/100 m) in the Prudhoe Bay area to about 2.47°F/100 ft (4.5°C/100 m) in the National Petroleum Reserve in Alaska (NPRA). The calculated and projected geothermal gradients from below the ice-bearing sequence range from about 0.88°F/100 ft (1.6°C/100 m) to about 2.85°F/100 ft (5.2°C/100 m).

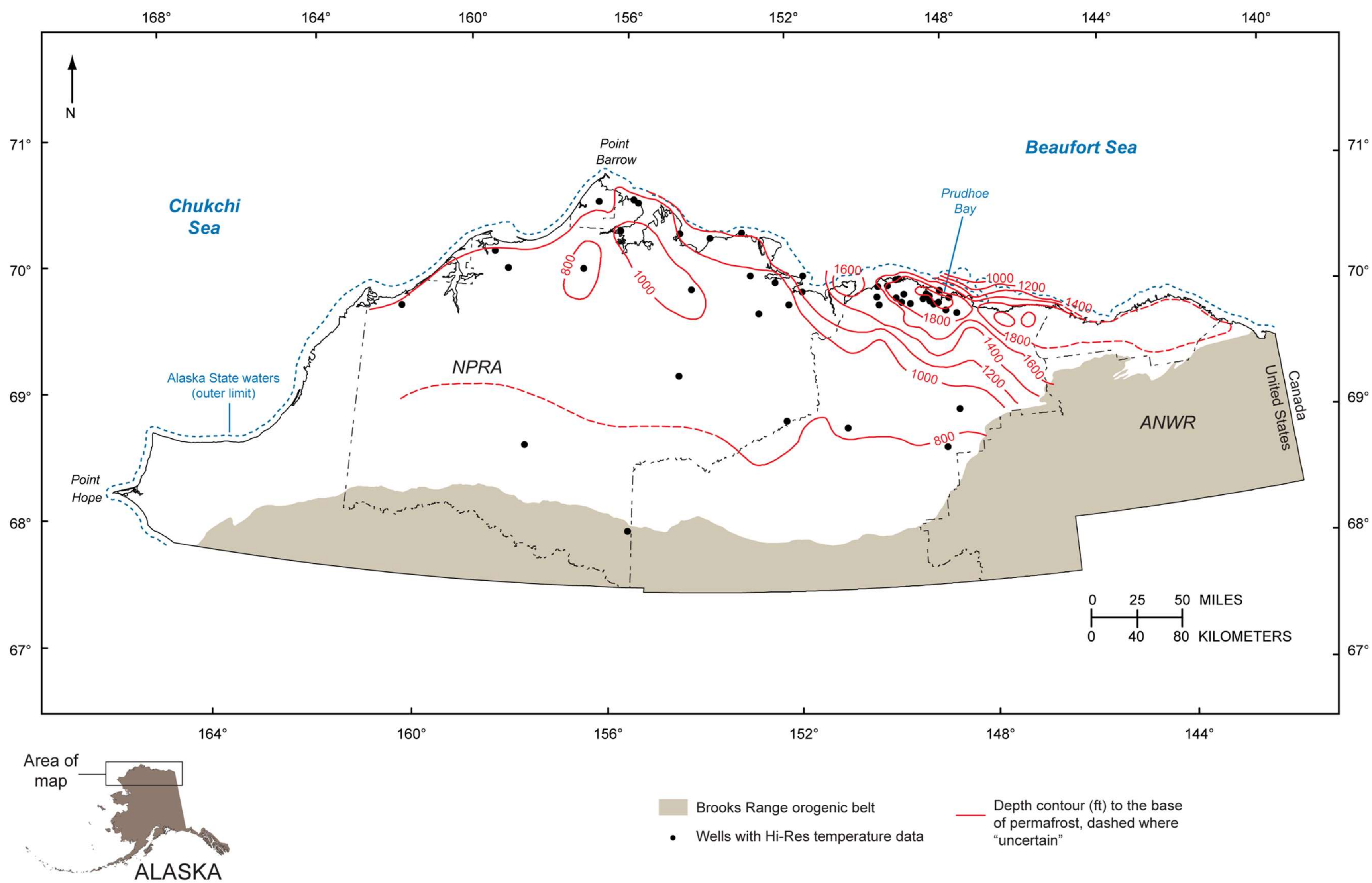

Figure 3. Map showing the depth to base of permafrost on the Alaska North Slope as determined from equilibrated well-bore temperature surveys in 46 wells (Table 1; Lee et al., 2008). Well log estimates for the base of ice-bearing permafrost in 102 other wells (Collett, 1993) were also used to draw the map contours. Contours in feet (ft). NPRA = Natural Petroleum Reserve in Alaska, ANWR = Alaska National Wildlife Refuge

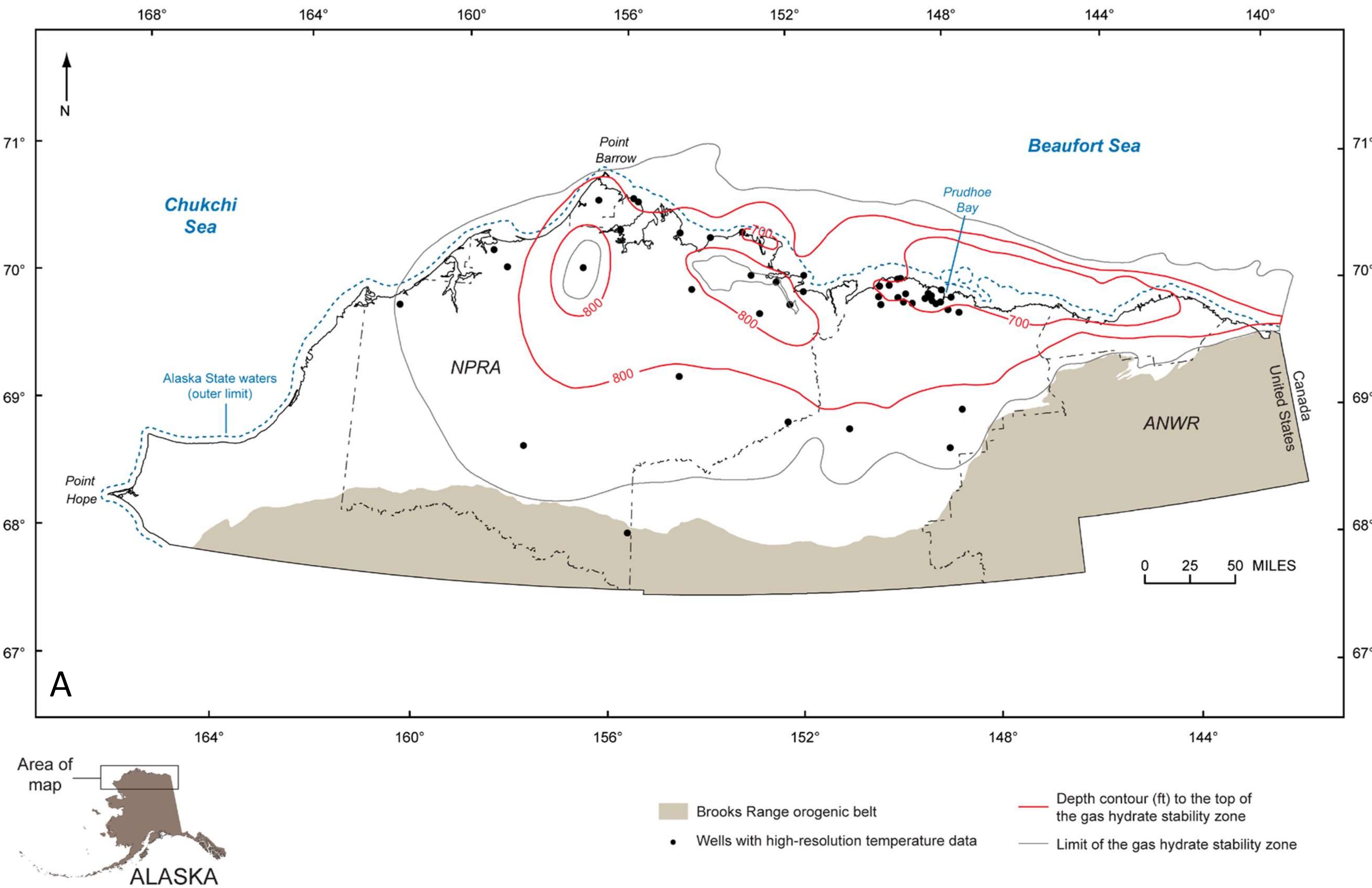

Figure 4. (A) Map of the Alaska North Slope gas hydrate stability zone (modified from Collett et al., 1988): Depth to the top of the hydrate stability zone. Contours in feet (ft). NPRA = Natural Petroleum Reserve in Alaska, ANWR = Alaska National Wildlife Refuge

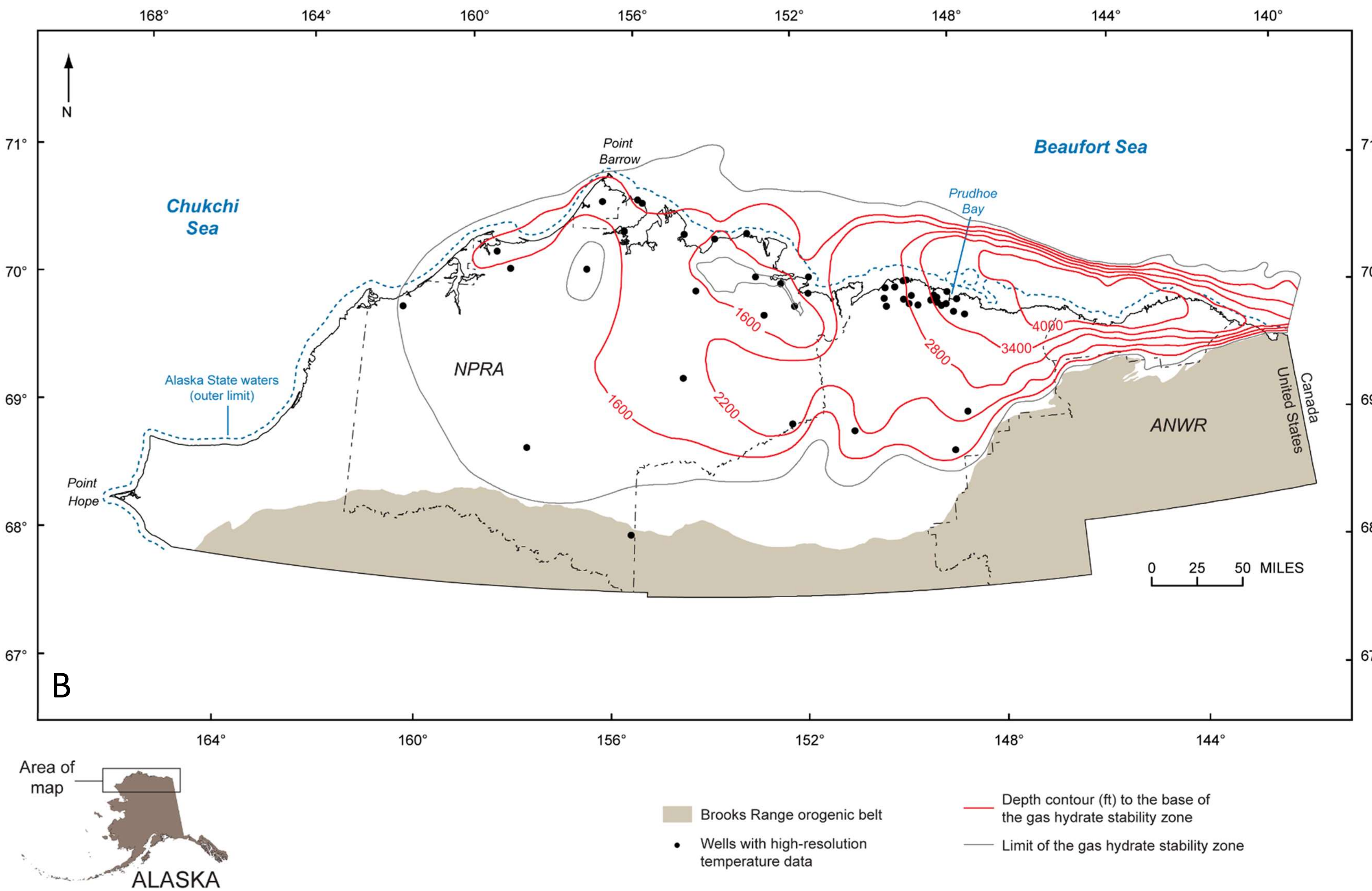

Figure 4. (B) Map of the Alaska North Slope gas hydrate stability zone (modified from Collett et al., 1988): Depth to base of the hydrate stability zone. Contours in feet (ft). NPRA = Natural Petroleum Reserve in Alaska, ANWR = Alaska National Wildlife Refuge

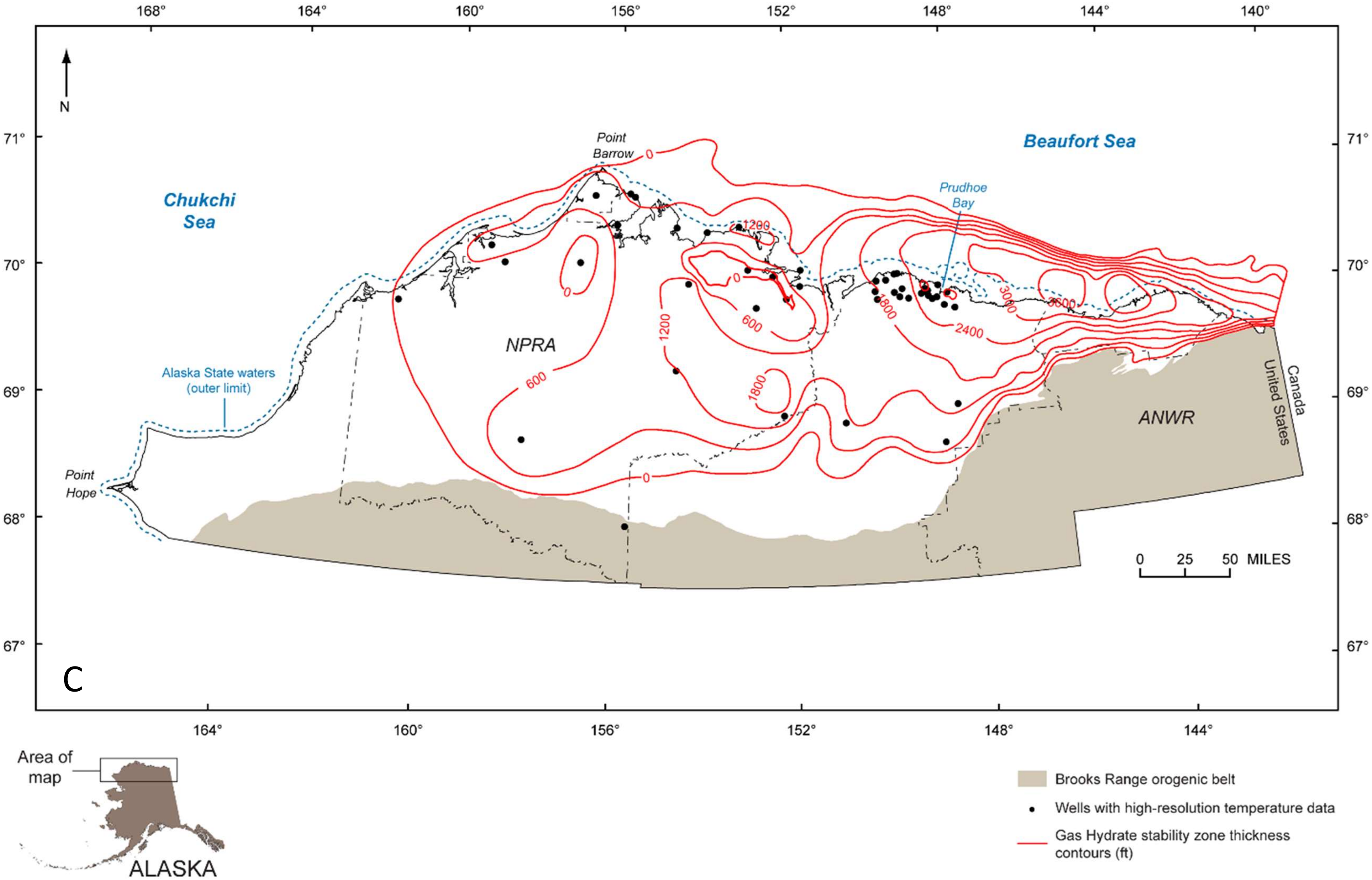

Figure 4. (C) Map of the Alaska North Slope gas hydrate stability zone (modified from Collett et al., 1988): Thickness of the hydrate stability zone. Contours in feet (ft). NPRA = Natural Petroleum Reserve in Alaska, ANWR = Alaska National Wildlife Refuge

API	Common well name	North Latitude	West Longitude	Depth (m) to 0°C	Depth (ft) to 0°C	Depth (m) to THSZ	Depth (ft) to THSZ	Depth (m) to BHSZ	Depth (ft) to BHSZ	Thickness (m) HSZ	Thickness (ft) HSZ
50301200010000	US TUNALIK #1	70.2062	161.0687	270	886	258	845	320	1,050	62	204
50301200020000	US PEARD #1	70.7156	158.9999	300	984	248	814	557	1,827	309	1014
50163200020000	HU KUGRUA #1	70.5866	158.6617	270	886	259	849	390	1,278	131	429
50163200010000	US SO MEADE #1	70.6147	156.8834	200	656	-	-	-	-	0	0
50023100110000	US SO BARROW #3	71.1652	156.5811	380	1,247	232	761	578	1,896	346	1135
50163200030000	US KUYANAK #1	70.9314	156.0368	320	1,050	233	763	500	1,640	267	877
50023200180000	US TULAGEAK 1	71.1885	155.7329	290	951	250	819	388	1,272	138	453
50023200140000	US WEST DEASE #1	71.1594	155.6296	270	886	257	842	352	1,155	96	313
50279200050000	US E SIMPSON 1	70.9178	154.6180	360	1,181	228	748	556	1,824	328	1076
50279200040000	HU IKPIKPUK 1	70.4555	154.3322	330	1,083	243	796	652	2,139	409	1343
50279200020000	HU DREW POINT 1	70.8794	153.8997	320	1,050	232	761	460	1,509	228	748
50279200060000	US J W DALTON 1	70.9209	153.1380	400	1,312	213	700	604	1,982	391	1282
50103200060000	HU E TESHEKPUK 1	70.5700	152.9447	250	820	-	-	-	-	-	-
50103200170000	US NORTH INIGOK 1	70.2576	152.7660	275	902	258	845	380	1,247	122	402
50103200110000	US NORTH KALIKPIK 1	70.5092	152.3668	210	689	-	-	-	-	-	-
50103200090000	HU WEST FISH CREEK 1	70.3267	152.0597	260	853	-	-	-	-	-	-
50103200070000	HU S HARRISON BAY 1	70.4245	151.7310	380	1,247	225	737	530	1,739	305	1002
50103200080000	HU ATIGARU PT 1	70.5561	151.7160	400	1,312	217	711	541	1,775	324	1064
50029202750000	WEST SAK 11	70.3569	149.9908	465	1,526	216	709	747	2,449	530	1740
50029204190000	SO WEST SAK 14	70.2935	149.9515	465	1,526	215	705	741	2,431	526	1726
50029205410000	WEST SAK 16	70.4433	149.9483	535	1,755	212	694	845	2,772	633	2078
50029205420000	SO WEST SAK 17	70.4463	149.7237	550	1,804	210	689	850	2,789	640	2100
50029200900000	AR WEST SAK RIVER ST 1	70.3397	149.5372	550	1,804	212	694	800	2,625	588	1930
50029215040000	MPU C-19	70.4915	149.5245	525	1,722	215	705	850	2,789	635	2083
50029209000000	MPU D-2	70.4905	149.4526	560	1,837	216	709	874	2,867	658	2159
50029205730000	MO KUPARUK 1	70.3020	149.4169	570	1,870	215	705	857	2,812	642	2106
50029200130000	AT NW EILEEN ST 1	70.3659	149.3559	530	1,739	207	679	860	2,822	653	2142
50029201990000	AT HIGHLAND ST 1	70.2869	149.2181	575	1,886	210	689	908	2,979	698	2290
50029200790000	PUT RIVER N-1: 08-11-13	70.3186	148.9097	615	2,018	209	687	1,019	3,343	810	2656
50029200250000	PUT RIVER J-3:04-11-13	70.3300	148.8467	635	2,083	209	684	1,063	3,488	855	2803
50029200470000	PUT RIVER 33-12-13	70.3561	148.8350	650	2,133	206	674	1,180	3,871	975	3197
50029200840000	PUT RIVER F-2-11-11-13	70.3347	148.7669	630	2,067	216	709	1,048	3,438	832	2729
50029200850000	PUT RIVER F-3-12-11-13	70.3353	148.7644	630	2,067	229	752	1,105	3,625	876	2873
50029200540000	PUT RIVER 23-11-13	70.2944	148.7525	540	1,772	210	688	1,065	3,494	855	2806
50029200590000	PUT RIVER 31-11-14	70.2683	148.6733	640	2,100	210	687	1,085	3,560	876	2872
50029200060000	PUT RIVER 27-11-14	70.2783	148.5656	615	2,018	211	693	1,050	3,445	839	2752
50029200490000	PRUDHOE BAY STATE 1	70.3764	148.5250	596	1,955	206	676	1,057	3,468	851	2792
50029200350000	PUT RIVER 19-10-15	70.2117	148.4125	585	1,919	218	715	1,048	3,438	830	2723
50029201330000	EAST BAY STATE #1	70.3106	148.3161	620	2,034	211	691	1,130	3,707	919	3016
50029200300000	SAG DELTA 31-10-16	70.1822	148.1581	590	1,936	224	734	1,010	3,314	786	2580
50155200010000	US AWUNA #1	69.1532	158.0214	236	774	264	865	468	1,535	204	670
50137200030000	US LISBURNE #1	68.4863	155.6935	264	866	264	866	783	2,569	519	1703
50119200010000	US KOLUKTAK 1	69.7524	154.6111	280	919	257	843	540	1,772	283	928
50287200070000	US SEABEE 1	69.3801	152.1753	300	984	258	845	1,070	3,510	812	2665
50287100180000	BP KUPARUK 1	69.3044	150.8093	265	869	262	860	595	1,952	333	1093
50223200110000	FO LUPINE 1	69.1009	148.6193	220	722	337	1,106	660	2,165	323	1060
50223200080000	MO ECHOOKA 1	69.4002	148.2680	265	869	263	864	787	2,582	524	1719

Table 1. List of Alaska North Slope wells with equilibrated borehole temperature surveys along with the estimated depth of the base of permafrost (32°F; 0°C) and the depth to the top (THSZ) and base (BHSZ) of the gas hydrate stability zone. Also listed is the estimated thickness (isopach) of the gas hydrate stability zone (HSZ) (modified from Lee et al., 2008; Collett et al., 2012). API = American Petroleum Institute, m = meters, ft = feet

Subsurface pore-pressure gradients calculated from shut-in pressures recorded during drill-stem testing in wells from the North Slope range from 0.41 to 0.50 psi/ft (9.3 to 11.2 kPa/m), with an average gradient of 0.43 psi/ft (9.7 kPa/m), near hydrostatic (Collett et al., 1988). To further evaluate pore-pressure conditions, we also used gamma ray and density well logs to study overburden compaction profiles. Within the near-surface (0–5000 ft; 0–1524 m) sediments of the North Slope, no significant pore-pressure discontinuities were observed. Thus, a hydrostatic pore-pressure gradient (0.433 psi/ft; 9.795 kPa/m) is generally assumed when considering gas hydrate stability conditions in northern Alaska.

Most of the previous studies of gas hydrate stability conditions in northern Alaska have assumed a pure methane chemistry for the gas being included in the gas hydrate structure (Collett, 1995). The analysis of mud-log gas-chromatographic data from industry exploratory wells generally indicates that methane is the dominant hydrocarbon gas in the near-surface (0–5000 ft; 0–1524 m) sedimentary section of the North Slope (Collett et al., 1988). Analysis of gas evolved from recovered cored gas-hydrate-bearing sedimentary sections in the Prudhoe Bay and Milne Point fields confirm that the in situ gas hydrates are composed mostly of methane in this portion of the North Slope (Collett, 1993; Lorenson et al., 2011; Lorenson and Collett, 2018).

Pore-water salinity data within the near-surface sediments of the North Slope are available from petroleum production tests, water samples from cores within and below permafrost, and spontaneous potential well-log calculations. These data indicate that the pore-water salinities within the sands both above and below the ice-bearing permafrost section are low, ranging from <1.0 parts per thousand (ppt) to as high as 19 ppt (Collett et al., 1988). Analysis of core-derived pore-waters from the Mount Elbert well (Torres et al., 2011) also confirm the presence of low-salinity pore water, with an average background concentration around 5.0 ppt. The updated gas-hydrate stability calculations in Lee et al. (2008) for northern Alaska were made assuming a pore-water salinity of 5.0 ppt.

The methane-hydrate stability zone in northern Alaska, as mapped (Figures 4A–C) (modified from Collett, 1993), covers most of the North Slope. The offshore extent of the gas hydrate stability zone is not well established. Geologic studies (for example, Molochushkin, 1978; Judge et al., 1994; Osadetz and Chen, 2005) and thermal modeling of subsea conditions (Osterkamp and Fei, 1993) indicate that permafrost and gas hydrate may exist within the continental shelf of the Arctic Ocean. Subaerial emergence of portions of the Arctic continental shelf to current water depths of approximately 400 ft (~122 m) (Bard and Fairbanks, 1990) during repeated Pleistocene glaciations subjected the exposed shelf to temperature conditions favorable to the formation of permafrost and gas hydrate. Thus, it is speculated that "relic" permafrost and gas hydrate may exist on the continental shelf of the Arctic Ocean to present water depths of approximately 400 ft (~122 m). We assumed the model-derived predictions for permafrost and gas hydrate stability conditions are accurate and the offshore limit of the nearshore permafrost-associated gas hydrate stability conditions as depicted in Figures 4A–C for the most part corresponds to the 400-ft (~122 m) bathymetric contour. However, more recent studies suggest that the present-day gas hydrate stability zone on the Alaskan Beaufort continental shelf may only extend to water depths of about 65 ft (~20 m) (Brothers et al., 2012, 2016; Ruppel et al., 2016).

2.B.2. Reservoir Rocks

The study of gas hydrate samples indicates that the physical nature of in situ gas hydrates is highly variable (reviewed by Sloan and Koh, 2008). Gas hydrates are observed as (1) occupying pores of coarse-grained sediment; (2) nodules disseminated within fine-grained sediment; (3) a solid substance, filling fractures; or (4) massive nodules composed mainly of solid gas hydrate with minor amounts of sediment. However, most gas hydrate field expeditions have shown that the occurrence of concentrated gas hydrate is mostly controlled by the presence of fractures and (or) coarse-grained sediments in which gas hydrate fills fractures or is disseminated in the pores of sand-rich reservoirs (Collett, 1993; Dallimore and Collett, 2005; Riedel et al., 2006; Collett et al., 2008a, 2008b; Park, 2008; Yang et al., 2008; Fujii et al., 2009; Lee et al., 2011; Collett et al., 2014; Kumar et al., 2014; Lee and Collett, 2005; Yamamoto, 2015; Konno et al., 2017; Collett et al., 2019c). Torres et al. (2008) concluded that hydrate accumulates preferentially in coarse-grained sediments because lower capillary pressures in these sediments permit the migration of gas and nucleation of hydrate. The growth of gas hydrate in clay-rich sediments, however, is less understood. Because high concentrations of gas hydrates in Arctic permafrost regions are in sand-dominated reservoirs, such lithologic units have been the focus of gas hydrate exploration and production studies in northern Alaska. Production testing and modeling have also shown that concentrated gas hydrate in sand reservoirs is conducive to existing well-based production technologies (Moridis et al., 2005, 2009; Anderson et al., 2008; Dallimore et al., 2008a, 2008b, 2012; Yamamoto and Dallimore, 2008).

The northern Alaska oil and gas province extends 600 miles (mi) from the Chukchi Sea on the west to the Canadian border on the east (Figs. 1A–B); its maximum width is about 200 mi and the total area is about 54,000 square miles (mi^2). The geology and petroleum geochemistry of rocks on the North Slope of Alaska are described in considerable detail in a number of publications (Gryc et al., 1951; Lerand, 1973; Grantz et al., 1975; Carman and Hardwick, 1983; Bird and Magoon, 1987; Gryc, 1988; Bird, 1998; Mull et al., 2003). The sedimentary rocks of the North Slope can be conveniently grouped into four sequences representing major episodes in the tectonic development of the region and, to a degree, reflecting its lithologic character. Defined on the basis of source area, these sequences (proposed by Lerand (1973) and applied to northern Alaska by Grantz et al. (1975) and modified by Hubbard et al. (1987)) are, in ascending order, the Franklinian (Cambrian through Devonian), the Ellesmerian (Mississippian to Jurassic), Beaufortian (Jurassic through Lower Cretaceous), and the Brookian (Cretaceous to Holocene). All of the known and inferred gas hydrate occurrences on the North Slope are in Cretaceous and Tertiary reservoirs of the Brookian sequence (Fig. 5), which are the focus of the following discussions on the geologic history of northern Alaska.

Before the completion of coring and downhole-logging operations in the BPXA-DOE-USGS Mount Elbert Gas Hydrate Stratigraphic Test Well in the Milne Point field (Hunter et al., 2011), the only direct confirmation of gas hydrate on the North Slope was obtained

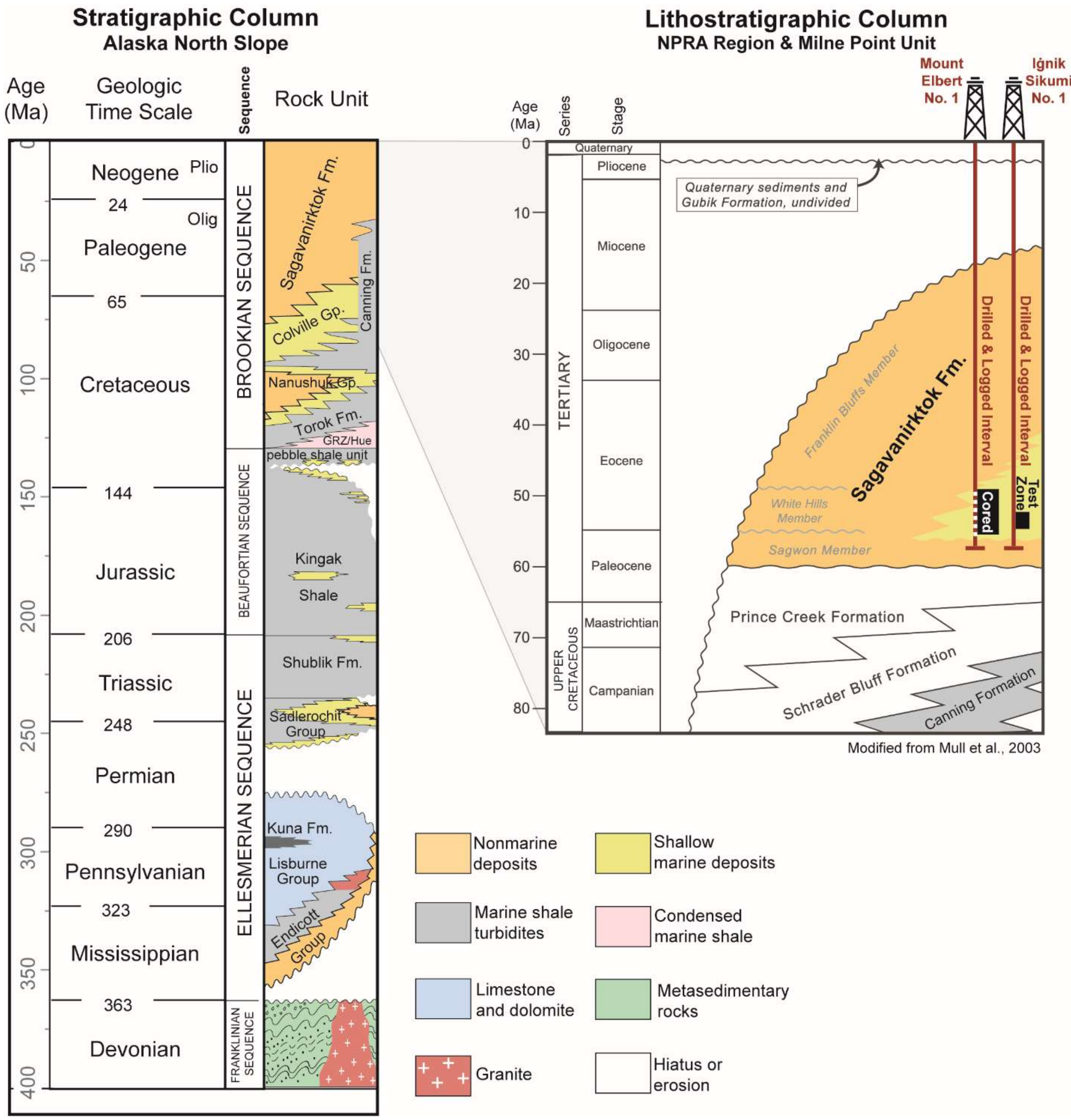

Figure 5. Lithostratigraphic column for the North Slope of Alaska (modified from Mull et al., 2003). The cored interval as shown from the Mount Elbert well recovered lower to middle Eocene marine and non-marine sediments of the Sagavanirktok Formation. GRZ = high gamma ray zone, Hue = Hugh Shale

in 1972 with data from the ARCO-Exxon Northwest Eileen State-2 well, located in the northwest part of the Prudhoe Bay field. Studies of pressurized core samples, downhole logs, and the results of formation-production testing confirmed the presence of three gas-hydrate-bearing stratigraphic units in the Northwest Eileen State-2 well (Fig. 6) (Collett, 1993). The gas-hydrate-bearing core in the Northwest Eileen State-2 well was recovered from a depth of 2156 ft (657 m). The well was drilled with chilled drilling muds in an attempt to reduce thawing of permafrost and decomposition of the in situ gas

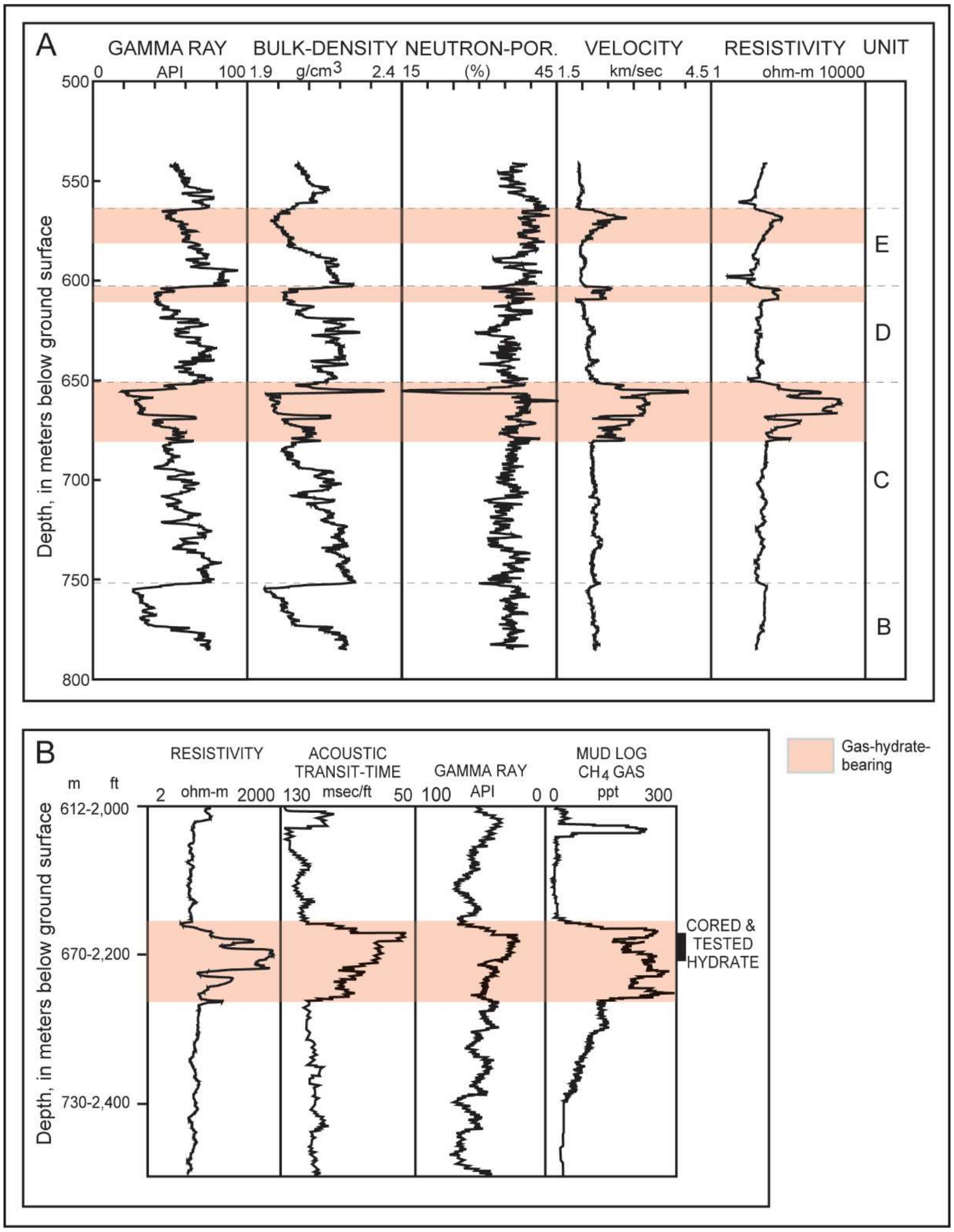

Figure 6. (A) Downhole logs from the Northwest Eileen State-2 well depicting the depth of Units B, C, D, and E; data shown include the natural gamma ray log, bulk-density, neutron porosity, acoustic velocity, and electrical resistivity data. (B) Insert of well logs from the cored gas hydrate interval (Unit C) in the Northwest Eileen State-2 well. Data shown include well logs and methane (CH_4) mud-log curve. See Figure 8 for well location. API = American Petroleum Institute, g/cm^3 = grams per cubic centimeter, % = percent, km/sec = kilometers per second, ohm-m = ohm-meters, msec/ft = milliseconds per foot, ppt = parts per thousand

hydrate that might exist. A pressure-core system was also used to recover core samples at near in situ conditions in order to reduce core disturbance attributed to gas hydrate dissociation. The presence of gas hydrate in the recovered core was confirmed by a pressure test as described by Hunt (1979, p. 167).

The confirmed gas hydrate occurrence in the Northwest Eileen State-2 well provided an ideal starting point for the development of gas hydrate well-log evaluation techniques (Fig. 6). Numerous studies since this early work, including Collett (1993), have shown that in most cases only two well-logging devices are needed to identify potential gas hydrates: they are the electrical resistivity and acoustic transit-time logs. For the most part, a gas hydrate-bearing sand reservoir is characterized by relatively high electrical resistivities and rapid acoustic transit times in comparison to water-saturated sands. However, resistivity and acoustic logs behave similarly within a sedimentary section that is saturated with either gas hydrate or ice. Hence, gas shows on the mud log produced from decomposing hydrate generally provide the only means of conclusively differentiating a gas hydrate from ice in Arctic permafrost regions.

Collett (1993) examined well-log data from 445 wells for evidence of gas hydrate based on the well-log responses observed in the Northwest Eileen State-2 well. Most of the wells were located in the greater Prudhoe Bay area; however, all wells in NPRA and most of the exploratory wells to the south and east of Prudhoe Bay were reviewed. Since this earlier work, Lee et al. (2008), Inks et al. (2009), and the U.S. Geological Survey Alaska Gas Hydrate Assessment Team (2013) examined the well log data from about 600 additional exploratory and development wells for the presence of gas hydrate. These well-log-based studies revealed the occurrence of two large gas hydrate accumulations, which have been named the Eileen and Tarn gas hydrate accumulations.

The Eileen gas hydrate accumulation was first described by Collett (1993) as six laterally continuous gas-hydrate-bearing sandstone units, each of which has been assigned a reference letter (A–F, in ascending order; Fig. 7). Many of the wells that penetrated the Eileen accumulation have multiple gas-hydrate-bearing units, with individual units ranging from 10 to 100 ft (3 to 30 m) thick. All the wells are geographically restricted to the area overlying the eastern part of the Kuparuk River field, the southern part of the Milne Point field, and the western part of the Prudhoe Bay field (Figs. 7–8). The lateral boundaries of the gas-hydrate-bearing units as mapped by Collett (1993) are based in many places on widely spaced well control and therefore are open to interpretation and further refinement. Also, the lateral continuity of gas hydrate occurrences between well sites is still poorly defined, but 3D seismic prospecting in the Milne Point area by Inks et al. (2009) has provided additional insight to the lateral nature and extent of the well log-inferred, gas hydrate-bearing units in the Eileen accumulation (discussed in a later section of this report). It is also important to emphasize that seismic surveys (reviewed by Inks et al., 2009; Lee et al., 2009) and downhole logs (Collett, 1993) from wells in the western part of the Prudhoe Bay field indicate the presence of several large free-gas accumulations trapped stratigraphically downdip below five (Units A–E) of the log-inferred gas hydrate-bearing units. The total mapped area of all six gas hydrate-units in the Eileen accumulation is about 635 mi^2 (1645 km^2); the areal extent of individual units range from 1 to 155 mi^2 (2.6-401 km^2) (Fig. 8).

Collett (1993) concluded that the Eileen gas hydrate accumulation is in rocks of the Mikkelsen Tongue of the Canning Formation (Fig. 5), which were deposited during a basin-wide marine transgression in the Eocene. This sequence (which is mostly marine)

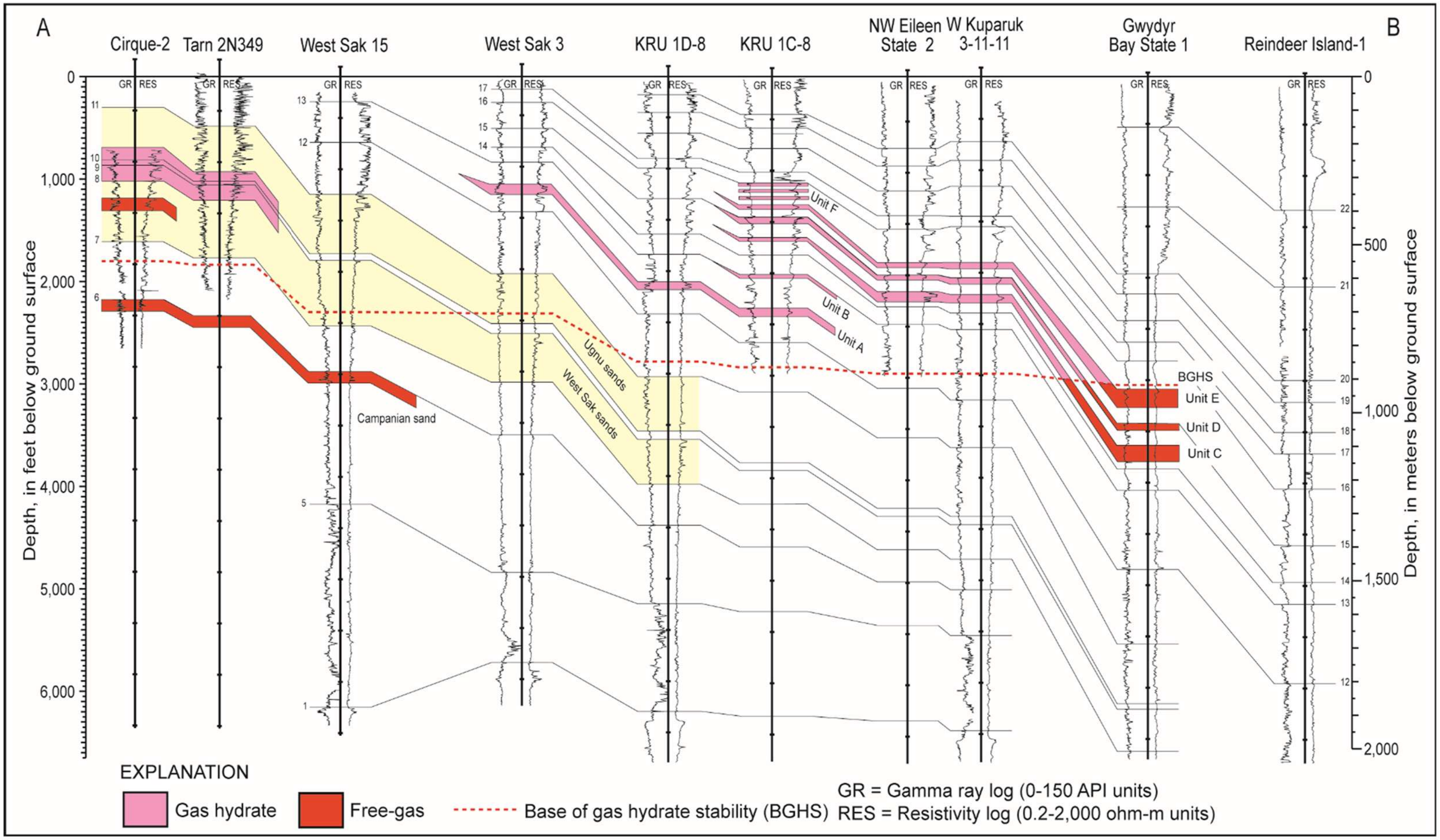

Figure 7. Well log cross section showing the lateral and vertical extent of the Eileen and Tarn gas hydrate accumulations and the associated underlying free-gas zones in the Prudhoe Bay and Kuparuk River oil fields. See Figure 8 for the location of the cross section. The gas hydrate-bearing units in the Eileen accumulation are identified with the reference letters A through F. The numbered solid lines are log correlation markers used to construct a regional stratigraphic framework (modified from Collett, 1993). The gas hydrate-bearing portions of units A and B in the Eileen accumulation are shown as ending above the base of the gas hydrate stability zone, which is correct along the path of this southwest- to northeast-trending cross section. However, to the east and south from the Kuparuk River field into the Prudhoe Bay field, Units A and B gas hydrates extend to the base of the gas hydrate stability zone and trap free gas in a downdip position.

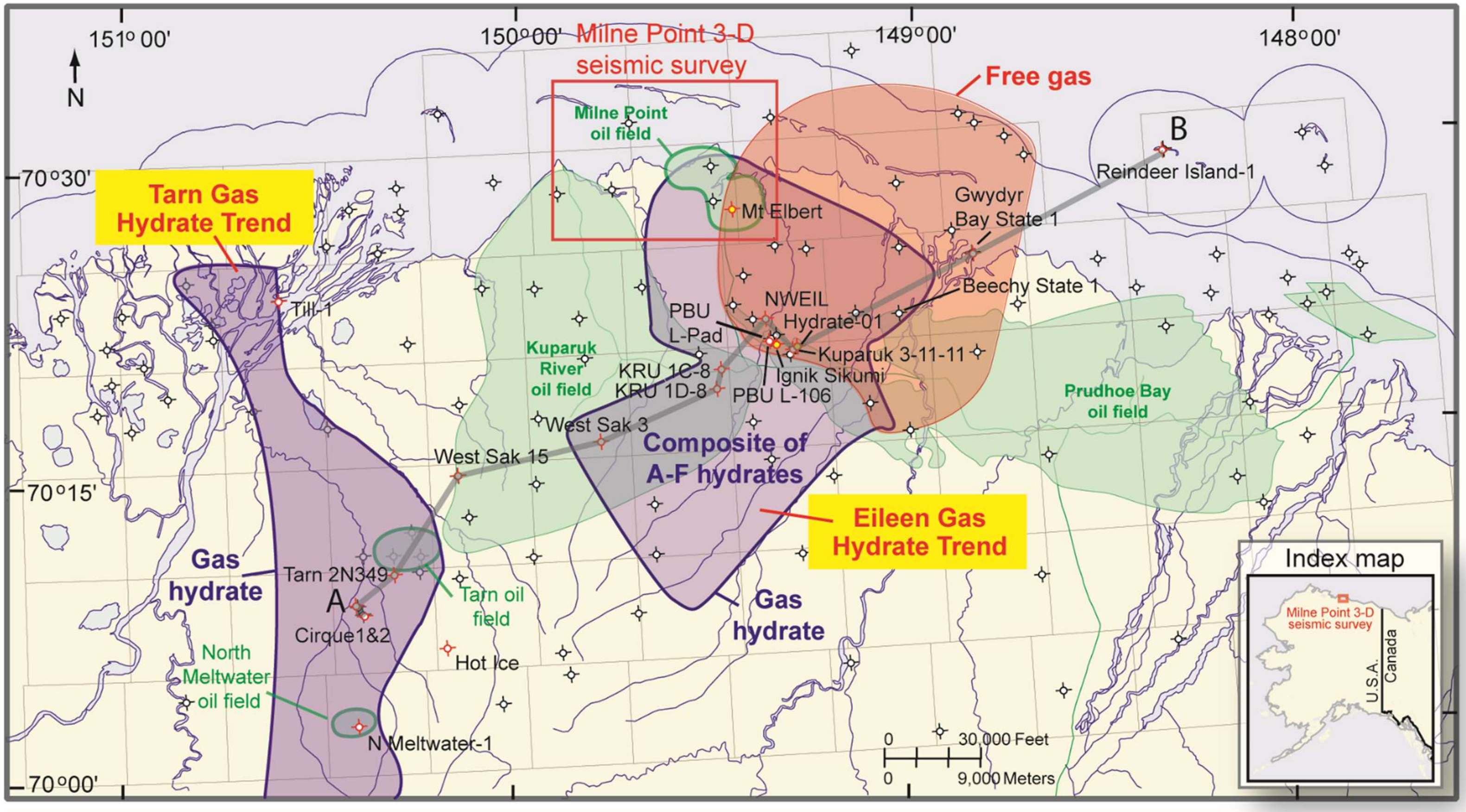

Figure 8. Map of the Eileen and Tarn gas hydrate accumulations overlying portions of the Prudhoe Bay, Kuparuk River, and Milne Point oil fields (modified from Collett, 1993). Also shown are the locations of the Northwest Eileen State-2 (NWEIL), Mount Elbert, Iġnik Sikumi, and Hot Ice gas hydrate research wells and the well log cross section A-B in Figure 7, along with the outline of the Milne Point 3D seismic volume used to identify and map gas hydrate prospects.

thins southwesterly and coarsens laterally into a sand-rich sequence in the western part of the Prudhoe Bay field. Analysis of drill cuttings (Collett, 1993) and core from the Mount Elbert well (Rose et al., 2011) indicates that the gas-hydrate-bearing reservoirs in the Eileen accumulation consist mostly of fine grained to very fine grained sands and coarse silts with minor amounts of interbedded coarse sands, conglomerates, and shales deposited in a range of nearshore marine and nonmarine environments. Considering the sand-rich nature of the section at the site of the Mount Elbert well, the interval containing the Eileen gas hydrate-bearing sands are now assigned to the Sagavanirktok Formation (Molenaar et al., 1987b; Bird, 1998; Rose et al., 2011) and are considered the age equivalent of the more distal early Eocene marine shales and minor sands of the Mikkelsen Tongue farther to the east.

In 1992, while drilling the Cirque-1 well near the western edge of the Kuparuk River field, a shallow gas zone (depth of about 2330 ft; 710 m) was encountered that subsequently blew out the well (Alaska Oil and Gas Conservation Commission, 1992). It was later determined that the well also encountered a thick gas-hydrate-bearing interval that contributed to the gas flow problem (Collett and Dallimore, 2002). Subsequent drilling of the Cirque-2 well confirmed the occurrence of gas hydrates near the base of permafrost within the depth interval of about 820 ft to 1150 ft (250-350 m) (Collett and Dallimore, 2002).

Downhole log data from industry exploratory and development wells located along the western margin of the Kuparuk River field, tied to the well-log responses in the Cirque-2 well, reveal a large gas hydrate accumulation that has been named the Tarn gas hydrate accumulation (Collett, 1993). As shown in Figure 8, the Tarn gas hydrate accumulation lies in a fairway extending from the Till-1 well in the north, through the Cirque-Tarn area, to near the North Meltwater field to the south. The gas-hydrate-bearing stratigraphic interval in the Tarn area appears to be the updip equivalent of the Upper Cretaceous West Sak Sands, which are estimated to contain more than 20 billion barrels of in-place viscous oil and are the focus of development activity in a downdip position to the east of the Tarn gas hydrate accumulation (Werner, 1987). Preliminary analyses of other recently completed wells along the western margin of the Kuparuk River field indicate that the Tarn gas hydrate accumulation may be larger than the Eileen accumulation; however, the Tarn accumulation lies mostly within permafrost unlike the Eileen accumulation, which straddles the base of permafrost.

In 2003, the USGS initiated a study to develop seismic interpretive methods to identify and characterize gas hydrate accumulations and to further characterize the nature of hydrate-bearing reservoirs on the Alaska North Slope. This study dealt primarily with the analysis of a 3D seismic data set from the area of the Milne Point field as provided to the USGS by BP Exploration Alaska, Inc. (Figs. 8–9). Detailed analysis and interpretation of available 3D and 2D seismic data sets, along with seismic modeling and correlation with specially processed downhole well log data, have led to the development of a viable method for identifying sub-permafrost gas hydrate prospects within the gas hydrate stability zone in the Milne Point area (Lee et al., 2009, 2011; Inks et al., 2009).

Initial seismic interpretation indicated a range of potential gas hydrate prospects, including accumulations at the base of the gas hydrate stability zone (in contact with

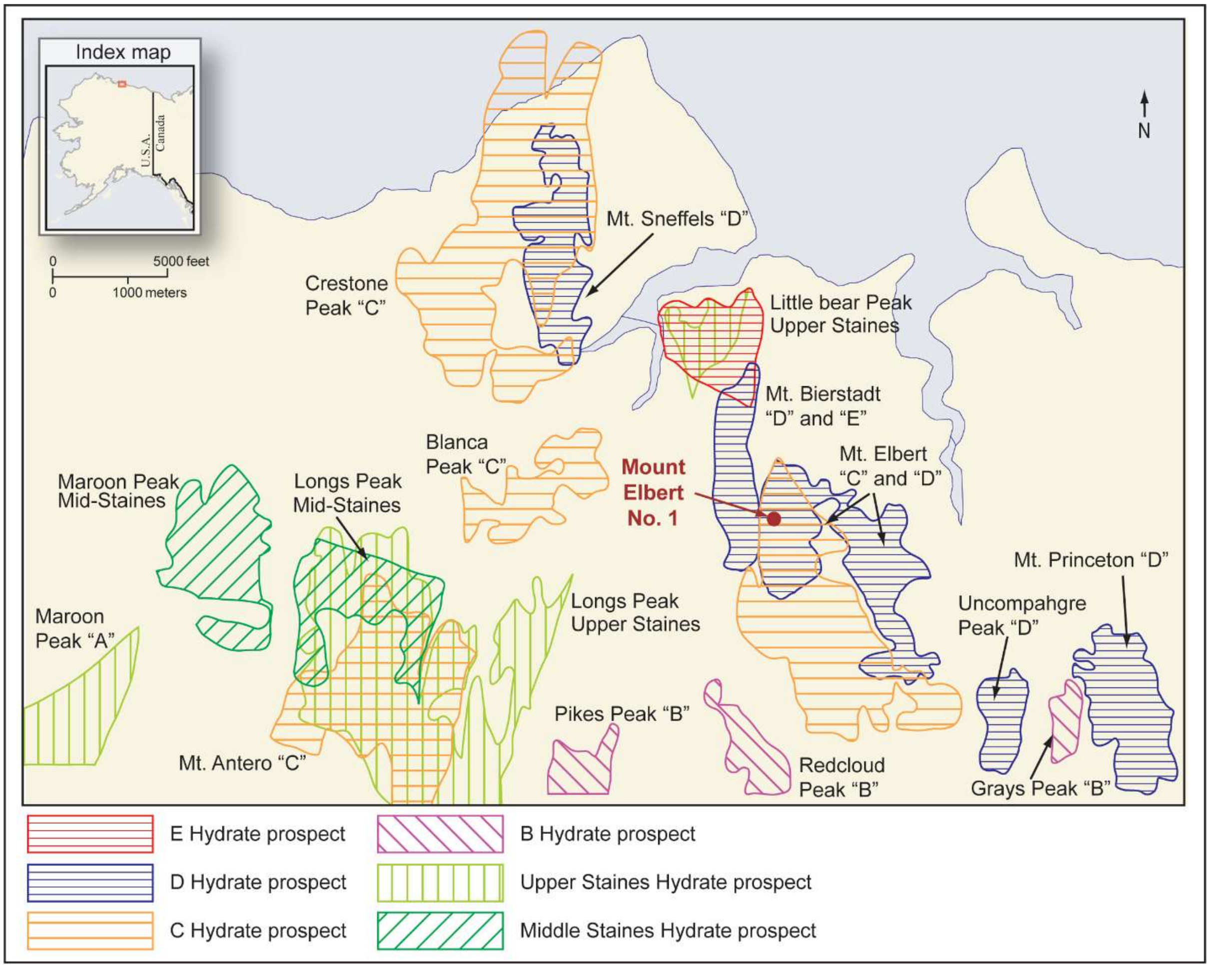

Figure 9. Milne Point area gas hydrate prospects identified with 3D seismic interpretation. Modified from Inks et al. (2009). As a condition of the seismic data use agreement, the latitude and longitude of the seismic data and the interpreted features cannot be shown on this map.

underlying free gas) and additional hydrate prospects higher in the stratigraphic section. However, well log data showed that the gas hydrate and free gas saturations in the deeper reservoirs were low (Inks et al., 2009). In 2005, the USGS project team completed their delineation, description, and ranking (including probabilistic volumetrics) of 14 gas hydrate prospects (Fig. 9) within the Milne Point area. The seismic characterization of the gas hydrate prospects was based on rock physics relations calibrated with downhole log data from nearby offset wells; this enabled the prediction of gas hydrate "pay" thickness and gas hydrate saturation from analyses of seismic amplitudes and peak-trough travel-times (Lee et al., 2009).

The highest ranked Milne Point gas hydrate prospect, named Mount Elbert, is depicted in Figures 9 and 10. The pre-drill site evaluation predicted that Mount Elbert would contain approximately 145 BCF (billion cubic feet) of in-place gas in two reservoir sands (Units C and D after Collett, 1993) (Inks et al., 2009). The Mount Elbert prospect, like all of the most promising Milne Point prospects, had not been penetrated by existing wells.

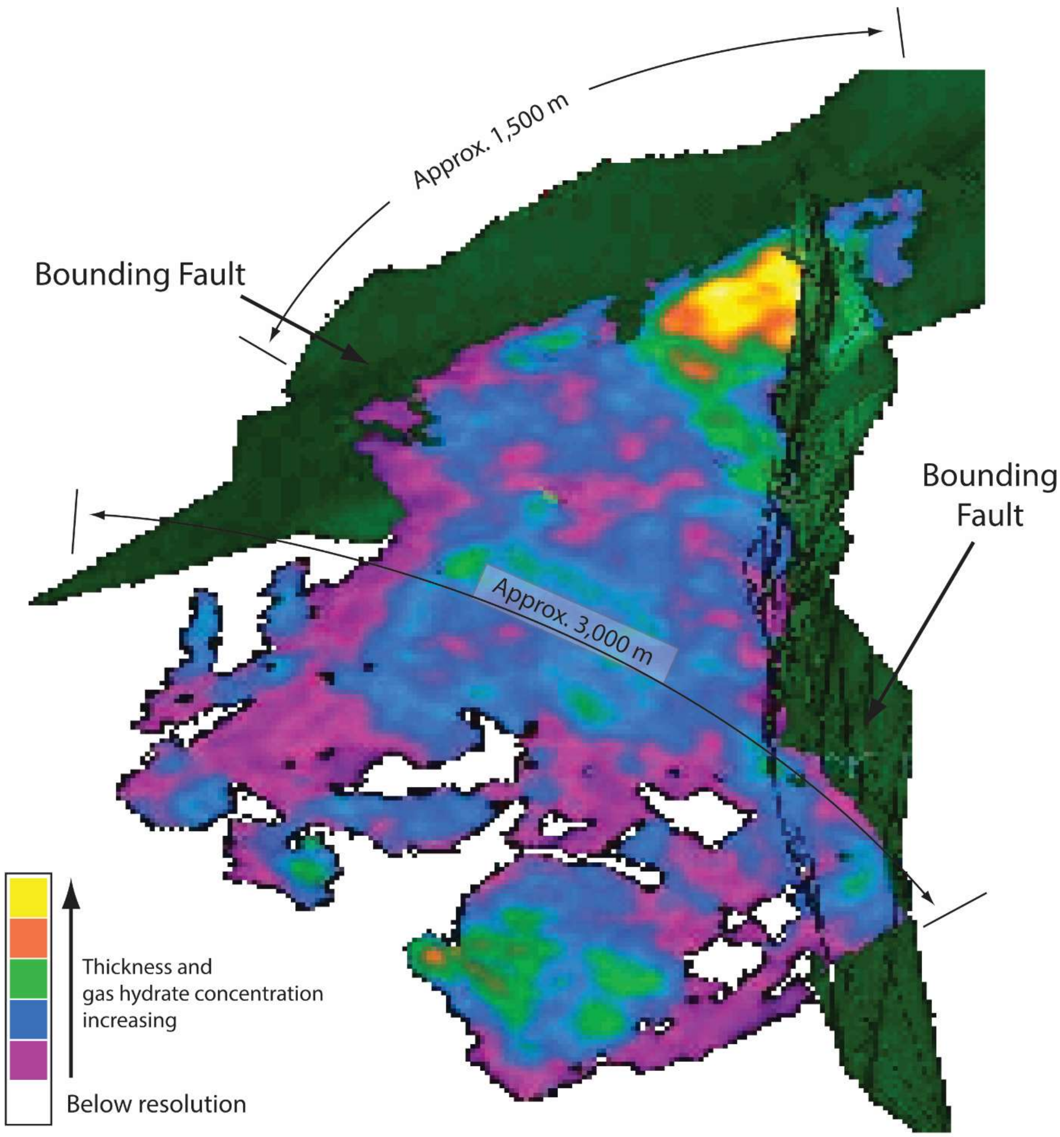

Figure 10. Milne Point Mount Elbert gas hydrate prospect. Shown are a three-dimensional image of a fault-bounded, high-amplitude feature (in a pallet of colors ranging from yellow to magenta, the yellow-imaged portion contains the thickest and most concentrated gas hydrate) and bounding faults (in green) (Modified from Inks et al., 2009). As a condition of the seismic data use agreement, the latitude and longitude of the seismic data and the interpreted features cannot be shown on this map.

Therefore, it was decided to drill a stratigraphic test well to confirm the existence of reservoirs, test the prospecting and assessment methodologies, and enable the collection of additional reservoir data to support reservoir-simulation modeling and production test design (Hunter et al., 2011). The Mount Elbert Gas Hydrate Stratigraphic Test Well was completed in February 2007 and yielded one of the most comprehensive data sets yet compiled on naturally occurring gas hydrates. The test well was designed as a 22-day program with the planned acquisition of cores, well-logs, and downhole production test data. It was first drilled and cased to a depth of 1952 ft (595 m), then was continuously cored to a depth of 2494 ft (760 m). After coring, the well was surveyed with a research-level wireline-logging program including nuclear magnetic resonance and dipole acoustic logging, resistivity scanning, borehole electrical imaging (Figs. 11–12), and advanced geochemistry logging. Following logging, Schlumberger Modular Dynamic Testing (MDT) was conducted at four open-hole stations in two hydrate-bearing sandstone reservoirs (Fig. 12). Each test consisted of flow and shut-in periods of varying lengths, with one lasting more than 13 hours (hr). Gas was produced from the gas hydrates in each of the tests. Gas hydrates were expected and encountered in two stratigraphic zones (Figs. 11–12): (1) an upper zone (Unit D) that contained approximately 46 ft (~14 m) of gas hydrate-bearing reservoir-quality sandstone, and (2) a lower zone (Unit C) that contained approximately 52 ft (~16 m) of gas-hydrate-bearing reservoir. Both zones displayed gas hydrate saturations that varied with reservoir quality as expected, with typical values between 60 and 75 percent. This result conclusively demonstrated the soundness of the gas hydrate prospecting methods developed primarily by the USGS (Lee et al., 2011).

The Milne Point 3D seismic gas hydrate prospecting effort also provided a greater appreciation of the lateral nature of the well-log-inferred, gas-hydrate-bearing sedimentary units in the Eileen accumulation. As reported by Collett (1993), the thickness of the well log-inferred gas hydrate intervals in the Milne Point area range from approximately 10 to 100 ft (~3–30 m). However, the nature of the gas hydrate occurrences between wells is poorly constrained. Collett (1993) assumed that the deposits were laterally continuous and were representative of hydrate occurrences throughout the Eileen accumulation. The Milne Point 3D seismic analysis, however, revealed a much more "patchy" nature, as depicted in the gas hydrate prospect map in Figure 9, with individual gas hydrate prospects ranging in size from about 0.1 to 2.7 mi^2 (~0.3–7.0 km^2). The thickness of the seismically imaged gas hydrate occurrences in the Milne Point effort were also determined to range from approximately 30 ft (~9 m) to a maximum thickness of approximately 65 ft (~20 m). However, Lee et al. (2009, 2011) demonstrated that within the Milne Point 3D seismic data volume, there is no significant seismic response to gas hydrate reservoirs with less than a cut-off thickness of about 25–30 ft (about 8–9 m). This indicates the probability that the relatively thinner log-inferred gas hydrate occurrences in the Milne Point area are not being seismically imaged. It is therefore likely that gas hydrates between well sites within a given stratigraphic unit are more regionally extensive than those imaged by Inks et al. (2009), but thicknesses can only be inferred from available data. The local variability in the nature of the Eileen gas hydrate accumulation is likely controlled by the components of the gas hydrate system (that is, reservoir conditions and continuity, hydrocarbon trapping relationships, gas source, and gas migration to name a few of the most important factors).

The Eileen and Tarn gas hydrate accumulations clearly demonstrate the role of the reservoir in a gas hydrate system. In both cases, gas hydrate is in pores of coarse-grained sedimentary rocks. It is also clear that the accumulation of gas hydrates is limited to the zone of methane hydrate stability in northern Alaska. Of most importance for this analysis of potential gas hydrate production test sites, however, is that the seismic-inferred hydrate accumulations on the Alaska North Slope occupy limited,

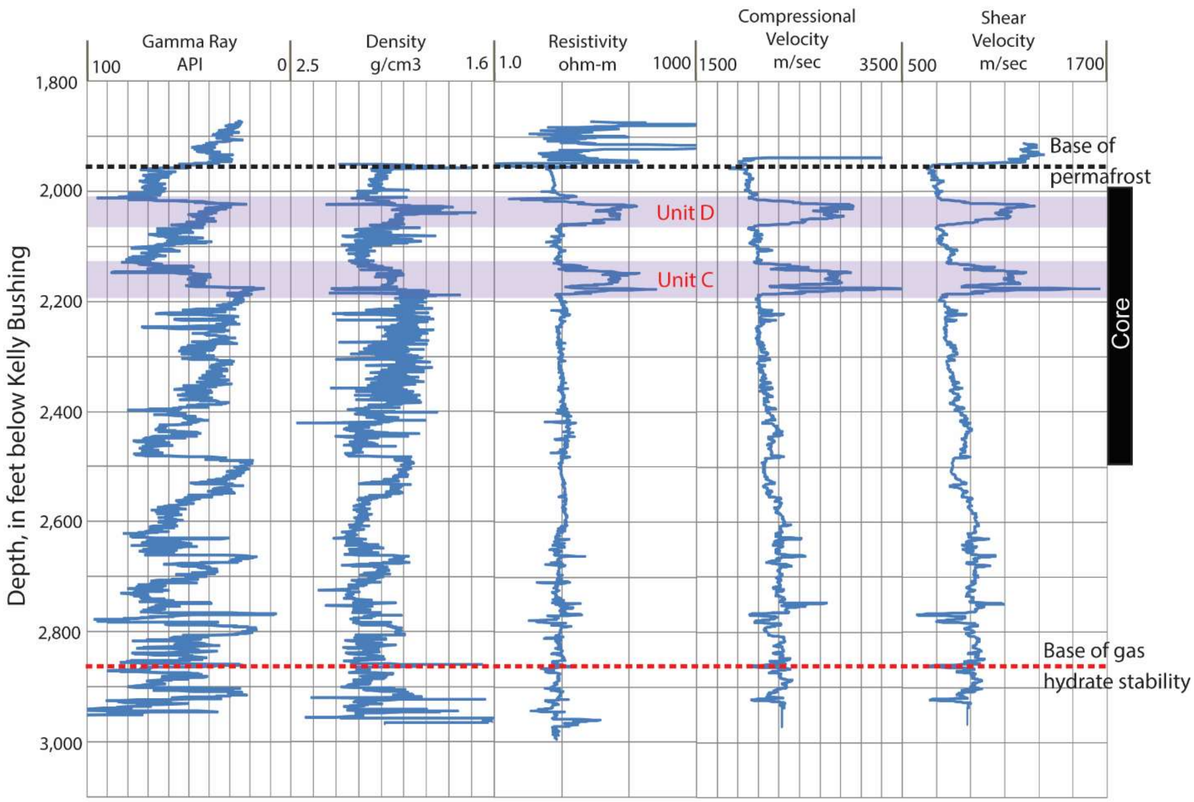

Figure 11. Open-hole well logs from the cored section of the Mount Elbert gas hydrate stratigraphic test well. Modified from Hunter et al. (2011). API= American Petroleum Institute, g/cm^3 = grams per cubic centimeter, ohm-m = ohm-meters, m/sec = meters per second

discrete volumes of rock bounded by faults, lateral stratigraphic changes, and downdip water contacts much like conventional hydrocarbon accumulations.

2.B.3. Gas Source and Migration

It has been shown that the availability of large quantities of hydrocarbon gas from both microbial and thermogenic sources is an important factor controlling the formation and distribution of natural gas hydrates (Collett, 1993; Kvenvolden, 1988,1993; Collett, 2002; Lorenson et al., 2011). Carbon isotope analyses indicate that the methane in many oceanic hydrates is derived from microbial sources; however, thermal sources have been observed within several hydrate deposits in the Gulf of Mexico, the Caspian Sea, the Black Sea, and onshore in the Mackenzie Delta of Canada and in northern Alaska (reviewed by Collett, 2002). Studies in northern Alaska (Lorenson et al., 2011) and Canada (Dallimore and Collett, 2005) have also documented the importance of thermogenic gas sources to the formation of highly concentrated gas hydrate accumulations.

Typically, not enough microbial methane is generated internally within the gas hydrate stability zone alone to account for the gas content of most gas hydrate accumulations (Kvenvolden, 1993). In addition, most gas hydrate accumulations are in sediments that have not been deeply buried or subjected to temperatures high enough to form

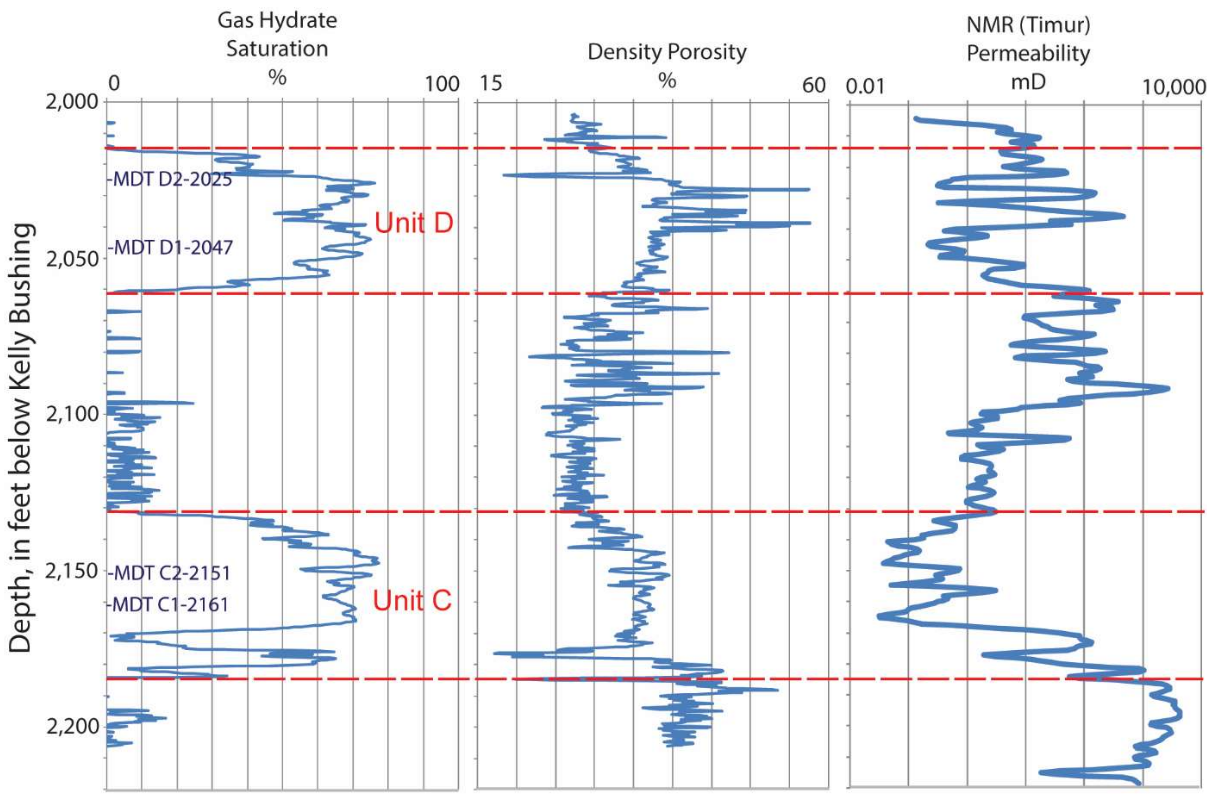

Figure 12. Well log-derived gas hydrate saturations, density porosities, and sediment permeabilities for the two gas hydrate-bearing intervals (Units C and D) cored in the Mount Elbert gas hydrate stratigraphic test well (modified from Hunter et al., 2011). The intervals tested (Schlumberger Modular Dynamic Testing (MDT) Tests C1, C2, D1, and D2) are also shown. NMR = nuclear magnetic resonance, % = percent, mD = millidarcy

thermogenic gas. Thus, in most cases, gas is likely concentrated in the hydrate stability zone by a combination of processes, one of which, gas migration, appears to be the critical component within most gas hydrate systems.

In the greater Prudhoe Bay area, the Sagavanirktok Formation (Fig. 5) is cut by a series of northwest-trending high-angle normal faults, generally downthrown to the east (Werner, 1987). Similar faults cut the underlying rocks in this area, suggesting a genetic linkage between the two fault systems that could provide conduits for oil and gas migration from the underlying Prudhoe Bay and Kuparuk River fields. Geochemical similarities suggest that oil and presumably the associated gas within the Sagavanirktok Formation were "spilled" from the underlying Sadlerochit Group reservoir as a consequence of regional tilting during the middle to late Tertiary (Carman and Hardwick, 1983; Masterson et al., 2001).

Geochemical analyses of drill cuttings and core samples from wells in both the Eileen and Tarn gas hydrate accumulations indicate that methane is the principal gas in these accumulations (Collett, 1993; Lorenson et al., 2011). Stable methane-carbon isotopic analyses show that the methane within the gas hydrate is likely from mixed microbial and thermogenic sources, with the apparent thermogenic methane migrating from deeper sources, including the Prudhoe Bay field. Masterson et al. (2001) and Lorenson et al. (2011) have shown that evaporative fractionation and biodegradation of the Sadlerochit-sourced oil in the Sagavanirktok Formation is also an important source of gas within the gas hydrates of both the Eileen and Tarn gas hydrate accumulations.

Collett (1993) adapted a generalized cross section (Fig. 13) from Carman and Hardwick (1983) to describe the history of the Eileen and Tarn gas hydrate accumulations. Collett postulated that as thermogenic gas and associated oil moved up the Eileen and other fault zones and encountered the relatively porous and permeable northeast-dipping sandstone reservoir units of the Sagavanirktok, some of the gas may have been rechanneled updip along these beds. The updip-migrating gas may have mixed with in situ microbial methane and collected in structural and stratigraphic traps where falling temperatures at the end of the Pliocene deepened the permafrost section and converted the trapped gas into gas hydrate.

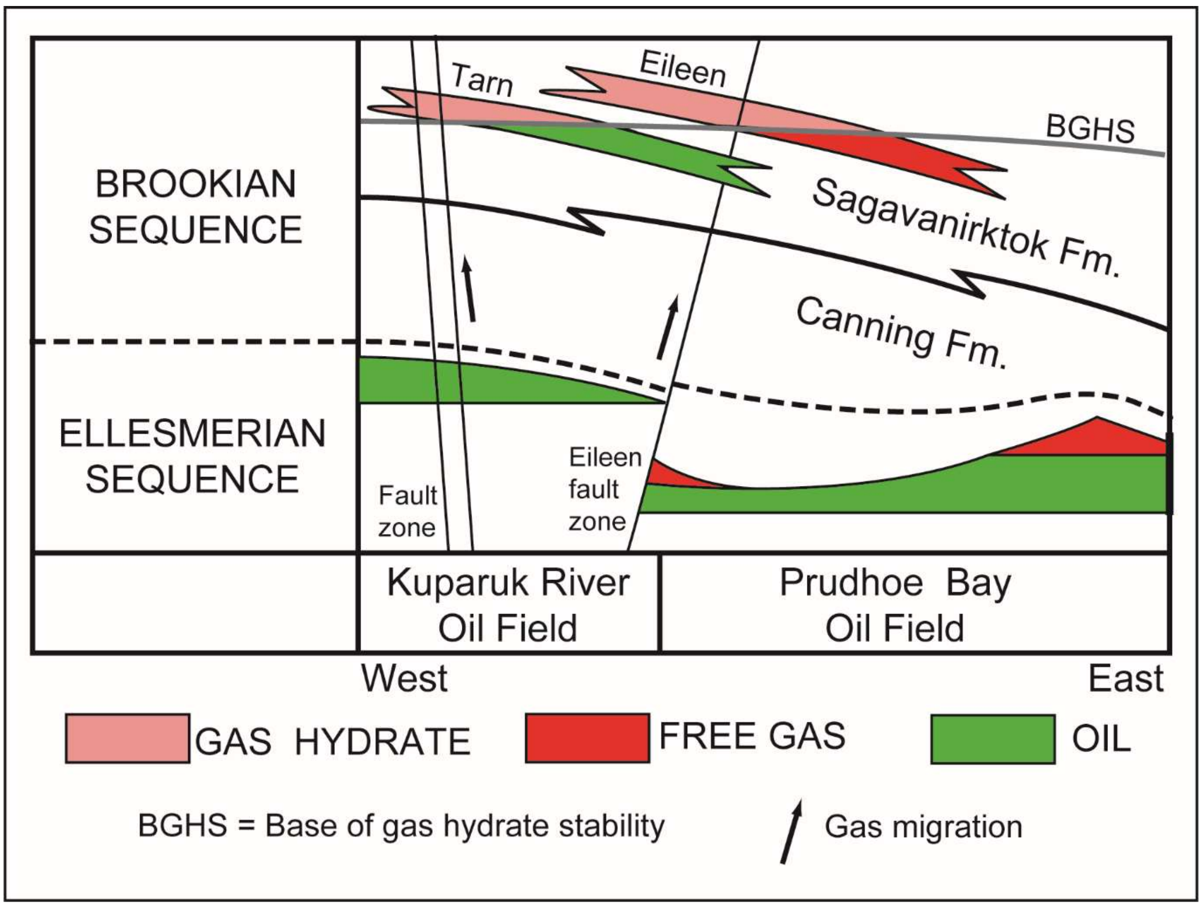

Figure 13. Schematic west to east cross section through the Prudhoe Bay and Kuparuk River fields illustrating possible gas-migration paths and spatial relations between the Eileen and Tarn gas hydrate accumulations, free-gas and oil accumulations, Eileen and other fault zones, and base of gas hydrate stability (modified from Carman and Hardwick, 1983).

As discussed above, gas hydrate in onshore Arctic environments is typically closely associated with permafrost. It is generally believed that thermal conditions conducive to the formation of permafrost and gas hydrate persisted in the Arctic since the end of the Pliocene (about 2.59 million years ago) (Collett, 1993, 2002; Lee et al., 2008). From Milne Point seismic and other studies, it also appears that most permafrost-associated gas hydrate accumulations probably developed from preexisting free-gas fields that originally formed in conventional hydrocarbon traps and were later converted to gas hydrate upon the onset of glaciation and cold Arctic conditions (Collett, 1993, 2002; Lee et al., 2009, 2011; Inks et al., 2009; Boswell et al., 2011a, 2011b).

2.B.4. Eileen Gas Hydrate Trend Petroleum System - Summary

In this section of the IA Final Report, well log and core derived data from industry and hydrate research wells, along with available seismic data, were analyzed to refine our understanding of the distribution of gas hydrate in northern Alaska. The occurrence of gas hydrate in the Eileen Gas Hydrate Trend at the reservoir pore-scale is controlled by the availability of gas supply as well as the petrophysical properties of the host reservoir. Stratigraphic variation (i.e., reservoir controls) within the reservoir unit, as discussed above, serves as a primary control on the petrophysical properties of the host reservoir. Finally, the interplay between the structural-stratigraphic relationships of the reservoir unit and the efficiency of gas delivery to the reservoir are collectively the fundamental controls on the occurrence of gas hydrate in the Eileen Gas Hydrate Trend.

Within this project, gas hydrate system analysis was one of the primary tools used in two closely related gas hydrate test site review and characterization studies. Understanding the geologic controls on the occurrence of gas hydrate through the above-described system analysis approach proved to be instrumental in the 2011 test site review effort that led to the identification of the site that ConocoPhillips ultimately drilled the Iġnik Sikumi test well. Similar analytical approaches, built on the 2011 test site review, were also used to support the second 2017 test site review effort that led to the selection of the PBU 7-11-12 test site and the drilling of the Hydrate-1 Stratigraphic Test Well in 2018.

3. TEST SITES REVIEW AND SELECTION

With the successful completion of the BP Exploration Alaska Incorporated (BPXA) 2007 Mount Elbert gas hydrate stratigraphic test well in the Milne Point Field, the Eileen Gas Hydrate Trend, located in the greater Prudhoe Bay area, became the focal point for gas-hydrate geologic and production studies. A critical goal of these new efforts became the identification of the most suitable site for gas hydrate production testing. A total of seven potential locations in the Prudhoe Bay (PBU), Kuparuk River (KRU), and Milne Point (MPU) production units were identified and assessed relative to their suitability as a long-term gas-hydrate-production test site. The test-site-assessment criteria included the analysis of the geologic risk associated with encountering reservoirs for gas-hydrate testing. The site-selection process also dealt with the assessment of the operational/logistical risk associated with each of the potential test sites. From this review, several sites in the PBU were determined to be the best locations for extended gas-hydrate production testing. The work presented in this report identifies the key features of the potential test sites in the greater Prudhoe Bay area and provides new information on the nature of gas-hydrate occurrence and the potential impact of production testing on existing infrastructure at the most favorable sites. These data were obtained from well-log analysis, geological correlation and mapping, and numerical simulation of expected gas production responses.

Before the start of this test site review effort under this IA, a series of short-term scientific tests (Dallimore and Collett 2005; Dallimore et al., 2008a, 2008b; Yamamoto and Dallimore 2008; Hunter et al., 2011) had provided a wealth of petrophysical information and insight on potential gas-hydrate reservoir performance. However, a reservoir's initial production response often provides limited insight into actual deliverability because of transient effects that are very difficult to understand. Because the time required for the production response to stabilize may be many months or more, a key criterion for gas-hydrate production testing is the availability of a site that allows continuous access over a sufficient duration to provide meaningful data on reservoir performance. This could mean only a month or so if the test produces large and stable volumes quickly; it could mean several years if all the planned contingencies for supplemental testing need to be invoked. Therefore, in addition to favorable geologic conditions, a potential field site also must provide year-round access to the well and needed services and infrastructure. On the ANS, this requires access to an existing gravel pad.

The remainder of this section of the report provides a summary of the geologic criteria and other considerations used to identify and characterize potential gas hydrate production test sites. The key geologic consideration that is discussed for each potential test site relates to the occurrence of gas hydrate reservoir sedimentary facies suitable for testing. Because of the long history of industry-led exploration activities and USGS resource assessments in northern Alaska, this study had access to a large number of pertinent published reports and databases. One of the more important sources of information was the various data sets published with the previously completed USGS assessments of unconventional and conventional resources in northern Alaska, including the following: (1) 1995 USGS Gas Hydrate Assessment (Collett, 1995); (2) 2008 USGS Geologic Assessment of Undiscovered Gas Hydrate Resources on the North Slope, Alaska (U.S. Geological Survey Alaska Gas Hydrate Assessment Team, 2013); (3) 2018 USGS Geologic Assessment of Undiscovered Gas Hydrate Resources on the North Slope, Alaska (Collett et al., 2019a); (4) 1999 Oil and Gas Resource Potential of the Arctic National Wildlife Refuge 1002 Area, Alaska (ANWR Assessment Team, U.S. Geological Survey, 1999); (5) 2002 Petroleum Resource Assessment of the National Petroleum Reserve in Alaska (Bird and Houseknecht, 2002); (6) 2005 Oil and Gas Assessment of Central North Slope, Alaska (Garrity et al., 2005); and (7) 2007 Geologic Assessment of Undiscovered Coalbed Gas Resources in Cretaceous and Tertiary Rocks, North Slope and Adjacent State Waters, Alaska (Roberts, 2008).

The USGS also maintains several specialized data sets that were used in this review. One of the most important data sets is a copy of the State of Alaska well log database (Alaska Oil and Gas Conservation Commission, 2020) — this database contains the publicly available downhole log data from more than 5,000 North Slope exploratory and development wells. For the most part, log data from wells in Alaska are released by the State two years after the completion of a well. This well log database was also used to develop an unpublished USGS Alaska formation tops file as maintained by Ken Bird (USGS, Menlo Park, California), Dave Houseknecht (USGS, Reston, Virginia), and Phil Nelson (USGS, Denver, Colorado). The USGS Alaska formation tops file, containing listings of penetration depths of all the major geologic "markers" and formations tops encountered during drilling, numbers about 450 wells as of December 1, 2020. This file was developed mostly as a product of the various USGS Alaska North Slope assessment studies.

A number of well log correlation sections were developed as part of this study and other USGS gas hydrate research projects in northern Alaska. Lewis and Collett (2013), for example, compiled a series of nine correlation sections, containing well log data from more than 122 wells, extending from just west of the Colville River in NPRA to the east near the Sagavanirktok River (Fig. 14). These sections include (1) "well log picks" for the tops of all the major formations and well log markers, (2) depths of the well log-inferred gas hydrate accumulations (including those within the Eileen and Tarn gas hydrate accumulations), (3) depths of the top and base of the gas hydrate stability zone, and (4) depths to the base of permafrost and (or) ice-bearing permafrost. Other important published well log correlation sections were available from Molenaar et al. (1987a) and Decker (2007).

This project also made use of several extensive grids of 2D seismic lines and 3D seismic volumes (Fig. 15). As part of the U.S. Government-managed NPRA exploration program in the 1970s and 1980s, the USGS supervised the acquisition of more than 15000 mi (24140 km) of 2D seismic data. Miller et al. (2000, 2001) included reprocessed digital seismic data for a series of regional reference seismic lines (approximately 4200 line-miles; 6760 km), which formed a 20×20-mi grid covering the entire NPRA. As discussed earlier, the 3D seismic data volume from the MPU covering an area of 155 mi^2 (400 km^2) (Figs. 8–10) (as released to the USGS by BP Exploration Alaska, Inc.) was used to develop and document seismic methods for identifying a series of nine gas hydrate prospects (accumulations) in the MPU (Lee et al., 2009, 2011; Inks et al., 2009).

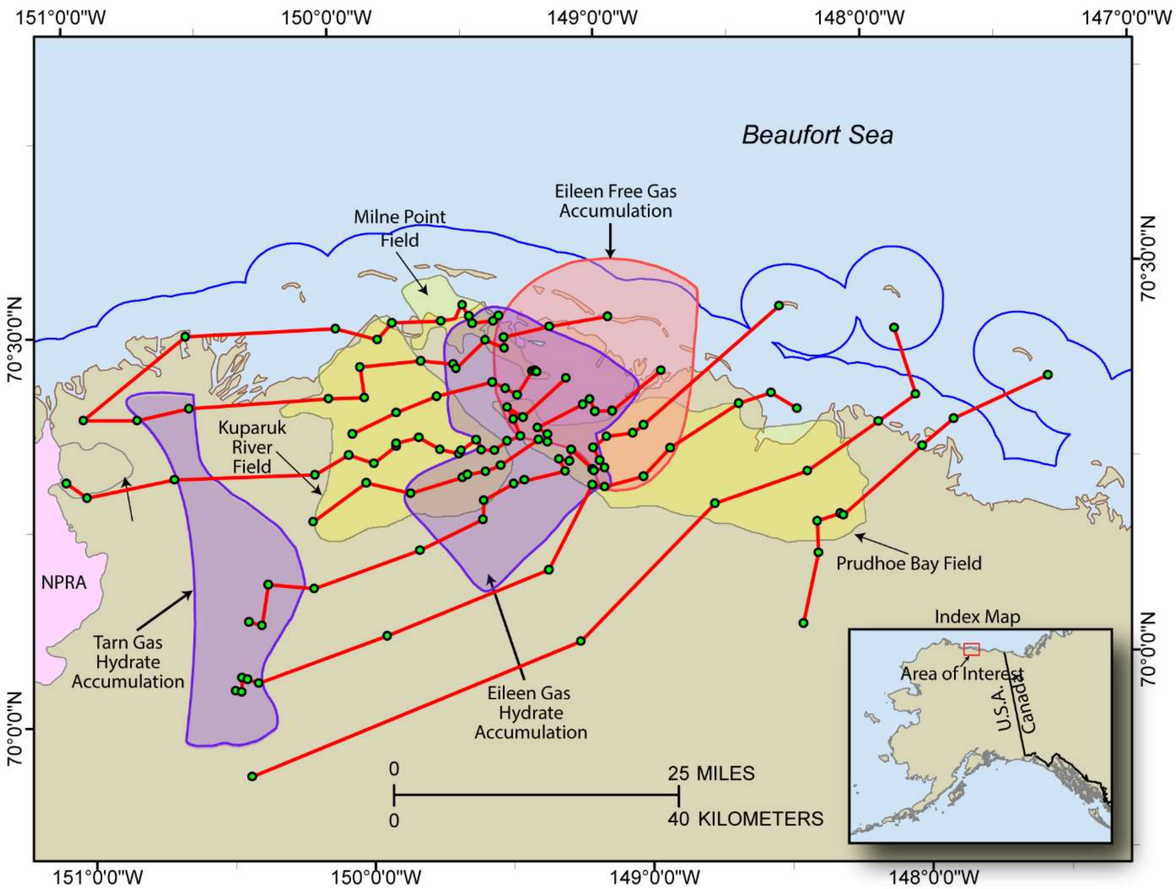

Figure 14. Map showing locations of well log correlation sections within the greater Prudhoe Bay area as compiled by Lewis and Collett (2013).

Another important USGS-acquired database that was used in this gas hydrate test site review effort included gas geochemistry data from 35 Alaska North Slope industry "wells of opportunity" (Table 2, Fig. 16; Lorenson et al., 2011; Lorenson and Collett, 2011). The "wells of opportunity," as described by Lorenson and Collett (2011), are mostly industry exploratory and development wells from which the USGS obtained drill cuttings and flowed gas samples in order to ascertain the composition and source of the gas within the inferred gas hydrate accumulations. For the wells listed in Table 2 and highlighted on the map in Figure 16 as wells with either significant or limited evidence of thermogenic gas in the gas hydrate stability zone, the area around these wells is more likely to contain a higher number of gas hydrate accumulations. The same is also true for the area around known conventional oil and gas fields. As discussed above, gas hydrate accumulations are commonly closely associated with more deeply buried conventional oil and gas fields that have leaked or possibly spilled gas that has migrated into the overlying gas hydrate stability zone, thus leading to a greater likelihood for the occurrence of gas hydrate.

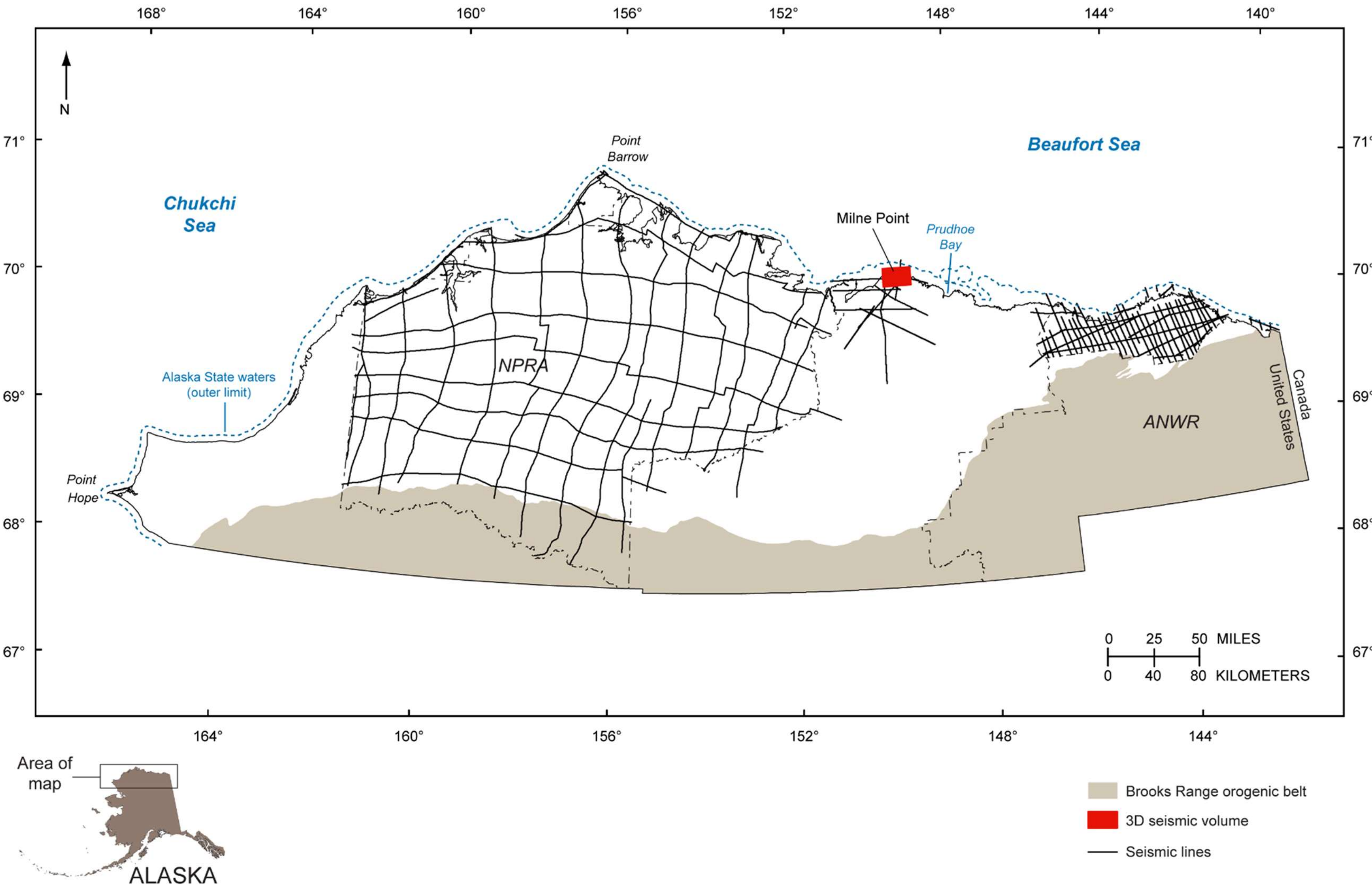

Figure 15. Map of 2D and 3D seismic profiles, the interpretation of which were used as the base data for this analysis of gas hydrate accumulations on the Alaska North Slope. Most of the 2D seismic lines depicted in or near NPRA are from Miller et al. (2000, 2001) and the 2D seismic lines shown in ANWR are from Bird and Magoon (1987). Also shown is the outline of the Milne Point unit 3D seismic volume used to identify and map gas hydrate prospects. NPRA = National Petroleum Reserve in Alaska, ANWR = Arctic National Wildlife refuge

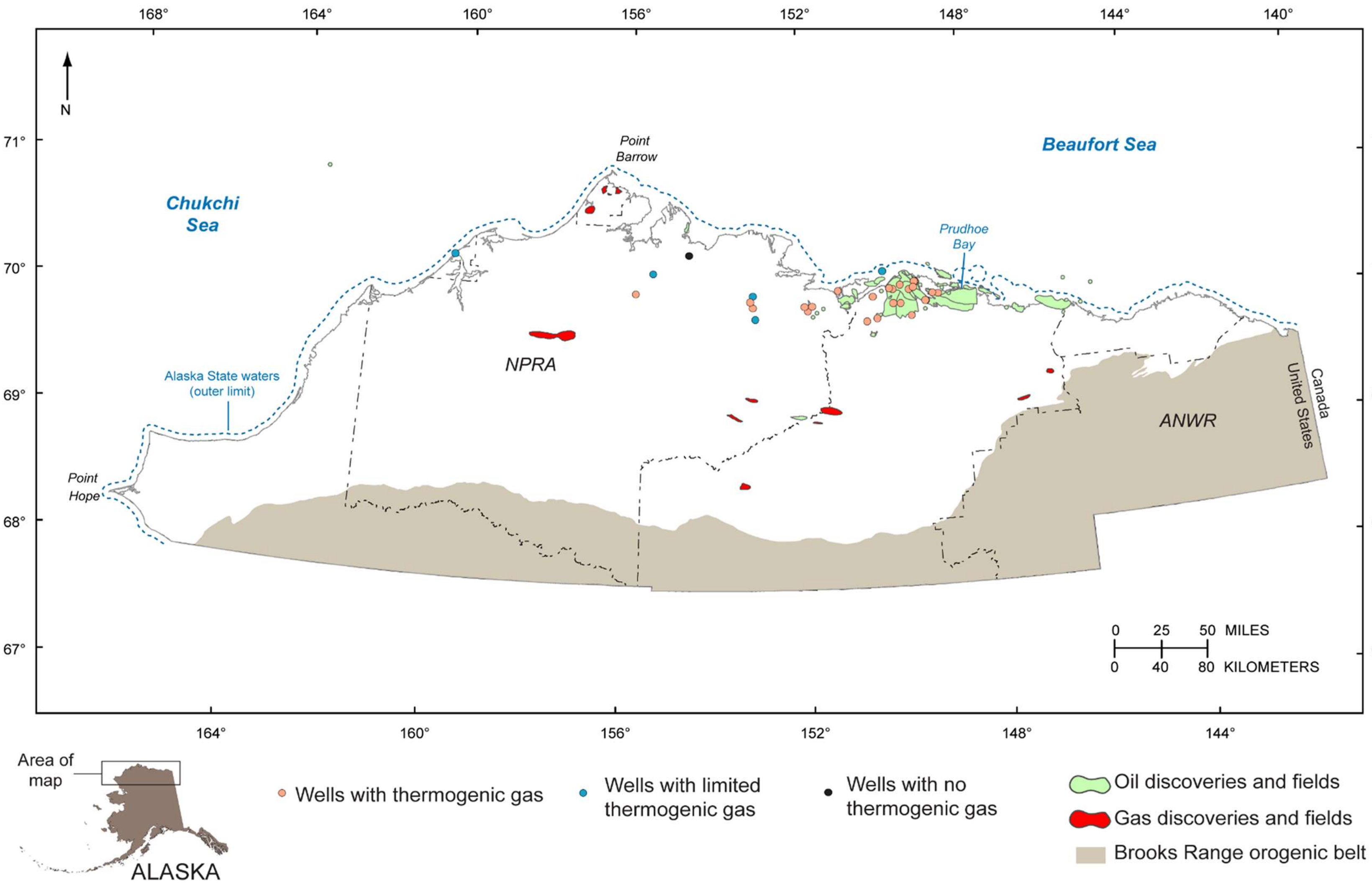

Figure 16. Map showing locations of the wells of opportunity (Table 2) from which the analyses of gas samples have been used to ascertain the composition and source of the gas within each of the gas hydrate assessment units in northern Alaska. Also shown are the locations of discovered conventional oil and gas fields. NPRA = National Petroleum Reserve in Alaska, ANWR = Alaska National Wildlife Refuge

Well API number	Operator at completion	Well name	Surface N latitude	Surface W longitude
Wells with significant evidence of thermogenic gas				
50029233020000	BP EXPL ALASKA INC	MT. ELBERT 1	70.4556	149.4132
50029232950000	CONOCOPHILLIPS AK	KUPARUK RIVER UNIT WEST SAK 1R-EAST	70.3954	149.5591
50029232960000	CONOCOPHILLIPS AK	KUPARUK RIVER UNIT WEST SAK 1H-SOUTH	70.3949	149.5579
50029210840000	ARCO ALASKA INC	KUPARUK RIVER UNIT 2B-10	70.2894	149.9375
50029211840000	ARCO ALASKA INC	KUPARUK RIVER UNIT 2D-15	70.2840	149.7617
50029206990000	ARCO OIL & GAS CORP	WEST SAK 23	70.4037	149.9383
50103200860000	ARCO ALASKA INC	KUPARUK RIVER UNIT 3H-9	70.4118	150.0117
50029216560000	ARCO ALASKA INC	KUPARUK RIVER UNIT 3K-9	70.4332	149.7608
50029219970000	CONOCO INCORPORATED	MILNE POINT UNIT E-4	70.4554	149.4367
50029203530000	SOHIO PETROLEUM CO	PRUDHOE BAY UNIT R-1	70.3455	148.9108
50029220470000	BP EXPL ALASKA INC	PRUDHOE BAY UNIT S-26	70.3536	149.0302
50029220460000	BP EXPL ALASKA INC	PRUDHOE BAY UNIT Z-7	70.2977	149.1955
50029217870000	BP EXPL ALASKA INC	PRUDHOE BAY UNIT Z-8	70.2978	149.1996
50103203490000	PHILLIPS ALASKA INC	KUPARUK RIVER UNIT TARN 2N-305	70.1713	150.3143
50103203600000	PHILLIPS ALASKA INC	ATLAS 1	70.1518	150.5505
50029230610000	BP EXPL ALASKA INC	MILNE PT UNIT SCHRADER BLUFF S-15	70.4097	149.4663
50103204770000	CONOCOPHILLIPS AK	CARBON 1	70.2479	151.8888
50103204800000	CONOCOPHILLIPS AK	SPARK 4	70.2884	151.7924
50103204790000	CONOCOPHILLIPS AK	SCOUT 1	70.2867	151.9571
50103205060000	CONOCOPHILLIPS AK	IAPETUS 2	70.4079	151.1831
50279200170000	FEX LP	AMAGUQ 2	70.3932	155.8066
50029232990000	CONOCOPHILLIPS AK	ANTIGUA 1	70.1809	149.5267
50279200110000	CONOCOPHILLIPS AK	KOKODA 1	70.2850	153.1375
50279200120000	CONOCOPHILLIPS AK	KOKODA 5	70.3344	153.2046
50103204810000	CONOCOPHILLIPS AK	PLACER 1	70.3467	150.3983
Wells with limited evidence of thermogenic gas				
50279200180000	FEX LP	AKLAQYAAQ 1	70.5573	155.4204
50279200130000	CONOCOPHILLIPS AK	NOATAK 1	70.3802	153.1335
50301200030000	U S DEPT OF INTER AK	WAINWRIGHT 1	70.6441	160.0237
50103201900000	EXXON CO USA	THETIS ISLAND 1	70.5539	150.1522
50279200090000	TOTAL E&P USA INC	CARIBOU 26-11 1	70.1898	153.0876
Wells with no evidence of thermogenic gas				
50279200190000	FEX LP	AKLAQ 6	70.7123	154.6077

Table 2. List of wells of opportunity (see Fig. 16) in which analyses of gas samples have been used to ascertain the composition and source of the gas within each of the gas hydrate assessment units in northern Alaska. Wells highlighted in blue are characterized by significant evidence for thermogenic gas in the mapped limits of the gas hydrate stability zone, whereas wells highlighted in green are assessed to have limited evidence of thermogenic gas in the gas hydrate stability zone (Collett et al., 2012). API = American Petroleum Institute

This part of the IA Final Report includes a review of ANS-gas-hydrate occurrences in the greater Prudhoe Bay area, with particular focus on the evaluation of their suitability for extended-duration gas-hydrate testing. This review summarizes the criteria used in the test-site-evaluation process and discusses the nature of the most favorable sites for testing. For these sites, the report includes detailed evaluation of well-log data and numerical simulation studies relevant to designing and conducting a gas hydrate production test. It is important to highlight that there were actually two different gas hydrate site review and selection efforts: (1) The first site review effort in 2011 led to selection of the PBU L Production Pad (PBU-L Pad) near where the Iġnik Sikumi well was eventually drilled and tested in 2011/2012; (2) The second test site review effort completed in 2017 led to the selection of the PBU 7-11-12 Pad in the PBU where the Hydrate-01 Stratigraphic Test was drilled in 2018.

Because the second 2017 test site review was partially based on the results of the first 2011 test site review and the related technical results associated with the drilling and testing of the Iġnik Sikumi well, this part of the IA Final Report includes reviews of both the 2011 and 2017 gas hydrate production test site selection efforts along with the analysis of the Iġnik Sikumi test well results.

3.A. Site Selection in Support of the Iġnik Sikumi Test Well

Within this project, USGS and DOE technical staff worked closely with State of Alaska Department of Natural Resources (SOA-DNR) staff and industry interest groups to develop a set of potential test site options. At the start of this project, two relatively mature DOE-led gas hydrate production research projects were being conducted in partnership with BPXA (Hunter et al., 2011) and ConocoPhillips (Farrell et al., 2010). The BPXA-DOE program had been underway since 2002 and produced many key contributions to the evaluation of ANS gas hydrates (as reviewed above in this report), including the successful drilling of the Mount Elbert stratigraphic test well in the MPU in 2007 (Hunter et al., 2011). Under the DOE-USGS IA, as described herein, the USGS first took the lead to work with the members of the BPXA and ConocoPhillips project teams to develop recommendations as to the most appropriate location of a proposed test site that could be the focus of a joint test and would address the interest of both industry partners. Given the primary criteria of access to infrastructure and reduced geologic risk by drilling offset wells with confirmed gas-hydrate occurrences, seven potential surface locations within the PBU, KRU, and MPU were considered. These sites were grouped into four locations for detailed evaluation (Tables 3 and 4; Fig. 17).

The criteria against which these sites were further evaluated are shown in Table 4. These criteria dealt primarily with two factors: (1) mitigating geologic risks that included reservoir quality, reservoir temperature, nature of bounding units, nature of production-modeling forecasts, and presence of multiple potential testable zones; and (2) mitigating operational/logistical risks including the ease of physical access to the test location, drilling/completion complexity, capability/capacity of local facilities, local need/use for gas produced during the test, disposal of water produced during the test, impact on ongoing industry operations, and overall program complexity.

3.A.1. Evaluation of Locations in the Milne Point Unit (MPU)

The 2007 BP-DOE-USGS Mount Elbert stratigraphic test well fully mitigated any geologic risk at the Mount Elbert test site prospect, and no other significant inferred gas-hydrate accumulation in the MPU has yet been confirmed by well data (as reviewed above in this report); consequently, any production test conducted in the MPU would likely test the Mount Elbert deposit. The occurrence of gas hydrate at the Mount Elbert site features two reservoirs (Units C and D) characterized by shallow marine sands with low clay content, high porosities, fine-grained sand, and high gas-hydrate saturations (Figs. 11, 12, and 17). However, log data indicate that the lower unit (Unit C) is likely in contact with free water, which could significantly complicate an extended well test. Most importantly, the position of this reservoir just below permafrost would pose additional operational difficulties related to the low formation temperature (between 36 and 37°F; 2 and 3°C;). Furthermore, drilling into the accumulation from one of the existing gravel pads (MPU B-Pad or E-Pad) would require a high-angle or horizontal well path that would cross at least one major fault, adding additional complexity to the well drilling and completion and logging operations, as well as to the analysis of the test data. Logistically, the MPU sites provide ample infrastructure support.

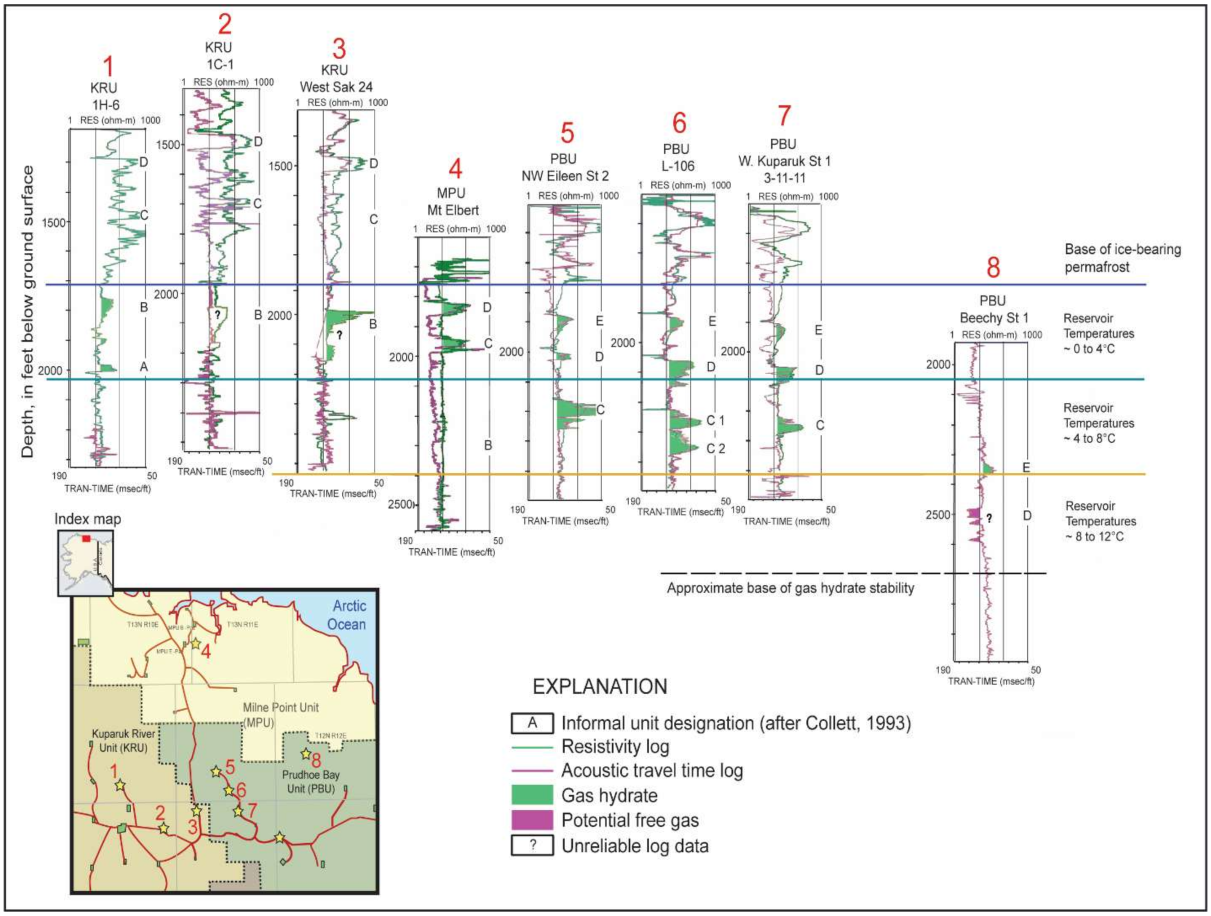

Figure 17. Montage of drill log data from Prudhoe Bay Unit (PBU), Kuparuk River Unit (KRU), and Milne Point Unit (MPU) area. The data are shown relative to interpreted base of ice-bearing permafrost. The indicated zones of reservoir temperatures are approximate only. Note that the PBU logs (Wells 5, 6, and 7) show inferred gas hydrate in multiple zones and are the deepest (warmest) identified locations of gas hydrate in areas with established surface facilities. The next data point downdip from these wells (Well 8) has relatively poor log data and anomalous responses that may reflect drilling effects.

3.A.2. Evaluation of Locations in the Prudhoe Bay Unit (PBU)

Two locations (PBU L-Pad and the site of the Kuparuk State 3-11-11 well) in the PBU area were evaluated. At both locations, a series of stacked gas-hydrate-filled sands have been identified in existing well data (Figs. 17 and 18). The sands (Units C, D, and E) are expected to be very similar petrophysically to the units cored and logged in both the Mount Elbert and Eileen State 2 wells. Furthermore, a well location closely offset to the PBU L-106 well will likely also encounter a fourth gas-hydrate saturated sand (Unit C2) at the base of the reservoir section. The gas-hydrate-bearing sands at the PBU L-Pad site total approximately 218 ft (66 m) in thickness. The primary test target, the Unit C sand, is approximately 30 ft (~10 m) thick, and is approximately 7°F (~4°C) warmer than the

Target	Depth (ft)	Lower contact	Thickness	Gas hydrate saturation (%)	Porosity (%)	Intrinsic permeability (mD)	Temperature (°C; °F)	Pressure gradient	Salinity (ppt)
Milne Point Unit – Mount Elbert Prospect									
Unit C	2132	Water	52 ft (16 m)	65	35	1000	3.6; 38.5	Hydrostatic	5
Unit D	2014	Shale?	47 ft (14 m)	65	40	1000	2.4; 36.3	Hydrostatic	5
Prudhoe Bay Unit – L-Pad vicinity									
Unit C2	2318	Shale	62 ft (19 m)	75	40	1000	5.7; 42.3	Hydrostatic	5
Unit C1	2226	Shale	56 ft (17 m)	75	40	1000	5.7; 42.3	Hydrostatic	5
Unit D	2060	Shale	50 ft (15 m)	70	-	1000	3.5; 38.3	Hydrostatic	5
Unit E	1915	Shale	50 ft (15 m)	60	-	1000	2.5; 36.5	Hydrostatic	5
Prudhoe Bay Unit Down-Dip from L-Pad									
Unit C*	2500	Shale	60 ft (18 m)	75	40	1000	~12; ~37	Hydrostatic	5
Kuparuk River Unit – West Sak 24 vicinity									
Unit B	2260	Shale?	40 ft (12 m)	65	40	1000	2.5; 36.5	Hydrostatic	5

*Conditions assumed for the Prudhoe Bay Unit Down-Dip "L-pad" site

Table 3. Summary of reservoir parameters for potential gas hydrate production test sites and targets in the Prudhoe Bay Unit (PBU), Kuparuk River Unit (KRU), and Milne Point Unit (MPU) area (Collett et al., 2012).

Parameter	MPU E Pad	MPU B Pad	PBU L Pad	PBU Kup St. 3-11-11	PBU Down-dip L-Pad	KRU West Sak 24	KPU 1H
Reservoir Temperature	H	H	M	M	L	H	H
Ownership	L	L	H	H	H	M-L	M-L
Site Access	M	M	L	L	H	L	L
Geologic Risk	L	L	L	L	H	M	M
Data Availability	L	L	L	M	H	M	M
Well Risk	L-M	L-M	M	M	H	M	M
Facilities Access	L	L	L	M	H	M	L
Gas Disposal	H	H	H	H	H	H	H
Interference w/Ops	L	?	H?	L	L	L	H?
Water Disposal	L	L	L	M	H	M	L
Use for Gas	L?	L?	M	M	M	L	L?
Test Options	M-H	M-H	L	L	M-H	H	H

Table 4. Information considered in the assessment of locations for a long-term production test. H = high risk associated with this parameter (unfavorable), M = medium risk, L = low risk (favorable), ? = Denotes uncertain conditions (Collett et al., 2012).

most promising target in the MPU. Units D and E also provide excellent uphole targets to accommodate operational contingencies or to provide testing options across a range of initial temperature conditions. Geologic risk for the Unit C, D, and E sands is low given the nearby well control. The second evaluated PBU location would closely offset the Kuparuk State 3-11-11 well. The geology seen in this well mimics that of the PBU L-106 well (Figs. 17 and 18), with the exception that the C2 sand does contain gas hydrate. Also, the Kuparuk State 3-11-11 well is not on an operational gravel pad and, therefore, would require significant investment in infrastructure development and greater operational logistical support for the testing program. In comparison to the L-Pad location, however, it would have reduced complexities related to potential interference with ongoing or planned near-term operations.

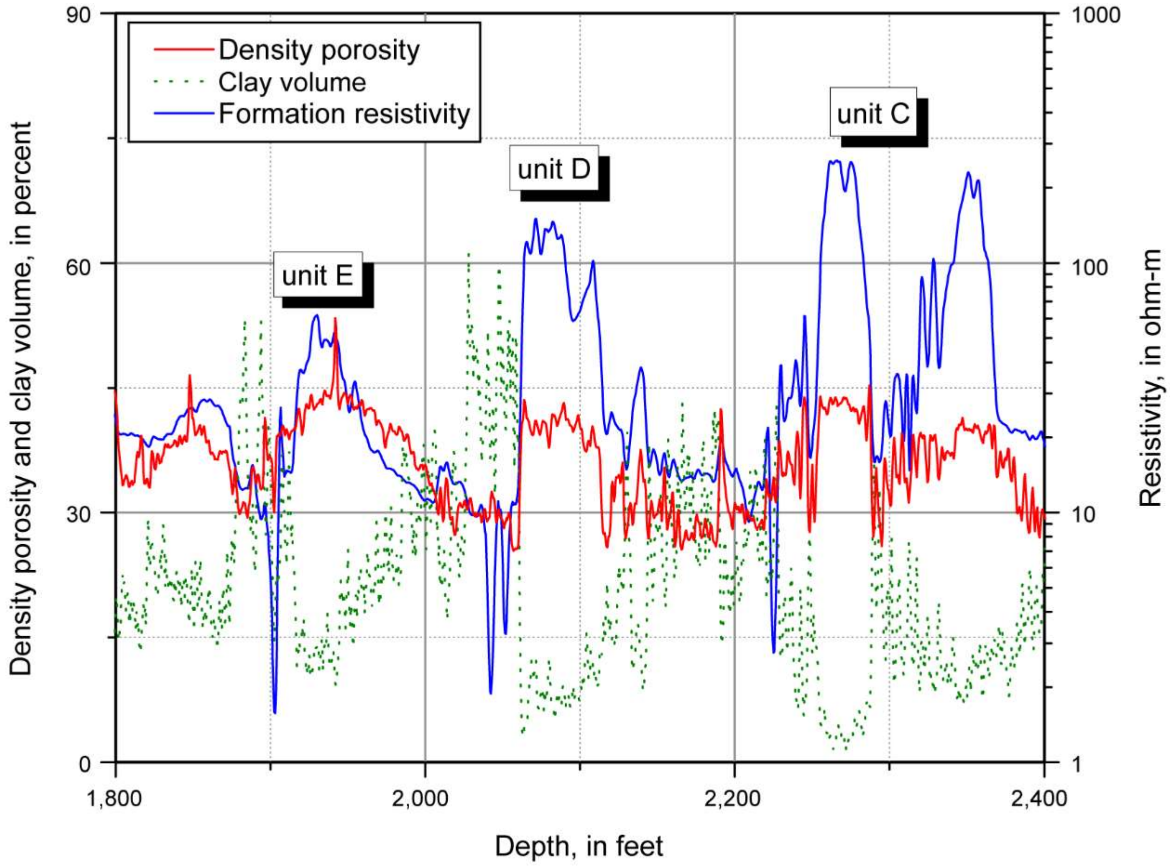

Figure 18. Gamma-ray, electrical resistivity, density porosity and sediment shale volume logs from the Prudhoe Bay Unit L-106 well, Alaska North Slope. Also shown is the approximate depth of Units C, D, and E (Collett, 1993).

3.A.3. Evaluation of Locations in the Kuparuk River Unit (KRU)

Gas hydrate reservoir targets are present along the eastern margin of the KRU and could be accessed from several existing well pads. However, well data from KRU are generally of lower quality than those at PBU, making geologic interpretations less certain. In addition, the reservoir sands occur structurally updip (to the west) of the potential PBU sites, placing the Unit C and D gas-hydrate reservoirs well within the permafrost section. However, Unit B, which is a very high quality reservoir throughout MPU and PBU but is often fully water saturated in those units, appears to be gas hydrate saturated from the available KRU log data. Overall, the temperature and reservoir quality of the KRU targets in the Unit B are expected to be very similar to those in MPU but with somewhat higher geologic risk. Operational risk in KRU is also elevated because of the occurrence of only a single reservoir target, providing limited testing flexibility.

3.A.4. Evaluation of Downdip Locations in the Prudhoe Bay Unit (PBU)

Given the prevailing easterly structural dip and the regional extent of the targeted sand units, there should be opportunities to track the gas-hydrate-bearing Unit C, D, and E sands downdip to the east of the PBU L-Pad site. Previous USGS mapping indicates that these units will cross below the base of gas-hydrate stability approximately 10 km to the east of the PBU L-Pad. Unfortunately, this area lacks existing surface facilities, rendering long-term testing unfeasible. Nonetheless, all options for establishing a test site were carefully reviewed because one could provide access to gas-hydrate-bearing reservoirs at temperatures as high as 54°F (12°C). However, there is a lack of well penetrations with suitable well-log data in this region as well. The only control point in the area is the Beechy State 1 well (Figs. 8 and 13), which encountered apparent free gas in the Unit D sand. Therefore, it is not possible to confirm with any confidence the continuity of the reservoirs between the Beechy State location and the western PBU wells. As a result, any location selected would have very high geologic risk. Significant additional seismic-interpretation and well-correlation work would be required to determine if gas hydrate exists at any potential site in this area.

3.A.5. Gas Hydrate Production Modeling in Support Test Site Selection

At the start of this test site review project, significant advancements in gas-hydrate production computer simulators had allowed for the first time the systematic analysis of the possible geologic and engineering controls on the production gas hydrates. Several previous studies (Moridis et al., 2009, 2010, 2011a, 2011b) that focused on simulating production from hydrates in northern Alaska had shown some promise.

To better understand the potential reservoir response for the locations considered in this study, the DOE and USGS collaborated with the participants of the International Code Comparison Group (Anderson et al., 2011a, 2011b) to conduct numerical gas-hydrate production simulations for the idealized MPU, KRU, PBU, and downdip-PBU settings (Figs. 17 and 19). These analyses relied heavily on the reservoir data acquired from the Mount Elbert test well in order to compare production between different geologic settings and between the various participating modeling approaches. To make these comparisons easier, the geologic representations entered into the models were simplified and homogenized. As a consequence, the most meaningful data from this effort are not the absolute predicted production values but instead are the comparative productivity between sites, the determination of those parameters to which productivity was most sensitive and the relative performance of the various models (Anderson et al., 2011b). Given the similarity between the KRU and MPU settings, only three sets of modeling runs were undertaken (Fig. 19). Although these cases differed somewhat in reservoir thickness and pressure, sensitivity runs clearly demonstrated that initial reservoir temperature is the primary control on the modeled production rates, with reservoir petrophysics, including intrinsic reservoir permeability, in situ permeability, and mobile-water saturation also being important (Anderson et al., 2011b). The initial MPU/KRU modeling results showed consistent predictions between the various participating codes, with very modest production rates and long lead times (time before first gas production). Analysis of the PBU case (production from the

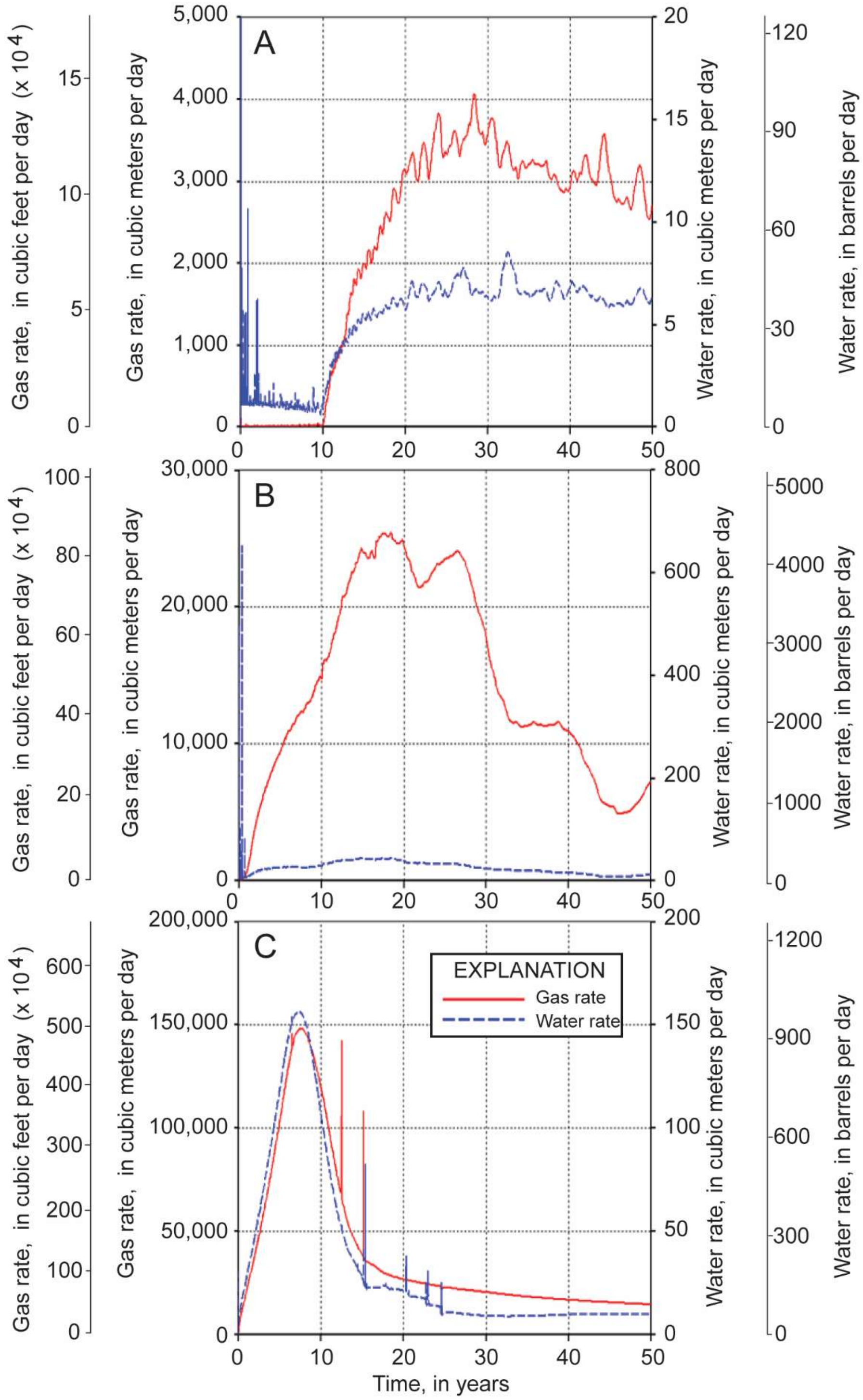

Figure 19. Comparison of typical production simulation results for Alaska North Slope gas hydrate reservoirs. (A) A setting typical for known Kuparuk River Unit (KRU), and Milne Point Unit (MPU) reservoirs (37–39°F; 3–4°C); (B) Westend Prudhoe Bay Unit (PBU) setting (41–43°F; 5–6 °C); (C) Downdip PBU setting (50–54°F; 10–12°C) (Anderson et al., 2011b).

composite Unit C sands) resulted in production rates about five times those of MPU and with zero production lead time. The downdip-PBU case revealed the clear benefits of higher temperatures, with rates increasing another five-fold (Anderson et al., 2011b). Subsequent incorporation of more detailed geologic input data sets for these locations, incorporating the detailed vertical reservoir heterogeneity, resulted in increased production and elimination of the production lead time (Anderson et al., 2011b). Additional production modeling of the gas-hydrate deposit at the PBU L-Pad site, as reported by Moridis et al. (2010), has contributed to our understanding of the production potential of this site and has been considered in the modeling work published in Anderson et al. (2011b).

3.A.6. Prudhoe Bay Unit L-Pad Test Site

From the review of the seven potential surface locations (Table 3 and Fig. 17) for a proposed gas-hydrate production test, the PBU site, particularly the L-Pad location, was determined to be the optimal site for any gas-hydrate production test on the ANS. The site offered the best combination of low geologic risk, maximum operational flexibility (multiple zones), low operational risk (ability to drill vertical wells adjacent to infrastructure), and, from the production modeling efforts, a high likelihood of near-term and meaningful reservoir responses. The primary concerns associated with this location were the logistical issues associated with gaining approval of three major resource industry partners as well as the ability to conduct the testing program in a manner that will not interfere with ongoing or planned future operations from the PBU L-Pad. Although MPU remained a possibility, the MPU sites were determined to be less favorable because of a much more complex operational environment (colder reservoirs, requirement for deviated wells, and limitation to a single potential target reservoir). The KRU locations were assessed as offering no geological advantages over the MPU location but with greater geologic risk because of generally poor well data. The PBU downdip location, though offering the potential for encountering the warmest reservoirs in the region (and, therefore, potentially the most successful test in terms of rates), was clearly impractical because of the lack of existing facilities to support a test and high geologic risk related to lack of well data.

The following subsection of this report deals with the detailed geologic and engineering analysis of the PBU L-Pad site that was ultimately selected for the ConocoPhillips/DOE Iġnik Sikumi CO2/CH4 exchange field trial (Silpngarmlert, 2010; Schoderbek et al., 2013; Boswell et al., 2017). The examination of the PBU L-Pad included the analysis of the downhole log data from the PBU L-106 well (Fig. 18) to develop a more complete understanding of the reservoir properties controlling the occurrence of gas hydrates at this site. Log data from another 54 PBU L-Pad wells were also examined to assess the potential structural complexity and reservoir-quality/-continuity issues throughout the L-Pad area. Finally, numerical modeling results relevant to determining the optimal final test site with respect to existing L-Pad wellbores were reviewed, including considerations of potential maximum areas of thermal disturbance from existing wells as well as the area of virgin reservoir conditions available to conduct the planned test without affecting the stability of existing wellbores.

High-quality well logs acquired in the PBU L-106 well (Fig. 18), as obtained from the public files of the Alaska Oil and Gas Conservation Commission (http://doa.alaska.gov/ogc/), were used to characterize the physical properties controlling the occurrence of gas hydrates in the vicinity of the PBU L-Pad. To analyze the acquired electrical resistivity log data, the Archie equation (Archie 1942; Pearson et al., 1983) with a shaly-sand correction described by Lee and Collett (2006) was used. To analyze the downhole acoustic log data, a rock-physics model proposed by Lee (2007, 2008) was used.

Gas hydrate saturations estimated from the resistivity log data in the L-106 well with a shaly-sand correction (Simandoux, 1963; Worthington, 1985; Western Atlas International Inc., 1995) (Figs. 20 and 21) are almost identical to those estimated without a shale correction. The relation between gas-hydrate saturations and acoustic velocities in this study were modeled using the three-phase Biot-type equation (TPE) (Lee, 2005, 2007) by assuming that gas hydrate acts as a load-bearing component of the sediments. Saturations estimated from the P-wave velocities (Fig. 20) are comparable to those from the resistivity, whereas saturations estimated from S-wave velocities (Fig. 21) are less than those from the resistivity log measurements. It was speculated that the differences in saturation calculations are primarily because of errors in the measured velocity log data, with the S-wave velocity measurements being most affected, because the saturations estimated from the P-wave velocities are close to those estimated from the resistivity log data.

The site selection review effort in support of the analysis of the PBU L-Pad location included the consideration of (1) avoiding the penetration of gas hydrate-bearing reservoir sections that may have been compromised (partial-to-full gas hydrate dissociation) by heat effects related to long-term production and injection of warm fluids in the L-Pad wells and (2) the gas hydrate test itself adversely affecting the mechanical stability of existing wells by gas hydrate dissociation related to the planned test. To pursue these issues, thermal- and production-modeling studies were conducted. The production modeling efforts were designed to determine the potential area of reservoir depressurization that would be associated with different test volumes so that the test can be halted before existing wells might be affected. The modeling efforts were based on earlier modeling scenarios performed by the International Methane Hydrate Reservoir Modeling Code Comparison Group (Anderson et al., 2011a, 2011b). The earlier reservoir descriptions, however, were homogeneous descriptions of the L-Pad area and neglected the reservoir complexities as shown in Figures 22, 23, and 24. As shown by Anderson et al. (2011b), significant differences between assumed homogeneous and heterogeneous reservoir conditions can yield very different model results. Therefore, to better constrain the possible extent of disturbance caused by long-term depressurization of a gas-hydrate reservoir and to more accurately model the possible gas- and water-production rates, a heterogeneous reservoir model was constructed.

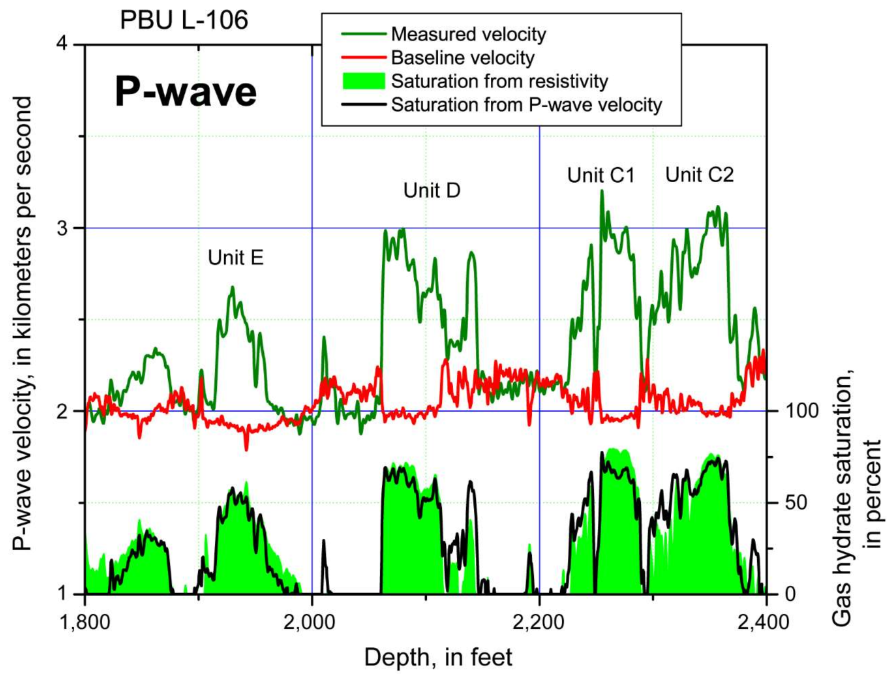

Figure 20. Measured and calculated baseline compressional-wave (P-wave) velocities along with gas hydrate saturations estimated from the P-wave velocity and resistivity logs in the Prudhoe Bay Unit L-106 well, Alaska North Slope (Collett et al., 2012).

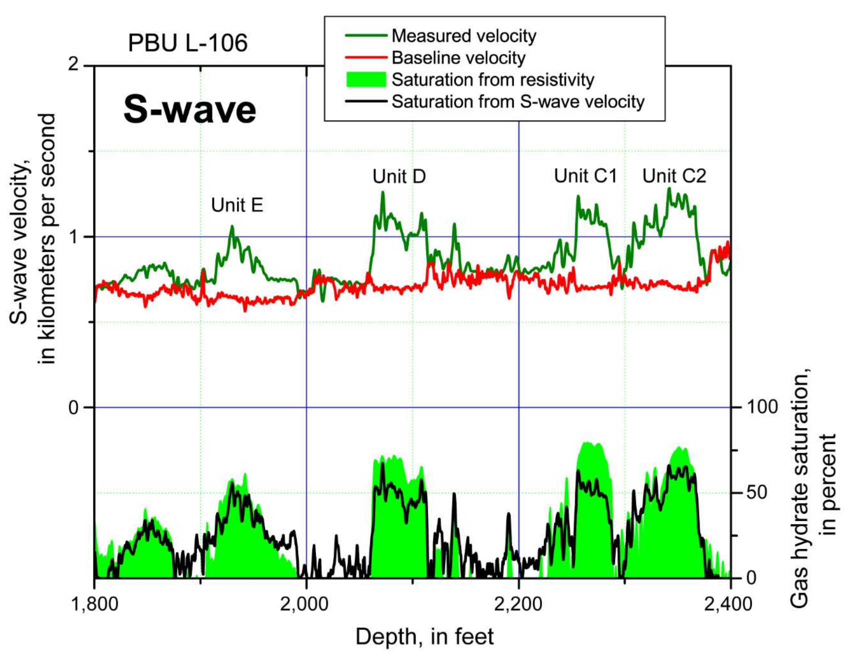

Figure 21. Measured and calculated baseline shear-wave (S-wave) velocities along with gas hydrate saturations estimated from the S-wave velocity and resistivity logs in the Prudhoe Bay Unit L-106 well, Alaska North Slope (Collett et al., 2012).

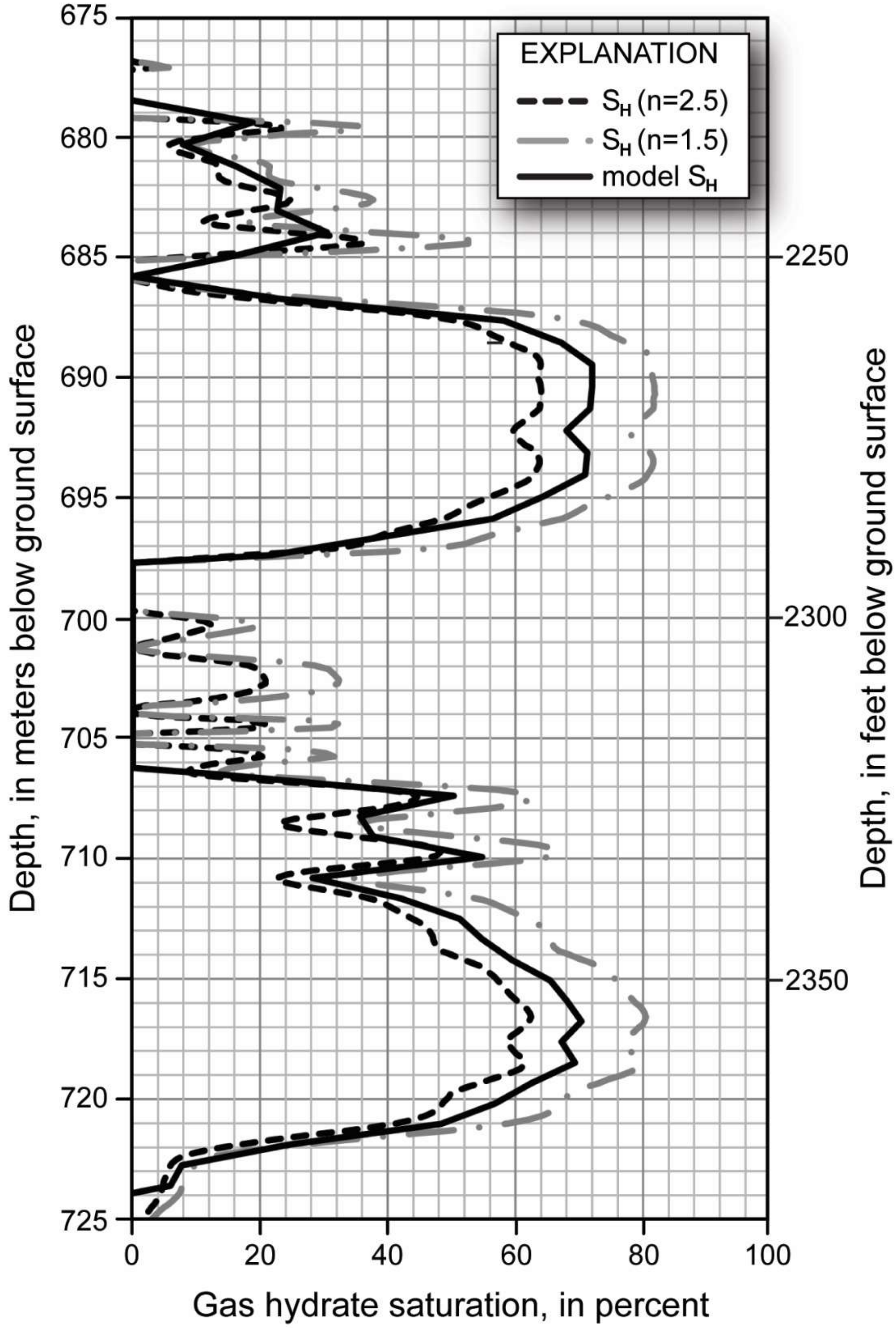

Figure 22. Hydrate saturation in the PBU L-106 well as calculated by Archie (1942) relationship for *n* = 1.5 and 2.5, and the assumed model S_H. The gas hydrate saturation in the reservoir model for the layers between 2289 ft (697.7 m) and 2317 ft (706.2 m) was assumed to be zero (Collett et al., 2012).

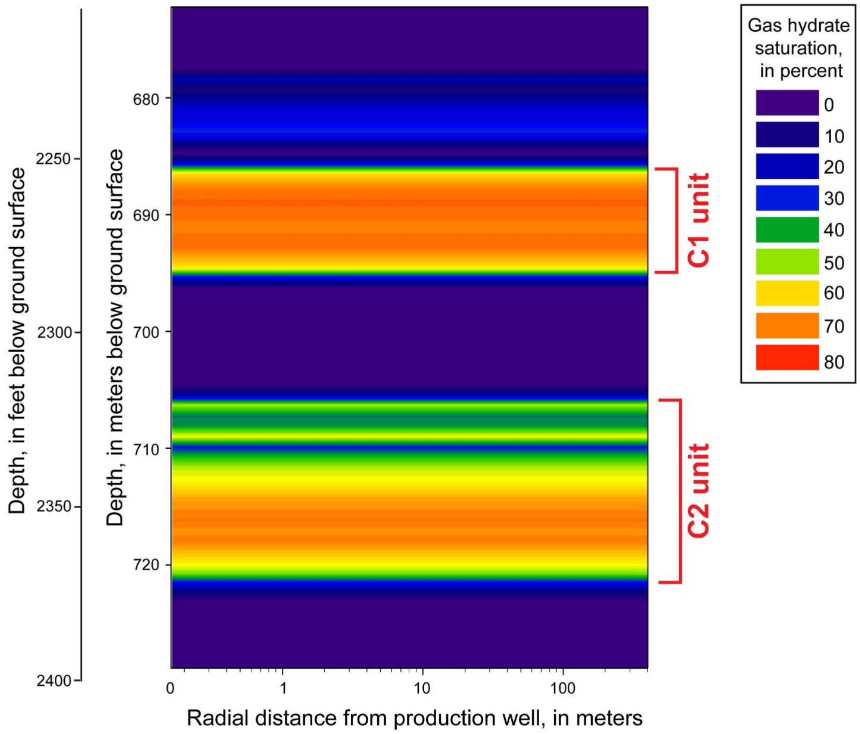

Figure 23. Initial gas hydrate saturations in the gas hydrate-bearing intervals in the PBU L-106 simulation (Collett et al., 2012).

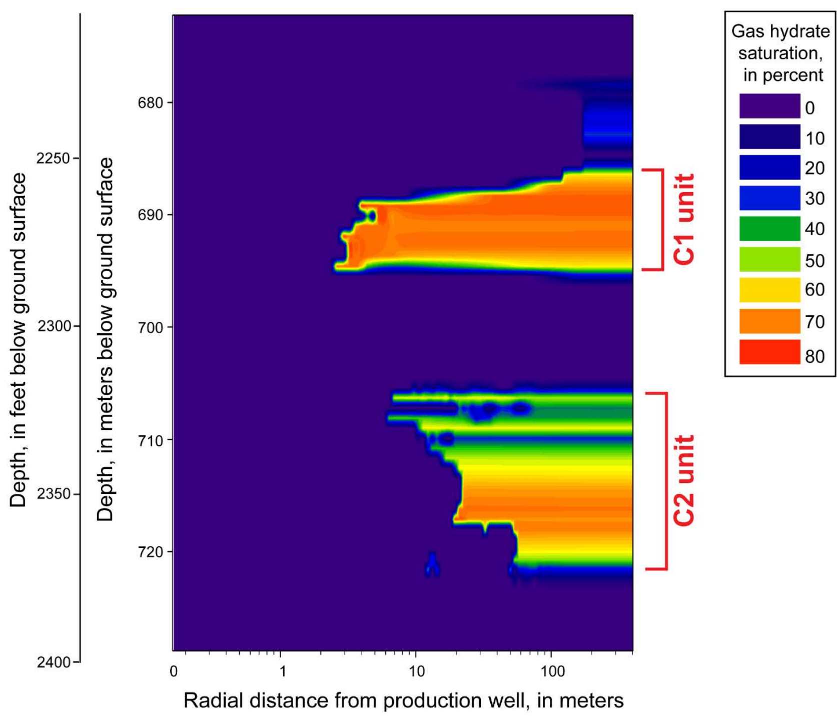

Figure 24. Predicted gas hydrate saturations in the gas hydrate-bearing intervals in the PBU L-106 well after 180 days of depressurization at a bottomhole pressure of 2.7 MPa. Maximum hydrate dissociation radius is approximately 100 m (~328 ft) (Collett et al., 2012).

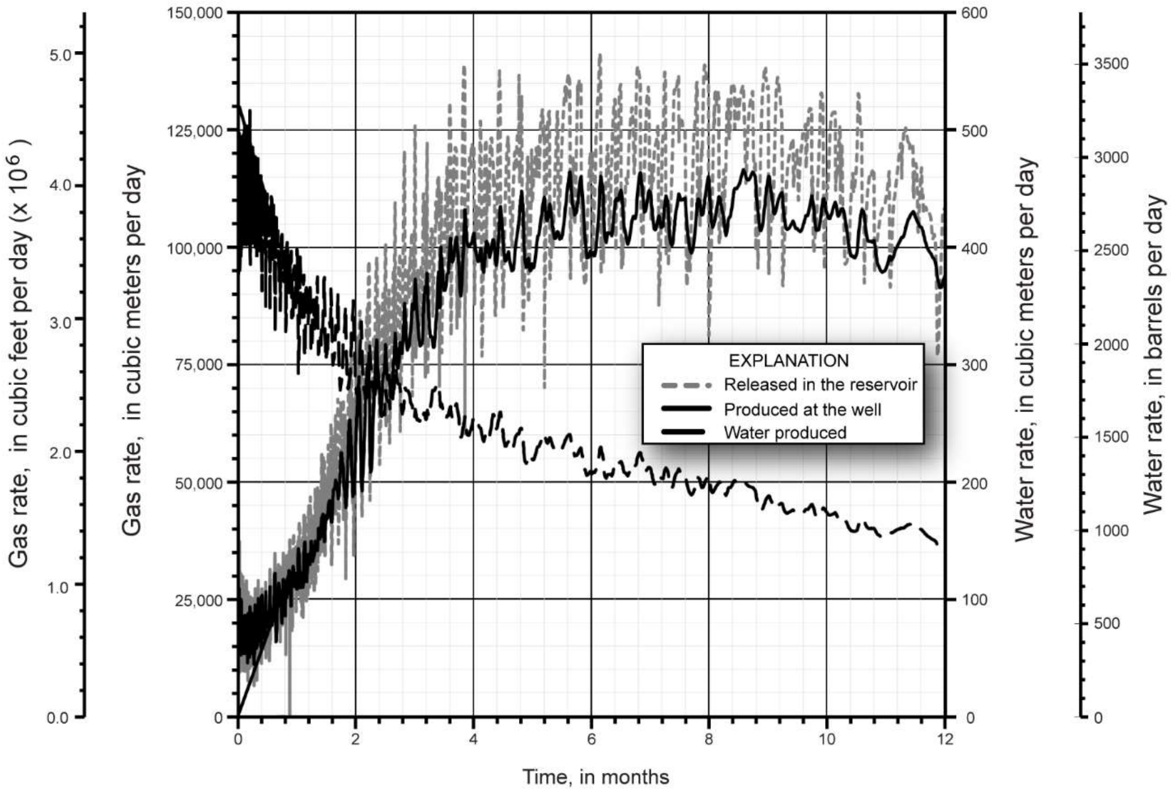

Figure 25. Predicted gas and water production from the PBU L-106 Unit C gas hydrate-bearing reservoir section at a constant bottom-hole pressure of 2.7 MPa. The solid black and dotted gray curves represent the rate of gas produced at the wellhead and gas released in the reservoir respectively and correspond to the left y-axis. The rate of water production is found on the right y-axis and is indicated by the dashed black line (Collett et al., 2012).

The initial hydrate saturation for the gas hydrate-bearing layers modeled for Unit C in this effort range from 0 to 72 % (Figs. 22 and 23). Figure 24 shows the predicted extent of hydrate dissociation from 180 days of depressurization (assumed constant bottomhole pressure of 2.7 MPa). Note that the x-axis is logarithmic and that the maximum perturbation is predicted to occur at the top (C1 unit) of the Unit C hydrate-bearing sand. This disturbance is on the order of 330 ft (approximately 100 m) radially from the wellbore, which is located along the left side of the image in Figure 24. Figure 25 shows the predicted gas and water production rates from the heterogeneous reservoir simulations of the PBU L-Pad Unit C hydrate-bearing sand deposit (C1 and C2 units). As one can see from Figure 25, the water rate is predicted to start at its maximum and decrease throughout production, while the modeled gas rate increases quickly throughout the early stages of production. As shown in Figure 25, the heterogeneous reservoir simulation results in predicted gas rates on the order of 3.5×10^6 ft^3/day (100000 std m^3/day), with produced-water rates ranging from 1000–3000 barrels/day (200–500 m^3/day) throughout the first 6 months of depressurization. After 180 days of production, it is predicted that a cumulative total of 458×10^6 ft^3 (13.0×10^6 std m^3) of gas would be produced. On the basis of the results of the production-modeling studies on a potential depressurization test of 180 days, it can be concluded that a hydrate-depressurization test should not be allowed to reach beyond approximately 330 ft (~100 m) from the center point of the proposed test well.

In conclusion, based mainly on the assessment of the geological conditions and operational risks associated with conducting a successful gas hydrate production test, the PBU L-Pad site was selected as the best candidate test site for the ConocoPhillips/DOE Iġnik Sikumi CO2/CH4 exchange field trial because of the unique combination of relatively warmer reservoirs (providing greater potential for successful testing in terms of measurable gas production rates) and the high likelihood of encountering multiple thick reservoirs suitable for long-term testing (providing for more testing options and flexibility).

3.A.7. Iġnik Sikumi CO2/CH4 Exchange Field Trial

The selected field test site for ConocoPhillips/DOE Iġnik Sikumi CO2/CH4 exchange field trial was initially to be located on the PBU L-Pad. The test well, Iġnik Sikumi, was eventually drilled from a temporary ice pad adjacent to the PBU L-Pad in early 2011 and the injection/production test was performed in early 2012. Production operations began in January 2012 and ended in May 2012, when the well was plugged and abandoned. The 2011 Iġnik Sikumi field program included drilling a single, near-vertical test well and performing extensive wireline logging through a thick section of gas hydrate-bearing sand reservoirs (Figs. 7, 8, and 26). A total of three hydrate-bearing stratigraphic units (Units C, D, and E) were encountered in the Iġnik Sikumi test well. For the purpose of this project, Unit C was further subdivided into a lower Unit C and an upper Unit C, also named C1 and C2, respectively, in other publications (Collett et. al., 2012, Boswell et al., 2017). In comparison to the upper Unit C, lower Unit C is more heterogeneous with a high number of interbedded prominent clay-rich beds (Schoderbek et al., 2013; Boswell et al., 2017). Sand-rich intervals below the hydrate-bearing portion of the upper Unit C and in Unit B are water-bearing at the site of the Iġnik Sikumi test well (Figures 7 and 26). Log analysis of hydrate-bearing reservoirs yielded gas hydrate saturations >75% in the more uniformly bedded upper Unit C. Scheihing (2010) also used available well log data and 3D seismic data to build a "highly generalized structural map" of several of the gas hydrate-bearing stratigraphic units in the area of the Iġnik Sikumi well. The resulting mapping showed that the gross interval thicknesses of the sand-dominated sections are fairly consistent across the area.

In 2012, the Iġnik Sikumi field testing program included a CO_2-CH_4 hydrate production test that consisted of an initial injection phase and a subsequent extended duration depressurization flow-back phase. The test was conducted in the same vertical well (total depth of 2597 ft; 792 m) drilled in 2011 and targeted the gas hydrate-bearing sands in the upper part of Unit C. The first stage of the test consisted of injecting 210000 ft^3 (5947 m^3) of a CO_2-N_2 mixture over a period of 13 days. Flowback of the well commenced following the reconfiguration of the surface equipment. Over four distinct well flow periods, the Iġnik Sikumi well produced nearly 1000 mscf of gas at peak rates as high as 175000 ft^3/day (4955 m^3/day) (Schoderbek et al., 2012, 2013; Boswell et al., 2017).

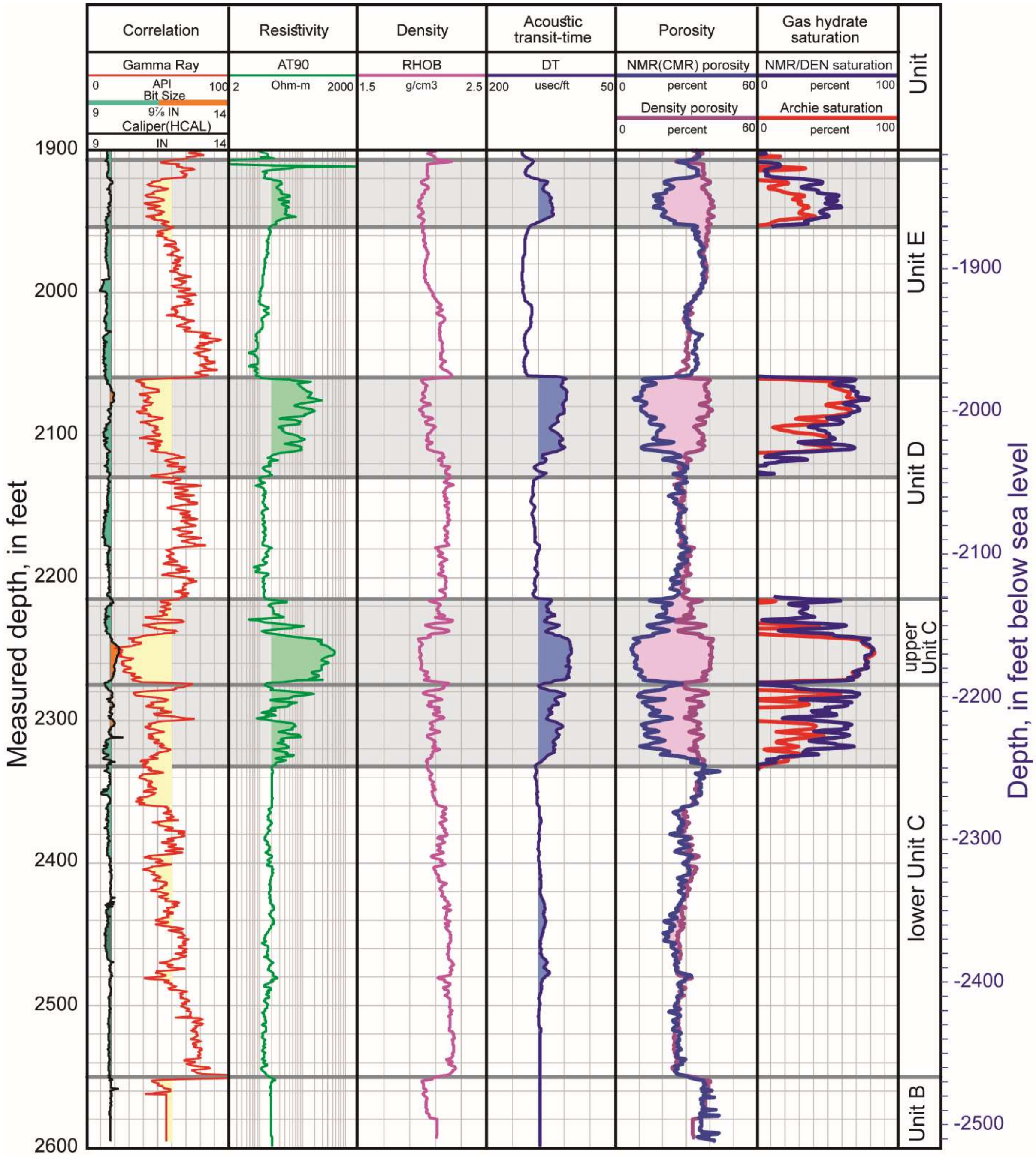

Figure 26. Well log display for the Iġnik Sikumi test well indicating Units B, C, D and E. Grey shading highlights the occurrence of gas hydrate within reservoir quality sands of Units C, D and E. Data shown include the natural gamma ray, caliper (HCAL), electrical resistivity (AT90), bulk density (RHOB), acoustic transit time (DT), neutron porosity, nuclear magnetic resonance porosity (NMR/CMR) logs, as well as calculated density porosity, NMR density-derived gas hydrate saturations, and Archie-calculated gas hydrate saturations.

3.B. Site Selection in Support of the PBU 7-11-12 Test Site

In 2011/2012, the Iġnik Sikumi gas hydrate test further confirmed the nature and occurrence of gas hydrate on the ANS and the short-term response of gas hydrate reservoirs to depressurization (Schoderbek et al., 2013; Boswell et al., 2017). Iġnik Sikumi test results indicated significant challenges to gas hydrate production by chemical injection and confirmed the favorability of reservoir depressurization as the primary production mechanism. In 2013, JOGMEC further demonstrated the potential effectiveness of depressurization technology relative to gas hydrates with a deepwater test in the Nankai Trough offshore Japan (Yamamoto et al., 2014). It remained unknown, however, how gas hydrate reservoirs will respond to depressurization over longer timeframes. There existed at the time only the wireline pressure transient tests from Mount Elbert (2007), the 6-day depressurization test at Mallik in Canada (2008), the 19 days of post-injection depressurization at Iġnik Sikumi (2012), and the 6-day (2013), 12-day (2017), and 24-day (2017) deepwater depressurization tests conducted by JOGMEC in the Nankai Trough (as reviewed by Boswell et al., 2020a). The global gas hydrate science community was in full agreement that tests of longer duration were required to advance the assessment of gas hydrate as a potential energy resource. With the goal of a long-term production test, from 2014 through 2017 the DOE, JOGMEC, and the USGS, along with contract support from PRA, and with the technical support of the SOA-DNR, worked to identify a potential location and develop a plan for an extended gas hydrate production test on the ANS. This effort included a comprehensive review of potential testing sites within the Eileen Gas Hydrate Trend, which had been the focus of the previous site review effort that eventually led to the drilling and testing of Iġnik Sikumi well. The new site review and selection effort again focused on assessing locations with favorable geologic conditions and limited logistical and operational risks for the proposed extended gas hydrate production test.

The results of the Mount Elbert and the Iġnik Sikumi test wells provided the data needed to further develop and calibrate geophysical and well log analysis methods used to characterize gas hydrate accumulations in both Arctic permafrost and marine environments (Lee and Collett, 2011; Schoderbek et al., 2013; Boswell et al., 2017). The production studies associated with the well tests in the Eileen Gas Hydrate Trend supplied important gas hydrate reservoir engineering data and provided insight to gas hydrate production concepts along with data to calibrate gas hydrate production simulators (Anderson et al., 2011b). As reviewed above in this report, the gas hydrate-bearing reservoirs in and around western portion of the PBU have also been the focus of several other detailed geologic and geophysical studies in support of the 2011/2012 Iġnik Sikumi gas hydrate production testing project (Collett et al., 2012; Schoderbek et al., 2012, 2013; Boswell et al., 2017).

The objective of this section of the IA Final Report is to describe the methodology and results of studies conducted by the USGS and others to characterize the occurrence and geologic controls on gas hydrate accumulations in the Eileen Gas Hydrate Trend. Building from previous analyses performed in the area (Collett et al., 2012), this investigation utilized borehole logs from additional wells and considered the results of published seismic framework studies (Schoderbek et al., 2012, 2013). This allowed us to expand the geologic framework and yielded an improved understanding of the local and regional occurrence of gas hydrate in the Eileen trend. A new Archie-based resistivity log analysis method, that includes special consideration to physical meaning of the empirical parameters within the Archie relationship (Archie, 1942), was used to generate a more complete gas hydrate reservoir saturation model for the Eileen trend. In addition, the acquisition of nuclear magnetic resonance (NMR/CMR) well logs and formation test data from the Mount Elbert (Collett et al., 2011b) and the Iġnik Sikumi (Schoderbek et al., 2012, 2013; Boswell et al., 2017) test wells provided critical information on the porosity and permeability relationships in the Eileen trend gas hydrate reservoirs. This section of the report further reviews the results and geologic findings from the Mount Elbert and Iġnik Sikumi gas hydrate test well projects and concludes with a systematic review of the structural-stratigraphic and reservoir controls on the occurrence of gas hydrate in the Eileen Gas Hydrate Trend.

3.B.1. Reservoir Controls on Gas Hydrate in the Eileen Gas Hydrate Trend

Well logs have been used to assess the occurrence of gas hydrate in numerous sedimentary basins (Collett and Lee, 2012) and have been used in this study to delineate and characterize the properties of the gas hydrate-bearing reservoirs in the western portion of the PBU. For a more complete review of well log responses to the presence of gas hydrate, see Collett and Lee (2012) and Schoderbek et al. (2013).

Reservoir Lithology

Clay content, which is often referred to as shale volume (V_{sh}) in conventional reservoir analysis, is one of the primary factors controlling the occurrence and concentration of oil and gas in conventional reservoir systems (Asquith and Krygowski, 2004). Collett and Lee (2012) also recognized that the occurrence of pore-filling gas hydrate in clastic reservoir sections is controlled in part by the presence of clay.

In this study of the occurrence of gas hydrate in the PBU, the volume of shale (V_{sh}) within the log-inferred gas hydrate intervals was calculated from gamma-ray logs using standard log analysis procedures for the type and age of sedimentary section in the Eileen Gas Hydrate Trend. The relationship between gamma-ray log values and sediment shale volumes (V_{sh}) used in this study area is shown in Equations 1 and 2 (Serra, 1984; Lee and Collett, 2011):

$$I_{GR} = \frac{GR - GR_{cln}}{GR_{sh} - GR_{cln}} \qquad (1)$$

$$V_{sh} = 0.083\ (2^{3.7 I_{GR}} - 1) \qquad (2)$$

where I_{GR} is a gamma-ray index or volume of shale, GR is a gamma-ray log value, GR_{cln} is a constant gamma-ray value for the cleanest (i.e., lowest shale content) sand in the reservoir section (lowest API log value), GR_{sh} is a constant gamma-ray value for a pure shale in the sedimentary section (the highest API log value), V_{sh} is a volume of shale corrected for Tertiary rocks, which is partially related to the degree of compaction that the sedimentary section has experienced.

Gamma-ray logs from a total of 90 wells located in the western portion of the PBU (Figs. 27, 28, and 29) were used to calculate V_{sh} in each well for the targeted reservoir sections of interest, from Unit B through Unit E. Since gamma-ray logs were not normalized in this study, the clean sand and shale baselines, required for the V_{sh} calculations (Equations 1 and 2), were selected on a well-by-well basis. For the sand-dominated portions of reservoir Units C and D, the estimated shale volumes (V_{sh}) ranged from near 0% to a maximum of about 30%.

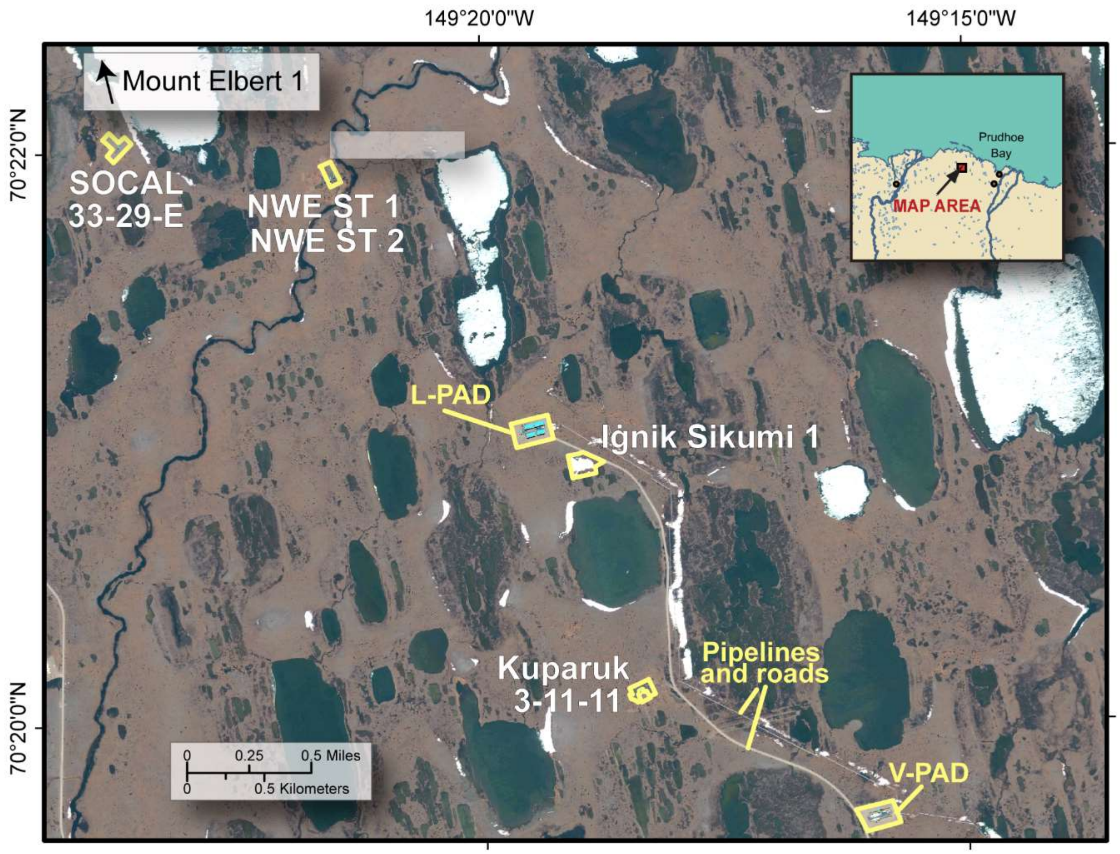

Figure 27. Satellite image showing the location of study area. Wells used in the study were drilled from PBU L-Pad, PBU V-Pad and the Kuparuk 3-11-11 Pad. The Northwest Eileen State 1 and 2 and State Socal 33-29-E wells were drilled from temporary ice pads. Location of the Mount Elbert well, also used in the study, not shown.

Reservoir Porosity

Advanced well logging tools are routinely used to examine petrophysical properties such as porosity and nature of pore-fill. In this study, the analysis of nine wells with sufficient log data to determine presence of gas hydrate, located in the western portion of the PBU (Figs. 27, 28, and 29), reveals the widespread occurrence of gas hydrate in Units C, D, and E (Collett et al., 2011a, 2012; Lewis and Collett, 2013). The same units were shown to be hydrate-bearing in three previously drilled gas hydrate research wells: Northwest Eileen State 2 (Collett, 1993), Mount Elbert (Boswell et al.,

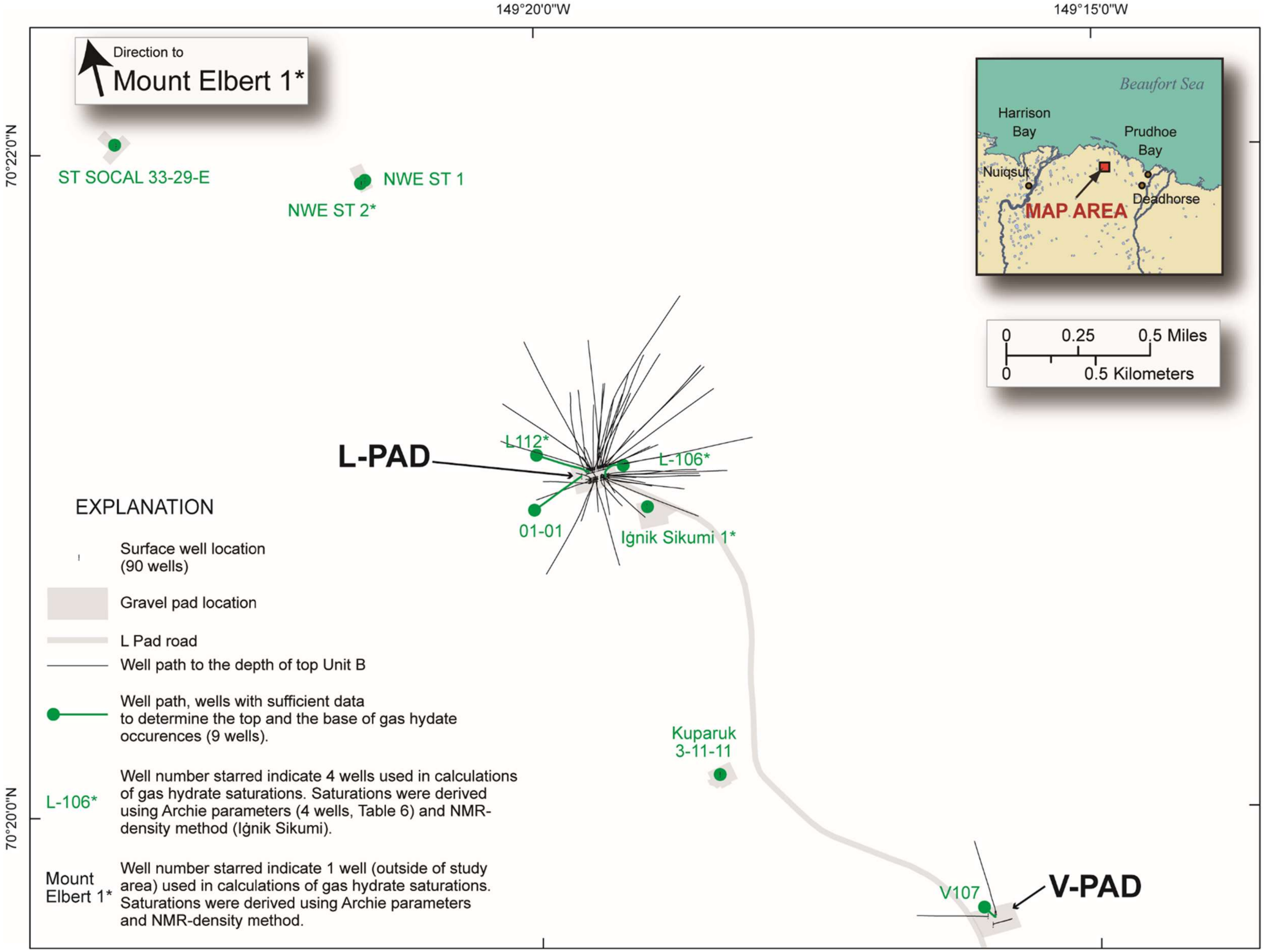

Figure 28. Map showing study area well paths to the depth of top Unit B. Well surface locations and well paths (grey lines) are shown for 90 wells with gamma-ray data in the interval of interest. Well surface locations and well paths for nine wells with enough log data to determine the top and the base of gas hydrate occurrence (green circles and lines). Log data from the Iġnik Sikumi, Northwest Eileen State 2 (NWE St 2), PBU L-106 and PBU L-112 wells were used to calculate gas hydrate saturations. Well data from the Mount Elbert well, located 9 km (5.5 mi) northwest of this map (indicated by arrow) were also used in calculation of gas hydrate saturations (not shown).

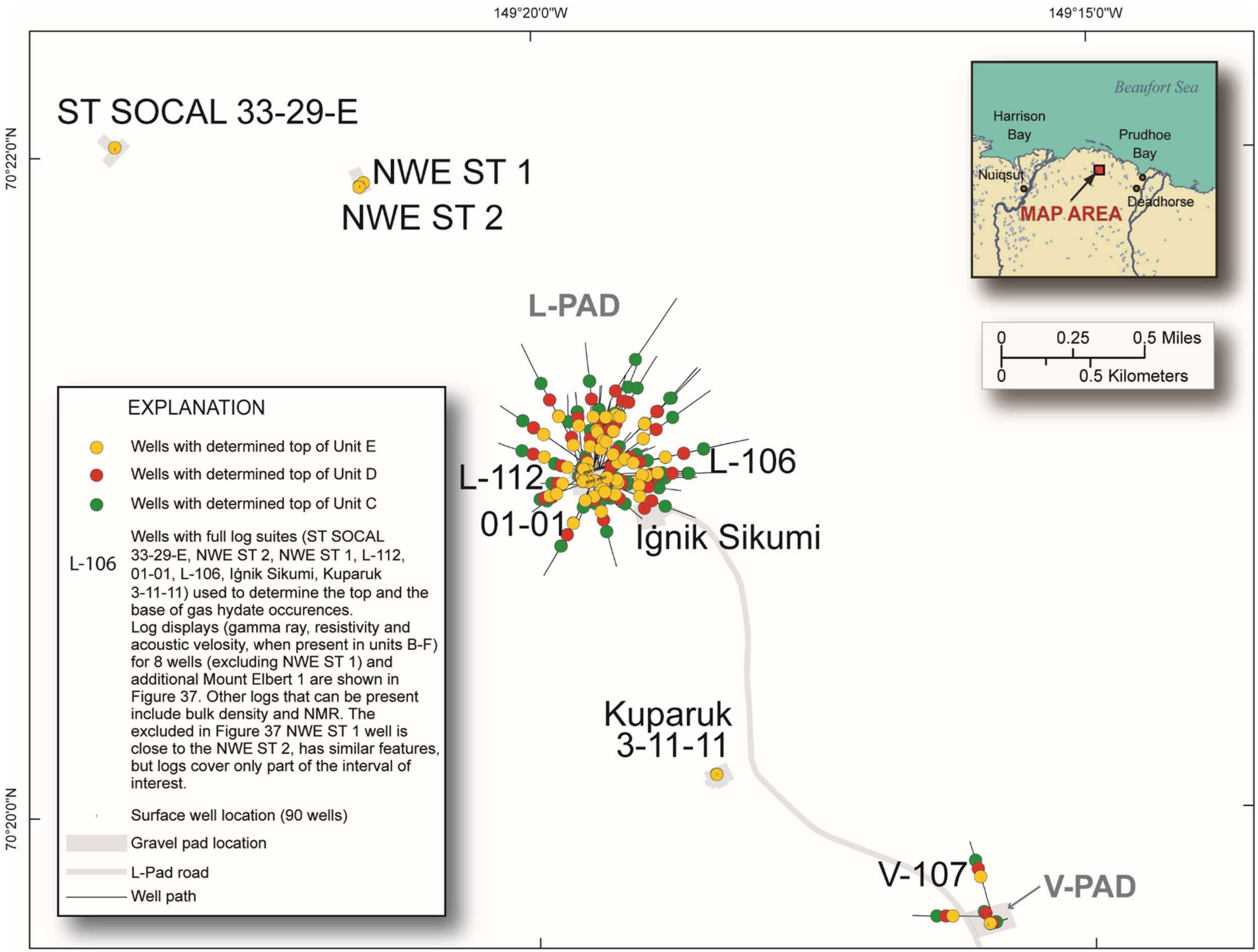

Figure 29. Map of data distribution at the tops of Units C, D, and E. NMR = Nuclear Magnetic Resonance

2011b), and Iġnik Sikumi (Schoderbek et al., 2013; Boswell et al., 2017). The well path trace map in Figure 29 shows the location of the top of Units C, D, and E as penetrated in each well. Density log data from available wells in the PBU study area were used to estimate porosity within the gas hydrate-bearing units of interest. The Archie relationship and the NMR-density log porosity data were used in this study to calculate gas hydrate saturations (as reviewed below).

The comprehensive well log data set from the Iġnik Sikumi well was an excellent starting point for the calculation of gas hydrate reservoir porosity and fluid saturations for the Eileen trend. For this test well, the presence of gas hydrate is inferred from resistivity (AT90) and acoustic sonic log data (DT). Resistivities of 20 ohm-m and greater and transit times less than 140 µsec/ft were determined as gas hydrate indicators (Fig. 26). Based on these criteria, three gas hydrate-bearing intervals are interpreted within the Iġnik Sikumi well: ~2215–2332 ft (~670–710 m) measured depth (MD) in Unit C, ~2060–2130 ft (~630–650 m) MD in Unit D, and ~1907–1954 ft (~580–600 m) MD in Unit E (Fig. 26). Unit C was also subdivided into an upper Unit C and a lower Unit C for description purposes. The 30-ft-thick (9-m) section within the upper Unit C (~2243–2273 ft; ~680–690 m MD) was selected for testing during the 2012 CO_2-CH_4 exchange trial.

The standard density porosity relationship was used to calculate porosity (ϕ_D):

$$\phi_D = \frac{\rho_{ma} - \rho_b}{\rho_{ma} - \rho_w} \qquad (3)$$

where ρ_{ma} is the matrix density (assumed value of 2.65 g/cm^3), ρ_b is formation bulk density (g/cm^3) as measured from the density log, and ρ_w is the formation water density (assumed value of 1.02 g/cm^3). Density log data from five wells with log data in gas hydrate intervals (Northwest Eileen State 2, PBU L-112, PBU L-106, Iġnik Sikumi, and Mount Elbert) were used to derive density-porosity trends throughout the delineated Eileen Gas Hydrate Trend. The density-log derived porosities in the gas hydrate-bearing portion of the upper Unit C in the Iġnik Sikumi test well averaged about 35 % (Fig. 26).

Reservoir Gas Hydrate Saturations

Gas hydrate saturations (Fig. 26) were determined through the Archie analysis methods utilizing measured resistivity log data (Archie, 1942; Collett and Lee, 2012), as well as a density and NMR porosity log method (Kleinberg et al., 2005). Gas hydrate saturations estimated from the NMR and density porosity approach do not depend on empirical relationships; thus, the accuracy of the estimation depends only on the accuracy of NMR and density log measurements. Therefore, NMR and density log-derived gas hydrate saturations were assumed as the most accurate and were used to constrain the hydrate saturation estimates derived using the Archie method for the Iġnik Sikumi well.

The NMR well logging tools primarily respond to the presence of movable hydrogen molecules in the rock formation. Thus, gas hydrates cannot be directly detected with a downhole NMR logging tool because they behave like they are part of the solid matrix.

Therefore, it can be concluded that NMR porosity is a measurement of the pore space that is not occupied by gas hydrate. It is a measurement of the pore space volume occupied by free water, capillary-bound water, and clay-bound water. As a result, the NMR derived porosities will significantly under-estimate the true or total-formation porosities in gas hydrate-bearing reservoirs. However, the comparison of accurate in situ total porosities from an independent source, such as those calculated from density log measurements (Equation 3), with apparent NMR-derived porosities, allows estimation of gas hydrate saturations from NMR measurements. A set of equations was developed for computing gas hydrate saturations using porosities estimated from density and NMR logs (Kleinberg et al., 2005; Collett and Lee, 2012):

$$\phi_{NMR} = (1 - S_h)\phi \qquad (4)$$

$$S_h = \frac{\phi - \phi_{NMR}}{\phi} \qquad (5)$$

$$\lambda_h = \frac{\rho_w - \rho_h}{\rho_{ma} - \rho_w} \qquad (6)$$

$$\phi = \frac{\phi_D + \lambda_h \phi_{NMR}}{1 + \lambda_h} \qquad (7)$$

where ϕ_{NMR} is the same as the water-filled porosity and is the NMR log reading itself, S_h is the NMR-density porosity-derived gas hydrate saturation, ϕ is the total porosity, representing the pore space occupied by water and gas hydrate, λ_h is a correction constant, ρ_w is the formation water density (assumed value of 1.02 g/cm^3), ρ_h is the gas hydrate density (assumed value of 0.9 g/cm^3 for structure I gas hydrate; Sloan and Koh, 2008), ρ_{ma} is the matrix density (assumed value of 2.65 g/cm^3), and ϕ_D is the density porosity derived assuming a two-component system (matrix and water; Equation 3).

For the NMR-density porosity derived gas hydrate saturations, the "total-porosity" value for the gas hydrate-bearing units was derived from bulk density well log data using Equation 3. Input parameters for the density porosity log calculations are summarized in Table 5. Grain or matrix density and fluid density values, required for the density porosity calculations, are usually derived from core data. These types of data were not generally available from the wells in the study area. Therefore, published grain (matrix), water, and gas hydrate densities, formation temperatures and pore water salinities from Mount Elbert acquired cores and other sources (Collett, 1992; Lee and Collett, 2011; Collett, et al., 2011a, 2011b; Collett and Lee, 2012; Lee and Waite, 2008) provided accurate estimates of these geologic and petrophysical parameters for the wells used in this study (Table 5). The calculated NMR porosity was compared with the density log derived porosity to identify gas hydrate-bearing intervals (Fig. 26, track 5) by the separation between the two porosity curves. The NMR-density derived gas hydrate saturation log for Units C, D, and E is shown in Figure 26 (track 6), with the gas hydrate saturations in the upper part of Unit C averaging about 75%.

Gas hydrate, much like oil or gas, acts as an electrical insulator, and can be detected with resistivity tools. Resistivity log measurements can also be used to estimate gas hydrate saturations. The Archie (1942) equation, which relates porosity, pore-fluid resistivity, and rock resistivity, is often used to calculate fluid saturations in gas hydrate-bearing sand reservoir systems (reviewed by Collett and Lee, 2012). According to Archie (1942), the water saturation (S_w) of a formation containing hydrocarbon-bearing sediments can be derived from the resistivity log as:

$$S_w = \left(\frac{aR_w}{\phi^m R_t} \right)^{1/n} \qquad (8)$$

$$S_h = 1 - S_w \qquad (9)$$

$$FF = \left(\frac{R_t}{R_w} \right) \qquad (10)$$

where, *a* and *m* are Archie constants, tortuosity factor, and cementation exponent, respectively, *n* is an empirically derived parameter, called saturation exponent, R_w is the resistivity of the connate water (ohm-m), ϕ is the porosity, R_t is the formation resistivity as measured by the deep-reading resistivity log (ohm-m), S_h is the Archie equation-derived gas hydrate saturation, and *FF* is a formation factor.

The parameter *n*, which depends on the reservoir lithology, has been shown to vary between 1.7 for unconsolidated sediment and 2.2 for sandstone and is typically 1.9 (Collett, 2001). The *a* and *m* are empirically derived parameters often obtained from logarithmic porosity-resistivity cross plots (Pickett, 1966), the physical meaning of which will be described in more detail below. Porosity values (Equation 3) can be estimated from other porosity logs, such as density logs. The resistivity of the pore water (R_w) can also be calculated using Arp's formula, if the salinity and temperature of the formation water are known (Arp, 1953; Schlumberger, 1998; Collett and Lee, 2012). The Archie method relies heavily on the selection of accurate values for the empirical parameters *a* and *m*, which can be derived from Pickett plots (Pickett, 1966; Hilchie, 1982; Serra, 1984; Asquith and Krygowski, 2004).

The Archie method is based on the general concept of comparing the resistivity of conventional hydrocarbon-bearing reservoirs with the resistivity of 100% water-saturated mostly sand-rich reservoirs. Since the gas hydrates in the Eileen trend are found mostly in conventional sand-rich reservoir sections and the gas hydrate-bearing reservoirs appear to contain an appreciable amount of free- and bound-water within interconnected pores (Collett et al., 2011a; Schroderbek et al., 2013; Boswell et al., 2017), it is reasonable to assume that the Archie method could be used to calculate accurate gas hydrate saturations with the well log data from the ANS as reviewed by Collett and Lee (2012).

In the Archie method, if the baseline salinity of the formation water is known within the stratigraphic section of interest, the data from the deep reading resistivity log can be plotted against the density porosity log values on a Pickett plot (Figs. 30 and 31) to derive the required Archie parameters, which can then be used to directly calculate the water saturations (Equation 8). The Archie *m* parameter can be derived from the slope of the "water-line," which is a line fitted through the data points representing 100% water-saturated sand units as posted on the Pickett plot. The intercept of the water-line with the porosity cross-plot axes at unity (which is ϕ equal to unity or 100% porosity) yields the value for the relationship of ($a*R_w$), where *a* is the Archie tortuosity factor (Equation 8). To simplify this process in this study, the formation factor (FF, Equation 10) was used instead of the well log-measured formation resistivity in the Pickett plots (Figs. 30 and 31). In this case, a plot of the water-line as projected to intercept the porosity axis at ϕ=100% (shown as 0.1 decimal percent) will yield the direct value for *a*, while *m* is derived from the slope of the water-line.

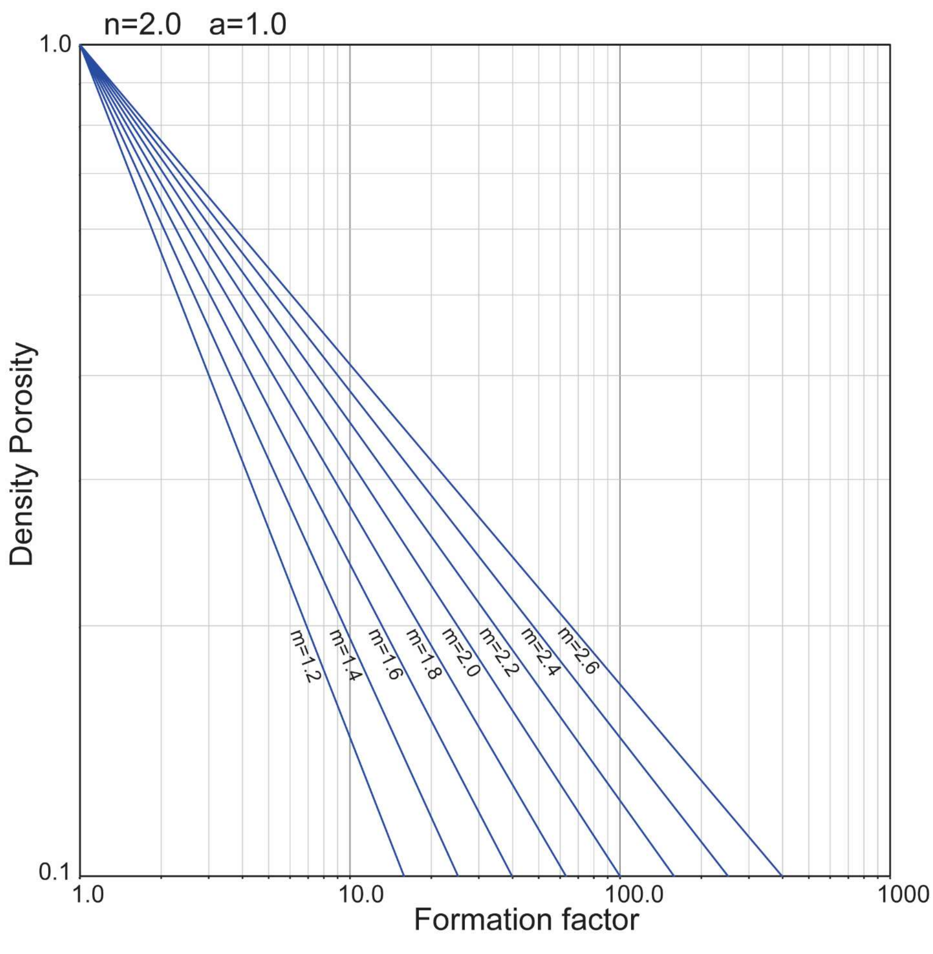

Figure 30. Example Pickett plot annotated to depict the cross-plot method used to derive Archie *a* and *m* parameters (modified from Serra, 1984). Porosity shown in decimal percent.

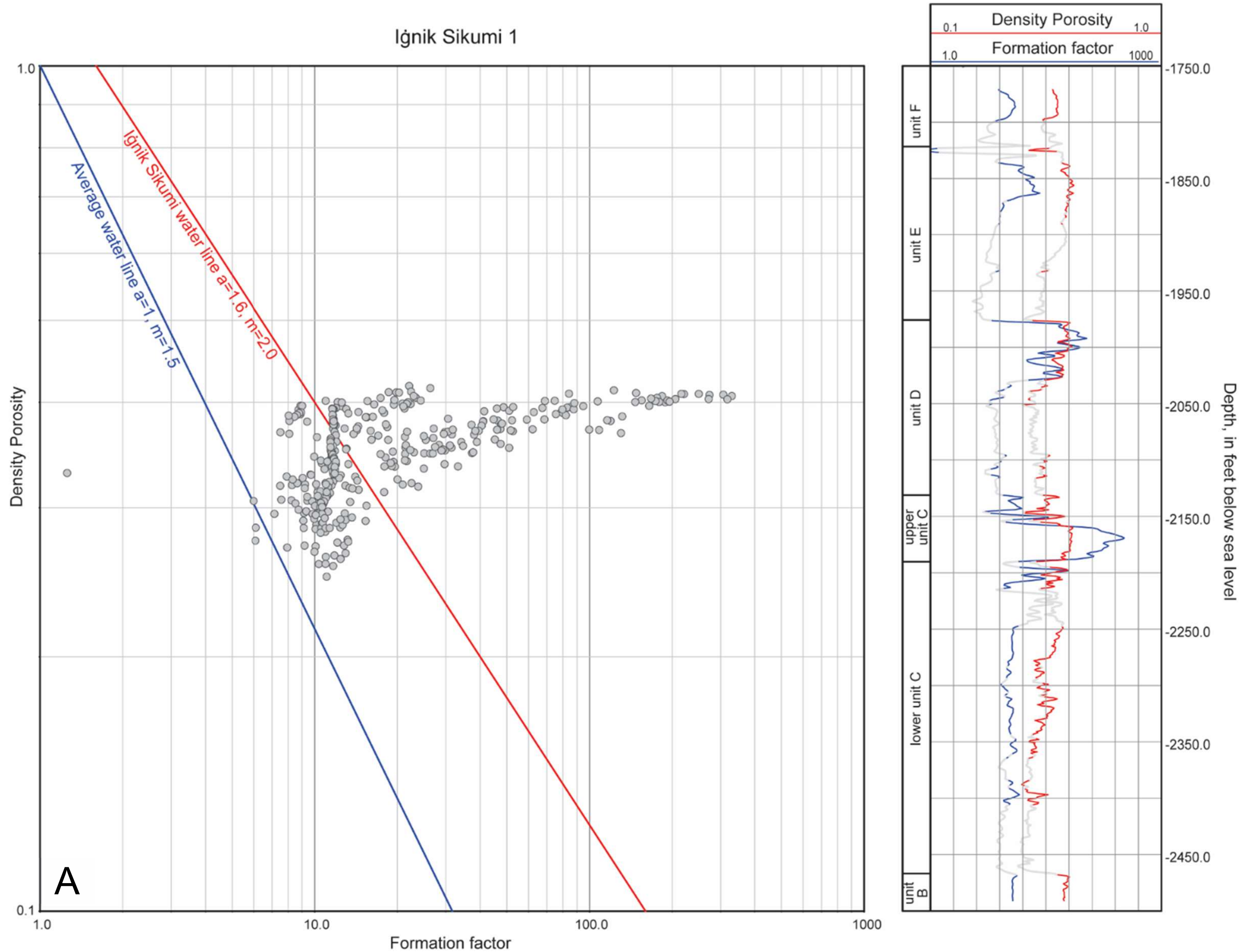

Figure 31. (A) Series of Pickett plots depicting the cross-plot methodology used to select the Archie *a* and *m* parameters for the water and gas hydrate-bearing units in the Iġnik Sikumi well for the Units B, C, D, and E reservoir sections. Also shown is the water line corresponding to the Archie parameters of *a*=1.0, and *m*=1.5 (blue line) and the water line corresponding to the Archie parameters of *a* = 1.6 and *m* = 2.0 (red line). Porosity shown in decimal percent.

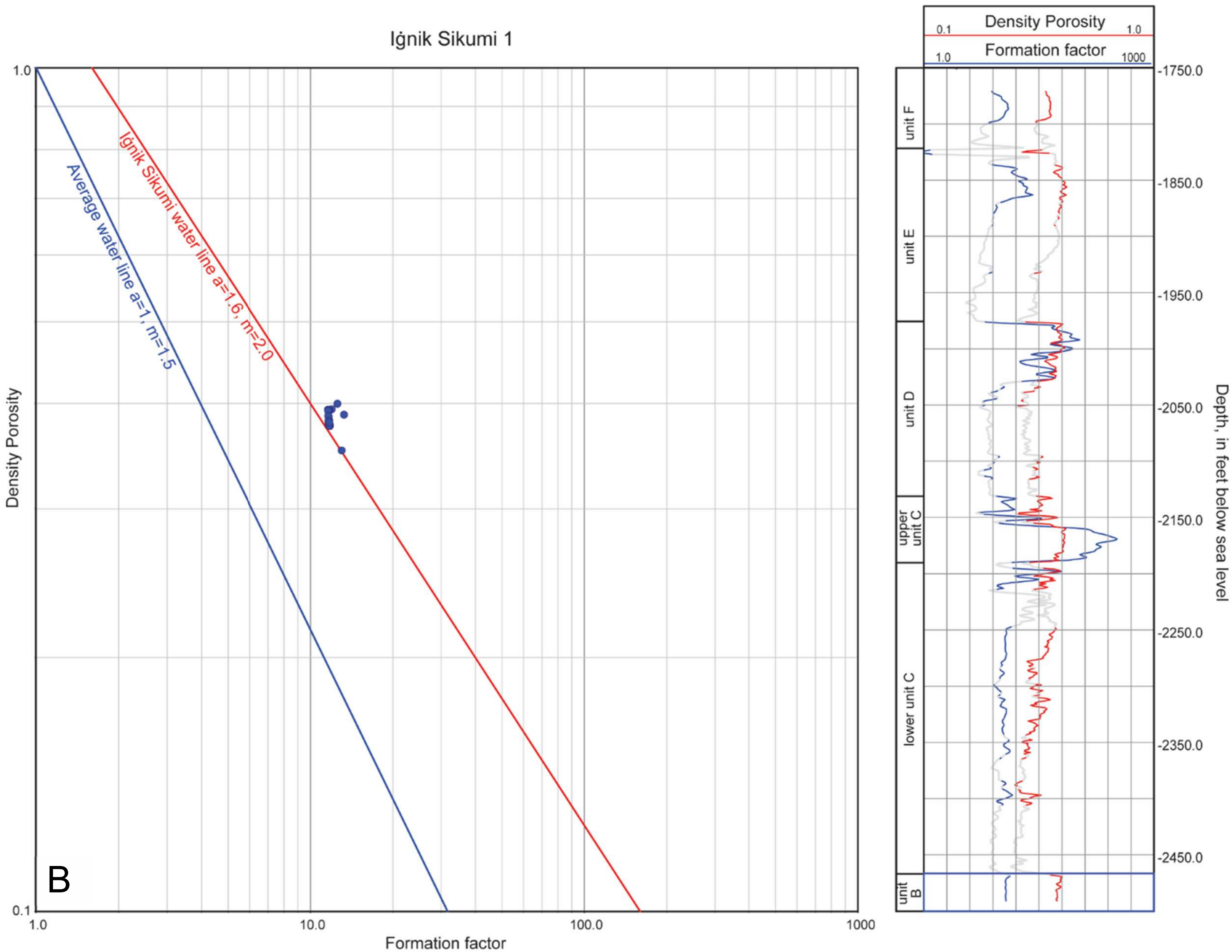

Figure 31. (B) Series of Pickett plots depicting the cross-plot methodology used to select the Archie *a* and *m* parameters for the water and gas hydrate-bearing units in the Iġnik Sikumi well for the Unit B reservoir section. Also shown is the water line corresponding to the Archie parameters of *a*=1.0, and *m*=1.5 (blue line) and the water line corresponding to the Archie parameters of *a* = 1.6 and *m* = 2.0 (red line). Porosity shown in decimal percent.

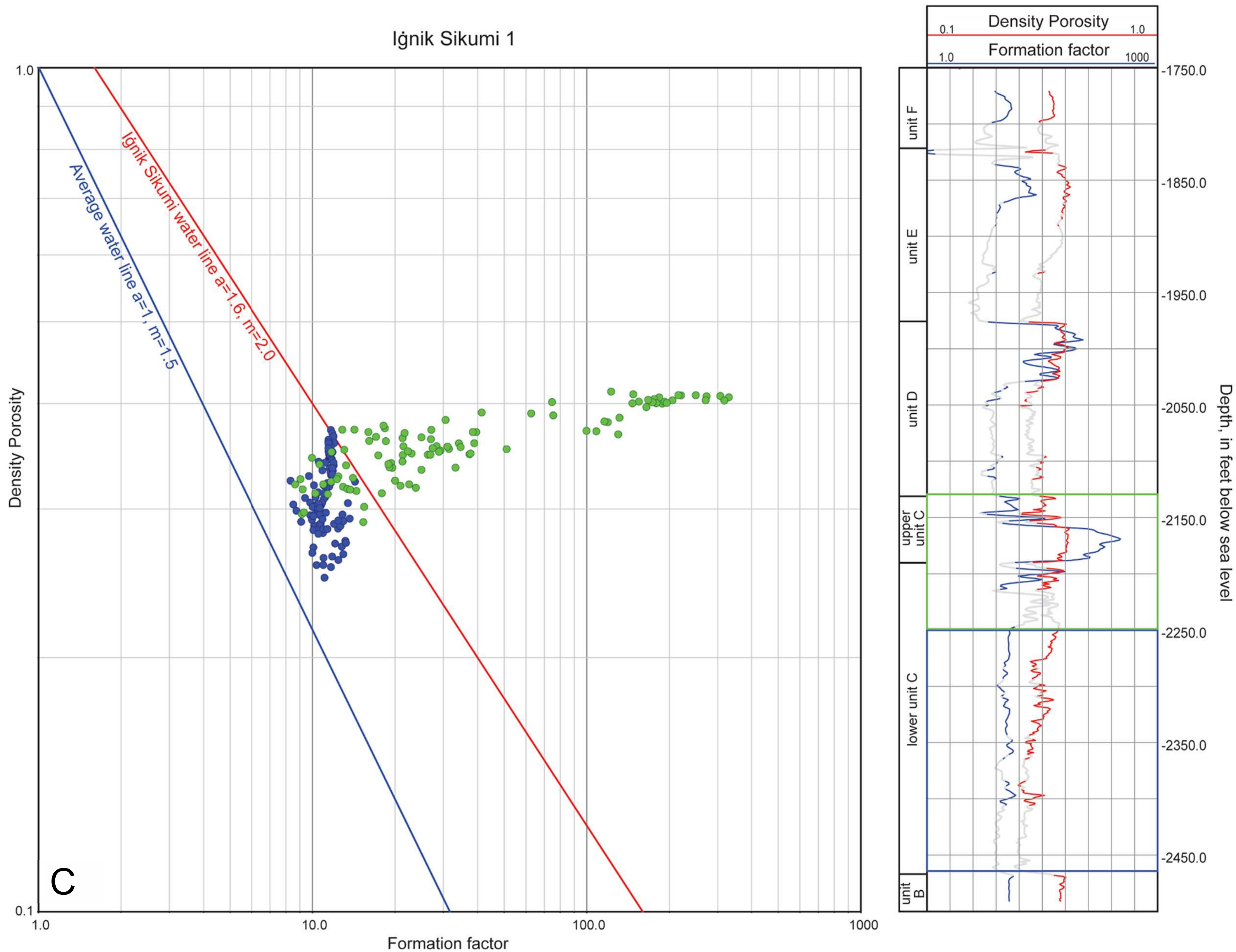

Figure 31. (C) Series of Pickett plots depicting the cross-plot methodology used to select the Archie *a* and *m* parameters for the water and gas hydrate-bearing units in the Iġnik Sikumi well for the Unit C reservoir section. Also shown is the water line corresponding to the Archie parameters of *a*=1.0, and *m*=1.5 (blue line) and the water line corresponding to the Archie parameters of *a* = 1.6 and *m* = 2.0 (red line). Porosity shown in decimal percent.

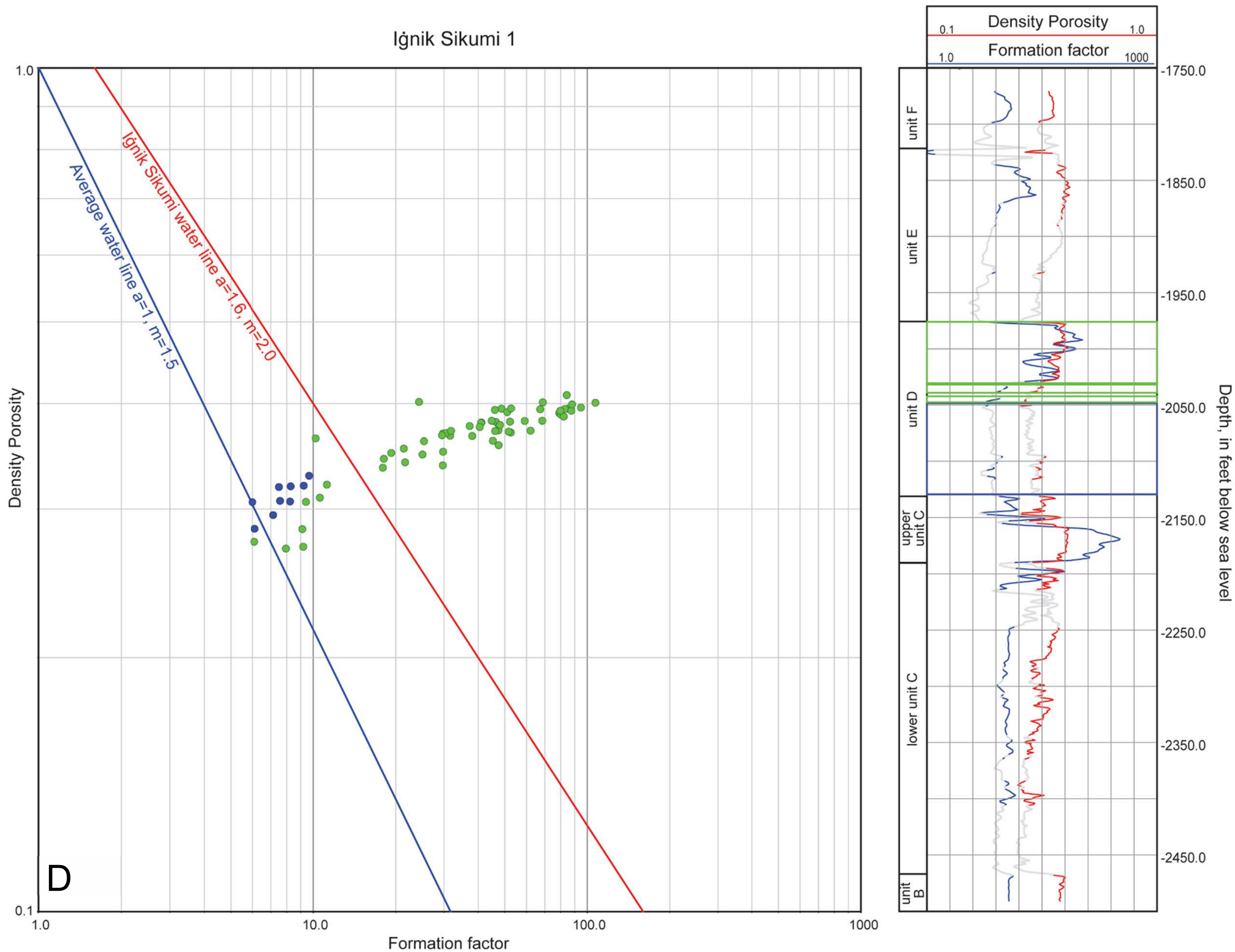

Figure 31. (D) Series of Pickett plots depicting the cross-plot methodology used to select the Archie *a* and *m* parameters for the water and gas hydrate-bearing units in the Iġnik Sikumi well for the Unit D reservoir section. Also shown is the water line corresponding to the Archie parameters of *a*=1.0, and *m*=1.5 (blue line) and the water line corresponding to the Archie parameters of *a* = 1.6 and *m* = 2.0 (red line). Porosity shown in decimal percent.

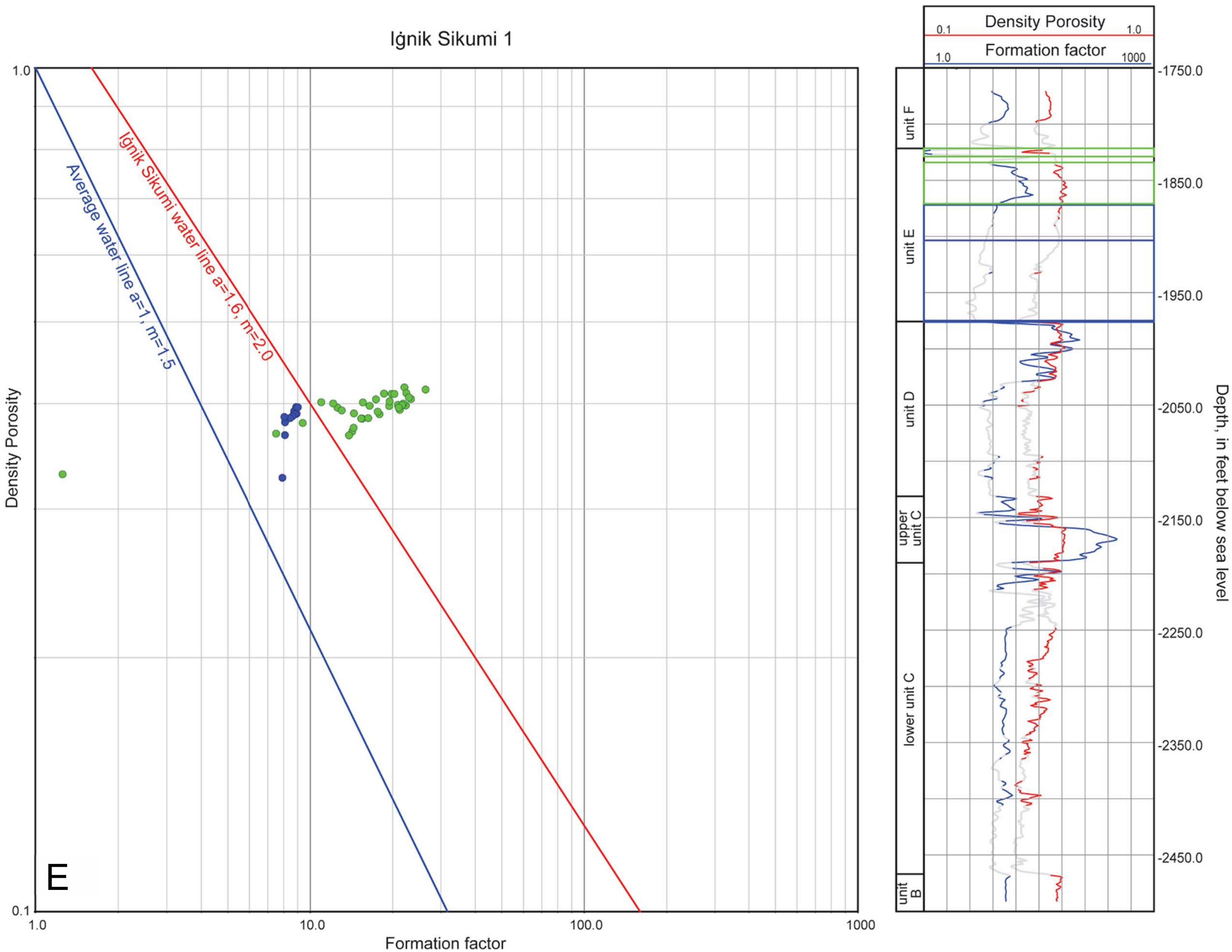

Figure 31. (E) Series of Pickett plots depicting the cross-plot methodology used to select the Archie *a* and *m* parameters for the water and gas hydrate-bearing units in the Iġnik Sikumi well for the Unit E reservoir section. Also shown is the water line corresponding to the Archie parameters of *a*=1.0, and *m*=1.5 (blue line) and the water line corresponding to the Archie parameters of *a* = 1.6 and *m* = 2.0 (red line). Porosity shown in decimal percent.

When NMR logs are not available, core data can be used to yield accurate values for the empirical Archie parameters. But in either case, it is important to consider the underlying physical controls and meanings of each of the Archie parameters. The Archie parameter a is often called the Archie tortuosity factor, and in some cases the cementation intercept, lithology factor, or lithology coefficient. This parameter is meant to correct for variation in compaction, pore structure, grain size, and matrix mineralogy (Archie, 1942). The value of a can range from 0.5 to 1.5 and is controlled by the electric current path length. A value of a = 1.0 is often used to represent clean (no clay), nonconductive, sand-rich reservoirs, while any variations from 1.0 are most often attributed to more clay-rich rocks that are relatively more conductive. Maute et al. (1992) presented an approach to determine Archie parameters m and n and in some cases a from standard resistivity measurements on cores. Maute et al. (1992) concluded that a is a "weak-fitting parameter with no physical significance," thus, it is recommended to fix a to unity. Mathematical analysis demonstrated that, for most reservoirs, the change of a=1 to $a \neq 1$ had a small effect on the Archie-derived saturation values. The Archie a parameter most likely accounts for hidden variables such as conductive minerals. In other words, a is a correction factor with no specific trends relative to lithology (clay), grain size or compaction, and it is used to adjust Archie-derived saturation values.

The Archie cementation exponent, m, models how much the pore network affects the conductivity of the reservoir, as the rock itself is assumed to be nonconductive. If the pore network is assumed to be represented by a set of parallel capillary tubes, a cross-sectional area average of the rock's resistivity would yield a porosity-dependent cementation exponent of m=1 (Archie, 1942). While this hypothetical rock does not exist in nature, the Archie parameter m does generally increase with increasing tortuosity of the pore space connectivity and decreases with increasing connectivity. The Archie cementation exponent, m, has been observed to range from 1.3 to 2.6, with lower values related to unconsolidated sands. Common values for the cementation exponent for unconsolidated rocks are expected to range from 1.3 to 1.8 (average 1.5), while for consolidated sandstones it usually ranges from 1.8 to 2.0 (Archie, 1942; Crain, 1986; Kadhim et al., 2013). The effect of gas hydrate growth on pore space tortuosity is not well known (Spangenberg, 2001). The permeability of the gas hydrate-bearing reservoirs is significantly impacted by the presence of gas hydrate (reviewed by Collett and Lee, 2012; Boswell et al., 2019), which may indicate that the conduction of electrical currents through a gas hydrate-bearing formation could be similarly impacted by the distribution and nature of gas hydrate at the pore-scale. Because of the unconsolidated nature of most of the cored gas hydrate occurrences on the ANS, the Archie cementation exponent, m, for these reservoirs would be less than 1.8, with an expected average value around 1.5 as derived below in this report. The Archie saturation exponent, n, is usually fixed to a value close to 2.0. The Archie saturation exponent is, for the most part, dependent on the wettability of the grain surfaces in the reservoir rock and is controlled by the presence of either conductive or nonconductive fluids bound to the grain surfaces. Water-wet rocks maintain a continuous film of conductive water along the pore walls making the rock conductive. Oil-wet rocks have discontinuous water films along the grain surfaces, making the rock less conductive. Since gas hydrate has not been observed growing on grain surfaces (as reviewed by Chaouachi et al., 2015) and the analysis of NMR and formation test data shows significant amounts of both bound water and free-water in gas hydrate sand reservoir systems (Collett and Lee, 2012; Schroderbek et al., 2013), the rock matrix in most gas hydrate-bearing sand reservoir systems can be considered water-wet, and the Archie saturation exponent, *n*, can be set to 2.0.

Four wells from the area of the PBU-L Pad in the Eileen trend had sufficient resistivity well log data to allow the calculation of gas hydrate saturations (Figs. 27, 28, 29, 30, 31A-E, 32, 33 and 34A-D) (Iġnik Sikumi, PBU L-106, PBU L-112, and Northwest Eileen State 2). As discussed previously, the Iġnik Sikumi well also had NMR log data from the gas hydrate-bearing reservoir, which aided the selection and calibration of the appropriate Archie parameters. A series of modified Pickett plots, as depicted in Figures 31A–E document the methodology used to select *a* and *m* parameters for the gas hydrate-bearing units in the Iġnik Sikumi and other wells analyzed in this study. As reviewed above, logarithmic cross plots (i.e., a modified Pickett plot) of porosities (ϕ) versus deep resistivity presented by *FF* in this case (Figs. 30 and 31A–E) can be used to select a "water-line" for the water-wet sands in the reservoir section being examined. The slope of the water-line and porosity axis intercept at 100% porosity (or unity) can be used to estimate the Archie *m* and *a* parameters, respectively. Analysis of the well log data from the Iġnik Sikumi wells revealed the presence of water-bearing sand intervals both within and below several of the gas-hydrate-bearing reservoir sections. Specifically, the sand-rich interval below the gas hydrate-bearing sand section in the lower part of Unit C in the Iġnik Sikumi well (Figs. 26 and 34A) and the entire B Unit were reported as water bearing in Schoderbek et al. (2013); therefore, these confirmed water-saturated sand units should help with the selection of the "water-line" for the water-wet sand units.

A critical assumption when using the Pickett plot method is that all the reservoir data points depicted on the plot have the similar matrix parameters and pore water salinities. These data points should form clusters, allowing to project a trend line. The series of modified Pickett plots in Figure 31A–E show results of well log data values distribution based on reservoir and lithology in the Iġnik Sikumi well. Figures demonstrate the methods used in this study to ascertain the required Archie *a* and *m* parameters. The goal is to understand the geologic nature of each data point as plotted and to select only the reservoir sections (within Units B, C, D, and E) with similar reservoir properties and that yield reasonable data distributions, leading to the accurate selection of Archie parameters from the cross plots. The first step in this process is to eliminate all the non-reservoir sections from consideration. This step was accomplished for each of Units B, C, D, and E by eliminating the reservoir sections with calculated V_{sh} values of 30% and greater (Figure 31A–E). The next step in the process was to determine if the pore fill in each of the remaining reservoir sections is either water or gas hydrate. The presence of gas hydrate was inferred from the deep-resistivity log data with gas hydrate being indicated by log values of 20 ohm-m and greater. In several cases, compressional-wave transit-time log data (sonic log) were also used to differentiate water-bearing from hydrate-bearing reservoir sections with travel times of 140 µsec/ft and less used as the gas hydrate-bearing threshold. The results of this reservoir discretization process for the Iġnik Sikumi well is depicted in Figure 34A, where the non-reservoir sections are identified in gray, the predominantly water-bearing reservoir sections are shown in blue, and the predominantly hydrate-bearing reservoir sections are shown in green. Figures 31A–E show Pickett plots with the mostly water-bearing reservoir sections data (shown in

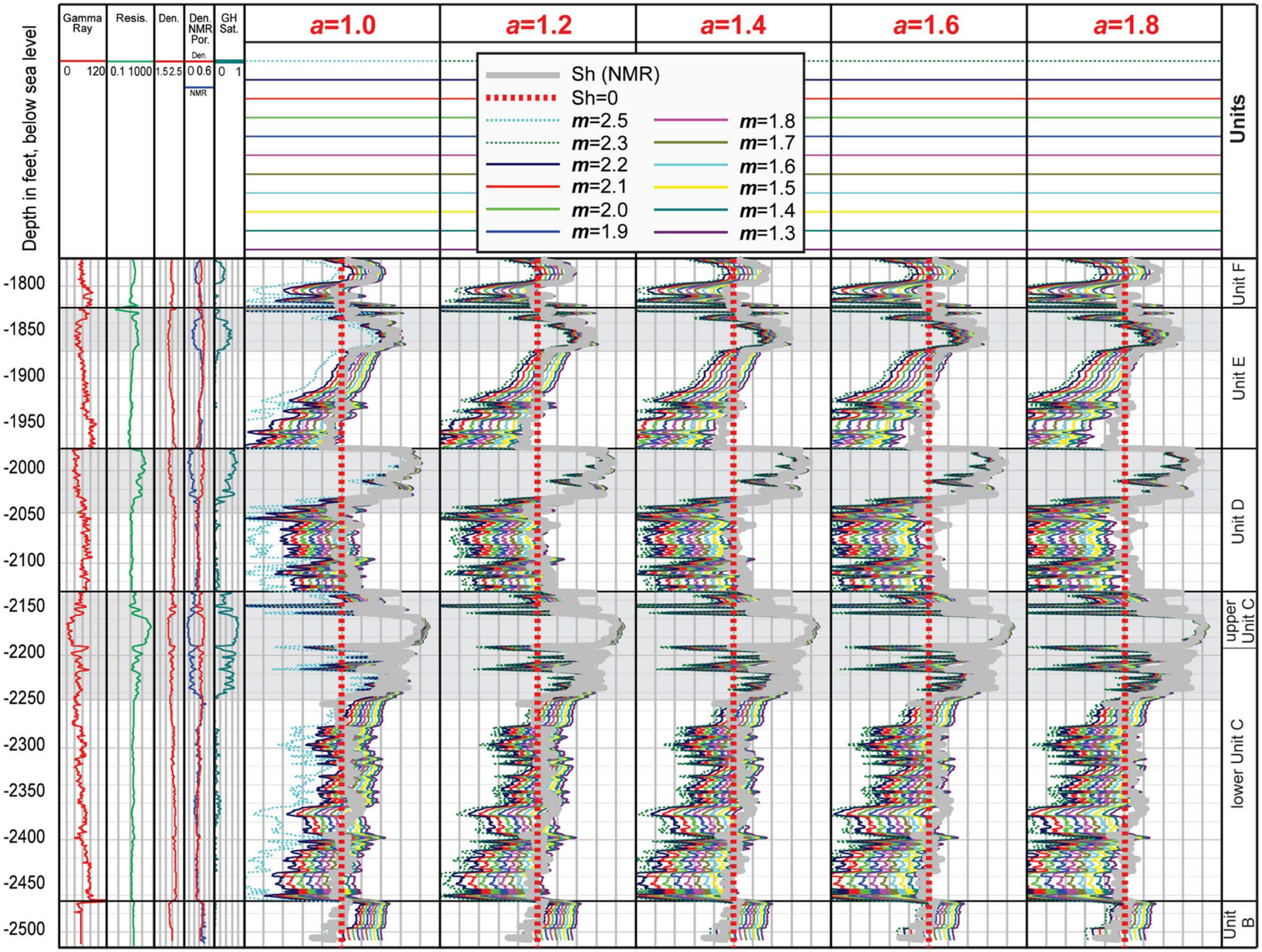

Figure 32. Display of calculated gas hydrate saturations for the Iġnik Sikumi well using different Archie parameters. Multiple calculated gas hydrate saturation log curves assuming different *m* values ranging from 1.3 to 2.5 are depicted in each of the tracks. Well log curves grouped in each track by the Archie parameter *a*. Also displayed in each track is the water line (0% gas hydrate saturation, red dashed line) and the NMR-derived gas hydrate saturation curve (gray curve). S_h = gas hydrate saturation, S_h (NMR) = gas hydrate saturation derived from DEN-NMR log method, NMR = Nuclear Magnetic Resonance, DEN = Density

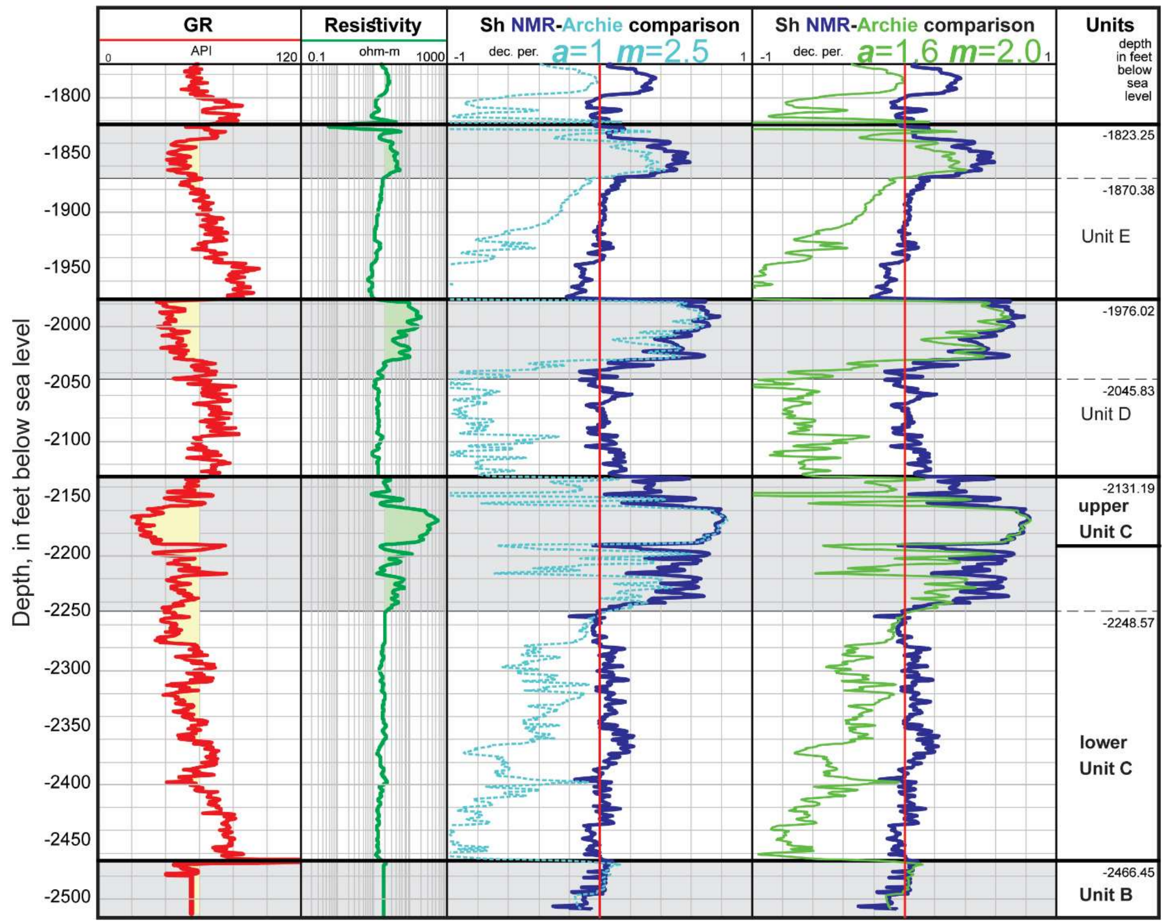

Figure 33. Log display for Iġnik Sikumi well depicting two scenarios for the selection of the Archie *a* and *m* parameters from Figure 32. Track 3 shows the scenario when Archie parameters *a*=1.0 and *m*=2.5 satisfy the selection criteria defined in the text. Track 4 shows the scenario when Archie parameters *a*=1.6 and *m*=2.0 satisfy the same selection criteria. However, only the second scenario provides physically reasonable parameters for gas hydrate saturation for this well data. Grey shading indicates the gas hydrate-bearing portion of the Units C, D and E. API = American Petroleum Institute, GR = Gamma ray, NMR = Nuclear Magnetic Resonance, S_h = gas hydrate saturation

blue) and the mostly hydrate-bearing reservoir sections (shown in green) in Units B, C, D, and E of the Iġnik Sikumi well. As previously discussed, the Archie parameters for unconsolidated rocks, like those expected in non-hydrate-bearing sediments of the Sagavanirktok should exhibit average values around *a*=1.0, and *m*=1.5. For reference purposes only, the "water-line" (blue line) corresponding to Archie parameters of *a*=1.0, and *m*=1.5 has been plotted in Figures 31A–E. It is important to highlight that this line does not correspond to any actual posted data trends in this example and is included for only reference purposes. Also plotted for reference purposes in Figures 31A–E (and will be discussed later in this report) is a "water-line" (red line) representing the Archie parameters of *a* = 1.6 and *m* = 2.0. In the cross plot of all the available log data from the potential sand-dominated water-bearing reservoir sections within Units B, C, D, and

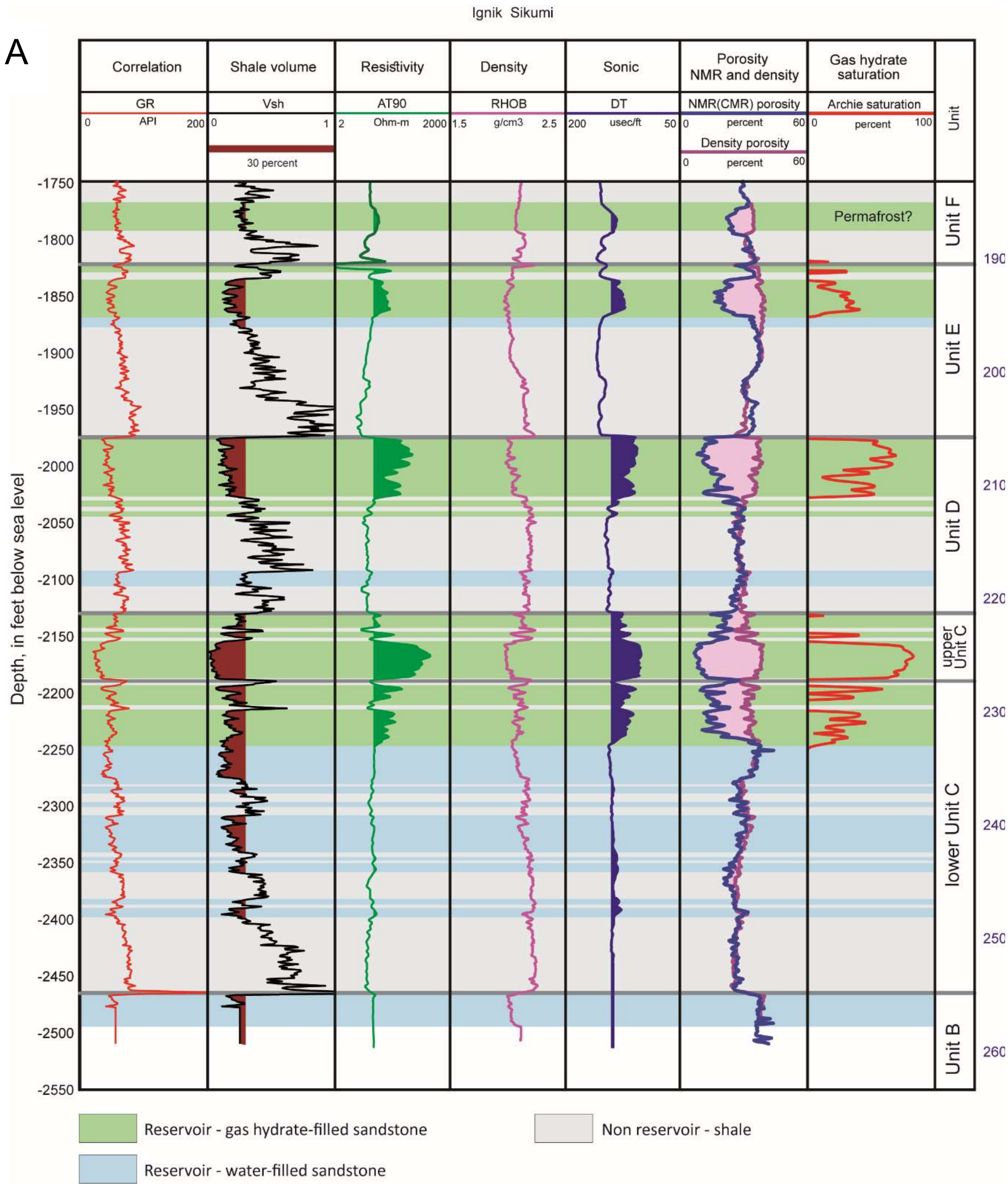

Figure 34. (A) Iġnik Sikumi well log display as drilled in the Eileen Gas Hydrate Trend depicting the vertical distribution of reservoir and non-reservoir sections within the Units B, C, D, and E and the reservoir fill type (i.e., gas hydrate or water). Shale volume shown in decimal percent. API = American Petroleum Institute, GR = Gamma ray, Vsh = Shale volume, AT90 = Resistivity log measurement, RHOB = Bulk density, DT = Sonic transit-time, NMR = Nuclear Magnetic Resonance, CMR = Nuclear magnetic resonance logging tool

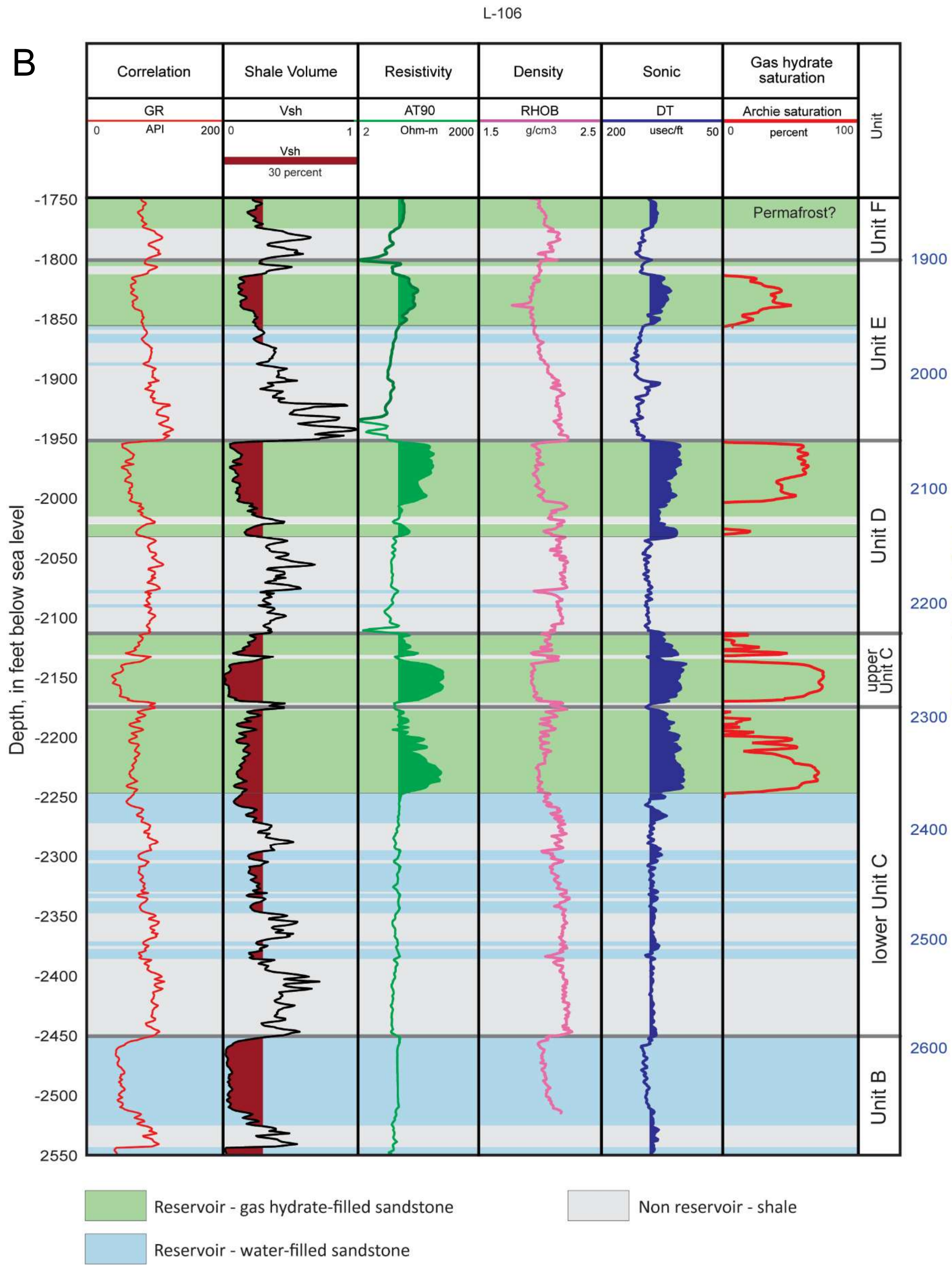

Figure 34. (B) PBU L-106 well log display as drilled in the Eileen Gas Hydrate Trend depicting the vertical distribution of reservoir and non-reservoir sections within the Units B, C, D, and E and the reservoir fill type (i.e., gas hydrate or water). Shale volume shown in decimal percent. API = American Petroleum Institute, GR = Gamma ray, Vsh = Shale volume, AT90 = Resistivity log measurement, RHOB = Bulk density, DT = Sonic transit-time

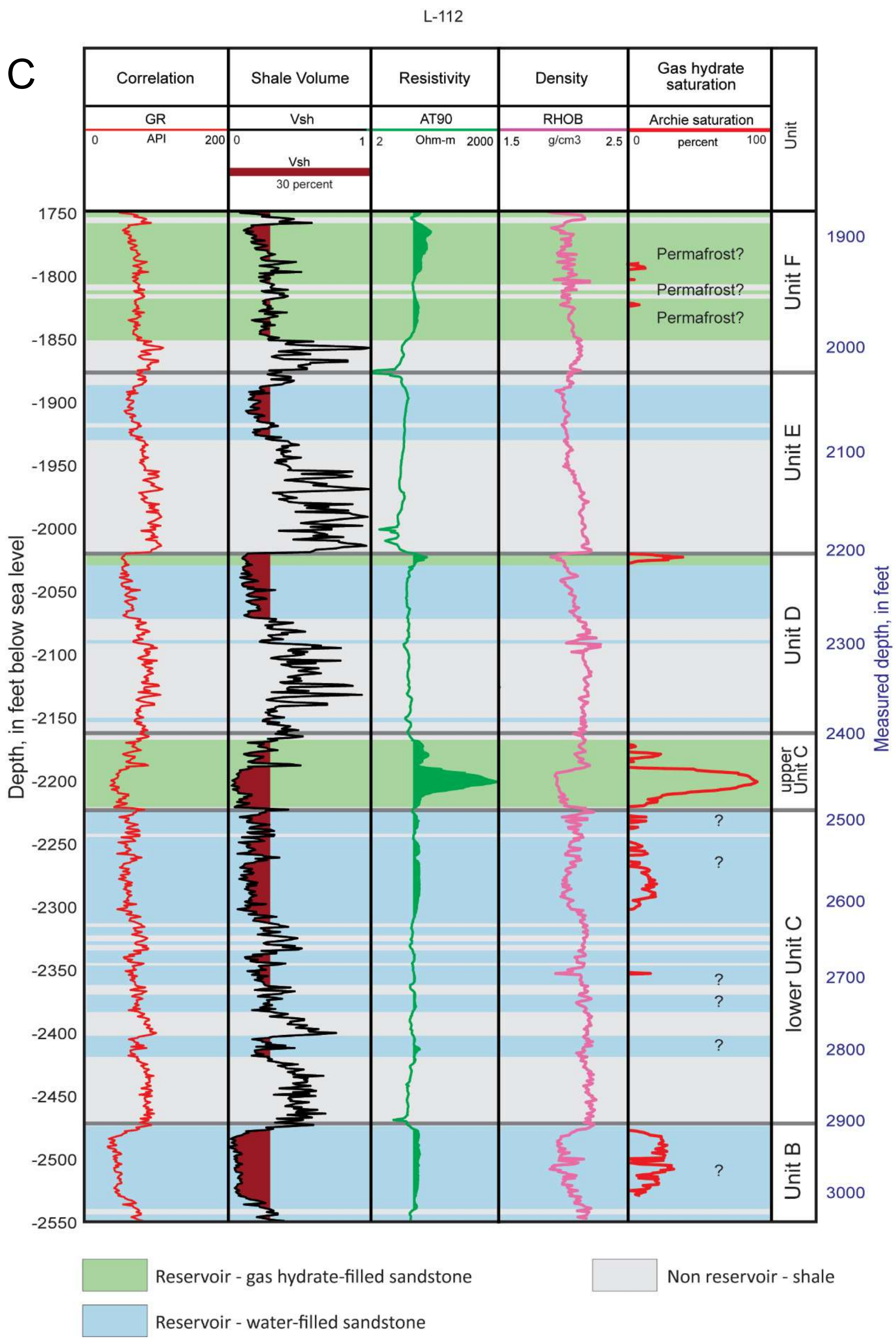

Figure 34. (C) PBU L-112 well log display as drilled in the Eileen Gas Hydrate Trend depicting the vertical distribution of reservoir and non-reservoir sections within the Units B, C, D, and E and the reservoir fill type (i.e., gas hydrate or water). Shale volume shown in decimal percent. API = American Petroleum Institute, GR = Gamma ray, Vsh = Shale volume, AT90 = Resistivity log measurement, RHOB = Bulk density

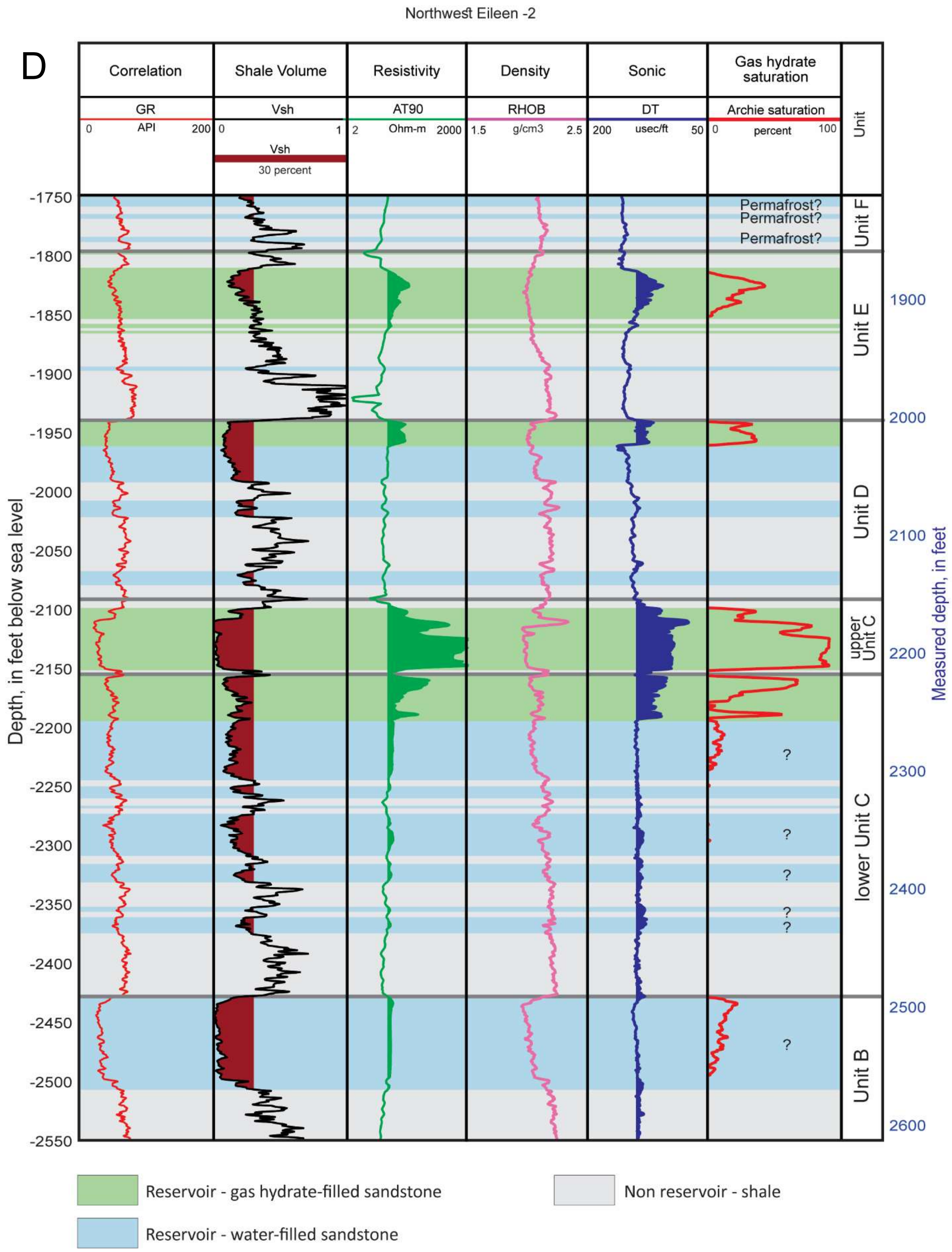

Figure 34. (D) Northwest Eileen State 2 well log display as drilled in the Eileen Gas Hydrate Trend depicting the vertical distribution of reservoir and non-reservoir sections within the Units B, C, D, and E and the reservoir fill type (i.e., gas hydrate or water). Shale volume shown in decimal percent. API = American Petroleum Institute, GR = Gamma ray, Vsh = Shale volume, AT90 = Resistivity log measurement, RHOB = Bulk density, DT = Sonic transit-time

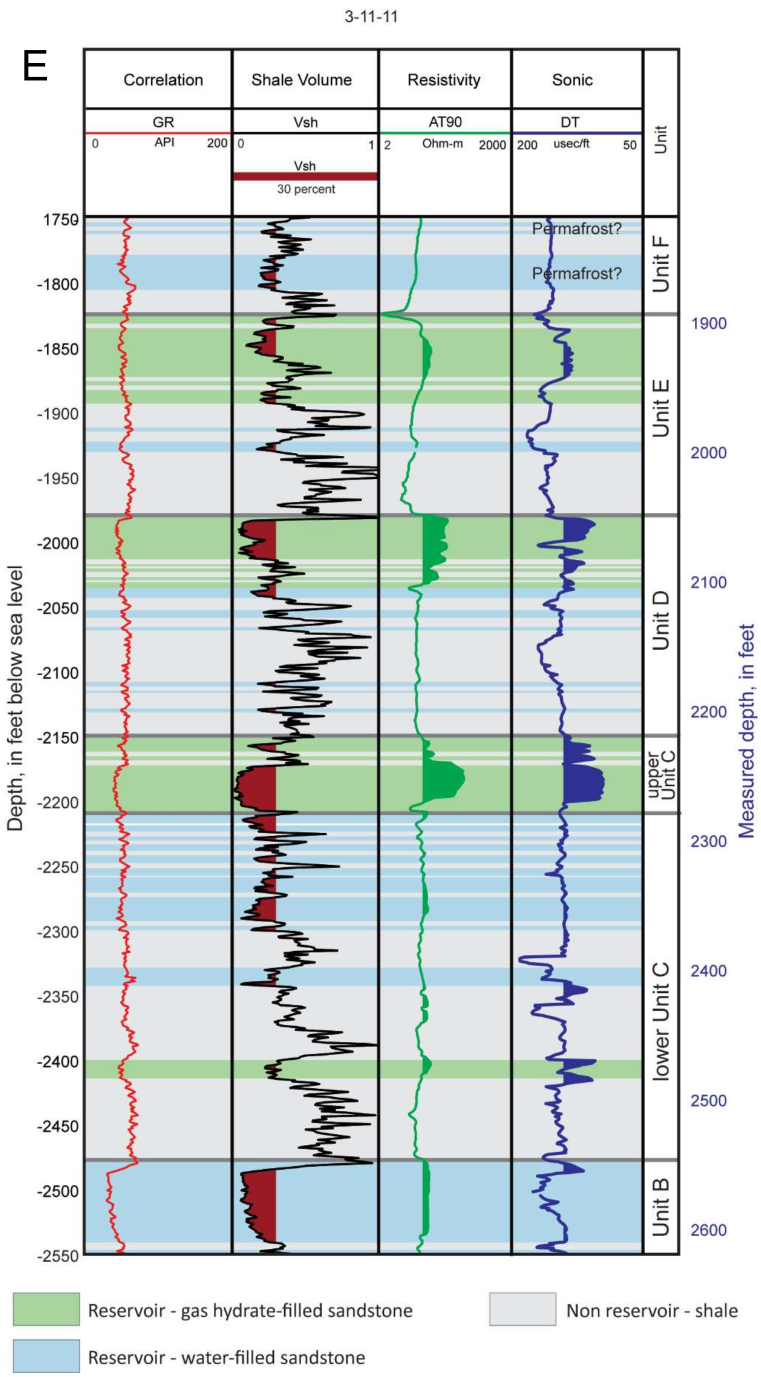

Figure 34. (E) Kuparuk 3-11-11 well log display as drilled in the Eileen Gas Hydrate Trend depicting the vertical distribution of reservoir and non-reservoir sections within the Units B, C, D, and E and the reservoir fill type (i.e., gas hydrate or water). Shale volume shown in decimal percent. API = American Petroleum Institute, GR = Gamma ray, Vsh = Shale volume, AT90 = Resistivity log measurement

E, the data points do not lend themselves to a confident determination of water-line; thus, Archie parameters using the Pickett method are hard to determine in this example from the Iġnik Sikumi well (Fig. 31A).

The next step in the process was to further subdivide the log data as shown in Figures 31B–E into the four sediment units defined in this study (i.e., Units B, C, D, and E). In Figure 31B, we consider only the log data from the Unit B in the Iġnik Sikumi well, which is known to be a sand-rich, water-saturated reservoir (Schroderbek et al., 2013). As shown in Figure 31B, there is no apparent data trend (water-saturated reservoir blue data points) that would yield reasonable Archie parameters for the Unit B. Next, we identify on the cross plot in Figure 31C the well log data values associated with the known hydrate- and water-bearing reservoir intervals in Unit C of the Iġnik Sikumi well (water-saturated reservoir blue data points and gas hydrate-bearing reservoir green data points). The data corresponding to the water-saturated intervals for Unit C, as shown in Figure 31C, are clustered together and exhibit lower *FF* log values. However, the data points as plotted for the water-bearing intervals again fail to yield a reasonable enough spread in the data distribution to allow selection of a unique water-line. The Pickett plots for Unit D (Fig. 31D) and E (Fig. 31E) known hydrate- and water-bearing intervals also do not exhibit enough of a data spread to fit unique water-lines to the data for either of the reservoir units. It was determined that, because of the limited distribution of the plotted well log-derived data values (ϕ and *FF*) for the wells examined in this study, the standard Pickett plot approach could not be used as a single method to yield reliable Archie a and m parameters.

To overcome the limitations of the Pickett cross-plot method, we have introduced another visual well log data plotting method to estimate the Archie a and m parameters. In this technique, a series of Archie resistivity log-derived gas hydrate saturation curves for a given well are calculated and plotted at the same scale assuming a range of probable Archie parameters (Fig. 32). As a starting point, the value for a was set to 1.0. The adjustments to the Archie a parameter were made if the value for a would not satisfy the physical properties of the sediments or the expected gas hydrate saturation conditions for values for a ranging from 1.0 to 1.8. The value for m, assuming unconsolidated rocks, should range from 1.3 to 1.8 due to the expected low tortuosity of the current flow path through these types of sand-rich reservoirs. However, it can be as high as 2.6 in consolidated rocks as reviewed previously in this report. Saturation curves were built to accommodate the whole range of the Archie parameter m. Archie parameter n was set to 2.0 as discussed earlier in this report. For the Iġnik Sikumi example well depicted in Figure 32, equations were formulated to generate a series of gas hydrate saturation log curves assuming the following range of Archie parameters: $1.0<a<1.8$, $1.3<m<2.5$ and $n=2.0$. Each of the calculated well log curves were grouped by their Archie parameter a in respective well log tracks. In addition, the data constraining NMR-density porosity-derived gas hydrate saturation well log curve for the Iġnik Sikumi well and the water-line (in this case, the calculated 0% gas hydrate saturation line) were plotted in each well log track (Fig. 32). The, overall, criteria for best fitting of the Archie-calculated gas hydrate saturations log curve in the Iġnik Sikumi well required that curve (1) cross the water-line at the top and base of each gas hydrate-bearing interval in Units C, D and E; (2) overlay the water-line in the hydrate-free Unit B (i.e., water saturated); (3) closely follow the NMR-derived gas hydrate saturation log; and (4) have Archie parameters that are within the expected range for the physical conditions for the reservoirs in the Iġnik Sikumi well. The format of the composite well log displays in Figure 32 allows for the quick visual comparison of the Archie-calculated gas hydrate saturation log curves and gas hydrate log saturations from other sources, such as NMR-derived. Although many curves could satisfy several of the key criteria defined above, the gas hydrate saturation curve calculated using a=1.6 and m=2.0 demonstrates the best fit to criteria for the Iġnik Sikumi well.

Figure 33 (tracks 3 and 4) demonstrates deeper understanding of the interrelationship between the Archie a and m parameters and saturations for Iġnik Sikumi well. The figure depicts two scenarios for the selection of Archie a and m parameters. As discussed earlier in this report, the Archie constant a does not have physical meaning and is mostly used to correct for hidden or unknown variables. In the first scenario, we set the value for the Archie parameter a to 1.0. Figure 33 (track 3) shows that when a=1.0, m must be as high as 2.5 to satisfy the defined criteria for the "water-line" and NMR-derived gas hydrate saturation line. Such a high m value suggests that the rocks are highly consolidated. Although gas hydrate has been shown in the Mount Elbert well to be "load bearing" and act as part of the matrix frame, it does not appear that gas hydrate plays a significant role in making the sediment matrix more rigid (Schroderbek et al., 2013). Therefore, we would not expect highly consolidated rocks in the Iġnik Sikumi well, and the value of 2.5 would be too high for accurate sediment representation. In the second scenario in Figure 33 (track 4), where a=1.6 and m=2.0, the Archie-derived gas hydrate saturation log curve closely matches the saturation log derived from the NMR and demonstrates zero gas hydrate saturation values in non-reservoir sections. In the water-bearing Unit B, both Archie- and NMR-calculated curves are matching. Also, the Archie parameters fall within the range of conditions believed to be suitable for the gas hydrate reservoir in the Iġnik Sikumi well (Figs. 32 and 33). Clearly, many different combinations of the Archie a and m parameters can be used to generate gas hydrate saturation log curves that can be fit to various independent data sets, but the selected parameters must be physically meaningful and accurately predict the physical conditions of the reservoir being examined. In this example, the parameter a was adjusted to keep the value for m within a reasonable range of values for the expected physical properties of the reservoir.

Results of the previously described integrated log display method are tested on the modified Pickett plots in Figures 31A–E The water-line (red line) representing the Archie parameters of a = 1.6 and m = 2.0, shown in each of the Pickett plots in Figures 31A–E, for the most part intercept the cluster of water-bearing data points for Units B and C. The analysis of the resistivity and acoustic sonic log data from the Iġnik Sikumi well also indicates that Unit B and a portion of Unit C were confirmed to be water saturated (Schroderbek et al., 2013). Thus, this indicates that the visual log display method used in this study appears to yield reasonable values which corelate with other approaches. Understanding the physical properties that control the selection of the Archie parameters allows the log display method to be used for wells without NMR- or core-derived saturations. This method was also applied to three additional wells (Table 6) in the area of the PBU-L Pad of the Eileen trend as depicted in Figures 34A–D.

Parameter	Value (unit)	Description
ρ_{ma}	2.65 (g/cm^3)	Matrix density
ρ_w	1.02 (g/cm^3)	Formation water density
ρ_h	0.9 (g/cm^3)	Gas hydrate density
R_w	1.08 (ohm-m)	Formation water resistivity at 5 ppm salinity

Table 5. Input parameters for gas hydrate porosity and saturation calculations using Equations 3, 6, and 8.

Well	*a*	*m*	*n*
Mount Elbert	1	1.9	2
Iġnik Sikumi	1.6	2	2
L-106	1.6	2.1	2
L-112	1.6	2.1	2
Northwest Eileen State 2	1.6	2.1	2

Table 6. Archie parameters *a*, *m*, and *n* for wells in which gas hydrate saturations have been calculated.

One of the goals in calculating gas hydrate saturations was the determination of whether one set of Archie parameters can be used for multiple units in the same well. Picket plot approach alone did not yield definitive results. The new log display method, however, allowed for greater flexibility in the calculation of gas hydrate saturations and one set of derived Archie parameters were able to reasonably predict gas hydrate saturations throughout all the hydrate-bearing units in each of the wells examined in this study (Table 2). It was also noted that the well log-derived gas hydrate saturations varied between the three gas hydrate-bearing units (Units C, D, and E) in all four wells examined in this study. The highest gas hydrate saturations were observed in the upper part of Unit C, with generally lower saturations in Unit D and the lower part of Unit C, and much lower values in Unit E. These variations in calculated gas hydrate saturations are not assumed to be an indication of partial filling of available pore space but are believed to be the product of the petrophysical properties of each unit as reviewed below. The water-saturated reservoir sand units (i.e., reservoir units with no gas hydrate), however, are likely the result of larger scale structural and stratigraphic controls and the source of the gas to charge the available reservoir sand units as reviewed below.

Reservoir Fluid Content and Permeability

As previously reviewed in this report, the permeability of the reservoir system to the migration of water and gas is an important control on the formation of gas hydrate in nature. Advances in NMR logging, formation wireline testing, and conventional formation testing yielded important information on how gas hydrates are physically distributed at the pore scale (Kleinberg et al., 2005) and the type and concentration of the pore-filling substances (i.e., gas hydrate, free water, clay- and capillary-bound water). Within the Eileen Gas Hydrate Accumulation, the hydrate-bearing reservoirs in the Mount Elbert and Iġnik Sikumi test wells were NMR logged and the formation was tested by a combination of wireline deployed tools and flow tests (Collett et al., 2011b;

Schroderbek et al., 2013; Boswell et al., 2017). Sediment cores recovered from the Mount Elbert well also yielded additional information on the petrophysical properties of the hydrate-bearing reservoir units in the Eileen trend. Porosity in the low-shale content sand reservoir sections of Units C, D, and E average about 40%. Core-derived estimates of intrinsic permeabilities in the hydrate-bearing reservoirs of the Mount Elbert well were high, with peak values measuring as high as 1000 mD (Boswell et al., 2011b). Sediment cores from the Mount Elbert hydrate-bearing units are generally fine-grained sands and coarse silts (Winters et al., 2011). Small changes in porosity (~4%), caused by going from poorly sorted to well-sorted intervals or due to modest decreases in grain size, result in significant changes in reservoir intrinsic permeability, thus, limiting the ability of gas and water to migrate into the potential reservoir sedimentary faces (Winters et al., 2011; Boswell et al., 2011b). Clay-dominated layers bounding the sand bodies also serve as low permeability impedance boundaries to the vertical flow of gas and water.

The in situ NMR log measurements of effective permeabilities in the Mount Elbert hydrate-bearing reservoirs yield low values (0.01 to 0.1 mD), which have been attributed to the presence of gas hydrate filling the larger pores and impeding fluid flow in the reservoir section. Evaluation of wireline formation tests of the upper Unit C in the Mount Elbert well also yielded low effective-permeability estimates in the range of 0.12 to 0.17 mD (Anderson et al., 2011a). The NMR log in the Mount Elbert well also indicates the presence of both bound and moveable water in the hydrate-bearing portion of the reservoir units, with the moveable water phase in the upper Unit C exceeding 15% of measured pore volume. The successful depressurization of the upper Unit C by fluid withdrawal during the formation wireline testing confirms the observation that even low effective-permeability hydrate-bearing reservoirs contain moveable water. The NMR log in the Iġnik Sikumi well (Fig. 35) also indicated the presence of clay-bound (~6%), capillary-bound (~7%), and movable water (~6%) in upper homogeneous and highly saturated hydrate bearing portions of Unit C (Schroderbek et al., 2013). Estimates of sediment permeabilities based on NMR measurements were calculated by both the Schlumberger-Doll Research (SDR) and Timur/Coates methods (Kleinberg et al., 2005). Both approaches generated permeability values greater than 1000 mD in the water-bearing portion of the Unit C and B sands, but effective permeabilities were calculated to be less than 1 mD in the hydrate-bearing portion of the upper Unit C.

The Schlumberger wireline deployed Pressure Express (XPT) and Modular Dynamic Tool (MDT) formation testing tools were used in the Iġnik Sikumi well to measure formation pressures and estimate fluid mobility (i.e., permeability) in Units C and D (Schroderbek et al., 2013). Estimated XPT- and NMR-derived effective permeabilities were in most cases <0.1 mD, similar to the values predicted from the NMR log. During the injection phase of the Iġnik Sikumi production test, where 215900 Msf (6113.6 m^3) of mixed N_2 and CO_2 gas was injected into the upper Unit C, the effective permeability at the start of the test was estimated to be 5.5 mD and it decreased to values as low as 0.6 mD by the end of the injection phase (Boswell et al., 2017).

Recent analysis of recovered pressure core samples from offshore Japan (Konno et al., 2015) and India (Yoneda et al., 2019) have shown that the effective permeabilities within gas hydrate-bearing reservoirs may actually be higher than those predicted from analyses of NMR log and MDT testing data from both Arctic terrestrial and marine gas

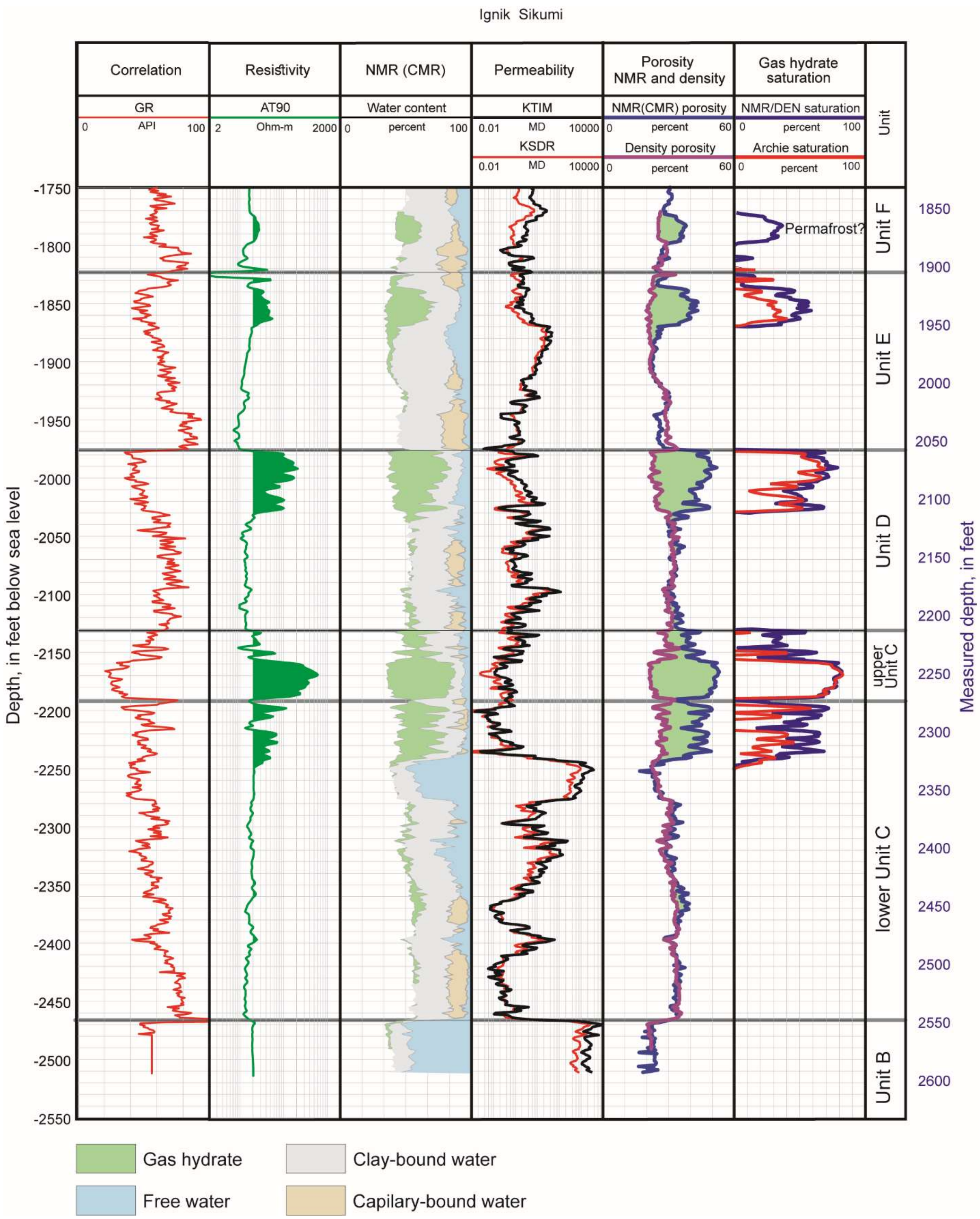

Figure 35. Log display for the Iġnik Sikumi well depicting NMR (CMR, Combinable Magnetic Resonance tool) log-derived sediment permeabilities and concentration of the pore-filling substances, including gas hydrate, free-water, and bound-water. API = American Petroleum Institute, GR = Gamma ray, Vsh = Shale volume, AT90 = Resistivity log measurement, RHOB = Bulk density, DT = Sonic transit-time, NMR = Nuclear Magnetic Resonance, CMR = Nuclear magnetic resonance logging tool, KTIM = Timur/Coates Permeability, KSDR = Schlumberger-Doll-Research Permeability

hydrate research wells (as reviewed by Boswell et al., 2019). These new pressure core results show that the effective permeability of hydrate reservoir systems may be more variable and range from less than 1 mD to several 10s of mD. The analysis of the Iġnik Sikumi production test injection data also indicated much higher initial reservoir permeability with a reported value 5.5 mD (as reviewed above in this report). No pressure cores have been recovered from the gas hydrate research wells drilled in the ANS; thus, we were unable to check the validity of the NMR- and MDT-derived permeabilities for the Eileen trend. For analysis of the permeability controls on the occurrence of gas hydrate in this review, we have assumed that the NMR log-derived permeabilities can still be used to assess the relative petrophysical controls on the occurrence of gas hydrate in the hydrate-bearing reservoirs encountered within the Eileen trend.

As shown in Figures 34A–D, the well log-derived gas hydrate saturations vary between Units C, D, and E in the Eileen trend. As reviewed above, the non-hydrate bearing portion of the pore-volume in each reservoir is occupied by a combination of clay-bound, capillary-bound, and movable water. We infer that each of the partially saturated hydrate-bearing reservoir sections are filled to their "petrophysically defined capacity," with the gas hydrate content varying with grain size, clay content, and bound- and free-water content. The dependency between petrophysical properties and gas hydrate and water content in a reservoir can be seen in the Iġnik Sikumi well display in Figure 35, where despite the fact that upper Unit C has the lowest observed water saturations (or highest S_h), this unit actually contains relatively more free-water and less bound water because of the low shale volume.

The concept of a petrophysically defined capacity for a gas hydrate occurrence was first developed in the 2008 U.S. Department of the Interior Minerals Management Service (now known as the Bureau of Ocean Energy Management) assessment of in-place gas hydrate resources in the Gulf of Mexico (Frye, 2008). In this assessment study, the fraction of a particular rock volume, identified by lithology type, that contains "effective" void space (i.e., porosity) and can contain gas hydrate was first calculated. For the next step in this process, the percent of the porosity that can be occupied by gas hydrate as a function of lithology and porosity type (sand, shale, and fractured reservoirs in this case) was derived from a database of wells where well logs and core data had been used to estimate gas hydrate saturations for a wide range of reservoir conditions.

Structural and Stratigraphic Controls on the Occurrence of Gas Hydrate

In this section of the report, we combine new information from this study on well log-determined gas hydrate occurrence and reservoir saturations with a refined structural and stratigraphic framework for the hydrate-bearing sand units to examine the structural and stratigraphic controls on the occurrence of gas hydrate within the Eileen Gas Hydrate Trend.

Pre Iġnik Sikumi Test Geological Framework Studies

One of the first critical steps in the Iġnik Sikumi test well project was the selection of a suitable production test site, which was conducted as a cooperative effort by geoscientists from the DOE, ConocoPhillips, and the USGS (Farrell et al., 2010; Collett et al., 2015; Schoderbek et al., 2013). As reviewed above in this report, seven sites, thought to contain gas hydrate within the Eileen trend, were examined based on criteria of infrastructure access and geologic risk of encountering gas hydrate, amongst other considerations. Eventually, two sites were selected for further detailed evaluation in the Westend of the PBU: (1) the PBU L-Pad and (2) the Kuparuk State 3-11-11 wellsite (Collett et al., 2012). Based on available log data, both locations were inferred to contain gas hydrate-bearing sands at the Unit C, D, and E levels, similar to the logged and cored gas hydrate occurrences in the Northwest Eileen State 2 and Mount Elbert wells.

Seismic data were not available in this initial evaluation of gas hydrate prospects in the Westend of the PBU; however, gamma-ray logs from 55 development wells from the PBU L-Pad were available and used to map the local distribution of potential gas hydrate reservoirs in and around the well pad, with only one well (PBU L-106) containing a full suite of well logs for gas hydrate saturation estimation. The Kuparuk State 3-11-11 well site was less developed, with only one well penetration, and a thinner gas hydrate reservoir section (Fig. 34E). Therefore, the PBU L-Pad became the focus of the Iġnik Sikumi test planning effort (Collett et al., 2012; Schoderbek et al., 2012, 2013) (Figs. 27, 28 and 29).

As part of the initial PBU L-Pad area test site review process, a numerical simulator was run to predict how a gas hydrate production test well would perform at this site. To construct the numerical simulator, gamma-ray log data were used to build a structural and stratigraphic framework for the area around the PBU L-Pad (Collett et al., 2012). Scheihing (2010) also used available well log data and a 3D seismic data volume to build a highly generalized structural map of several of the potential gas hydrate-bearing stratigraphic units in the area of the PBU L-Pad (Fig. 36A-B). The structure map on the top of the youngest known gas hydrate-bearing unit (i.e., Unit F) in Scheihing (2010) was used by ConocoPhillips to construct a 3D structural model for the PBU L-Pad gas hydrate accumulation. The resulting map and reservoir model showed that the gross interval thicknesses of the sand-dominated sections are fairly consistent across the area. Based on previous studies, Scheihing (2010) described Units C, D, and E as gas hydrate-bearing and Units B and F as water saturated.

Post Iġnik Sikumi Test Geological Framework Studies

In support of the analysis of the Iġnik Sikumi test results, the USGS conducted an expanded and more detailed field study of the gas hydrate occurrences both in and around the PBU L-Pad. This new effort refined our understanding of the geologic controls on the occurrence of gas hydrate within the greater Eileen Gas Hydrate Trend, supported gas hydrate production modeling studies (Anderson et al., 2014; Boswell et al., 2017), and contributed to gas hydrate assessment efforts in the USGS.

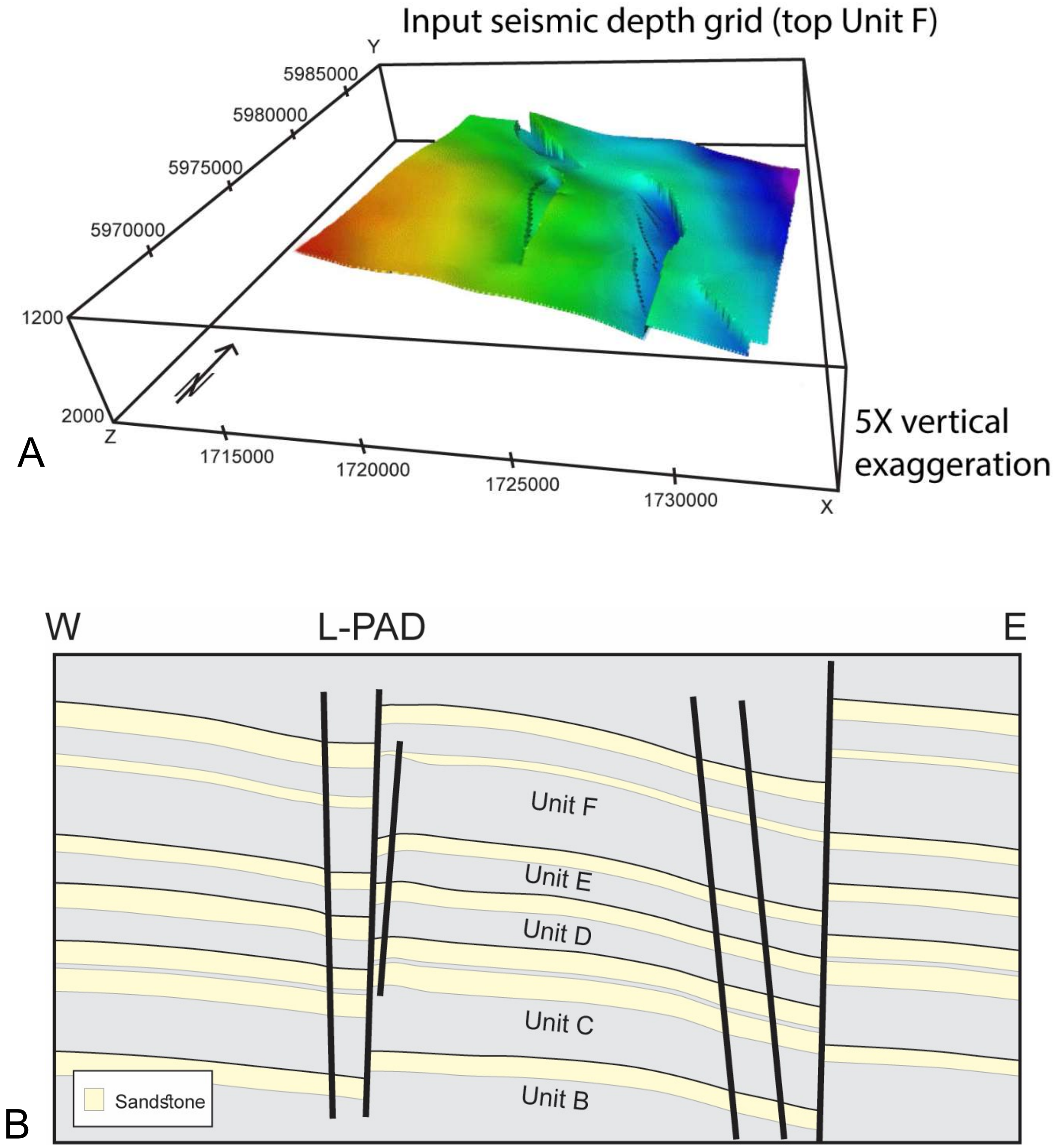

Figure 36. (A) Seismically defined structure grid of the top of Unit F in the area of the PBU L Pad. (B) Generalized stratigraphic cross section with inferred fault positions for the Units B–F in the area of the PBU L Pad derived from available 3D seismic data volumes. Both displays were modified from Schoderbek et al., (2013), location and depth scales of the depicted cross section and structure images were not provided.

Well log data from a total of 112 wells in the Westend of the PBU and surrounding areas, including the State Socal 33-29-E, Northwest Eileen State 1 and 2, PBU L-112, Northwest Eileen 01-01, PBU L-106, Iġnik Sikumi 1, Kuparuk 3-11-11, PBU V-107, and Mount Elbert 1 wells, along with additional oil field development wells drilled from the PBU L-Pad and the PBU V-Pad (Figs. 27, 28 and 29) were acquired from public files maintained by the Alaska Oil and Gas Conservation Commission (2020). As reviewed previously, a total of 90 wells that had sufficient gamma-ray log data through the target interval of interest (Units B through E) were used to map the geologic structure and determine the reservoir properties of the gas hydrate-bearing reservoirs (Figs. 28 and 29). Most of the wells in study area are located on oil field development gravel pads and were drilled as deviated wells from the pads to penetrate the deeper oil reservoirs some distance from the pads as shown in Figs. 28 and 29.

Access to only published seismic images and analysis (Silpngarmlert, 2010; Schoderbek et al., 2013) and the limited nature of the well data in the study area made it challenging to thoroughly characterize and map the geologic structure, the distribution of the major reservoir sand units, and the occurrence of gas hydrate within them. Previous studies on the ANS indicated that the general orientation of the regional deep faults in the oil-bearing Sadlerochit sandstone are northwest to southeast (Fig. 36A-B) (Chatterton, 1983; Schoderbek et al., 2012, 2013; Boswell et al., 2017). Deep faults in the vicinity of PBU L-Pad also have a nearly north-south orientation (Chatterton, 1983). Additional structural studies along the western margin of the Prudhoe Bay oil field have described the local faults as near vertical, connecting deep and shallow sediments that have served as migration conduits, in some cases, seals (Chatterton, 1983; Silpngarmlert, 2010; Boswell et al., 2011b; Collett et al., 2011a, 2011b; Schoderbek et al., 2012, 2013; Boswell et al., 2017). Because of the highly deviated nature of most of the wells utilized in this study, the well log data were analyzed for distortions related to high-angle penetrations of both geologic units and faults. As a starting point, all the available well log gamma-ray signatures were converted to true-vertical depth (TVD) displays and correlated across the study area (Fig. 37A–B). Evidence of fault-related displacements were inferred where wells showed repeated (or anomalously thickened) or missing (or anomalously thinned) sections. Discontinuities along some of the shallow mapped horizons were attributed to sediment erosion rather than to faulting.

The stratigraphic framework as shown on north-south and west-east oriented cross sections (Fig. 37A, B), through the approximate center of the study area, showed the presence of potential multiple thick sand reservoir units. Gross interval thicknesses are generally consistent across the study area. The upper boundaries of the major gas hydrate-bearing sand reservoir units (Units A–F) appear as well-defined, continuous features on the well log correlation sections and are indicated by low gamma ray log values associated with increased sand volume.

The map of seismically defined geologic structure map of the top of Unit F (Silpngarmlert, 2010) (Fig. 36A) was georeferenced with maps created in this study for the Units C and D (Fig. 38A, B) to verify and extend the well log-derived structural framework. The locations of the faults as determined from the well log interpretation agree well with the seismically imaged faults mapped by Silpngarmlert (2010). The well log-inferred faults in the area of the PBU L-Pad are mostly high angle normal faults and

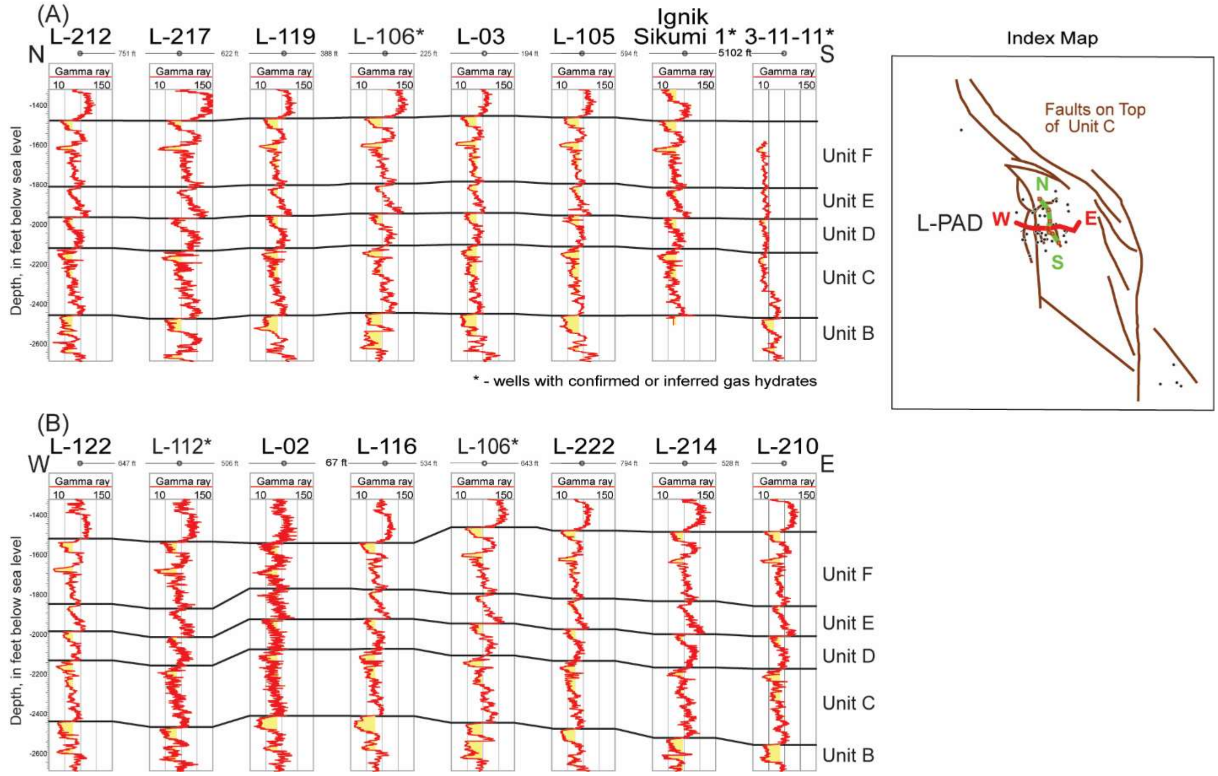

Figure 37. (A) North-south and (B) west-east cross sections though the PBU L-Pad. Wells PBU L-02 and PBU L-116 both show missing section associated with faults. Index map indicates the locations of the cross sections relative to the PBU L-Pad and major faults depicted in Figure 38.

their mapped locations are nearly coincident with the published seismically mapped location of the faults at the top of Unit F. The more deeply buried, nearly vertical fault systems mapped by Chatterton (1983) were also georeferenced with the structures defined in this study and showed close spatial correlation between the two mapped systems. The close correlation between the well log- and seismic-inferred structural framework in the area of available overlapping data allowed the well-log-inferred structural framework to be projected beyond the limits of the well log database. Seismically imaged, large-displacement faults as shown by Silpngarmlert (2010) were included in the composite structural-stratigraphic map (Figure 38A, B). The maps on the top of Units C and D developed in this study reveal a monoclinal structure with a dip of about 3–5° to the east-northeast. This monocline is disrupted by several large arcuate, down-to-the-east, normal faults that trend roughly northwest-southeast.

A stratigraphic cross section using select wells with enough log data to distinguish the presence of gas hydrate has been plotted in Figure 39 through a portion of the Eileen Gas Hydrate Trend and the location of the PBU L-Pad and the Iġnik Sikumi well. Figure 39 also depicts the relationship of the delineated reservoir sections to the base of ice-bearing permafrost (BIBPF) and the predicted base of the gas hydrate stability zone. In the area of the PBU L-Pad (Fig. 39), the upper Unit C in the Iġnik Sikumi and PBU L-106

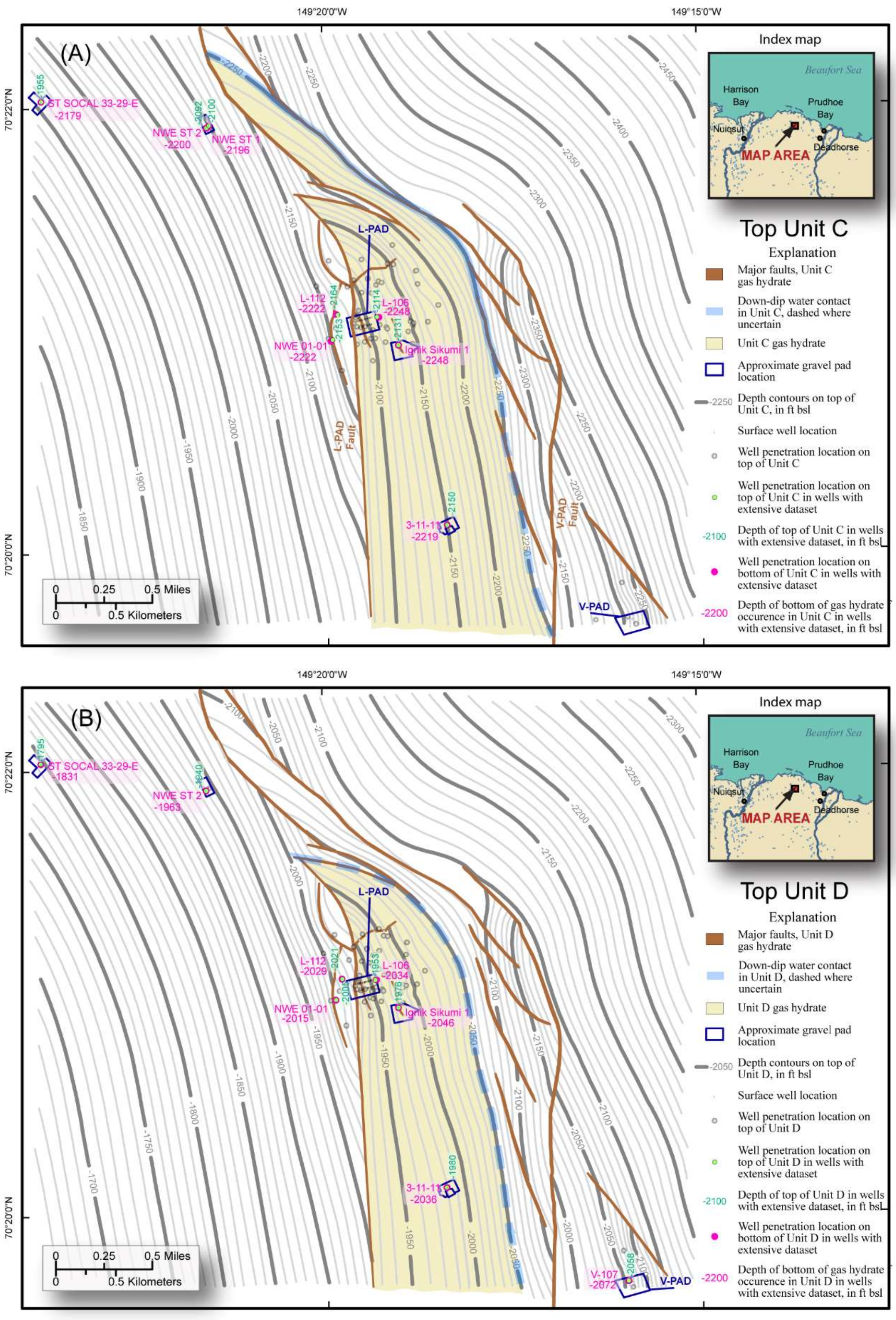

Figure 38. Structure map on top of (A) Unit C and (B) Unit D (modified from Collett et al., 2012). Contour interval is 10 ft. Yellow shading indicates the inferred minimal gas hydrate occurrence. bsl = below sea level

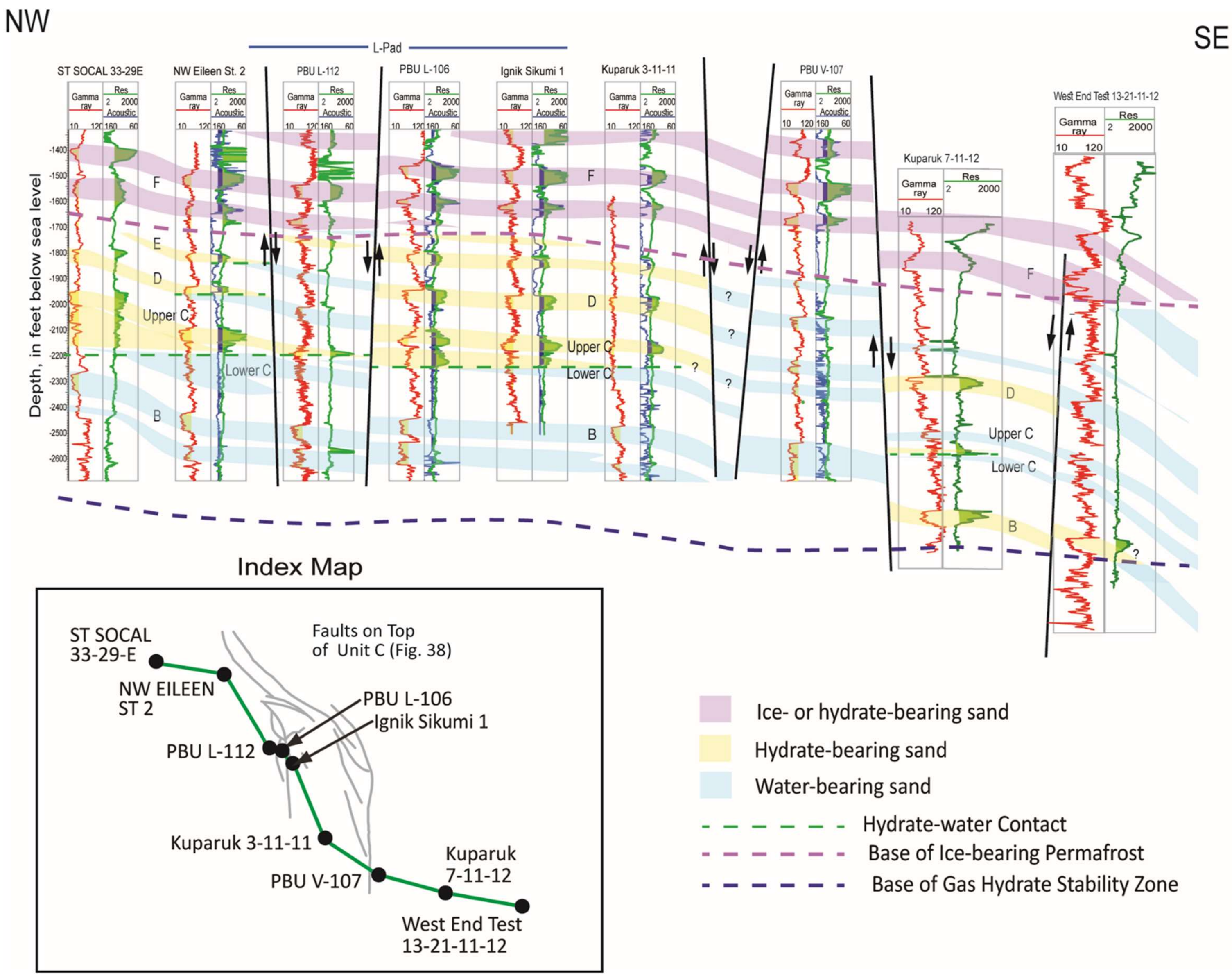

Figure 39. Well log cross section showing the lateral and vertical extent of the predominantly gas hydrate- and water-bearing reservoirs extending from the State SOCAL 33-29E well to the West End Test 13-21-11-12 well that crosses the area of the PBU L-Pad (modified from Boswell et al., 2017). The gas hydrate-bearing units in the Eileen trend are identified with the reference letters B through F (modified from Collett, 1993). The relationship of the gas hydrate-bearing portions of Units F through B to nearby faults and the gas hydrate-water contact are also shown. Res = Resistivity well log, Acoustic = Acoustic (sonic) well log

wells are inferred to be occupied fully by gas hydrate at high concentrations (Figs. 34A, B). The lower Unit C, however, is only partially filled with gas hydrate, with a gas hydrate/water contact occurring at depth of approximately 2248 ft (685 m) below sea level in both the PBU L-106 and Iġnik Sikumi wells. Considering the common gas hydrate/water contact depth in both the PBU L-106 and Iġnik Sikumi wells, and the fact that both wells are located in the same mapped fault block (Fig. 38A), it is likely that the hydrate/water contact extends throughout the mapped fault bock. Assuming the occurrence of gas hydrate in the Unit C conforms to the structure map on top of Unit C, the "PBU-L pad gas hydrate accumulation" can be mapped as shown by the yellow shading in Figure 38A.

The major PBU L-Pad "west bounding fault" showed more than ~100 ft (~30 m) of throw at the depths of Units C and D (Figs. 38A and 39) and is interpreted to act as the lateral trap to the gas-hydrate-filled portions of Units C and D in the mapped structure. The eastern limit of the lower Unit C gas hydrates accumulation at the PBU L-Pad is defined by the hydrate/water contact observed in the PBU L-106 and Iġnik Sikumi wells at a common depth of 2248 ft (685 m). The closure along the northern part of the structure appears to be against a series of northwest- to southeast-trending arcuate faults. The control on the occurrence of gas hydrate in Unit C to the south is less clear. In Figure 38A, the PBU L-Pad west bounding fault and the Unit C structural contours are shown extending to the south with the southern limit of the gas hydrate accumulation in this fault block depicted as unknown. As shown in the map of Unit C in Figure 38B and the well log cross section in Figure 39, the Kuparuk 3-11-11 well is inferred to be located in the same fault block with the PBU L-106 and Iġnik Sikumi wells, as such it would be reasonable to expect that the gas hydrate/water contact could be at the same depth in all three wells. In the Kuparuk 3-11-11, however, the occurrence of gas hydrate is limited to the upper Unit C (base of which is at a depth of 2219 ft (676 m), with no gas hydrate in the lower C Unit (Figs. 34E, 38A, and 39).

As shown in Figures 38A and 39, the PBU L-112 and Northwest Eileen 01-01 wells also penetrated gas hydrate-bearing sediments in the upper Unit C in a down-thrown fault block west of the PBU L-Pad "west bounding fault." In both wells, the upper C Unit is only partially filled with gas hydrate, with a gas hydrate/water contact occurring at a common depth of approximately 2222 ft (677 m). The Northwest Eileen State 2 and State SOCAL 33-29-E wells are located to the northwest of the PBU L-112 and Northwest Eileen 01-01 wells and are separated from them by an up-to-the-northwest normal fault (Figure 39). Unit C in the Northwest Eileen State 2 (Fig. 34D) and State SOCAL 33-29-E wells appears to be partially filled with gas hydrate with the well-log inferred gas hydrate/water contacts at depths of 2196 ft (670 m) and 2179 ft (664 m), respectively.

At the far downdip end of the cross section in Figure 39, the PBU V-107 well is separated from the Units C, D, and E gas hydrate occurrences in the greater PBU L-Pad area by a series of north-south trending faults (Figs. 38A, B) and the well logs from PBU V-107 did not indicate the presence of gas hydrate at any depth in the PBU V-107 well.

The structure map of the top of Unit D closely matches that of the top of Unit C (Figs. 38A and B). The top of Unit D is marked by an abrupt contact from what appears to be a high-quality sand reservoir section into an overlying high gamma-ray shale (Fig. 39).

Using the same well log analysis criteria to identify the presence of gas hydrate as was used for the analysis of Unit C, it appears that Unit D is gas hydrate bearing throughout most of the area examined in this study (Fig. 38B). Within the fault block penetrated by the PBU L-106, Iġnik Sikumi, and Kuparuk 3-11-11 wells, the depth to the base of the gas hydrate occurrence in Unit D varies between wells and conforms to the stratigraphic dip, unlike that for Unit C. In addition, the reservoir portion of Unit D is inferred to be fully occupied by gas hydrate at high concentrations (i.e., to its "petrophysically defined capacity") in the immediate area of the PBU-L Pad. Thus, the occurrence of gas hydrate in Unit D appears to be controlled in part by stratigraphy and reservoir quality.

The areal extent of gas hydrate occurrence in the shallower Unit E could not be determined with certainty due to the poor data quality and distribution of the wells at shallow depths around the PBU-L Pad. As depicted in Figure 39, it appears that the Unit E reservoir section is completely filled with gas hydrate much like Unit D in the PBU L-Pad fault block. However, both Units D and E were determined to be void of or only partially filled with gas hydrate in the wells drilled updip of the PBU-L Pad.

Finally, the more deeply buried, massively bedded, high porosity, sand-rich Unit B in the PBU L-Pad area wells was interpreted to be only water bearing with no gas hydrate (Lee et al., 2011; Lee and Collett, 2011; Torres et al., 2011), which has been attributed to the lack of trap development in this reservoir section.

The Eileen Gas Hydrate Trend - Controls on the Occurrence of Gas Hydrate – Summary

Gas hydrate in the Eileen Gas Hydrate Trend occurs over a wide range of conditions as shown in the well log correlation section depicted in Figure 39, where the lower boundary of the well log-inferred gas hydrate occurrences is often marked by sharp contacts, despite the reservoir, in some cases, having additional sand-rich, water-saturated reservoir units below the base of the deepest gas hydrate occurrence. This suggests that the reservoir intervals were only partially filled to their capacity by gas hydrate as seen in lower Unit C in the Iġnik Sikumi (Fig. 34A), PBU L-106 (Fig. 34B), PBU L-112 (Fig. 34C), Northwest Eileen State 2 (Fig. 34D), and Northwest Eileen 01-01 wells. Further analysis of gas hydrate to water contacts across the study area suggests the presence of laterally extensive hydrate- and water-bearing reservoir sections along with a series of major north-south trending faults that compartmentalize the reservoirs into several discrete structural fault blocks. These fault blocks contain thick gas hydrate accumulations often in contact with underlying water-bearing reservoir sections.

The examination of the well log correlation section depicted in Figure 39 and well log displays of the hydrate-bearing reservoir sections in Figures 34A–E also indicates that the occurrence of gas hydrate in the Eileen Gas Hydrate Trend is controlled in part by the "quality" or clay content (defined as volume of shale or V_{sh} within this study) of the potential reservoir sections. For example, the Unit D reservoir section in the PBU L-106 (Fig. 34B) and Iġnik Sikumi (Fig. 34A) wells (as defined by sedimentary sections with V_{sh} values of <30%) appear to be completely filled with gas hydrate at high saturations. However, the gas-hydrate-bearing portion of the Unit C reservoir section in the same two wells is underlain and is in direct contact with water-saturated reservoir sections (i.e., with V_{sh} values of <30%). Along the well log correlation section in Figure 39, the Unit

C gas-hydrate-bearing reservoir section in the Kuparuk 3-11-11 well (Fig. 34E) thins to about half of the thickness of the reservoir section observed in the PBU L-106 and Iġnik Sikumi wells (Figure 34A, B), and the gas-hydrate-bearing reservoir section appears to be underlain by both thinly bedded non-reservoir V_{sh}-rich sections and water-saturated reservoir sections. A critical question reviewed here is what are the geologic and reservoir controls on these two very different gas hydrate occurrences in the same stratigraphic section?

A closer examination of the well log data in Figures 34A, B reveals that the hydrate- and water-bearing reservoir section in Unit C of the PBU L-106 and Iġnik Sikumi wells are about 297 and 203 ft (91 and 62 m) thick, respectively. However, the hydrate- and water-bearing reservoir section in Unit C of the Kuparuk 3-11-11 (Fig. 34E) is only about 151 ft (46 m) thick. In comparison, the lower Unit C in Kuparuk 3-11-11 consists mostly of a series of thinly bedded non-reservoir shale-rich sections and interbedded water-saturated sands.

As previously discussed, the petrophysical properties of the sedimentary section are important controls on the occurrence of gas hydrate. The well log displays (Figures 34A–D and 35) clearly show that the occurrence of gas hydrate within the stratigraphic section (Fig. 39) at a given site is controlled in part by the quality of the reservoir or in this case the volume of clay (in this study described as shale volume, V_{sh}) within the stratigraphic section. All the well log inferred, gas hydrate-bearing reservoir sections in the Eileen trend exhibit well log-inferred V_{sh} values of less than 30%. It is assumed that clays dispersed in the coarse-grained sediment matrix in each potential reservoir section limit the entry of gas into the available pore-space and subsequent nucleation of gas hydrate; thus, limiting the "petrophysically defined capacity" of the fine-sand and coarse-silt reservoirs to contain gas hydrate. In the case where the sedimentary section has V_{sh} values of less than 30%, gas hydrate or water is found completely filling the available reservoir section.

The analysis of the well log data and insights gained from previous published seismic data studies has clearly shown that the occurrence of gas hydrates in the Eileen Gas Hydrate Trend is controlled by a series of interrelated petrophysical, stratigraphic, and structural controls. The major results of the analysis of the geologic controls on the occurrence of gas hydrate in the Eileen Gas Hydrate Trend include the following:

- Structural-stratigraphic mapping, based on well log correlation studies and previously published seismic mapping projects yielded a more detailed understanding of the occurrence and distribution of three prominent gas hydrate-bearing stratigraphic units (Units C, D, and E) within the Eileen Gas Hydrate Trend.

- Reservoir quality indicators (including gamma-ray derived shale volumes) and the analysis of the well log data (including resistivity and acoustic transit-time logs) provided the criteria to accurately define the limits and geologic controls on the occurrence of gas hydrate in the Eileen Gas Hydrate Trend.

- NMR log data, when combined with independent sources of accurate in situ sediment porosities (such as from density log data), was shown to yield accurate gas hydrate saturations and reservoir petrophysical data on the hydrate-bearing reservoirs as penetrated in the Iġnik Sikumi gas hydrate test well in the Westend of the PBU.

- Various forms of the Archie relationship, with special consideration given to the values of the required Archie *a, m,* and *n* parameters, yielded gas hydrate saturations from resistivity log data that compare favorably with gas hydrate saturations calculated by other methods. It was also shown that the Pickett plot method alone did not yield reliable empirical parameters for Archie calculated gas hydrate saturations in this study; however, a new visually based well log data plotting method was developed and shown to yield accurate Archie parameters within the hydrate-bearing reservoir sections in the Eileen Gas Hydrate Trend.

- The Archie-derived gas hydrate saturations for the five wells (Northwest Eileen State 2, PBU L-112, PBU L-106, Iġnik Sikumi, and Mount Elbert wells) examined in this study from the Eileen Gas Hydrate Trend varied between well locations and gas hydrate-bearing units (Units C, D, and E). These variations were shown to be a product of the petrophysical properties of the host reservoir.

- In the Eileen Gas Hydrate Trend, the hydrate-bearing reservoirs were shown to be limited to sedimentary sections with clay content (shale volume as defined in this study) of 30% and less. The "petrophysically defined capacity" of a reservoir to contain gas hydrate was attributed to the relative volume of clay (shale) in the reservoir section.

- Well log correlation studies and petrophysical analysis of available log data have shown that the lateral distribution of gas hydrate in at least one of the mapped hydrate-bearing units (Unit C) is controlled by changes in stratigraphy from areas of more massive and thicker sand-rich reservoir sections to more thinly interbedded non-reservoir clay- and sand-rich sections.

- One of the more striking discoveries in the area of the PBU L-Pad is the presence of laterally continuous, flat-lying, gas-hydrate/water contacts that revealed the presence of laterally continuous down-dip water accumulations that are in direct contact with overlying hydrate-bearing reservoir sections; thus, documenting the presence of partially hydrate filled reservoir sections.

3.B.2. Reevaluation of Test Site Locations in the Eileen Gas Hydrate Trend

The science and engineering studies in support of the 2007 Mount Elbert Gas Hydrate Stratigraphic Test Well project and the 2011/2012 Iġnik Sikumi Gas Hydrate Production Test Well project yielded two of the most comprehensive datasets on the occurrence of gas hydrates in an Arctic permafrost setting including those within the Eileen Gas Hydrate Trend. This section of the IA Final Report provides a detailed reexamination of the potential test sites along the Eileen Gas Hydrate Trend with a focus on the gas hydrate accumulations in the PBU.

This new 2017 test site review considered similar criteria to the initial 2011 site review effort that led to the selection of the PBU L-106 test site and the drilling of the Iġnik Sikumi test well. The site selection criteria used in this new 2017 effort were similar to the approach used in the 2011 review, as listed in Table 4; several additional more complex concerns were also evaluated as listed below:

- State of Alaska regulations required that all producing ("live wells") wells be accessible by either ice roads or all-season gravel roads.

- As previously reviewed in this report, the use of ice roads and ice drill pads are limited most years to the months of January through mid-May, thus limiting the duration of any testing program.

- Other access options like insulated ice roads/pads that have been used for the summer storage of drilling rigs were considered to extend the proposed gas hydrate testing operation window; however, it was concluded that these more complex options were not feasible.

- Another consideration included the construction of a new gravel pad and/or building an extension onto an existing gravel development pad or road. It was determined that the length of time required to build a new gravel pad (12–18 months) and the associated cost and permitting process would add significant challenges to the project.

- The primary option for a test site became gaining access to an active development pad or possibly an old exploration pad that had been either abandoned and/or converted to a storage pad with no facilities, which are often used to support other general field operations.

- In this new site review effort, additional emphasis was also given to the requirements to effectively and safely dispose of both fluids and gas produced during the gas hydrate test.

Given the various considerations of site access, favorable geologic conditions, testing requirements, and limiting impact on unit operations, a total of six surface locations in the MPU and PBU were evaluated as candidate sites for an extended gas hydrate production test (Table 7; Figs. 40, 41).

Evaluation of Locations in the Milne Point Unit (MPU)

Mount Elbert Well Site

The reevaluation of potential gas hydrate production test sites in the MPU included the consideration of testing the Mount Elbert Prospect, which was previously drilled and confirmed to contain significant gas hydrate accumulations with the completion of the

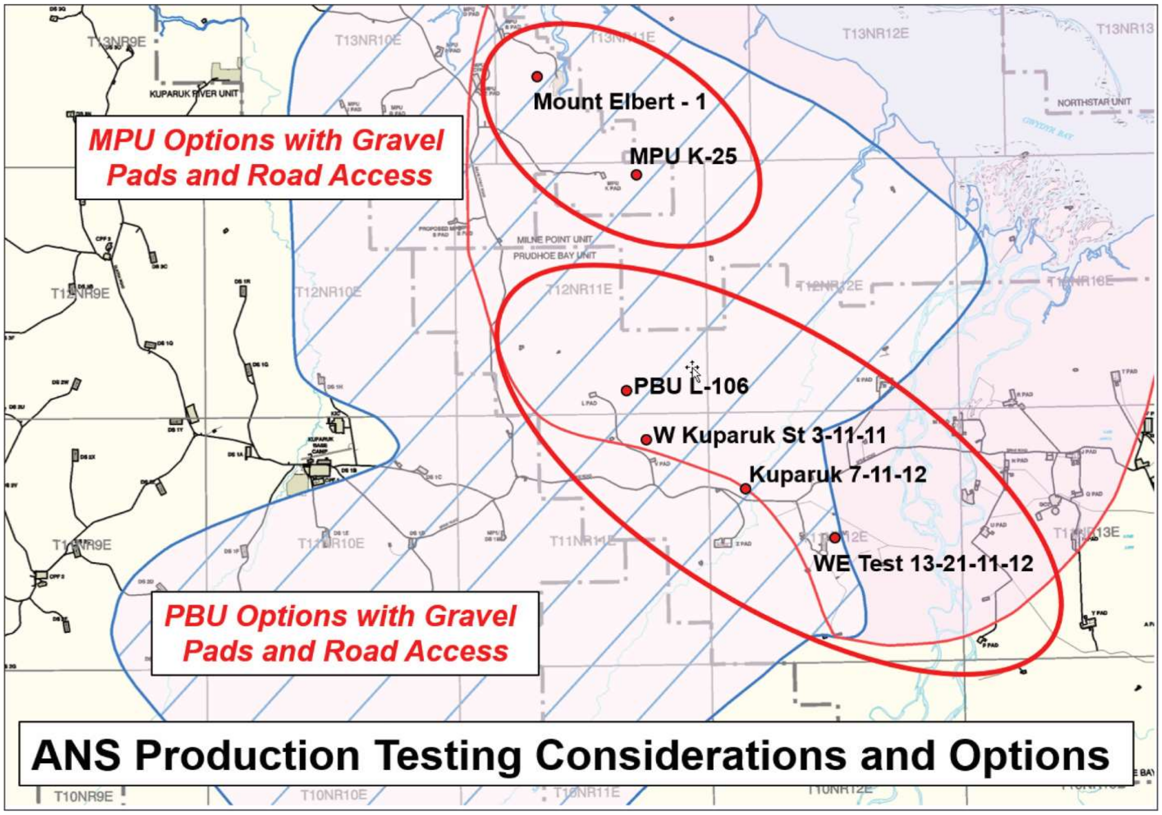

Figure 40. Map of candidate sites (Table 7) for gas hydrate production testing as targeted in the Prudhoe Bay Unit (PBU) and Milne Point Unit (MPU) during the 2016-2017 test site review effort as conducted under the DOE-USGS Interagency Agreement.

Candidate test sites	Reference well names	Well API number
Milne Point Unit Sites		
Mount Elbert	Mount Elbert - 1	50029233020000
MPU K Pad	MPU K-25	50029226500000
	MPU K-38	50029226490000
	Cascade-1	50029223260000
Prudhoe Bay Unit Sites		
PBU L Pad	PBU L-106	50029230550000
	PBU L-112	50029231290000
	NW Eileen 01-01	50029228580000
	Ignik Sikumi - 1	50029234430000
West Kuparuk State 3-11-11	West Kuparuk State 3-11-11	50029200140000
Kuparuk 7-11-12	Kuparuk State 7-11-12	50029200620000
West End Test 13-21-11-12	West End Test 13-21-11-12	50029210330000

Table 7. List of candidate sites (Fig. 40) for gas hydrate production testing as targeted in the Prudhoe Bay Unit (PBU) and Milne Point Unit (MPU) during the 2016–2017 test site review effort as conducted under the DOE-USGS Interagency Agreement.

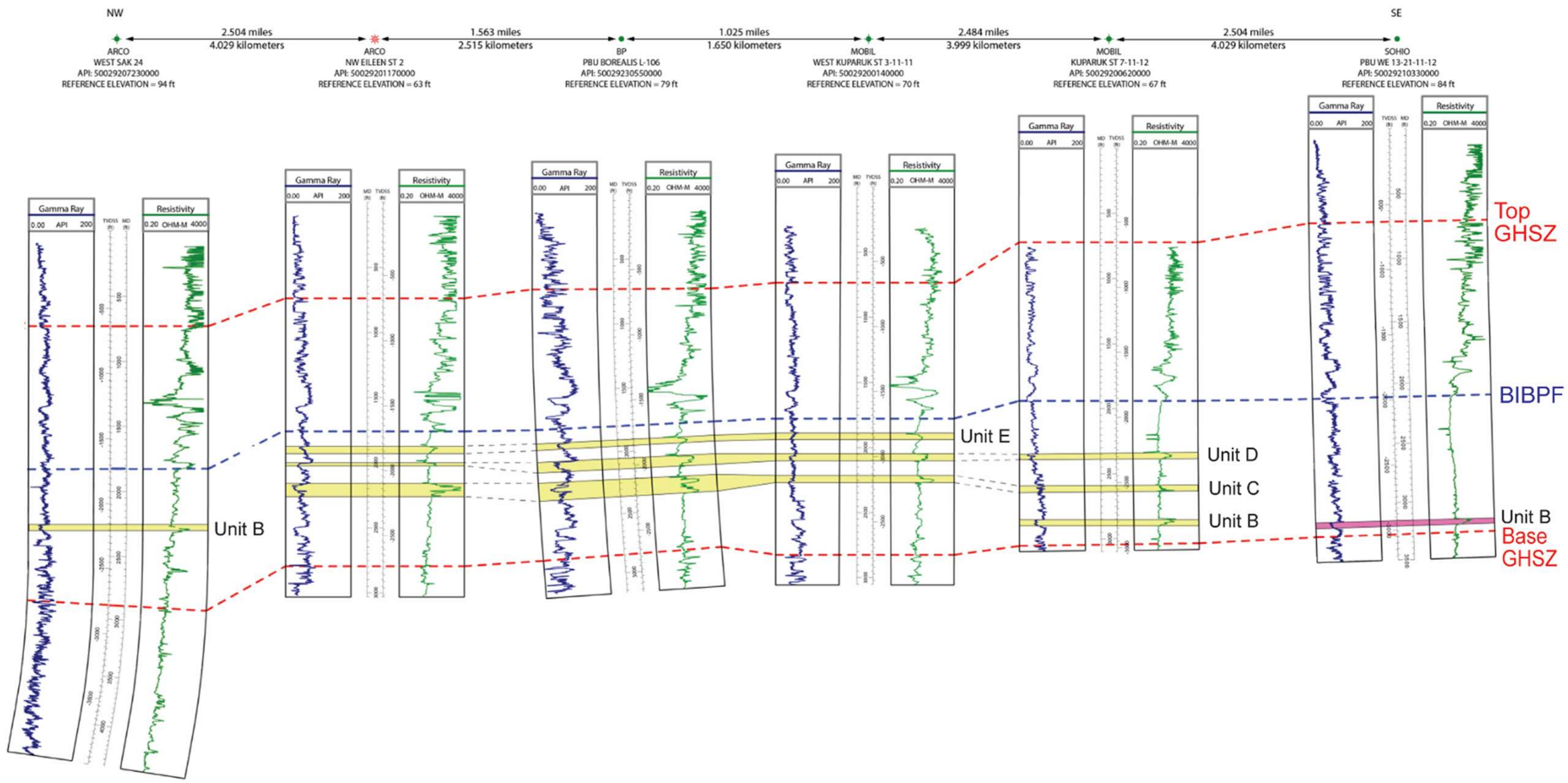

Figure 41. Well log cross section showing the lateral and vertical extent of the prominent gas hydrate-bearing reservoir units (Units B-E) associated with the candidate sites (Table 7; Fig. 40) for gas hydrate production testing as targeted in the Prudhoe Bay Unit (PBU) and Milne Point Unit (MPU) during the 2016-2017 test site review effort, conducted under the DOE-USGS Interagency Agreement. Yellow shading indicates well log inferred occurrence of gas hydrate. Red shading indicates the uncertain occurrence of gas hydrate or free gas. BIBPF = Base of ice-bearing permafrost, GHSZ = Gas hydrate stability zone

2007 Mount Elbert stratigraphic test well (Figs. 9–12). In this reexamination of the Mount Elbert Prospect option, it was determined that the Unit C and Unit D gas hydrate-bearing reservoir sections (Figs. 9–12) could be drilled from the either the MPU-A or MPU-B production pads, which would provide year-round access to the proposed gas hydrate producing test well(s). The possibility of also establishing the test well with a high-angle completion through the hydrate-bearing test interval provided the project with additional testing options. Additional engineering analysis and new production modeling efforts, however, indicated that the low temperature conditions (between 36 and 37°F; 2–3°C) of the Mount Elbert Prospect gas hydrate reservoirs and the added engineering complexity of drilling a "long-reach" well at this site would add a significant degree of risk to this project. Thus, the MPU Mount Elbert Prospect option was not further considered in this test site review effort.

Milne Point Unit K Pad Site

Within this project, remapping the Eileen Gas Hydrate Trend in the greater Prudhoe Bay area provided critical new insight into the occurrence of gas hydrate on the ANS and a detailed appreciation of the reservoir parameters needed to understand the production response of the gas hydrates. As a product of this effort, a new potential gas hydrate test site was identified in the southeast corner of the MPU associated with the conventional oil and gas Cascade Prospect (Table 7, Figs. 40-41). Well log data acquired from the industry drilled Cascade #1 exploratory well and two development wells drilled from the MPU K production pad (MPU K-25 and MPU K-38 wells) revealed an ~500-ft-thick (~152-m-thick) resistivity log inferred hydrocarbon-bearing stratigraphic section occurring near the base of the regionally projected gas hydrate stability zone (Figs. 42, 43). The well log correlation section shown in Figure 43 displays the lateral characteristics of the anomalous resistivity log inferred hydrocarbon-bearing stratigraphic section, which correlates to the Unit B gas hydrate-bearing reservoir section (top of Unit B defined by the log correlation marker C13) as originally defined by Collett (1993). In this case, however, the analysis of the acoustic wireline log from the Cascade #1 exploratory well revealed that the anomalous resistivity log inferred hydrocarbon-bearing stratigraphic section is characterized by low acoustic velocity log values that are indicative of the presence of free gas and not gas hydrates. Also as displayed in Figure 43, the Unit B reservoir section in the area of the Cascade #1 well and the MPU K Pad is shown to occur below the predicted base of the gas hydrate stability zone, further indicating that the anomalous resistivity log interval actually contains free gas and not gas hydrate.

To further assess the potential for gas hydrate prospects along the southern border of the MPU, the USGS also analyzed the 3D seismic data volume that had been provided to the USGS by BPXA to reexamine the previously identified gas hydrate prospects in the MPU (Fig. 9). As shown in the seismic section depicted in Figure 44, we have highlighted the seismic inferred occurrence of hydrate and free-gas reservoir sections in the area of the MPU K Pad. As shown, it again appears that the Unit B reservoir section is free-gas bearing and does not contain gas hydrate. Because the MPU K Pad is located along the edge of the provided 3D seismic data volume, we were not able to fully evaluate the lateral nature of the Unit B gas-bearing section as drilled and logged from the MPU

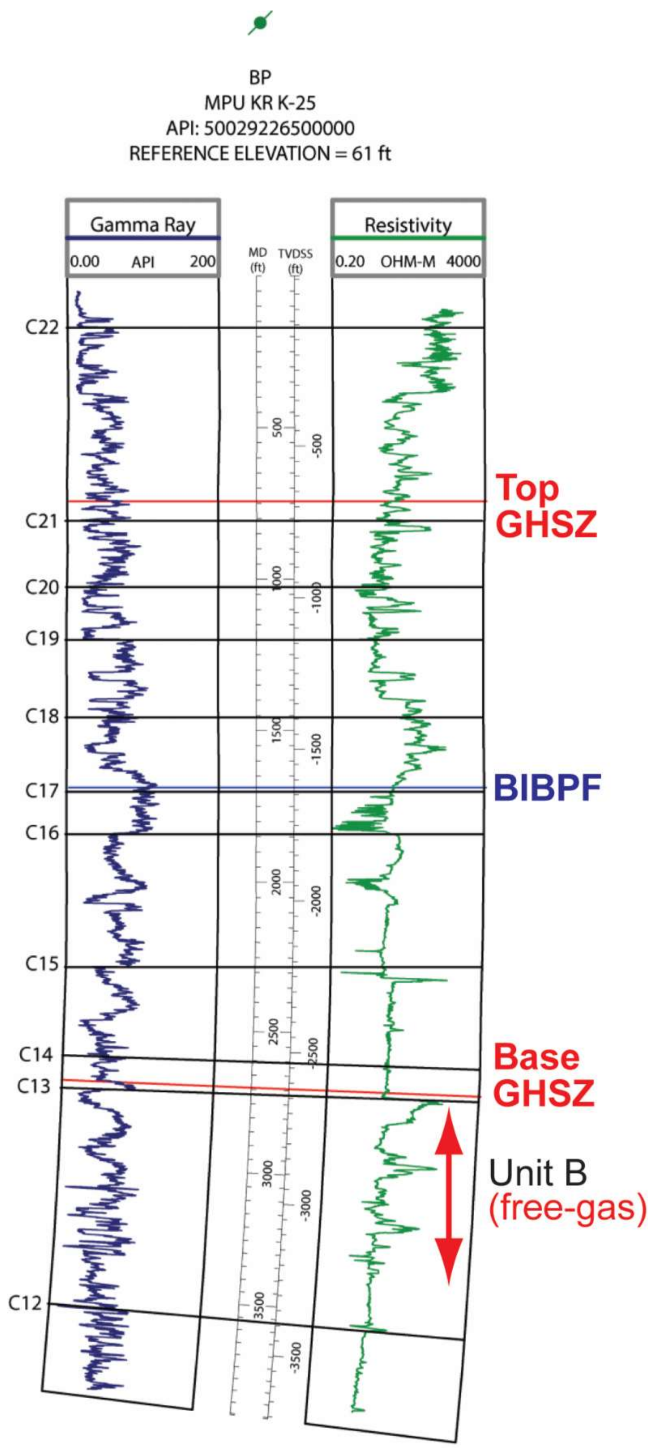

Figure 42. Well log display for the Milne Point Unit (MPU) K-25 related candidate production test site (Table 7; Fig. 40) showing the well log inferred occurrence of free gas associated with Unit B. BIBPF = Base of ice-bearing permafrost, GHSZ = Gas hydrate stability zone

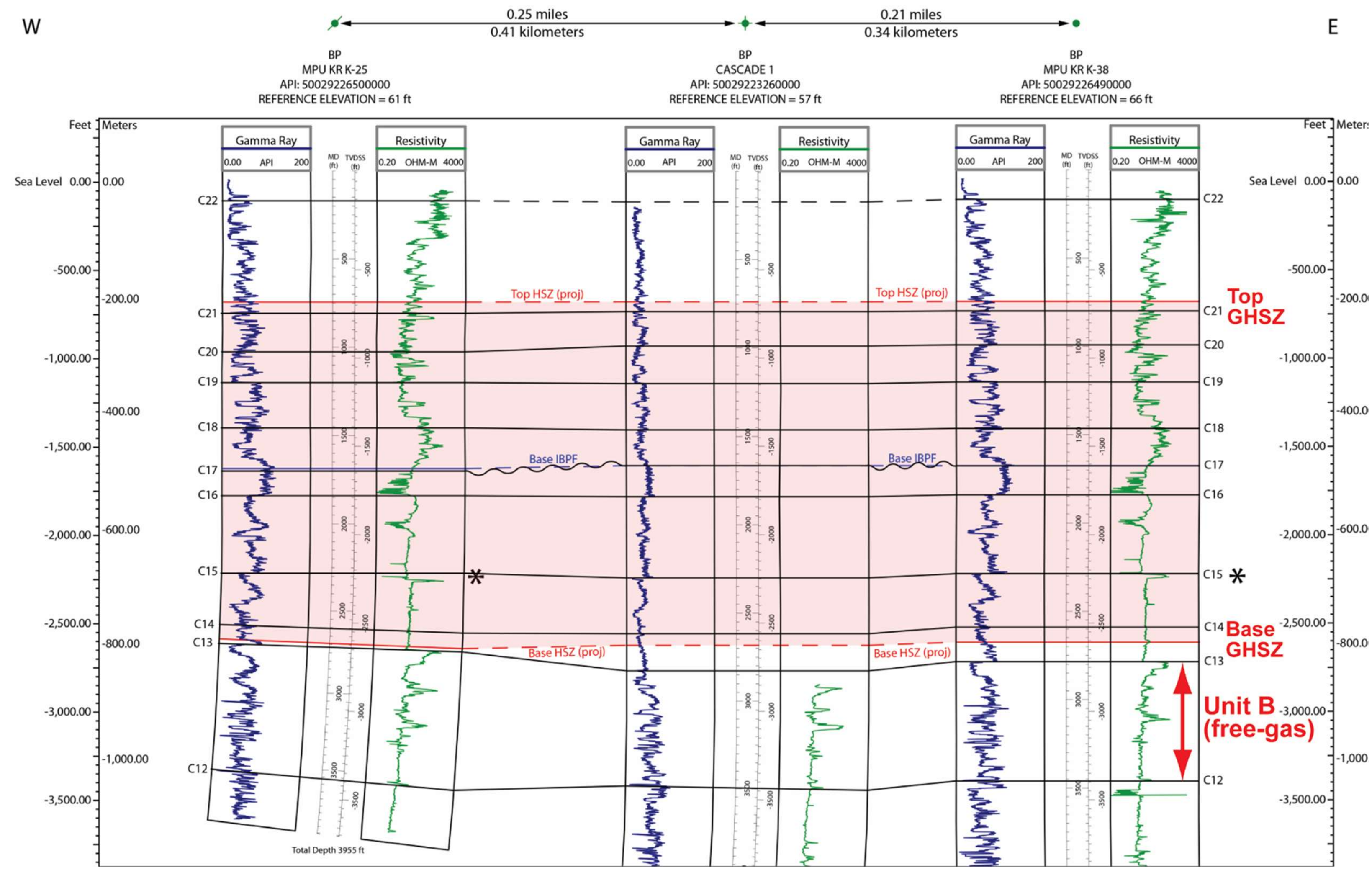

Figure 43. Well log cross section showing the lateral and vertical extent of the Unit B free gas-bearing stratigraphic interval associated with MPU K Pad and Cascade Prospect in the Milne Point Unit (MPU) (Table 7; Fig. 40). Asterisk (*) denotes the potential occurrence of gas hydrate. BIBPF = Base of ice-bearing permafrost, GHSZ = Gas hydrate stability zone

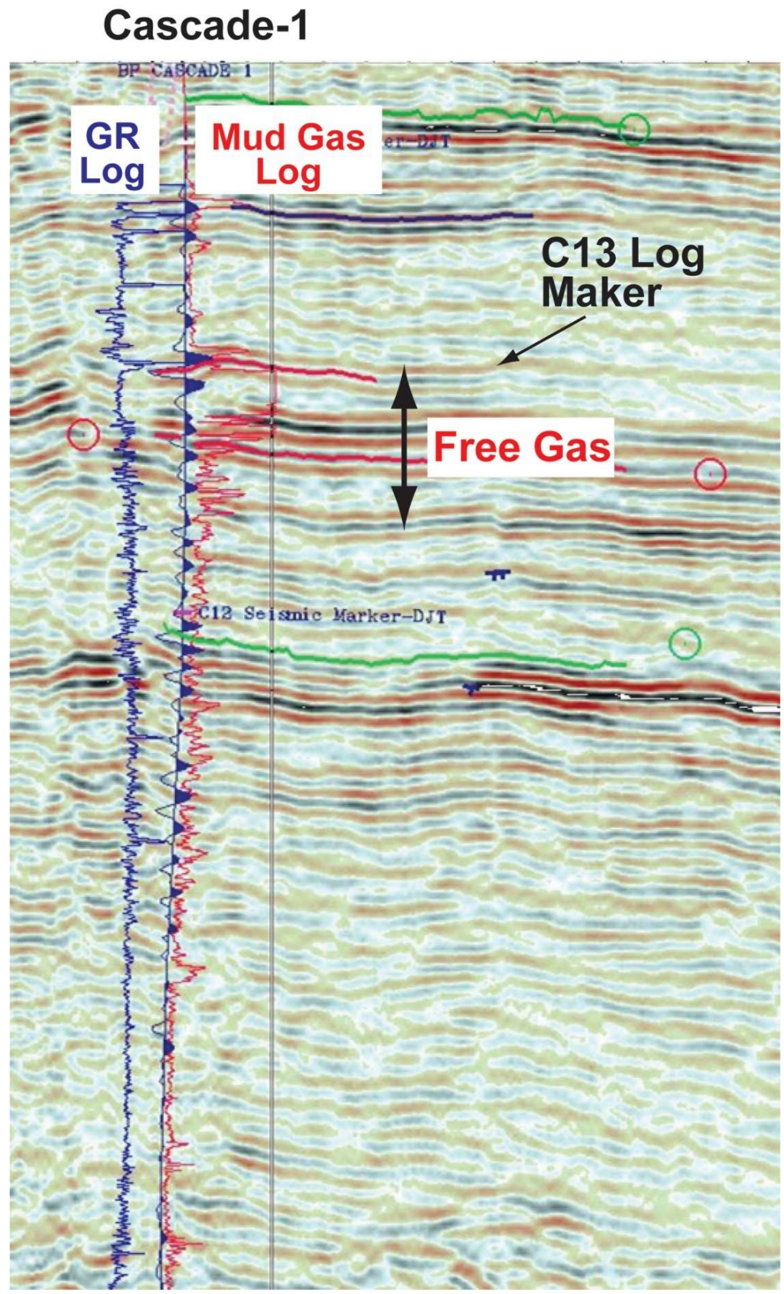

Figure 44. Seismic section showing the lateral and vertical extent of the Unit B free gas-bearing stratigraphic interval associated with Cascade Prospect (Cascade-1 Well) in the Milne Point Unit (MPU) (Table 7; Fig. 40). As a condition of the seismic data use agreement, the location and associated depth scale of the depicted seismic line cannot be shown in this display. GR = Gamma ray log, Mud Gas Log = Mud loggers total gas log as recorded during the drilling of the Cascade-1 Well, C13 Log Marker = Well log stratigraphic correlation as shown in Figure 43

K Pad. In 2017, with approval from the PBU Working Interest Owners (WIOs), USGS scientists worked with SOA-DNR technical staff to further characterize the potential occurrence of gas hydrate around the area of the MPU K Pad. This cooperative effort, which made use of an extensive regional proprietary seismic database, concluded that the MPU K Pad would not be a suitable site for an extended gas hydrate production test.

Evaluation of Locations to the East of the Milne Point Unit (MPU)

In April 2013, the DOE and the SOA-DNR signed a Memorandum of Understanding (MoU) designed to collaborate on the pursuit of gas hydrate research opportunities in Alaska. One of the outcomes of this cooperation included a comprehensive review of potential testing sites within an area of unleased acreage adjacent to the east of the MPU. In November 2014, DOE-NETL also signed an MoU with JOGMEC to collaborate on the development of a long-term testing opportunity in northern Alaska. These new cooperative agreements expanded the test site review effort to include two new data/knowledge streams in support of (1) the remapping and detailed reservoir characterization of the Eileen Gas Hydrate Trend in the PBU-MPU and (2) the identification and detailed characterization of gas hydrate prospects on the SOA unleased lands (also known as North Shore area) east of the MPU. Under the new DOE-NETL/JOGMEC MOU, the USGS worked with JOGMEC and DOE technical staff on the gas hydrate prospecting effort on the SOA land that was set aside for gas hydrate research. This effort, as coordinated by JOGMEC, led to the identification of a series of eight new seismic inferred gas hydrate prospects in the area of the SOA unleased lands east of the MPU. These newly proposed test sites were assessed to have unfavorable geologic, logistical, and operational risks as compared to the proposed test sites within the western portion of the PBU.

Evaluation of Locations in the Prudhoe Unit (PBU)

Prudhoe Bay Unit L Pad Site

In 2017, the USGS reexamined the potential gas hydrate accumulations in and around the PBU L-Pad, which is located near the site of the Iġnik Sikumi test well as drilled and tested in 2012/2013. This study again included the integrated analysis of well log data from more than 70 wells across the Eileen trend to yield one of the most detailed reservoir models for any known gas hydrate accumulation. The primary reservoir test section in the Iġnik Sikumi test well was the “upper Unit C” (also named the “C1 sand”) at a depth of 2243–2273 ft MD (684–493 m MD) (Figs. 26 and 34A), which was confirmed to be at an in situ temperature of about 5°C (41°F). These same reservoir conditions would be expected for the Unit C reservoir section in any well drilled from the PBU L-Pad (Fig. 45). During the later stages of the Iġnik Sikumi test, gas production was maintained by flowing the well at bottom-hole pressures below those that would destabilize methane hydrate (i.e., depressurization production). The endothermic cooling associated with in situ gas hydrate disassociation and gas production resulted in a drop of the reservoir temperature to about 1°C (34°F) over about 18 days of nearly continuous production. This significant drop in reservoir temperatures would have eventually led to the formation of ice in the reservoir section and likely the reformation

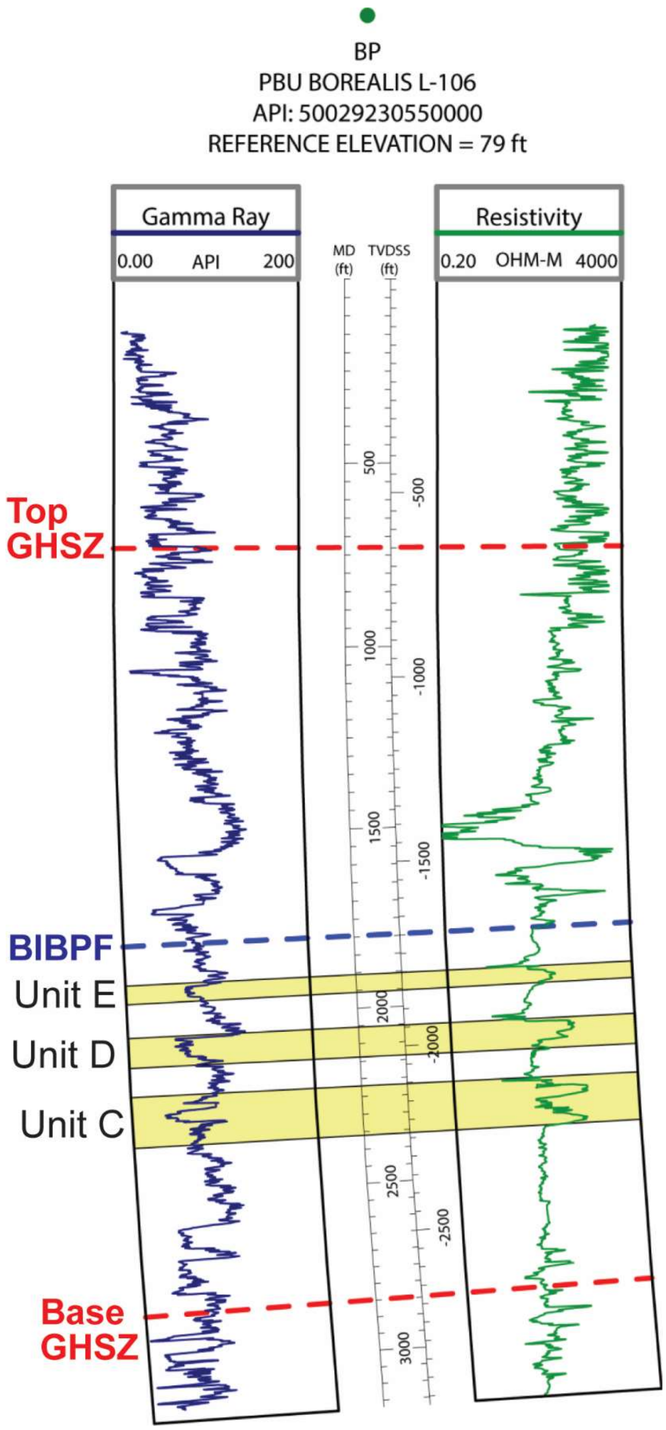

Figure 45. Well log display for the Prudhoe Bay Unit (PBU) L-106 related candidate production test site (Table 7; Fig. 40) showing the well log-inferred occurrence of gas hydrate (yellow shading) associated with Units C, D, and E. BIBPF = Base of ice-bearing permafrost, GHSZ = Gas hydrate stability zone

of the gas hydrate. In planning for the proposed extended gas hydrate production test, it was decided that the in situ temperature of the Unit C reservoir section in the area of the PBU L-Pad would be too low to conduct a useful long-term gas hydrate production test. It was also determined that because of the large number of industry development wells drilled from the PBU L-Pad, any gas hydrate testing operations conducted from the pad would have a relatively high probability of negatively impacting PBU operations.

Kuparuk State 3-11-11 Well Site

The Kuparuk State 3-11-11 well pad test site in the Westend of the PBU was also evaluated in 2011 as a potential test site in advance of the Iġnik Sikumi test as reviewed above in this report. The Kuparuk State 3-11-11 well pad is located about 2 miles to the south of the PBU L-Pad (Figs. 17, 38, 39, 40, and 46). The geologic conditions of the gas hydrate reservoir section (Units C–E) at the Kuparuk State 3-11-11 site are similar to those encountered in the Iġnik Sikumi test well. However, the "lower Unit C" (also named the "C2 sand") does not appear to be gas hydrate bearing in the Kuparuk State 3-11-11, which represents a likely production testing challenge with potential water production negatively impacting the results of any test of Unit C. In addition, the expected in situ temperature of the Unit C reservoir section at the Kuparuk State 3-11-11 site would be too low for long-term gas hydrate production testing. During this site review effort, it was determined that the gravel exploration pad associated with the Kuparuk State 3-11-11 well site had been removed and the site was revegetated. Considering the limited nature of the available reservoir testing options at this site, the low in situ temperature of the deepest target gas hydrate-bearing reservoir section, and the lack of a useable gravel pad, the proposed Kuparuk State 3-11-11 site was removed from further consideration for future testing.

West End Test 13-21-11-12 Well Site

The Prudhoe Bay Unit West End Test 13-21-11-12 well pad overlies the most structurally downdip targeted gas hydrate-bearing reservoir section in the Eileen Gas Hydrate Trend (Figs. 39–41, 47). The well log data as acquired in the West End Test 13-21-11-12 industry exploration well (Fig. 47) indicated that only the Unit B reservoir section at a depth of 3155–3210 ft MD (3071–3126 ft below mean sea level – MSL) exhibits the well log responses indicative of the presence of gas hydrate. The considerable depth of the Unit B reservoir section in the West End Test 13-21-11-12 well and relatively low quality acoustic log data from this well added considerable geologic risk to the selection of this site for future testing. In addition, the presence of only one possible gas hydrate-bearing reservoir section would also limit the testing flexibility at this site. The West End Test 13-21-11-12 well site has no current production and is used for staging drilling rigs and other field equipment. Based on the geologic uncertainty associated with this site and the apparent limited number of testable reservoir targets, the West End Test 13-21-11-12 site was not advanced for further consideration as a long-term gas hydrate production test site.

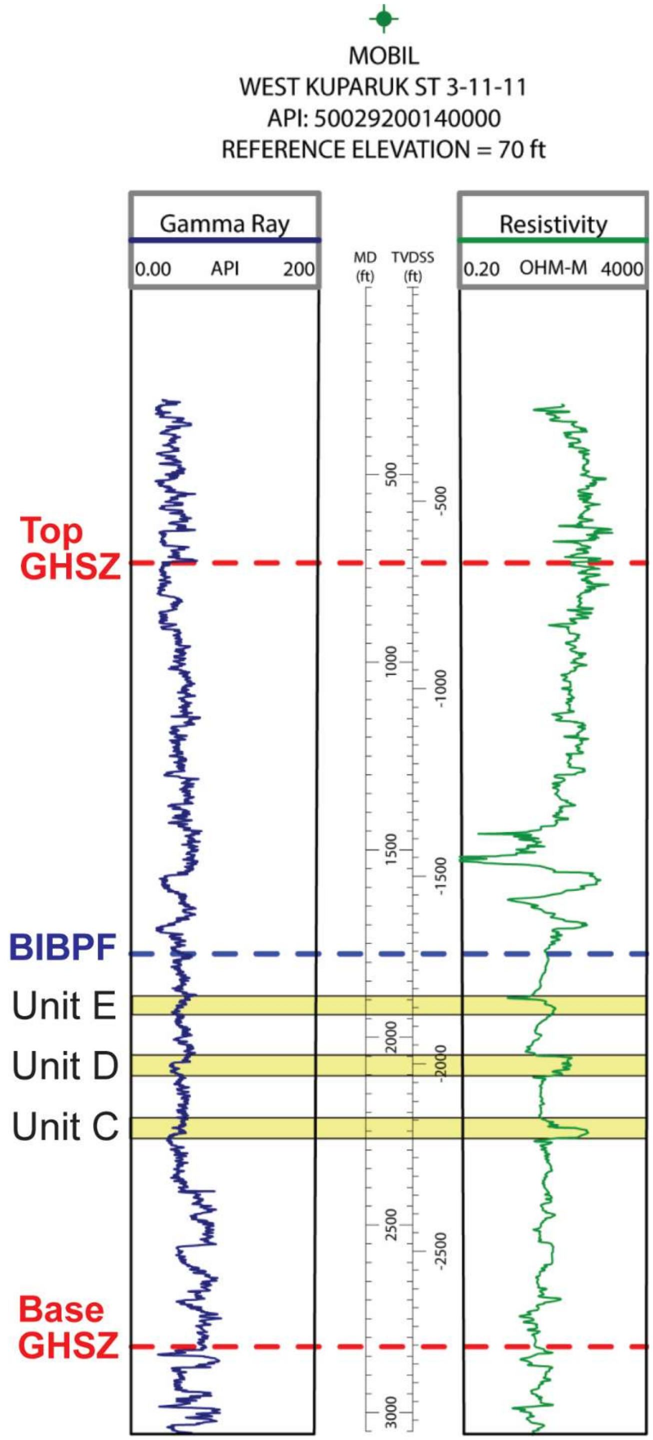

Figure 46. Well log display for the Prudhoe Bay Unit (PBU) West Kuparuk State 3-11-11 related candidate production test site (Table 7; Fig. 40) showing the well log-inferred occurrence of gas hydrate (yellow shading) associated with Units C, D, and E. BIBPF = Base of ice-bearing permafrost, GHSZ = Gas hydrate stability zone

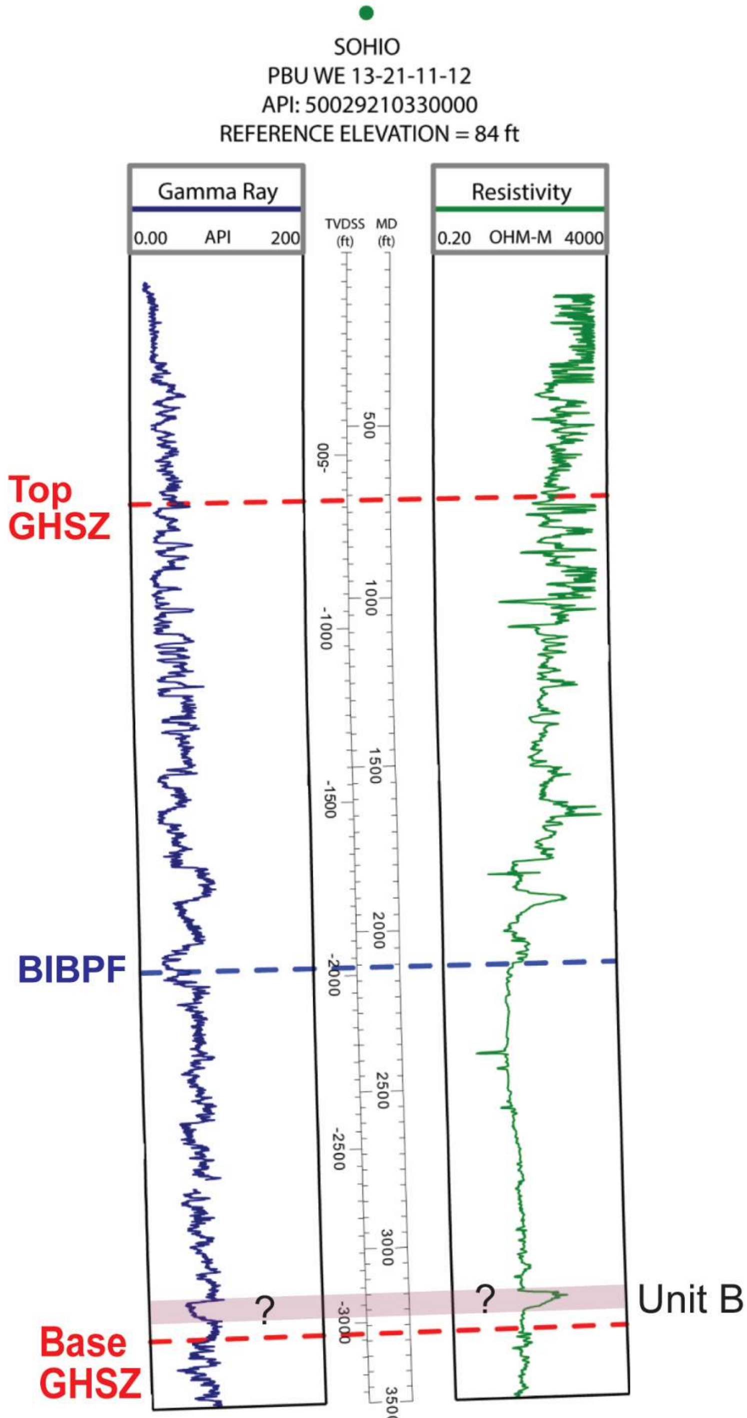

Figure 47. Well log display for the Prudhoe Bay Unit (PBU) West End Test 13-21-11-12 related candidate production test site (Table 7; Fig. 40). Red shading associated with Unit B indicates the uncertain occurrence of gas hydrate or free gas. BIBPF = Base of ice-bearing permafrost, GHSZ = Gas hydrate stability zone, ? = denotes either free gas-bearing or gas hydrate-bearing

Kuparuk 7-11-12 Well Site

As previously reviewed in this report, the 2017 test site review and selection process was based upon the physical accessibility of the site (gravel pad and road access), proximity to ANS infrastructure, confidence in the presence of gas hydrate-bearing reservoirs, and the possibility of multiple reservoir targets suitable for testing. The targeted reservoirs for this field test should possess high porosity, high (intrinsic) permeability clastic sand-rich reservoirs as previously documented in the Tertiary Sagavanirktok Formation reservoir section in the Eileen Gas Hydrate Trend (Collett et al., 2011a, 2011b; Boswell et al., 2020b). For the field test, reservoirs below the permafrost with an in situ temperature no lower than ~40°F (~5°C) were targeted. Wireline-deployed well logs, as acquired from industry exploratory and development wells, were the primary dataset used to identify and evaluate potential gas hydrate reservoir targets. Eventually, the 2017 test site review and selection process determined that the western PBU location that best combines known and possible gas hydrate occurrences with an existing gravel pad and no ongoing industry activities was the gravel pad at the site of the Kuparuk 7-11-12 exploration well (Figs. 39-41 and 48-51). The pad lies at the intersection of the main PBU Spine Road and the road to the PBU Z-Pad to the south. As part of the test site review and well-planning effort, a portion of an industry-acquired 3D seismic data volume was made available to the project partners through agreements with PBU WIOs, which allowed for more detailed mapping of the potential hydrate reservoir sections in the area of the gravel pad from which the Kuparuk 7-11-12 exploration well was drilled (Boswell et al., 2020b; Lim et al., 2020).

The gas hydrate accumulations in the western part of the PBU occur within the Tertiary Sagavanirktok Formation. The Project Partner site review process indicated that two hydrate-bearing stratigraphic units (Units B and D) had the potential to be encountered with suitable reservoir conditions to conduct the desired gas hydrate testing. These reservoirs are well known from log data acquired at the NW Eileen State-2 well in 1970, from log and other data acquired at the Iġnik Sikumi test well in 2012, from log data acquired in the Kuparuk 7-11-12 well, and from log data acquired in numerous industry exploratory and development wells drilled throughout the PBU, MPU, and the KRU (Collett et al., 2011a).

Detailed analysis of the log data acquired from the Kuparuk 7-11-12 well (Figs. 48-50), indicated the potential occurrence of three hydrate-bearing reservoir sections, including the following: Unit B reservoir section at a depth of 2845–2895 ft MD (2778–2828 ft below mean sea level – MSL); Unit C reservoir section at a depth of 2590–2640 ft MD (2523–2573 ft below mean sea level – MSL); and Unit D reservoir section at a depth of 2340–2390 ft MD (2273–2323 ft below mean sea level – MSL). As shown in Figures 48 and 50, the hydrocarbon-bearing reservoir sections associated with Units B, C, and D are characterized by high resistivity log values ranging from 50 to over 100 ohm-m. The fast-acoustic transit-time well log values (averaging about 105 microseconds per foot) acquired in Unit D appear to confirm the presence of gas hydrate. However, acoustic well log data acquired in Units B and C appear "cycle skipped," which often indicates the presence of free gas (i.e., not gas hydrate). However, the analysis of borehole temperature data (Lachenbruch et al., 1987a, 1987b) obtained in nearby wells (Fig. 51) and the analysis of the gas hydrate stability conditions indicated that the base of the

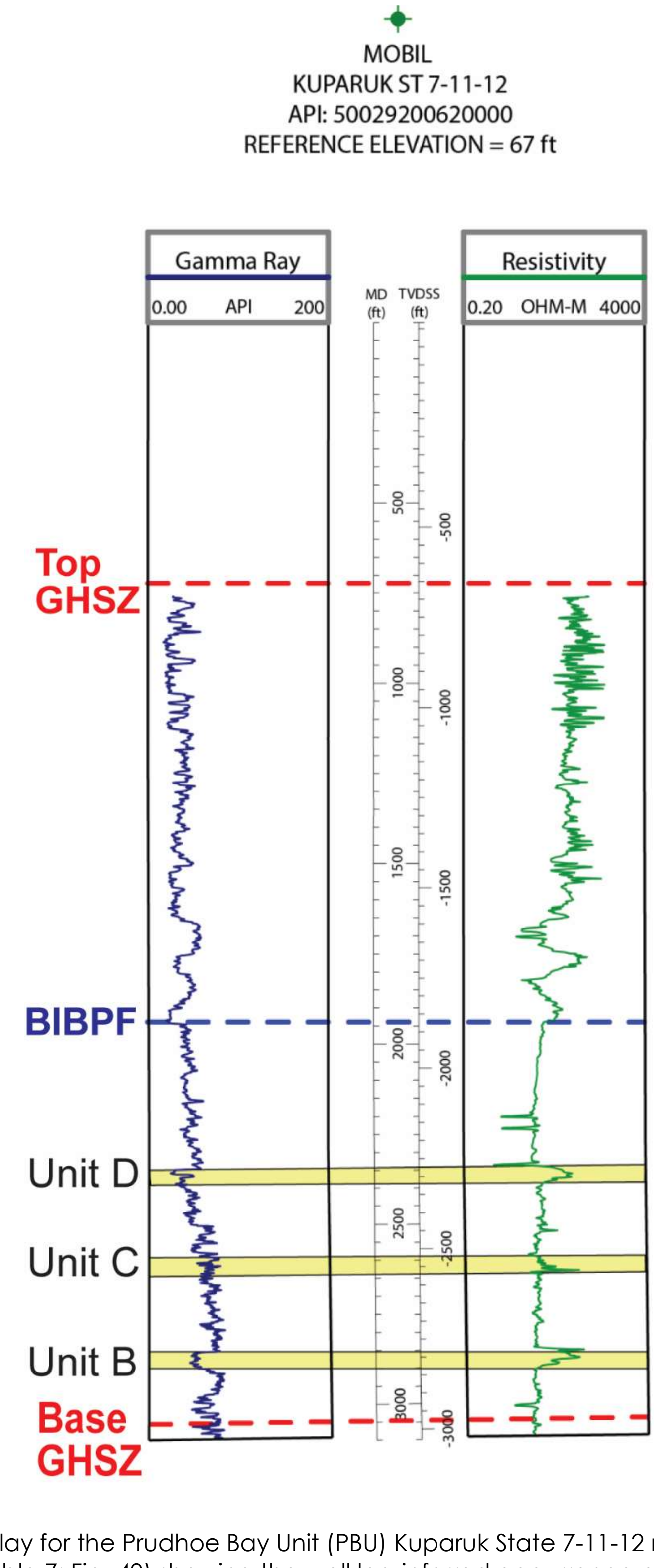

Figure 48. Well log display for the Prudhoe Bay Unit (PBU) Kuparuk State 7-11-12 related candidate production test site (Table 7; Fig. 40) showing the well log-inferred occurrence of gas hydrate (yellow shading) associated with Units B, C, and D. BIBPF = Base of ice-bearing permafrost, GHSZ = Gas hydrate stability zone

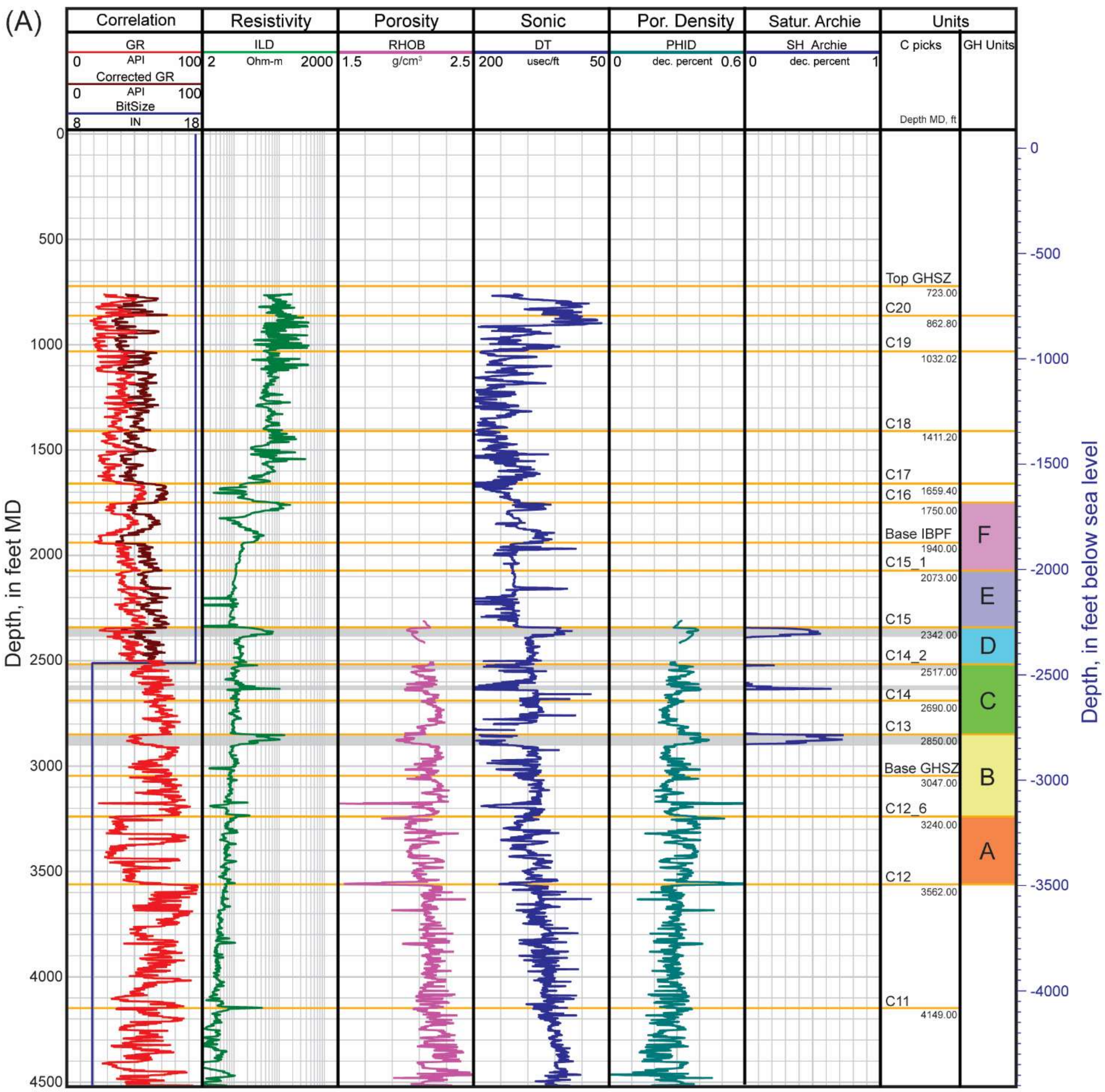

Figure 49. (A) Well log montage for the Prudhoe Bay Unit (PBU) Kuparuk State 7-11-12 related candidate production test site (Table 7; Fig. 40) showing the well log-inferred occurrence of gas hydrate (gray shading) associated with Units B, C, and D. Also shown as numbered solid (yellow) lines are log correlation markers used to construct a regional stratigraphic framework in the greater Prudhoe Bay area (modified from Collett, 1993). The gas hydrate related stratigraphic units in the Eileen accumulation are identified with the reference letters A through F.

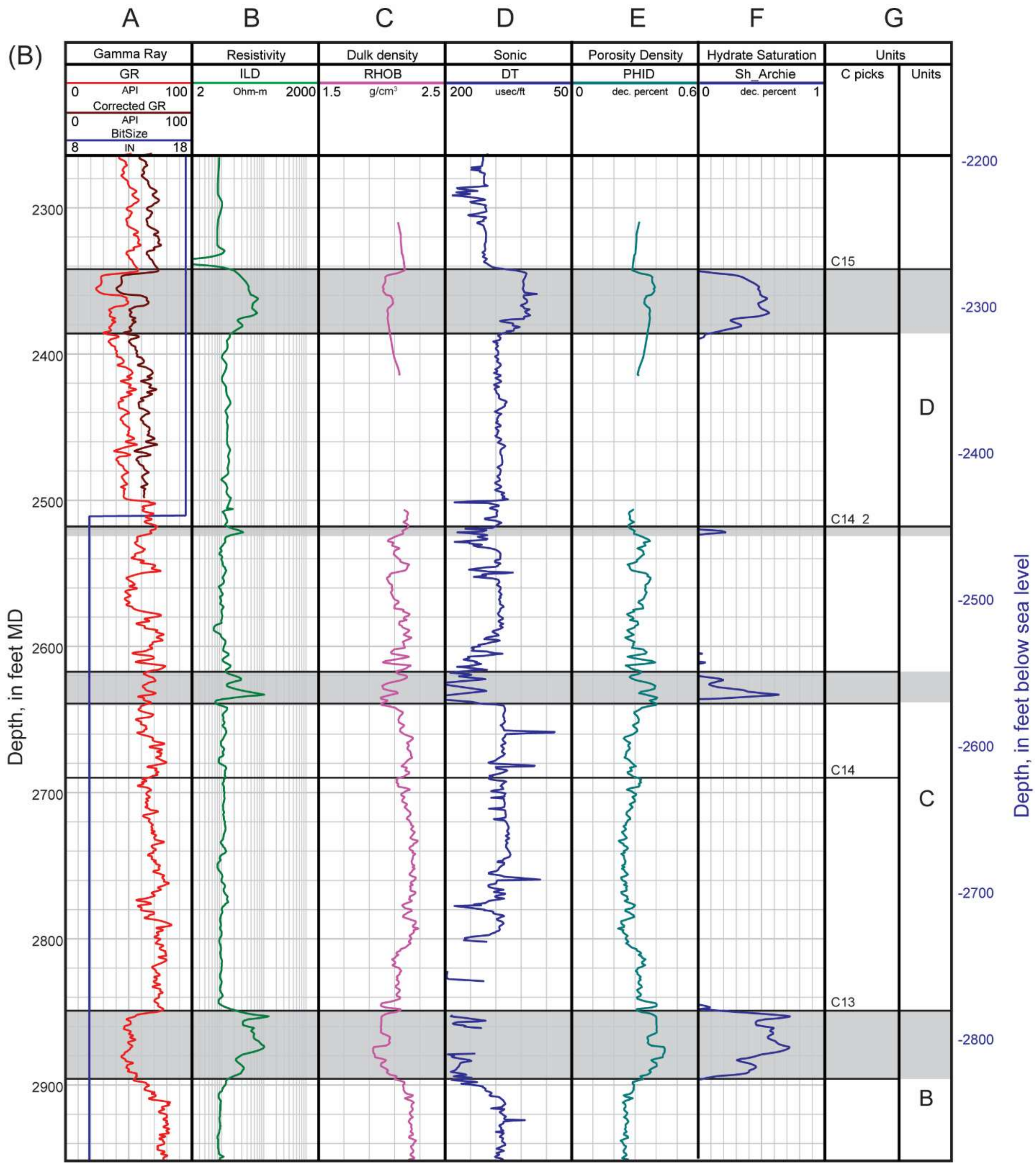

Figure 49. (B) Expanded scale well log montage for the Prudhoe Bay Unit (PBU) Kuparuk State 7-11-12 related candidate production test site. Columns are as follows: (A) Gamma ray and caliper, (B) Resistivity, (C) Bulk density, (D) Sonic, (E) Density porosity, (F) Archie resistivity derived gas hydrate saturation, (G) Eileen Gas Hydrate Trend stratigraphic units. Gas hydrate saturation (Sh Archie) and porosity density (PHID) shown in decimal percent. BIBPF = Base of ice-bearing permafrost, GHSZ = Gas hydrate stability zone

methane hydrate stability zone should extend to a depth of 3025 ft MD (922 m MD) or about 40 ft (about 12 m) below the base of the Unit B resistivity log inferred hydrocarbon-bearing reservoir section. During the site review process, it was theorized that drilling operations below the surface casing set at 2500 ft MD (762 m MD) in the Kuparuk 7-11-12 well negatively impacted the stability of gas hydrates in Unit B leading to the dissociation of the in situ gas hydrate. Thus, when the stratigraphic section was eventually logged some 19 days later, the acoustic log indicated the presence of high transit-time (i.e., low velocity) free gas in these two reservoir sections. To better constrain these risks, USGS scientists obtained the necessary confidentiality agreements to view PBU seismic data and worked with SOA-DNR geophysicists to provide an initial assessment of the geologic conditions at the site. Despite the available log data from the Kuparuk 7-11-12 exploration well and seismic data analysis of the candidate test site, geologic risk remained with respect to the condition of the target reservoirs. It was determined that a stratigraphic test well would be required to confirm reservoir occurrence and condition (Okinaka et al., 2019, 2020).

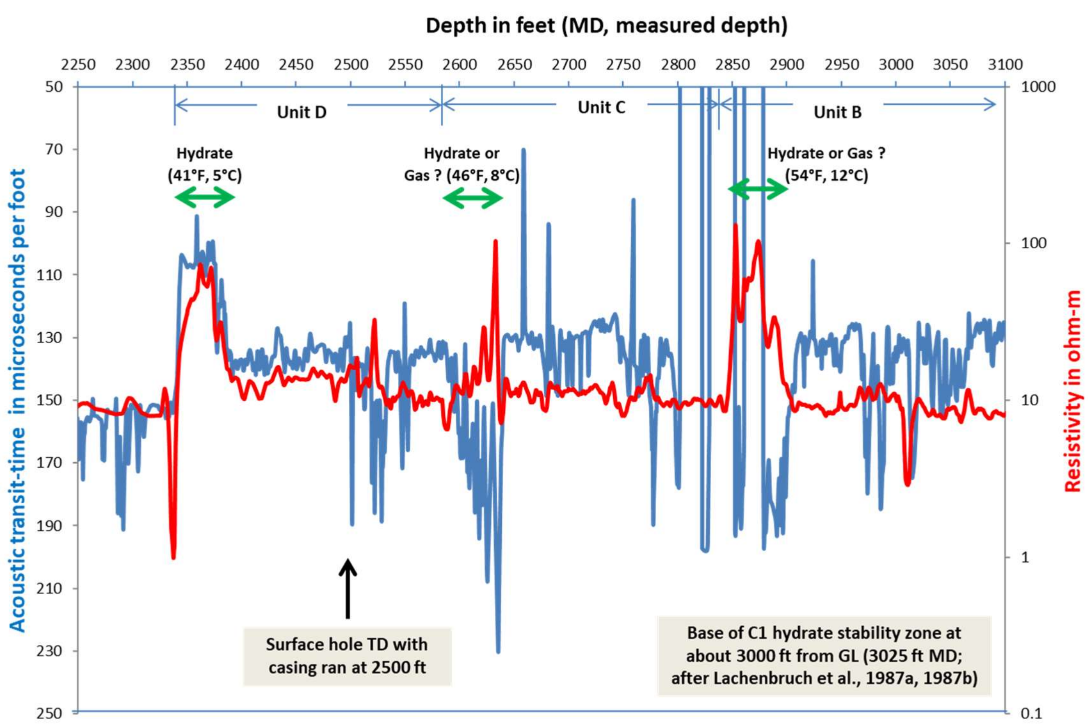

Figure 50. Resistivity and acoustic transit-time log display for Units B, C, and D in the Prudhoe Bay Unit (PBU) Kuparuk State 7-11-12 showing evidence for the resistivity log inferred presence of hydrocarbons and acoustic log evidence for the occurrence of gas hydrate and possible free gas.

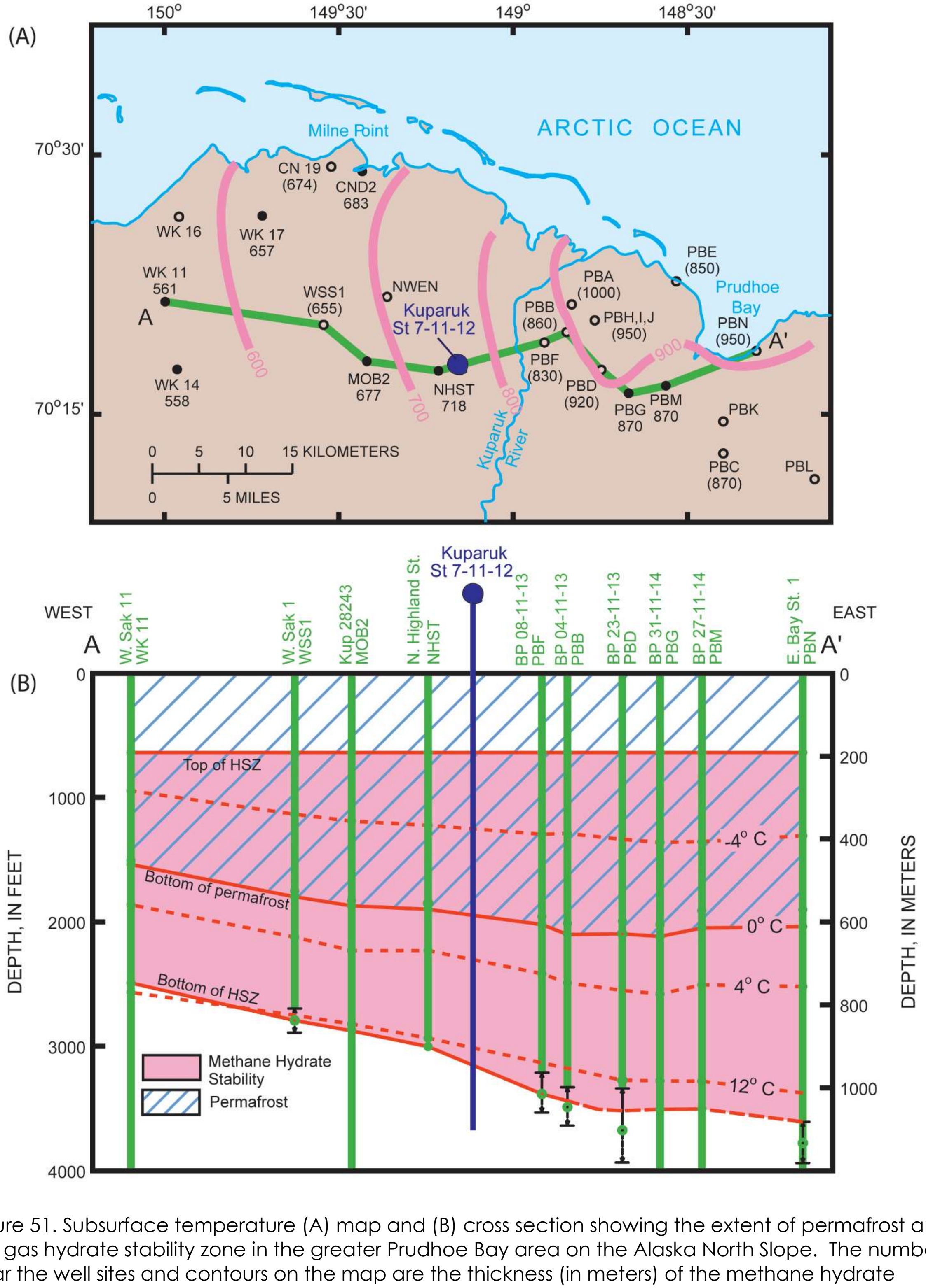

Figure 51. Subsurface temperature (A) map and (B) cross section showing the extent of permafrost and the gas hydrate stability zone in the greater Prudhoe Bay area on the Alaska North Slope. The numbers near the well sites and contours on the map are the thickness (in meters) of the methane hydrate stability zone. Also shown is the projected location of the Prudhoe Bay Unit (PBU) Kuparuk State 7-11-12. Both the map and cross section are modified from Lachenbruch et al. (1987a, 1087b).

4. PBU 7-11-12 Test Site Planning, Operations, and Technical Findings

In review, the primary goal of the Alaska gas hydrate production testing program is to conduct a scientific field production test from one or more gas hydrate-bearing sand reservoirs using conventional "depressurization" technology. The project was designed to include the drilling and evaluation of a stratigraphic test well, followed by the establishment of a production test site (including a geoscience data well and two production test wells that will also be instrumented as monitoring wells), and then the testing of reservoir response to pressure reduction over a period of 12 months or for whatever period the parties find operations at the site valuable (Fig. 52).

As reviewed above, from 2015 through 2017, DOE, JOGMEC, the USGS, and the SOA-DNR worked together to assess potential locations for an extended gas hydrate test on the ANS. This review conclusively determined that the one location that combines known gas hydrate occurrences with an existing gravel pad with no ongoing industry activities was the gravel pad at the site of the Kuparuk 7-11-12 exploration well, within the Westend PBU (Fig. 53).

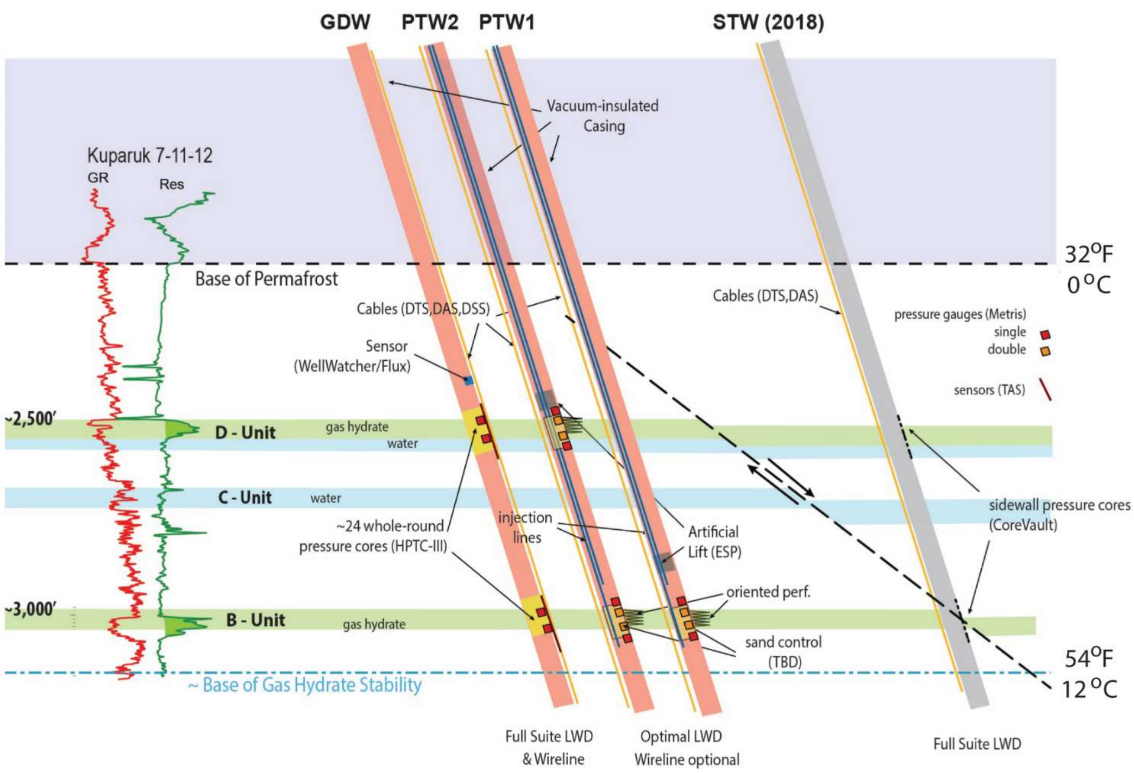

Figure 52. Schematic of the nominal 7-11-12 site field test design. The location of monitoring systems and associated gauges and other well completion design elements are shown for planning purposes and are subject to change. Dashed line depicts the approximate position of a fault crossing the Hydrate-01 Stratigraphic Test Well. PTW1 = Production Test Well Number 1, PTW2 = Production Test Well Number 2, STW (2018) = Stratigraphic Test Well (Hydrate-01), GDW = Geoscience Data Well, GR = Gamma ray well log, Res = Resistivity well log, LWD = Logging while drilling, DTS = Distributed temperature system, DSS = Distributed shear system, DAS = Distributed acoustic system, ESP = Electrical submersible pump, HPTC-III = High Pressure Temperature Corer

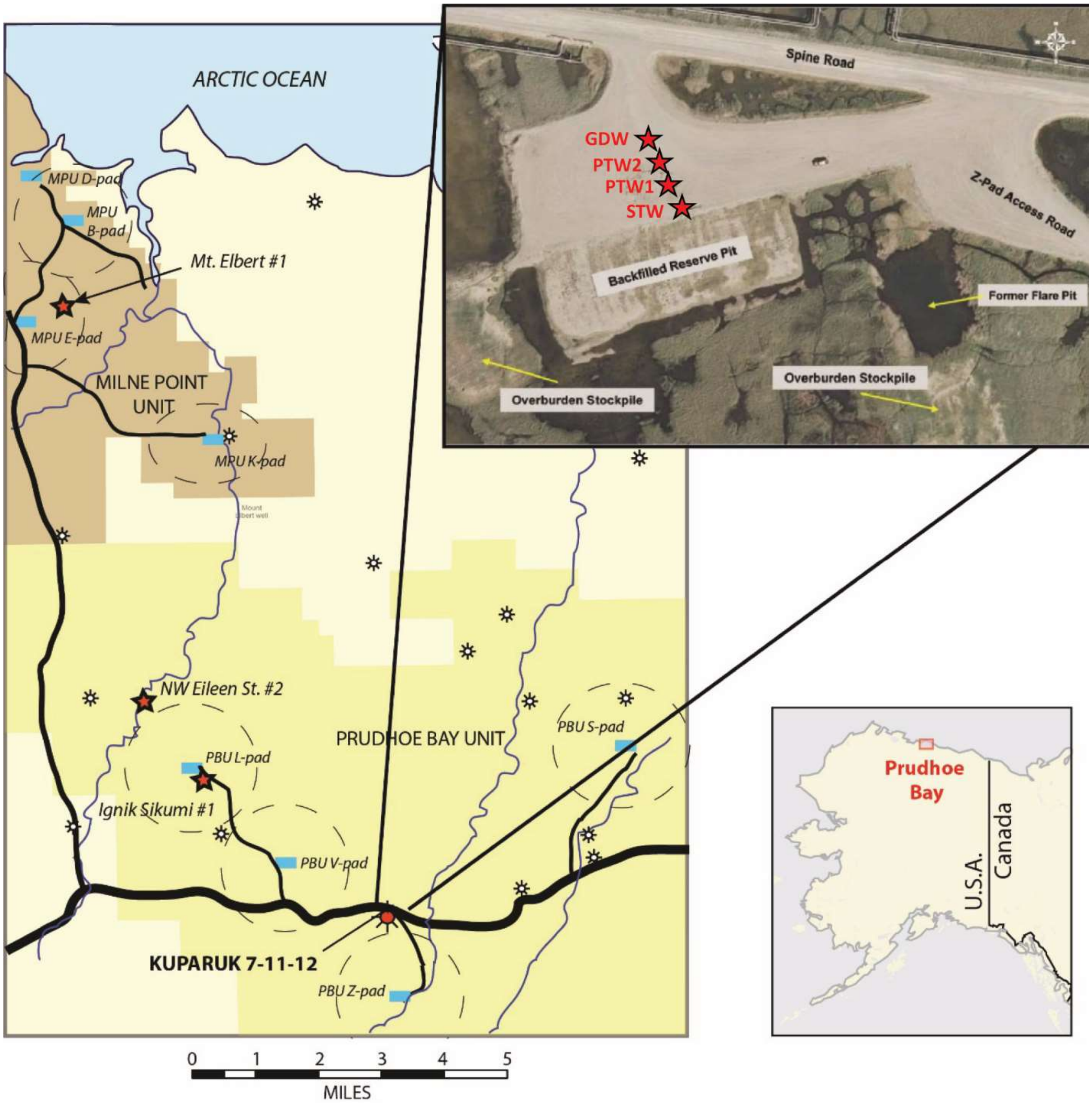

Figure 53. Image of the 7-11-12 pad in the western part of the Prudhoe Bay Unit (PBU). The 7-11-12 pad is located immediately adjacent to the PBU Spine Road. Also shown is the location of other wells with data used to study gas hydrates. Photo insert of the 7-11-12 pad shows the location of Hydrate-01 (STW) and other planned wells. STW = Stratigraphic test well, GDW = Geoscience data well, PTW1 = Production test well 1, PTW2 = Production test well 2

Despite the available log data from the 7-11-12 site and other nearby wells, geologic risk remained after the site review effort with respect to the condition of the target test reservoirs. The 7-11-12 data confirmed the presence of gas hydrate within Unit D and within lower-quality reservoirs of Unit C. However, the upper reservoir section in Unit C, which was the primary reservoir target at the Iġnik Sikumi test, appears to be mostly water wet at the 7-11-12 location. The reservoir section associated with Unit B is clearly hydrocarbon-bearing, and the log data appear to suggest the presence of gas, but there are good reasons to believe that the unit lies within the gas hydrate stability zone and the observed gas is derived from gas hydrate destabilized during the drilling process. The primary target interval (Unit B) was anticipated to occur at a depth of ~2900 ft TVD (~885 m TVD), approximately 1000 ft (~305 m) below the base of ice-bearing permafrost. This unit was the primary target given its greater depth and expected warmer temperature (~50°F or ~10°C). The upper reservoir section of Unit C lies at ~2550 ft MD (~777 m MD); however, this unit appears largely water-wet at the 7-11-12 location. Unit C does contain gas hydrate at the 7-11-12 well, but it appears to be only minimally charged. Unit D presents the lowest geologic risk of the examined targets and exists at conditions very similar to those of Unit C that were tested at the Iġnik Sikumi location. Units B and D were not expected to be in direct contact (vertically or laterally) with hydrate-free, water-bearing stratigraphic sections, the presence of which could complicate the proposed test. Within the 7-11-12 well, each unit was assessed to be ~30 to ~50 ft (~9 to ~15 m) thick, with elevated gas hydrate saturations of 70% and higher. The remaining pore fill was expected to include bound and free water only (i.e., no free gas). In order to refine the final location of the bottom hole for the stratigraphic test well, the project proponent team worked with the PBU WIOs to further access and analyze seismic data in the vicinity of the Kuparuk 7-11-12 pad to build on the seismic studies completed by the SOA-DNR.

4.A. Planning and Operations of the Site 7-11-12 (Hydrate-01) Stratigraphic Test Well

The stratigraphic test well was to be drilled for the purpose of confirming reservoir occurrence and conditions suitable for a successful long-term gas hydrate production test and for collecting information needed to enable the design of production test completion components. In review, the preferred test reservoir conditions included the following: (1) at least 41°F (5.0°C) formation temperature, (2) at least 15 ft (5 m) of net reservoir thickness, (3) no direct communication with water-saturated units, and (4) high-quality (high intrinsic porosity and permeability with high gas hydrate saturation) reservoir conditions. For planning, the stratigraphic test well would be drilled to a depth of ~3000 ft (~915 m) using chilled oil-based drilling fluids to impede gas hydrate dissociation and assure acquisition of high-quality logging while drilling (LWD) and wireline (WLL) log data. The well would also be drilled directionally to reach the identified bottom hole location to the east of the 7-11-12 pad (Figs. 54–56).

This part of the IA Final Report provides an overview of the operational aspects of the Hydrate-01 STW, including (1) pre-drill project and operational planning, (2) review of drilling operations, (3) synopsis of the completed logging operations, (4) acquisition of sidewall pressure cores, (5) a review of the well completion including the installation of fiber-optic monitoring cables, and (6) an analysis of the major lessons learned from the operational review of the Hydrate-01 well.

4.A.1. Hydrate-01 Pre-Drill Project and Operational Planning

In January 2016, the SOA-DNR reviewed the physical condition of the PBU 7-11-12 pad. The pad was remediated in the winter of 2005, which included filling reserve pits and returning them to natural habitat, removing berms, and other activities which left approximately 1.62 acres of useable area. The pad had been used for temporary storage activities and as a vehicle turnout. Site reviews indicated potential contamination at the interface of the gravel and tundra within the center of the pad, which was carefully characterized prior to any site remediation operations. Additional gravel was added to the pad in 2018. The pad was found likely to be suitable in size and condition for the drilling of the stratigraphic test well.

From 2017 to 2018, DOE, JOGMEC, and the USGS developed an operational drilling plan that enabled the needed science to be conducted in a manner that would not disrupt industry's ongoing field operations in the area. In 2018, BPXA proposed to operate the ANS Site 7-11-12 Stratigraphic Test Well, which was given the official name of the PBU Hydrate-01 Stratigraphic Test well (also known as the Hydrate-01 STW) in cooperation with the PRA-lead project team as a means to "warm up the rig" to be used for the PBU 2019 industry drilling program. After an extensive planning effort, the project partners moved forward with the Hydrate-01 STW, which was drilled and completed in December 2018 by BPXA as the PBU Operator. BPXA drilled the well using the Parker 272 rotary drilling rig through a Drilling Services Agreement executed with PRA in association with a contract between DOE and PRA. The operational plan for the Hydrate-01 STW was developed under a modified version of the BPXA "Decision Support System," which featured the development of a "Statement of Requirements" (SOR) document that specifically describes the project objectives and requirements (Okinaka

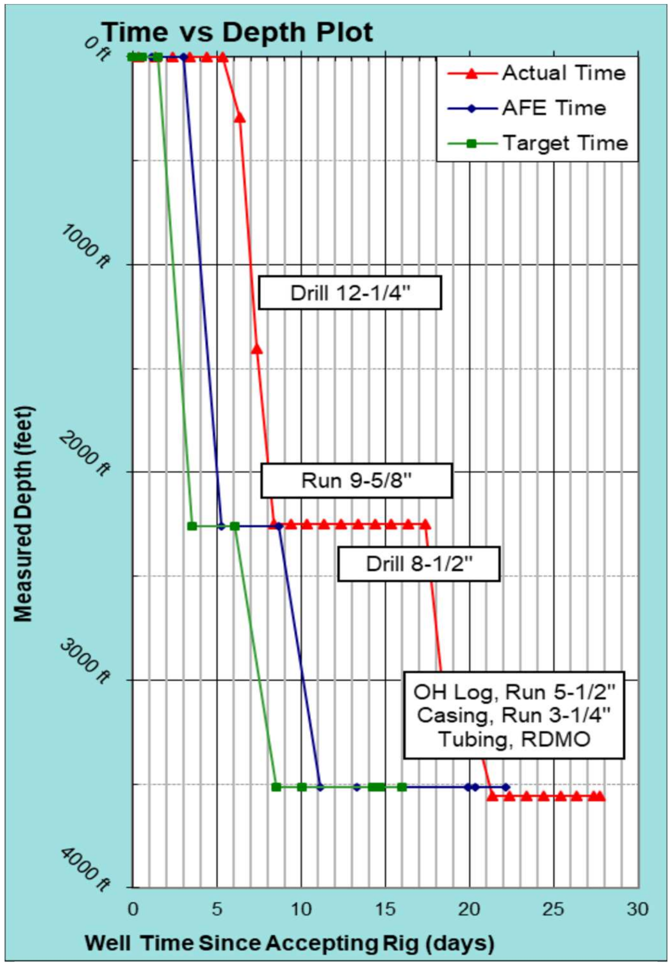

NPT	Time (hrs)
Rig stood down by IMT for DS02	~48
Gyro failure	2
Frozen cuttings chute	2
MWD sync issues	1
Surface casing top jobs	~48
Troubleshoot mud chiller	~85
Additional CoreVault run	4.5
Thermal issues while PT packoff	4.5
Attempt to PT 5-1/2" casing (leaking shoe track)	3
Run EZSV on E-Line to isolate shoe track	4
Issues setting TWC	4.5
Total NPT	**~9 days**

Figure 54. Drilling and operational performance analysis of the Hydrate-01 Stratigraphic Test Well. Shown is the actual well schedule as compared to the pre-drill well plan (modified from Collett et al., 2020). AFE = Authorization for expenditure, EZSV = Easy sliding valve, IMT = Incident Management Team, MWD = Measurement while drilling, NPT = Non-productive time, PT = Pressure testing, TWC = Two-way communication

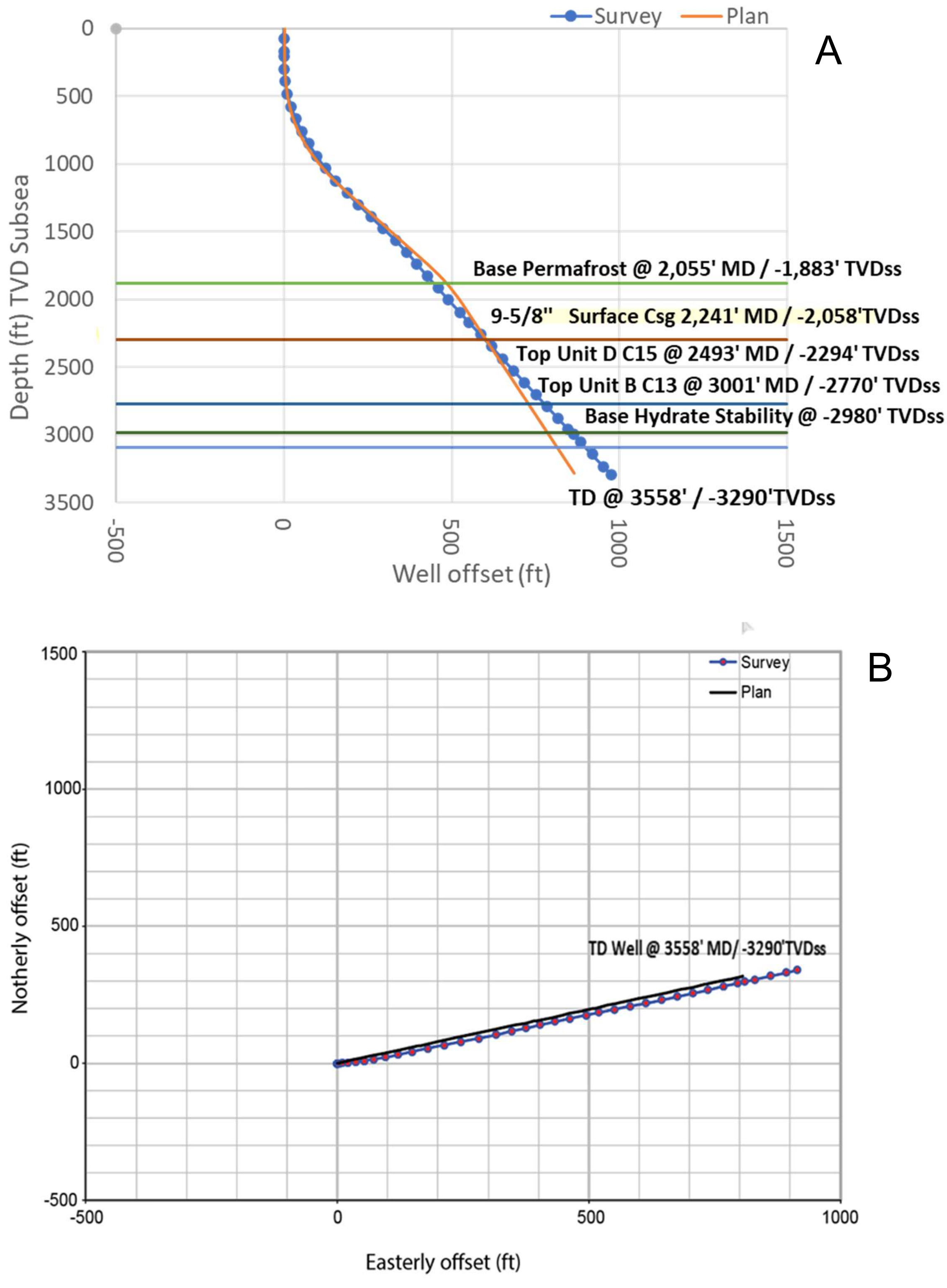

Figure 55. End-of-well vertical section image of the Hydrate-01 Stratigraphic Test Well profile; shown is the completed path (Survey) for the well in both (A) cross section and (B) map view relative to the original well design (plan). Also shown are the depths of the major well targets and features. Csg = Casing; MD = Measured depth, TVDss = True vertical depth subsea

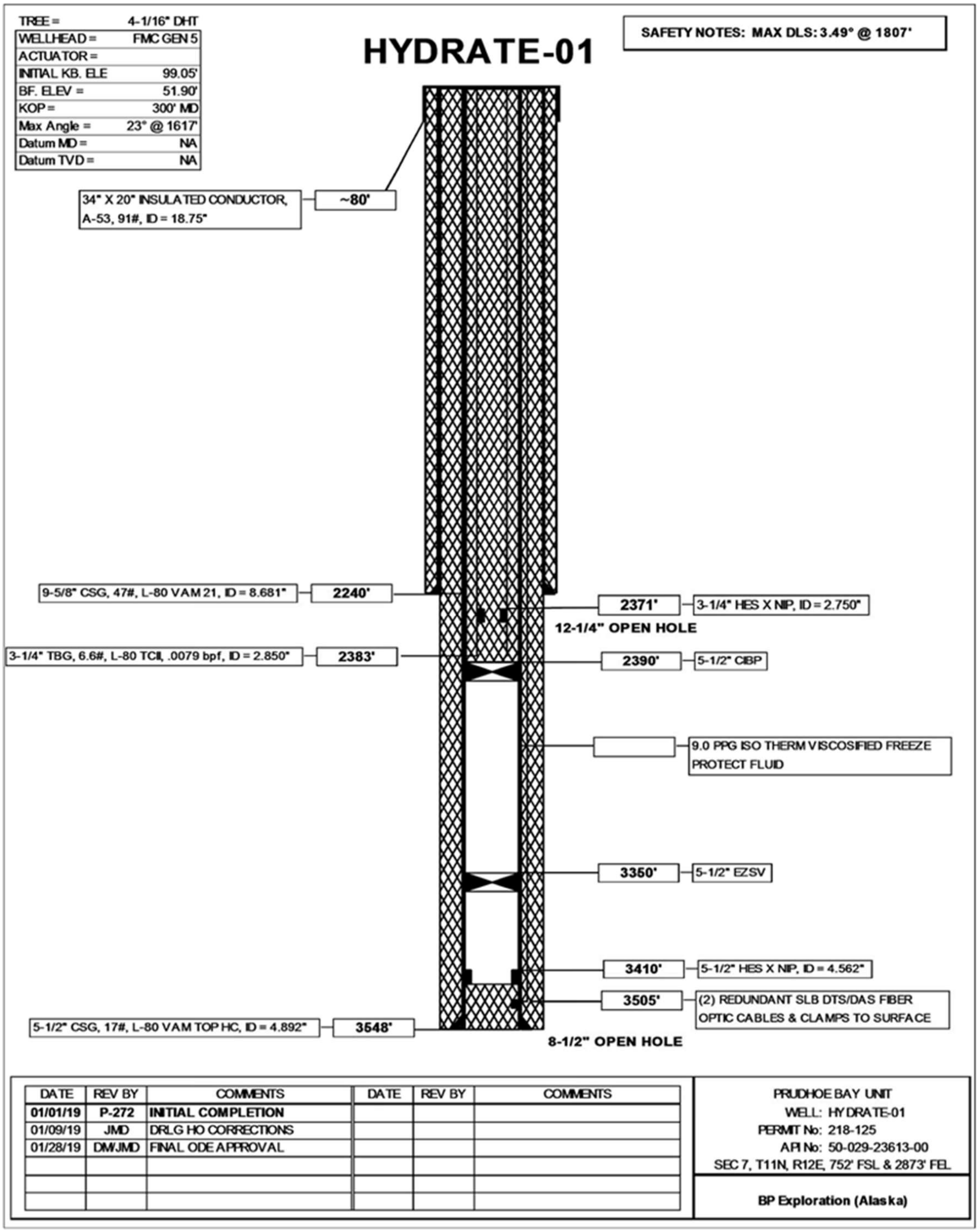

Figure 56. Engineering completion for the Hydrate-01 Stratigraphic Test Well depicting how the well was drilled and completed. DHT = Dry hole tree, FMC GEN 5 = FMC company generation 5 well head, KB ELE = Kelly busing elevation, BF ELEV = Below floor elevation, KOP = Kickoff point, MD = measured depth, TVD = True vertical depth, ID = Inside diameter, Max = Maximum, DLS = Dogleg severity, CSG = casing, VAM = Threaded connection, HES X NIP = Hess Corporation nipple, TBG = Tubbing, CIBP = Cast iron bridge plug, ISO THERM = Viscous anti-freeze fluid, EZSV = Easy Sliding Valve, SLB DTS/DAS = Schlumberger distributed temperature system and distributed acoustic system, API = American Petroleum Institute

et al., 2020). The following operational planning documents were generated in support of the Hydrate-01 STW:

- Hydrate-01 BPXA Statement of Requirements Report
- Hydrate-01 Well Operations Program Plan
- Hydrate-01 Well Construction Plan
- Hydrate-01 Well Plan Survey Report
- Hydrate-01 Well Anticollision Summary Report
- Hydrate-01 Drilling and Completion Fluids Plan
- Hydrate-01 Fiber Optic Installation Plan
- Hydrate-01 Drilling Fluid Temperature Control Plan
- Hydrate-01 MWD/LWD Data Acquisition Program Plan
- Hydrate-01 Contingent Wireline Logging Program Plan
- Hydrate-01 Mud Logging Program Plan
- Hydrate-01 SOA-AOGCC Permit to Drill Application

As defined during the project planning effort, the primary objectives of the Hydrate-01 well included the following:

- Confirm the presence, temperature, thickness, reservoir saturation, and grain size of gas hydrate-bearing Sagavanirktok Units B (primary target), C, and D (secondary targets) in the target area in order to determine if the site is suitable for a future gas hydrate production test well(s) and a geologic data collection well.

- If a suitable gas hydrate accumulation is confirmed, complete the STW as a monitoring well for the future production testing phase of the project. If logging data do not indicate sufficient hydrate presence, abandon the well.

Upon approval of the SOR by all stakeholders, the engineering design, contracting, and permitting phases of the project were performed by PRA and the research partnership under the operatorship of BPXA.

4.A.2. Hydrate-01 Drilling Operations

Drilling and data acquisition operations were conducted by BPXA in the Hydrate-01 STW from the acceptance of the Parker 272 drilling rig on 05-December-2018 through the release of the drilling rig on 01-January-2019 (Fig. 54). Program objectives were to acquire geologic and engineering data including sidewall pressure cores, LWD data, wireline-acquired log data (as a backup to LWD data, if required), and the deployment of formation monitoring systems pending the confirmation of suitable gas hydrate accumulations for production testing.

The Hydrate-01 STW was initially drilled as a vertical well to a depth of about 600 ft MD (183 m MD) and then deviated to target a bottom hole location about 1000 ft (305 m) to the northeast of the well's surface location on the Kuparuk 7-11-12 gravel pad (Figs. 55 and 56). The Hydrate-01 STW was completed to a total depth of 3558 ft MD (1085 m MD) or 3290 ft TVDss (1003 m TVDss) (TVDss = true vertical depth subsea).

Much like typical industry wells on the ANS, the Hydrate-01 STW drilling operations included the installation of surface casing below the permafrost section to help maintain borehole stability (Fig. 56). The 9-5/8" surface casing was landed and cemented in place to a depth of 2440 ft MD (744 m MD). The 8-1/2" production hole section was drilled with refrigerated (chilled) mineral oil-based mud (MOBM) drilling fluid to limit the dissociation of in situ gas hydrate and to maintain in-gauge borehole conditions to enable the acquisition of high-quality LWD data and sidewall pressure cores. The MOBM was cooled to a targeted temperature ranging from 15 to 35°F (about -9 to 2°C) by circulating the drilling fluids through a heat-transfer chilling unit connected to the Parker 272 drilling rig. Mud logging-acquired drill cuttings samples and gas geochemistry data were collected within both the surface and production hole section of the Hydrate-01 STW for real-time geologic characterization, archival storage of drill cuttings samples, and to fulfill USGS geochemical sampling requirements and protocol.

In support of the primary objectives of the Hydrate-01 STW, LWD tools were included within the bottom-hole assemblages (BHA) used to drill both the surface hole (12-1/4" hole) and production hole (8-1/2" hole) sections of the STW to enable the assessment of the targeted reservoir units (Table 8) as reviewed later in this report. The downhole logging program also included a contingency open hole wireline logging program. Contingency wireline logging was included in the well plan to deal with the possibility that the LWD data proved to be insufficient to characterize the presence of hydrates in the target intervals. Ultimately, the analysis of the LWD-acquired logging data confirmed the occurrence of gas hydrate and suitable reservoir conditions for production testing in both Unit B and Unit D, thus eliminating the need for contingency wireline logging. The determination of suitable reservoirs for testing also led to the decision to move ahead with the acquisition of sidewall pressure cores (Yoneda et al., 2020a, 2020b) and the installation of casing with fiber-optic cables for the measurement of formation temperatures and the acquisition of acoustic geophysical data (Lim et al., 2020).

Pressurized sidewall core samples were acquired from the reservoir and non-reservoir stratigraphic section associated with Units B and D (Table 9; Yoneda et al., 2020a, 2020b) in the Hydrate-01 STW as reviewed later in this report. The Hydrate-01 STW well was also outfitted with continuous fiber-optic monitoring cables, which were used to acquire a 3D vertical seismic profile (VSP) after the completion of the well (Lim et al., 2020). These same cables will be used to monitor downhole temperature conditions and acquire additional 3D VSP data throughout the remainder of the gas hydrate testing program.

After the completion of the production hole section of the Hydrate-01 STW with the running and cementing in place the 5-1/2" production casing to a depth of 3548 ft MD (1081 m MD) (Fig. 56), a wireline deployed gyroscope directional survey tool was run in the 5-1/2" casing to acquire highly accurate downhole well placement information. In addition, thermally insulating fluid was placed inside the casing, a bridge plug was set at 2390 ft MD (728 m MD) (Fig. 56), a 3-1/4" abandonment tubing was run to a depth of

BHA	LWD Log Run	Hole Section	Comments	Date Started	Date Finished	MWD Top (ft MD)	MWD Bottom (ft MD)	MAD Top (ft MD)	MAD Bottom (ft MD)	LWD and MWD Tools Primary Measurements
1		12.25 in	No data							
2	LWD001	12.25 in	Drill to casing point	11-Dec-18	13-Dec-18	318.25	2205	100	318.25	arcVISION 825 (gamma ray, resistivity) TeleScope 825 MWD (survey-power-com) SonicScope 825 (acoustic velocity) SadnVISION (neutron-density porosity)
3		12.25 in	No data: Clean Out							
4	LWD002	8.5 in	No data: Remove RSS							
5	LWD003	8.5 in	Drill to core point	20-Dec-18	23-Dec-18	2205	3224	2229.75	3256.83	arcVISION 675 (gamma ray, resistivity) TeleScope 675 MWD (survey-power-com) SonicScope 675 (acoustic velocity) proVISION 675 (NMR) adnVISION (neutron-density porosity)
6	LWD004	8.5 in	Drill to TD	25-Dec-18	26-Dec-18	3224	3522	2726	3160	arcVISION 675 (gamma ray, resistivity) TeleScope 675 MWD (survey-power-com) SonicScope 675 (acoustic velocity) proVISION 675 (NMR) adnVISION (neutron-density porosity)

Table 8. Logging while drilling (LWD) and measurement while drilling (MWD) program as completed in the Hydrate-01 Stratigraphic Test Well (Collett et al., 2020). com = communication, in = Inch, MAD = Measurements-After-Drilling, MD = Measured depth, NMR = Nuclear Magnetic Resonance, RSS = Rotary steerable system, TD = Total depth of well drill

2383 ft MD (726 m MD), and cement was pumped to fill the casing and tubing from the bridge plug to the surface.

It is important to highlight that the Hydrate-01 STW was completed without any recordable safety incidents. When considering the overall drilling and associated operational performance of the Hydrate-01 STW (Figs. 54-55), the pre-drill estimated 22.1-day program plan was exceeded by 5.6 days. The recordable "non-productive time" associated with Hydrate-01 STW operations can be mostly attributed to (1) an operational stand-down due to field operations outside the scope of this project, (2) unplanned surface casing completion "top job" remediations, and (3) performance issues associated with the mud chiller system.

4.A.3. Hydrate-01 Logging Operations

The primary well data obtained from the Hydrate-01 STW featured the acquisition of a full suite of Schlumberger LWD and measurement-while-drilling (MWD) well logs (Table 8). LWD/MWD operations in the 12-1/4" surface hole included the deployment of arcVISION, SadnVISION, Sonic Scope, and TeleScope tools. The LWD/MWD program in the 8-1/2" production hole section included the deployment of arcVISION, adnVISION, Sonic Scope, proVISION, and TeleScope tools. Table 8 contains a complete summary of Schlumberger LWD tools that were run in the Hydrate-01 STW along with the depth of each LWD log run. The primary log run was Run LWD001 within the 12-1/4" surface hole. Drilling/logging operations in the 8-1/2" production hole section were conducted in two parts: Runs LWD003 and LWD004. As shown in Table 8, the three primary log runs in the Hydrate-01 (i.e., LWD001, LWD003, and LWD004) each included additional measurement-after-drilling up-hole running surveys to acquire additional repeat log data over important and/or anomalous stratigraphic intervals.

Due to the careful control of drilling rates, the use of MOBM, and attention to maintaining cold mud temperatures throughout the drilling process, the 8-1/2" production hole section was in very good condition resulting in outstanding LWD data quality. The acquisition of a full suite of high-quality MWD/LWD data, including gamma-ray, resistivity, acoustic, and NMR well logs enabled the assessment and confirmation of the occurrence of gas hydrate in the targeted Unit B and Unit D reservoirs (Suzuki et al., 2019; Boswell et al., 2020b; Haines et al., 2020), achieving one of the primary objectives of the Hydrate-01 STW.

4.A.4. Hydrate-01 Acquisition of Sidewall Pressure Cores

To gather grain size and other data needed for the design of the production test well, sidewall pressure cores were collected in the Hydrate-01 STW using Halliburton's CoreVault tool (Okinaka et al., 2020; Yoneda et al., 2020a, 2020b). After the 8-1/2" production hole was advanced to a depth of 3260 ft MD (994 m MD), the CoreVault tool was run to obtain pressurized sidewall cores from the hydrate-bearing portions of Units B and D, along with additional core samples from the non-reservoir shale bounding stratigraphic sections associated with Units B and D. A total of 34 cores were successfully recovered during five runs of a wire-line deployed pressure corer in the Hydrate-01 STW (Table 9). A total of 13 pressure core samples were extracted,

Core Run and Core Number	Core Depth (ft MD)	BP Sample ID	BP Sample Depth (ft MD)	Stratigraphic Unit	Assigned Laboratory
1 - 2	3,006.01	1-2	3,006.00	Unit B	Stratum
1 - 3	3,007.04	1-3	3,007.00	Unit B	Stratum
1 - 4	3,008.05	1-4	3,008.00	Unit B	Stratum
1 - 5	3,009.05	1-5	3,009.00	Unit B	Stratum
1 - 6	3,011.02	1-6	3,011.00	Unit B	Stratum
1 - 7	3,013.08	1-7	3,013.00	Unit B	Stratum
1 - 8	3,015.01	1-8	3,015.00	Unit B	Stratum
1 - 10	3,019.02	1-10	3,019.00	Unit B	Stratum
1 - 12	3,023.05	1-12	3,025.00	Unit B	Stratum
1 - 13	3,026.03	1-13	3,027.00	Unit B	Stratum
2 - 1	3,032.00	2-18	3,032.00	Unit B	Stratum
2 - 2	3,033.01	2-19	3,033.00	Unit B	Stratum
2 - 3	3,035.05	2-20	3,035.00	Unit B	AIST
3 - 1	2,498.02	3-22	2,498.00	Unit D	AIST
3 - 2	2,501.07	3-23	2,501.00	Unit D	AIST
3 - 3	2,501.07	3-24	2,504.00	Unit D	Stratum
3 - 4	2,504.15	3-25	2,507.00	Unit D	AIST
3 - 5	2,511.04	3-27	2,511.00	Unit D	AIST
3 - 6	2,513.05	3-28	2,513.00	Unit D	Stratum
3 - 7	2,516.07	3-29	2,516.00	Unit D	AIST
3 - 8	2,519.03	3-30	2,519.00	Unit D	AIST
3 - 9	2,522.06	3-31	2,522.00	Unit D	Stratum
3 - 10	2,525.10	3-32	2,525.00	Unit D	AIST
4 - 1	3,010.04	4-33	3,010.00	Unit B	AIST
4 - 2	3,014.09	4-34	3,014.00	Unit B	Stratum
4 - 3	3,016.04	4-35	3,016.00	Unit B	AIST
4 - 4	3,018.04	4-36	3,018.00	Unit B	AIST
4 - 5	3,024.02	4-38	3,024.00	Unit B	AIST
4 - 6	3,040.01	4-39	3,040.00	Unit B	AIST
5 -1	3,078.07	5-44	3,078.00	Lower Seal	Stratum
5 - 2	3,074.03	5-45	3,074.00	Lower Seal	Stratum
5 - 3	3,070.02	5-46	3,070.00	Lower Seal	Stratum
5 - 4	Unknown	Unknown	Unknown	Lower Seal	Stratum
5 - 5	Unknown	Unknown	Unknown	Lower Seal	Stratum

Table 9. Listing of sidewall pressure cores recovered in the Hydrate-01 Stratigraphic Test Well using the Halliburton CoreVault system (Collett et al., 2020). Also shown is the laboratory to which each core was assigned. AIST = National Institute of Advanced Industrial Science and Technology in Sapporo, Japan; Stratum = Stratum Reservoir labs in Golden, Colorado, U.S.

preserved in liquid nitrogen, and shipped to the laboratories of the National Institute of Advanced Industrial Science and Technology in Sapporo, Japan, for advanced laboratory analysis (Yoneda et al., 2020a, 2020b). The remaining 21 core samples were shipped to the Stratum Reservoir labs in Golden, Colorado, for routine and advanced core analysis.

4.A.5. Hydrate-01 Well Completion and Monitoring Systems

With the confirmation of gas hydrate-bearing reservoirs within the Hydrate-01 STW, the decision was made to move ahead with the conversion of the Hydrate-01 STW to a monitoring well. This conversion included outfitting the well with continuous fiber-optic monitoring cables (clamped the casing and cemented in place). Two redundant sets of distributed temperature sensors (DTS) and distributed acoustic sensors (DAS) fiber-optic cables were clamped to the outside of the 5-1/2-inch production casing (Fig. 56), deployed to the bottom of the hole, and cemented in place. This installation completed the second major objective of the Hydrate-01 drilling program as defined within the project SOR. The DTS was used to collect formation temperatures over the entire length of the Hydrate-01 well during the 5-1/2-inch production casing cementing operations, over a short operational window of several days in the middle of March-2019, and continuous DTS monitoring was started in May 2019. The deployed DAS cables were used in March 2019 to obtain a large 3D VSP dataset over the site of the planned gas hydrate production test (Lim et al., 2020).

4.A.6. Hydrate-01 Operational Lessons Learned

At the end of the Hydrate-01 STW project, BPXA convened an "End of Well Review," which included the analysis of the lessons learned based on actionable conclusions about what went right, what went wrong, and what could be done to better prepare for future operations. The major actionable lessons learned from the Hydrate-01 STW operations included the following:

- Directional drilling vendor delivered the planned directional drilling program, despite removing the rotary steerable system (RSS) from the BHA.

- Drilling fluids vendor successfully ran a mineral-oil-based mud system with no issues; the rig team handled the mud without any contamination problems.

- The volume of surface casing cement was insufficient and did not circulate to the surface due to likely considerable surface hole enlargement within the ice-bearing permafrost section, causing the need for surface casing top jobs.

- The time required for the unplanned surface casing cement "top job" remediations were impacted by the lack of 24-hour coverage of the cement crew and lack of available lightweight cement on the ANS. Additionally, the time needed to develop the required compressive strength of the pumped cement was longer than anticipated, thus indicating the need for additional "pilot testing" of all cement products.

- The performance issues associated with the mud chiller system were attributed to the fact that the impact of a reduced internal mud chiller flow-rate was not fully appreciated; additional flow-rate sensitivity analysis should help understand the effect of the flow regime on the performance of the mud chiller system. For future projects, include both active (primary system) and passive (backup system) mud chiller systems.

- Improve ability to monitor mud temperatures in a digital format at various locations on the rig (i.e., before/after mud pumps, possum belly, pits).

- Despite causing drilling delays, the deployed mud chiller system was able to adequately cool mud and provide the conditions for obtaining excellent LWD data and sidewall pressure cores.

- The equipment configuration used to run and cement the 5-1/2-inch production casing was successful in delivering the second primary well objective to deploy DTS/DAS monitoring system.

- The lack of lead time restricted equipment options and added cost; planning for equipment orders should begin about 8-12 months before the start of operations.

4.A.7. Hydrate-01 Operational Summary

The Prudhoe Bay Unit Hydrate-01 STW was spudded by BPXA on 10-December-2018. Downhole data acquisition was completed on 25-December-2018 and the rig was released on 01-January-2019. The STW was drilled in two sections. The surface hole was drilled to a depth of 2248 ft MD (331 m MD) and cased, the "production hole section" was drilled to a depth of 3558 ft MD (1085 m MD) and also cased. A thermally chilled mineral-oil-based mud was used to maintain drillhole stability and quality of the borehole-acquired data. The primary borehole data were acquired using a suite of Schlumberger LWD tools. To gather grain size and other data needed to inform the design of the production test well, sidewall pressure cores were collected using Halliburton's CoreVault tool. In addition to confirming the geologic conditions at the test site, the Hydrate-01 well was designed to serve as a monitoring well during future field operations. Therefore, two sets of fiber-optic cables, each including bundled DAS and DTS, were clamped to the outside of the well casing and cemented in place. In March 2019, the project team worked with SAExploration to acquire 3D DAS VSP data in the Hydrate-01 STW, which was the largest 3D DAS-VSP ever conducted. Additionally, since the December 2018 completion of the STW, borehole temperature surveys have been acquired with the DTS deployed in the Hydrate-01 well.

The Hydrate-01 STW that was drilled in support of a proposed ANS gas hydrate production test project was completed in December 2018 with the following major results:

- The Hydrate-01 STW was drilled without any recordable incidents or injuries.

- The well confirmed the occurrence of gas hydrate in two targeted reservoir sections.

- A complete research-level suite of LWD downhole log data was acquired in the Hydrate-01 STW, which confirmed the presence of two high-quality reservoirs, each with high gas hydrate saturations that are suitable for gas hydrate production testing.

- The targeted reservoirs were determined to be acceptable for production testing; therefore, the DTS and DAS systems were installed in Hydrate-01 STW, allowing the well to serve as a monitoring well for future testing.

- Pressurized sidewall cores were recovered from both targeted gas hydrate reservoir units and their associated seals. Results of laboratory analysis of the petrophysical and geomechanical properties of the recovered sidewall pressure cores have been used to design the completion requirements for the future production test wells.

4.B. Hydrate-01 Stratigraphic Test Well Technical Findings

The Hydrate-01 STW met all project objectives and confirmed the occurrence of highly saturated gas hydrate-bearing reservoirs (Boswell et al., 2020b), which were designated Unit B and Unit D by Collett et al. (2011a, 2011b) (Fig. 57). Unit B, the deeper of the two reservoirs, comprised of well-sorted, very fine grained sand to coarse silt. The hydrate was interpreted to be filling 65 percent to more than 80 percent of the porosity in the upper ~40 ft (~12 m) of Unit B (Boswell et al., 2020b; Haines et al., 2020; Suzuki et al., 2019). Unit D, the shallower of the two reservoirs, exhibits similar gas hydrate saturations to that observed for Unit B. In addition, Unit D has a water-bearing section at its base, which could provide opportunities to investigate additional scientific and well design options as a potential follow-on to the testing of the primary Unit B target (Suzuki et al., 2019; Boswell et al., 2020b; Haines et al., 2020).

Critical to this effort is the evaluation of potential reservoir conditions in three dimensions. To support that assessment, the program acquired and evaluated a DAS 3D vertical seismic profile dataset (Lim et al., 2020) in March 2019. Mapping of local and bounding faults and interpretation of any major lateral changes in reservoir character in the area will inform the final selected location for subsequent wells in the planned testing program.

4.B.1. Hydrate-01 Gas Hydrate Reservoir Conditions

As described by Boswell et., (2020b), Unit D was encountered at a depth of 2493 ft MD (760 m MD) and consists of two zones (Fig. 57). The upper 37 ft (11 m) of the unit (to 2531 ft MD; 721 m MD) is relatively massive, with density porosities averaging ~37%. Resistivity is consistent at 100 ohm-m and shows no significant separation between the various measured resistivity logs. Comparison of density porosity and NMR porosity indicates gas hydrate saturation throughout the upper part of Unit D is ~70%. Initial interpretation of NMR transverse relaxation (T2) data indicates that the 30% water

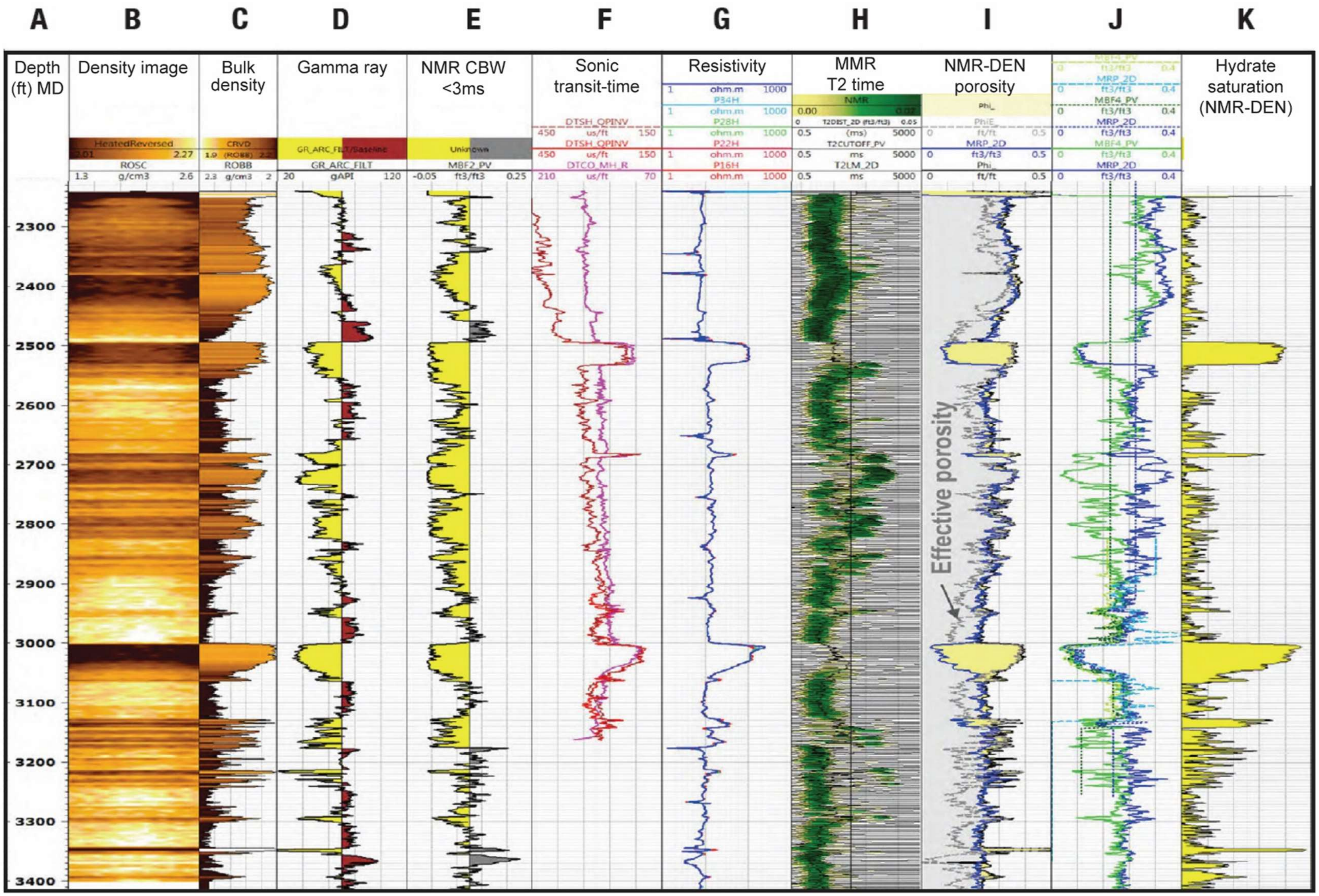

Figure 57. Summary of logging while drilling (LWD) and interpretations for the Hydrate-01 Stratigraphic Test Well, western Prudhoe Bay Unit, Alaska North Slope. Columns are as follows: (A) Measured depth, (B) Density image, (C) Bulk density, (D) Gamma ray, (E) Clay-bound water (NMR CBW), (F) Acoustic transit-time, (G) Resistivity, (H) Nuclear magnetic resonance (MMR) transverse relation times (T2 time), (I) NMR-density porosity and others, (J) NMR pore volume fractions, (K) Gas-hydrate saturation calculated by NMR-DEN porosity method (Boswell et al., 2020). Hydrate saturation (NMR-DEN) and porosity (NMR-DEN) shown in decimal percent.

content is defined as 88% bound- and 12% free-water. The lower 24 ft (7 m) of Unit D (to 2555 ft MD; 779 m MD) exhibits a gradual decrease in porosity and increase in gamma ray with depth. However, despite the generally gradual change in reservoir quality, NMR and resistivity data show a sharp transition (~2531 ft MD; 771 m MD) from highly gas hydrate saturated to water saturated with a high percentage of the water (~80%) being mobile, which appears to be a gas hydrate/water contact within the Unit D reservoir section.

Unit B was encountered at 3001 ft MD (915 m MD) (Boswell et al., 2020b) (Fig. 57). The reservoir appears massive and homogeneous to a depth of 3031 ft MD (924 m MD). This upper section of Unit B has a density porosity of ~40%. Resistivity consistently averages ~100 ohm-m, but the upper ~5 ft (~2 m) shows slightly higher values (up to 250 ohm-m) in those tools with greater depth of investigation. The lower 36 ft (11 m) of the unit shows a gradual decrease in reservoir quality that is matched by a similar decrease in inferred gas hydrate saturation. This indicates that the reservoir is fully charged with gas hydrate from top to base, with the degree of gas hydrate saturation being controlled by the petrophysical properties of the reservoir. NMR log data show no evidence of any substantial free-water zones in the Unit B reservoir section. Assuming gas and water chemistries that are typical of the ANS (Collett et al., 2011a), the base of gas hydrate stability is likely to occur from 50 to 100 ft (15 to 30 m) below the base of Unit B.

4.B.2. Hydrate-01 Gas Hydrate Reservoir Petrophysical Properties

As described by Boswell et al. (2019, 2020b) and Yoneda et al. (2020a, 2020b), planning for subsequent test wells necessitated the collection of grain-size data from the Hydrate-01 STW. Given the unconsolidated nature of the units and the inevitable loss of sample with dissociation upon retrieval, the acquisition of pressure cores was necessary to assure recovery of physical samples. To gather the samples, Halliburton's CoreVault system was deployed, collecting samples from both the reservoirs and the bounding units associated with Units B and D (Collett et al., 2019b, 2020). Mineralogy and grain-size studies (Yoneda et al., 2020a, 2020b) indicate the reservoirs are well sorted and quartz rich, with the grain size of the sampled reservoir section ranging from coarse silt to very fine sand. Additional analysis of the recovered pressure cores yielded in situ effective permeabilities measured in Units B and D on the order of 10 mD (Yoneda et al., 2020a, 2020b).

Evaluation of LWD NMR data provided a second interpretation of in situ effective permeabilities within the gas hydrate reservoirs. Standard methods of NMR analyses suggest low values (on the order of 0.1 mD) associated with high bound-water fractions. However, reevaluation of the NMR log data (Yoneda et al., 2020b) indicates that higher permeability values consistent with those obtained from pressure cores are possible for the gas hydrate-bearing reservoir sections logged and cored in the Hydrate-01 STW.

The USGS (Haines et al., 2020), using an effective medium theory rock-physics approach (Helgerud et al., 1999), has estimated gas hydrate saturations from compressional (P) and shear (S) wave log data acquired in the Hydrate 01 STW (Fig. 58). Haines et al. (2020) assumed that gas hydrate occurs as load-bearing material (i.e., part of the grain matrix). For Unit D, approximately ~500 ft (~150 m) above the base if gas hydrate

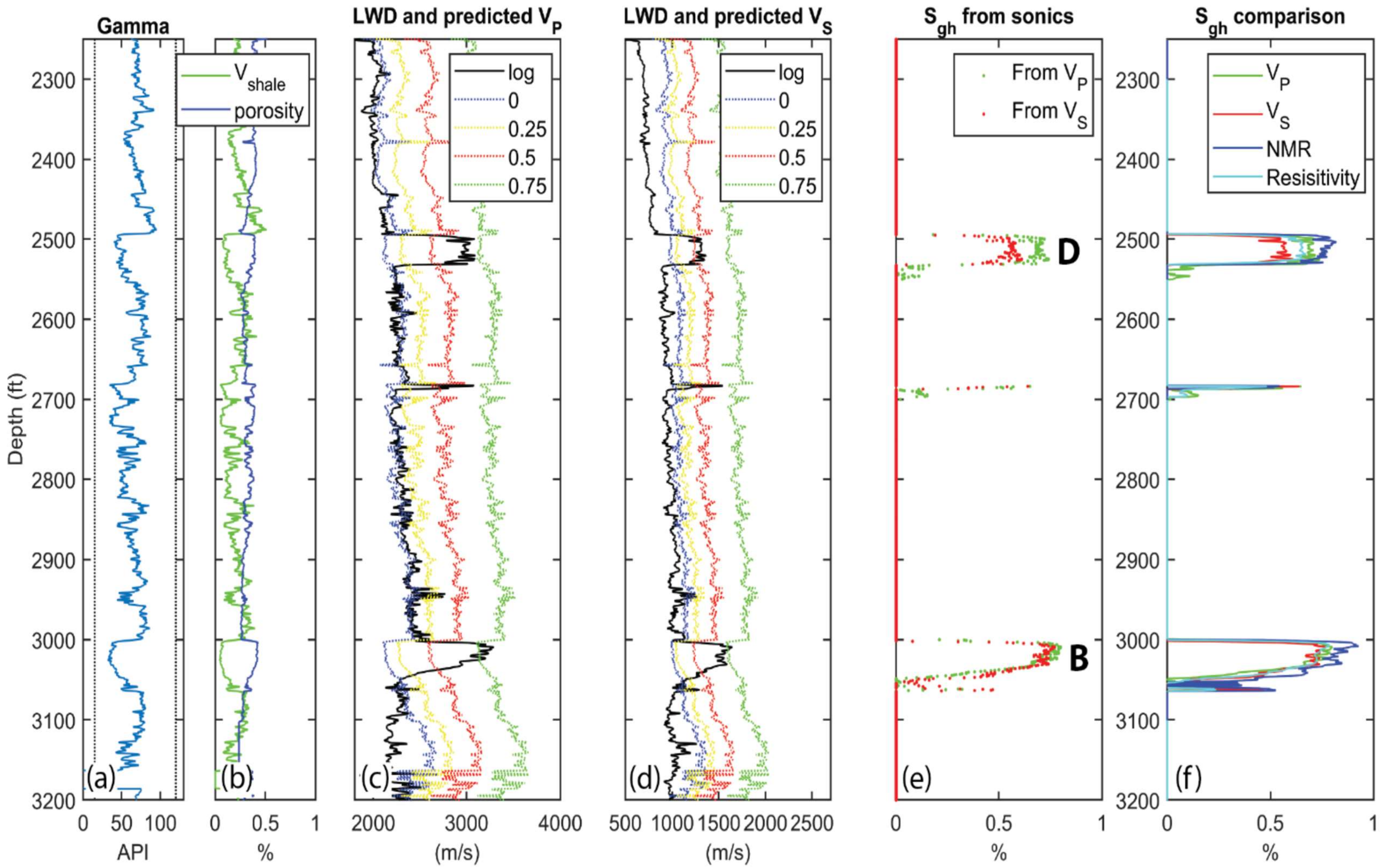

Figure 58. Gas hydrate saturation (S_{gh}) from sonic and other log data. (a) Logging while drilling (LWD) gamma ray log, (b) V_{shale} and porosity, (c) LWD-measured V_P (black line) and predicted V_P for S_{gh} values as indicated in the legend, (d) LWD-measured V_S (black line) and predicted V_S for S_{gh} values as indicated, (e) comparison of S_{gh} values estimated from V_P and V_S, (f) comparison of all four S_{gh} estimates. The reservoir portion of Units B and D is indicated with bold letters. Modified from Haines et al. (2020). Hydrate saturation (S_{gh}) shown in decimal percent.

stability (BGHS), both P-wave and S-wave acoustic logs indicate moderate gas hydrate saturations (75 %) with S-wave results slightly lower than those for P-waves. For the Unit B, located just above the BGHS, we obtain moderate to high gas hydrate saturation estimates (approaching 80%) from both the P-wave and S-wave sonic logs. The P-wave saturation estimates agree well with results from electrical resistivity-based estimates, whereas estimates from NMR LWD data generally suggest 5 to 10 % higher saturations; the S-wave results suggest lower saturations. These differences likely indicate complexities in the distribution of gas hydrate at the pore scale in Units B and D (Haines et al., 2020).

4.B.3. Hydrate-01 Gas Hydrate Reservoir Production Modeling

Gas hydrate production models based on the analysis of Hydrate-01 STW acquired LWD data and sidewall pressure core samples were developed through a collaborative DOE-JOGMEC numerical simulation effort to predict the thermodynamic and hydraulic response of the Hydrate-01 STW gas hydrate-bearing reservoir sections to depressurization (as reviewed by Myshakin et al., 2020). The developed gas hydrate production models combine both gas hydrate-bearing sections in Unit B and Unit D together with the intermediate Unit C and the over- and under-burden sand and shale sections. The vertical heterogeneity in porosity, gas hydrate saturation, and permeability distributions for reservoir and non-reservoir units was assigned using "fine mesh discretization" (Myshakin et al., 2020) (Fig. 59). Given the uncertainty regarding effective in situ permeability, geologic models constructed for reservoir simulations represent an integration of measurements, including (1) a conservative (low-permeability) case (Case-B) was built using standard NMR methods, (2) a core-calibrated (higher permeability) case (Case-A) that uses sidewall core data (available only from the reservoir sections), and (3) a third "most likely" case (Case-C) that uses the initial NMR-based values in the non-hydrate-bearing sections and the relevant core-calibrated values within the reservoir sections (Figs. 59 and 60). The depressurization method was applied to Unit B to induce gas hydrate destabilization at constant bottom hole pressure values. The results of the initial numerical simulations (Fig. 60) were used to support the development of production scenarios, well design, surface facilities design, and field test procedures with the main goal to perform efficient and safe scientific production testing.

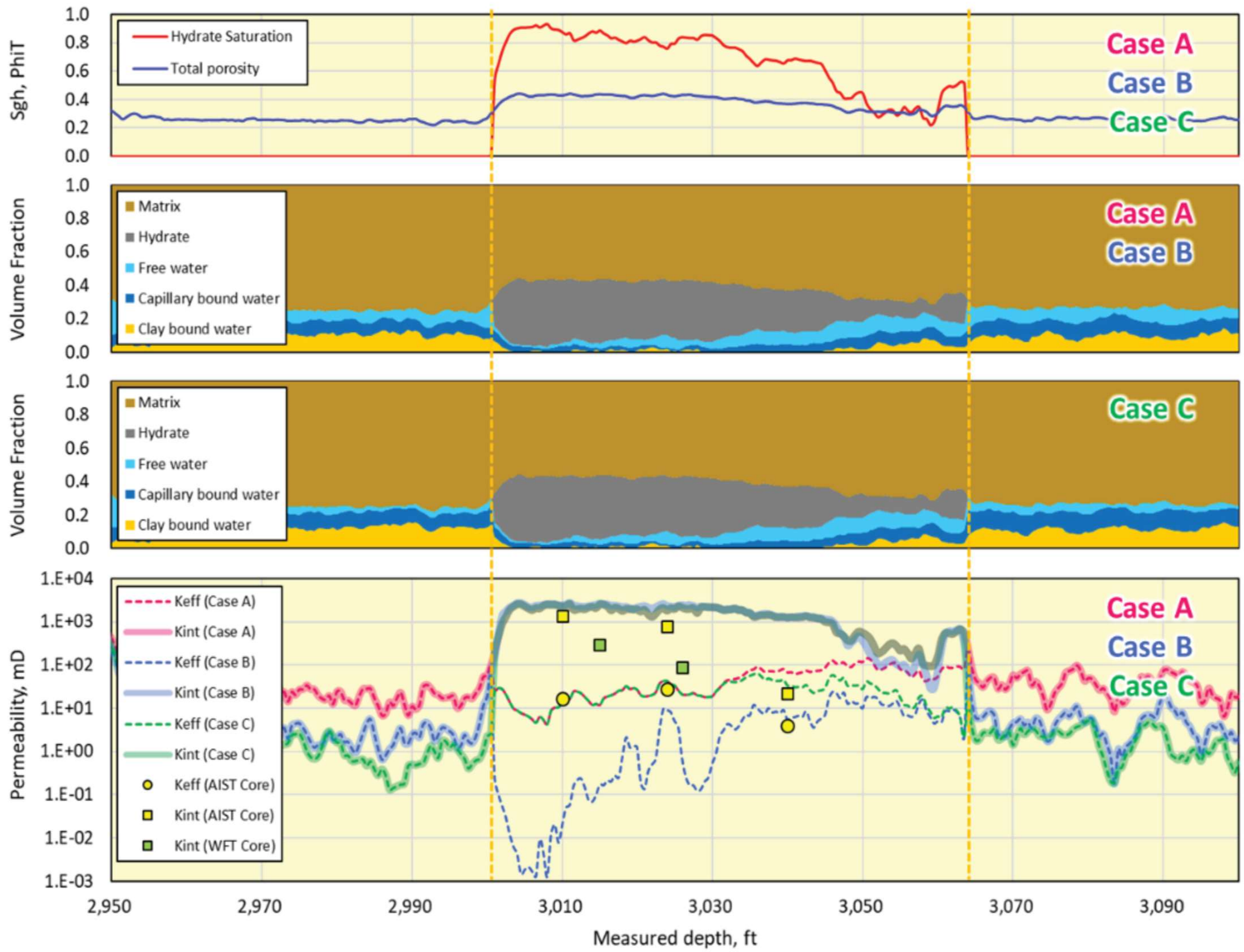

Figure 59. Geological input data from the Hydrate-01 Hydrate Stratigraphic Test Well used for Unit B reservoir response modeling. Data shown include sediment porosity, gas hydrate saturation, pore fluid volume fractions, and permeabilities. Hydrate saturation (S_{gh}) and volume fraction are shown in decimal percent. Yellow dashed lines define the boundaries of Unit B. Modified from Myshakin et al. (2020). Three production cases were designed based on three different permeability models: Case A = NMR log derived values; Case B = Core data corrected NMR log values; Case C (assumed "best case") = Combination of Cases A and B.

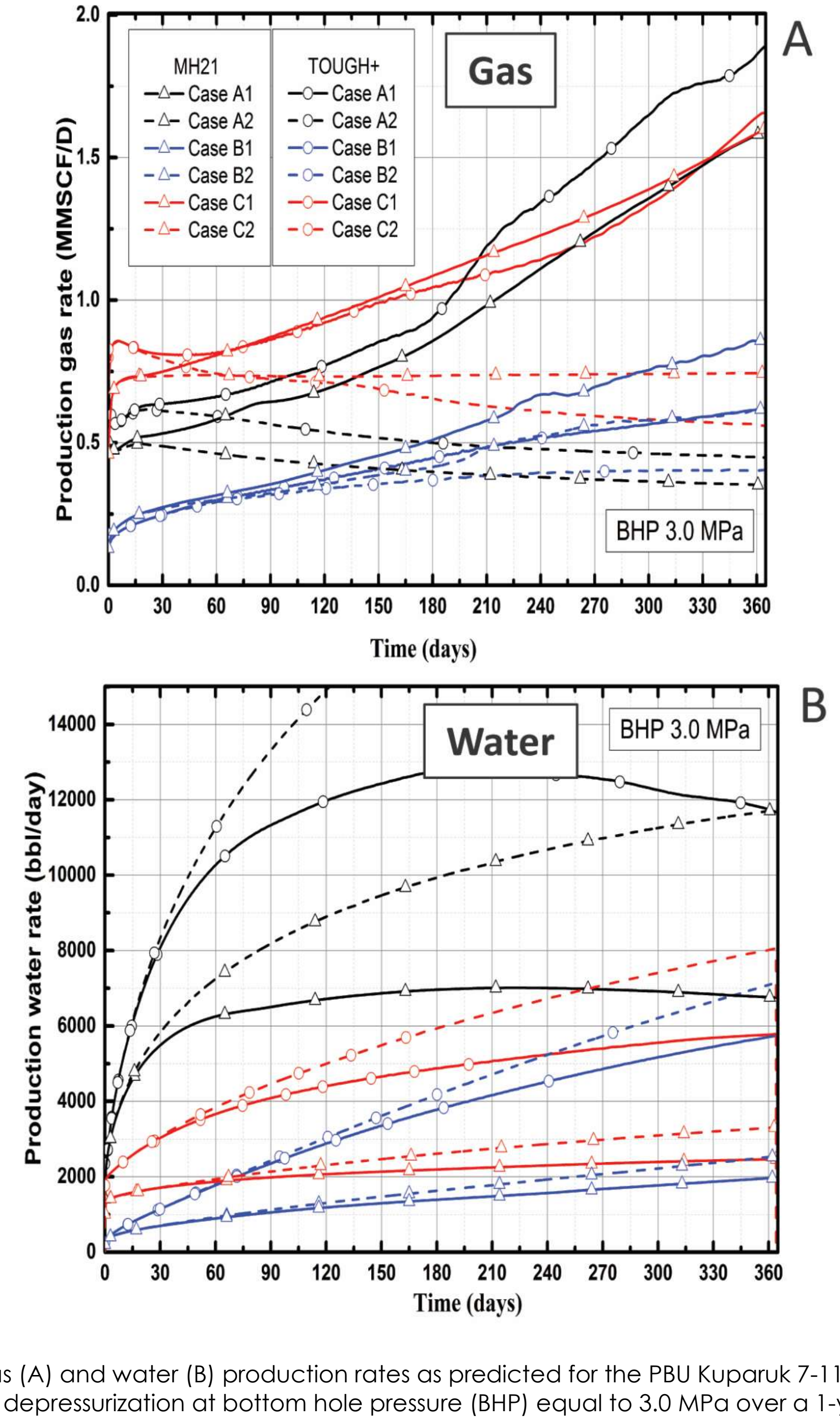

Figure 60. Gas (A) and water (B) production rates as predicted for the PBU Kuparuk 7-11-12 reservoir (Unit B) using depressurization at bottom hole pressure (BHP) equal to 3.0 MPa over a 1-year period for three production cases, the "1" (solid curves) and "2" (dashed curves) designate 500 and 3000 m (~1640 and 9843 ft) radii for the 2D reservoir models, respectively. The production data predicted using the MH21 code are given by the curves with open triangles, those made by the Tough+ code are depicted using open circles. Modified from Myshakin et al. (2020). Results shown assume three production cases based three different permeability models: Case A = NMR log derived values; Case B = Core data corrected NMR log values; Case C (assumed "best case") = Combination of Cases A and B. BBL = Barrels, MMSSCF = Million standard cubic feet), NMR = Nuclear Magnetic Resonance

5. PBU 7-11-12 Test Site Production Testing Planning

With the successful confirmation of the presence of hydrate-bearing reservoir sections suitable for production testing at the site of the Hydrate-01 STW, the next goal of the ANS gas hydrate production testing effort was to partner with an experienced industry operator for the planned production test (Okinaka et al., 2020). The project partners, including DOE, JOGMEC, and the USGS have worked together to recommend the design of the remaining wells, surface production facilities, and testing procedures to allow the implementation of efficient and safe scientific production testing and monitoring that will address a range of questions associated with the response of gas hydrate-bearing reservoirs to depressurization. The PBU 7-11-12 test site production testing plan as reviewed in the following part of this report is the last project deliverable included within the DOE-USGS IA.

As reviewed previously in this report, the plan for the "Alaska Gas Hydrate Production Field Experiment" is to conduct a long-term (12 months or more) scientific reservoir response test utilizing depressurization production technology, currently scheduled to start in 2022. These activities will provide an initial assessment of the potential to successfully produce gas hydrate resources in similar settings throughout the U.S. and the world.

The DOE-JOGMEC-USGS partnership, also known as the "Collaborative Gas Hydrate R&D in Alaska Project Owners Group (POG)," is responsible for developing the scientific objectives and for recommending well designs and operational procedures for the ANS gas hydrate production test. The planning efforts in support of this project included the modification and generation of existing and new planning documents, including the following: (1) an updated version of the project prospectus that deals with the major goals and design aspects of the planned ANS gas hydrate production test, (2) a comprehensive outline of the gas hydrate production test data acquisition requirements, and (3) the development and refinement of a detailed depressurization well test plan and a contingency test well intervention plan.

As noted above, the POG's efforts have looked beyond the stratigraphic test well phase of the project to determine design requirements for the testing phase. Cooperative gas hydrate production modeling studies conducted within the project partnership (as reviewed above in this report) have been used to predict what flow rates are to be expected during a test of the Unit B reservoir section (Myshakin et al., 2020). These studies have also been used to consider the test well design requirements (completion design, sand control, flow assurance systems, gauges/measurement and control systems, production monitoring systems) to implement a successful production test.

Within the gas hydrate field test planning effort, the USGS coordinated the effort to develop and maintain the project "Science and Operational Plan" for the "Alaska Gas Hydrate Production Field Experiment." This "Science and Operational Plan" (Table 10) represents both an internal project planning and briefing document intended to provide a comprehensive systematic review of the objectives of the entire "Alaska Gas Hydrate Production Field Experiment." This project planning document is also intended

Alaska Gas Hydrate Production Field Experiment
Science and Operational Plan

Part I. Introduction and Science Plan
- **I.1. Executive Summary**
- **I.2. Data to be Acquired to Achieve Science Objectives**
- **I.3. Test Site G&G Characterization**
  - *I.3.1. Hydrate-01 Stratigraphic Test Well Results*
  - *I.3.2. DAS-VSP (MARCH-2019) Data Analysis*

Part II. Operational Recommendations
- **II.1 Well Delivery GDW/PTW-1/PTW-2: Drilling**
- **II.2. Well Delivery GDW/PTW-1/PTW-2: Completion**
- **II.3. Well Delivery PTW-1/PTW-2: Sand Control**
- **II.4. Well Delivery PTW-1/PTW-2: Artificial Lift**
- **II.5. Well Delivery PTW-1/PTW-2: Intervention Plan**
- **II.6. Operational Facilities**
  - *II.6.1. Testing Procedure PTW-1/PTW-2B/PTW-2D*
  - *II.6.2. Subsurface Facilities*
  - *II.6.3. Surface Testing Facilities*
  - *II.6.4. Well Production Intervention Plan*
  - *II.6.5. Data Acquisition and Management*
- **II.7. Well Derived Geoscience Data Acquisition**
  - *II.7.1. Mud Logging Program*
  - *II.7.2. Downhole LWD/Wireline Logging Program*
  - *II.7.3. DTS/DAS/DSS and Gauge Based P&T Systems and Surface Monitoring Systems*
  - *II.7.4. Stabilization of Borehole Temperature Conditions*
  - *II.7.5. Pressure Coring System & Operations*
  - *II.7.6. Coring Plan*
  - *II.7.7. Well Site Core Flow and Analysis*
  - *II.7.8. Post Well Site Core Shipping, Processing and Analysis*
- **II.8. Production Data Analysis and Decision Making**
  - *II.8.1. Decision-Making on Test Progression*
  - *II.8.2. Decision-Making on Intervention*
- **II.9. Geophysical Data Acquisition**
  - *II.9.1. DAS-VSP Data Analysis - Before and After Production Test*
  - *II.9.2. CWT Data Analysis - Before and After Production Test*

Table 10. Outline of the "Science and Operational Plan" that was prepared as part of the project planning effort in support of the "Alaska Gas Hydrate Production Field Experiment" under the direction of the Japan Oil, Gas, and Metals National Corporation (JOGMEC), the U.S. Department of Energy – National Energy Technology Laboratory (DOE-NETL), and the U.S. Geological Survey (USGS) "Collaborative Gas Hydrate R&D in Alaska" Project Owners (POs).

to provide the POG selected Third Party Operator (TPO) with a comprehensive review of the project technical requirements and expert recommendations to advance the design and implementation of the "Alaska Gas Hydrate Production Field Experiment."

The operational recommendations included in this project planning document provide expert insight to gas hydrate specific operational tasks and concerns. As such, this planning document makes extensive use of lessons learned from previous partner-led field projects, with particular importance placed on the review of the operational results of the 2018 ANS PBU Hydrate-01 Stratigraphic Test Well (Collett et al., 2020) as compiled and reviewed in this planning document. The provided expert insight and lessons learned entries within this planning document are intended to communicate to the selected TPO specific technical information that can be considered in the development of the well drilling and testing program plans to be generated by the TPO.

6. Accomplishments of the Alaska Gas Hydrate Interagency Agreement

In review, the objective of this DOE and USGS IA was to provide geologic and geophysical technical support to identify and characterize gas hydrate production test sites on the ANS and to develop plans for an extended gas hydrate production testing program. In addition, the primary goal of the project supported by this IA is to conduct a scientific field production test in northern Alaska from one or more gas hydrate-bearing sand reservoirs using conventional "depressurization" technology. The project has included the drilling and evaluation of a stratigraphic test well, which was completed in December 2018. This will be followed by the establishment of a production test site (including a geoscience data well, two production test wells, deployment of well monitoring systems, and surface monitoring), and the testing of reservoir responses to pressure reduction over a period of about 12 months or for whatever period the parties find operations at the site to be valuable.

The technical support provided by the USGS under this cooperative IA was organized under two project subtasks: *Subtask 1.1. Geologic Occurrences of Gas Hydrate, Analyzing Available Eileen Geologic and Geophysical Data, and Subtask 1.2. Gas Hydrate Field Test Technical and Operational Support*. Under *Subtask 1.1,* the USGS led the effort to refine the interpretations of the regional ANS gas hydrate stability field as well as the distribution and properties of previously identified gas hydrate accumulations in the Eileen Gas Hydrate Trend through the collection and incorporation of new well log and seismic data. Under *Subtask 1.2,* the USGS has (1) provided technical leadership and advice for formulation of a research drilling and production testing program designed to assess the nature and production potential of gas hydrates on the ANS, (2) provided personnel and resources to enhance field and laboratory analyses of material recovered by pressure core systems, and (3) partnered in the synthesis of data from logging, direct sampling, and geophysical and geologic characterization studies conducted under this agreement. The collective accomplishments of the research efforts conducted under this cooperative IA are further reviewed below in this section of the report and summarized in Tables 11 and 12.

Research conducted under this cooperative IA revealed the relatively complex nature of the occurrence of gas hydrate in the Eileen Gas Hydrate Trend, with gas hydrates occurring in a series of coarsening upward, laterally pervasive, sand reservoirs systems with mostly fine-grained sand beds exhibiting high gas hydrate saturations that are interbedded with non-reservoir shale (clay-rich) beds. For the most part, the IA managed partnership identified gas hydrate occurrences were laterally segmented into distinct northwest- to southeast-trending fault blocks with often well log-inferred downdip water contacts. Depositional facies control on the occurrence of gas hydrate in the study area, presented in the form of reservoir shale content, porosity, and permeability trends, was also observed within Eileen Gas Hydrate Trend. The USGS-supported efforts revealed that most of the gas hydrate-bearing reservoirs in the Eileen trend are found in combination structural-stratigraphic traps and are only partially hydrate filled with distinct downdip water contacts. These findings suggest that traditionally recognized parts of a petroleum system that control the occurrence of conventional gas accumulations (i.e., reservoir, gas source, gas migration, and timing of

Alaska Gas Hydrate Production Field Experiment – Planning & Accomplishments

- USGS research and resource assessments in Alaska
- Gas hydrate production testing interest in Alaska – Before 2016
- Mapping and characterization of gas hydrate accumulations in the Eileen Trend
- Production test site G&G analysis and selection – MPU Cascade and PBU 7-11-12
- Development of the initial goals of the Alaska Gas Hydrate Production Field Experiment
- Public and private sector outreach and engagement in Alaska
- Detailed G&G and reservoir engineering examination of the PBU 7-11-12 Test Site
- Development science and operational project plans and task specific Statements of Requirements
- Planning and execution of the Hydrate-01 Stratigraphic Test Well drilling program
- Analysis of geologic (well logs and core derived) and geophysical data acquired from the Hydrate-01 well
- Gas hydrate production modeling studies with data from the Hydrate-01 well
- Production testing monitoring technology R&D review – distributed and gauge-based systems
- Gas hydrate geophysical response modeling – focus on 3D/4D VSP acquisition, processing, and analysis
- Development of the Alaska Gas Hydrate Production Field Experiment Science and Operational Plan
- Development of the GDW/PTWs well delivery, completion, monitoring, and production testing plans
- Development of the GDW and PTWs G&G and production testing data (logging, coring, geophysical, monitoring, etc.) acquisition and analysis plan
- Review and development of well response systems to measure produced fluid/gas volumes and P/T responses with surface and down hole equipment
- Execution of the Geoscience Data and Production Test wells drilling and data acquisition program
- Conduct production testing in PTW-1 and as appropriate in PTW-2 consisting of pressure reduction and monitoring, with intervention as needed and surface operations including gas, water, and solids disposal
- Test results data analysis, post-testing production modeling code calibration studies, and reporting

Table 11. Completed project planning and accomplishments associated with the Interagency Agreement (IA) between the Department of Energy (DOE) and the U.S. Geological Survey (USGS) under DOE Award Number DE-FE0022898.

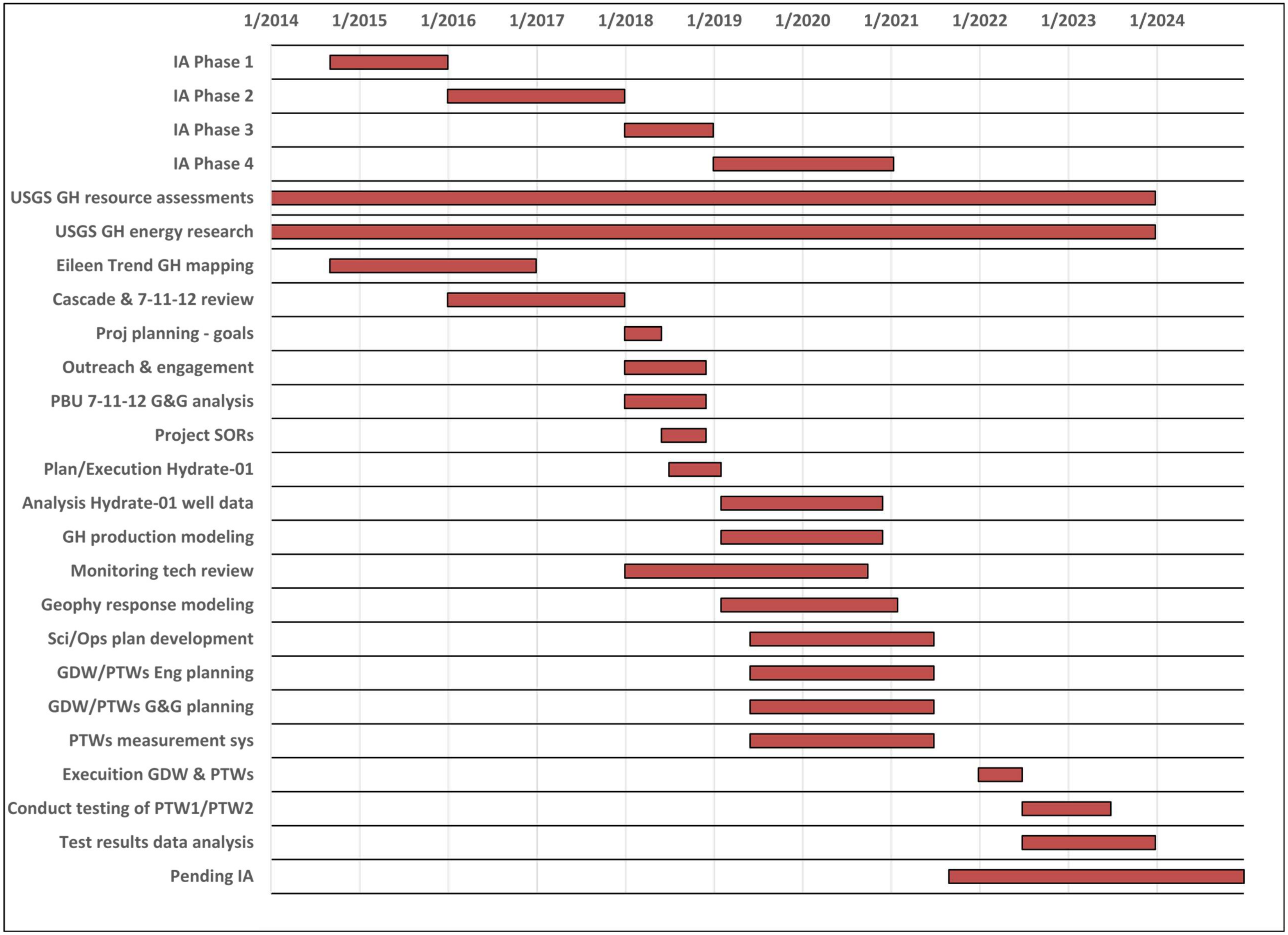

Table 12. Completed project planning and accomplishments, as well as the timeline associated with the Interagency Agreement (IA) between the Department of Energy (DOE) and the U.S. Geological Survey (USGS) under DOE Award Number DE-FE0022898.

factors controlling the accumulation of gas with the reservoir-trap system) also control the occurrence of gas hydrate in the Eileen Gas Hydrate Trend.

The test site review effort under this agreement focused on the known and expected gas hydrate occurrences in the Grater Prudhoe Bay area and their suitability for extended-duration production testing. The first test site review effort as described in this report dealt with the 2011 analysis of the Eileen Gas Hydrate Trend and the selection of the PBU L Production Pad site, near which the Iġnik Sikumi well was drilled and tested in 2011/2012. Building on the results of the Iġnik Sikumi test well program and the information gained from this project, the USGS coordinated a second (2017) test site review and analysis effort that led to the selection of the PBU 7-11-12 test site and the drilling of the Hydrate-01 Stratigraphic Test Well.

The Hydrate-01 Stratigraphic Test Well was drilled in 2018 from the PBU 7-11-12 test site in the western portion of the PBU to verify the geological and reservoir conditions at a proposed gas hydrate production test site. The Hydrate-01 Stratigraphic Test Well met all project objectives and confirmed the occurrence of highly saturated gas hydrate-bearing reservoirs in the identified Unit B and Unit D Eileen Gas Hydrate Trend stratigraphic units. The reservoirs were found as expected; Unit B was confirmed to hold gas hydrate at high concentrations, and the Unit D reservoir section was found to be only partially charged, with the lower part of the reservoir section being water wet. With the success of the Hydrate-01 Stratigraphic Test Well, the project leadership group moved on to develop the project "Science and Operational Plan" for the "Alaska Gas Hydrate Production Field Experiment" production testing effort at the PBU 7-11-12 test site.

Cited References

Alaska Oil and Gas Conservation Commission, 1992, Summary of the Cirque-1 Blowout of February 12, 1992, Public Record Letter from D.J. Ruckel, ARCO Alaska, to D. Johnston: State of Alaska Oil and Gas Conservation Commissioner, Anchorage, Alaska, 32 p.

Alaska Oil and Gas Conservation Commission, 2020, Well file images database (web page): State of Alaska, Alaska Oil and Gas Conservation Commission (last viewed April 13, 2020). http://aogweb.state.ak.us/WebLink/Browse.aspx

Anderson B., Boswell R., Farrell H., Ohtsuki S., White M., and Zyrianova M., 2014, Review of the findings of the Iġnik Sikumi CO2-CH4 gas hydrate exchange field trial: Proceedings of the 8th International Conference on Gas Hydrates (ICGH8-2014), Beijing, China, 28 July - 1 August, 2014, 38 p.

Anderson, B., Hancock, S., Wilson, S., Enger C, Collett T., Boswell R., and Hunter R., 2011a, Formation pressure testing at the Mount Elbert Gas Hydrate Stratigraphic Test Well, Alaska North Slope: operational summary, history matching, and interpretations: Marine Petroleum Geology, v. 28, no. 2, p. 478-492. http://dx.doi.org/10.1016/j.marpetgeo.2010.02.012.

Anderson, B.J., Kurihara, M., White, M.D., Moridis G.J., Wilson S.J., Pooladi-Darvish M., Gaddipati M., Masuda Y., Collett T.S., Hunter R.B., Narita H., Rose K., and Boswell R., 2011b, Regional long-term production modeling from a single well test, Mount Elbert Gas Hydrate Stratigraphic Test Well, Alaska North Slope: Marine Petroleum Geology, v. 28, no. 2, p. 493-501. http://dx.doi.org/10.1016/j.marpetgeo.2010.01.015.

Anderson, B.J., Wilder, J.W., Kurihara, M., White, M.D., Moridis, G.J., Wilson, S.J., Pooladi-Darvish, M., Masuda, Y., Collett, T.S., Hunter, R.B., Narita, H., Rose, K., and Boswell, R., 2008, Analysis of modular dynamic formation test results from the Mount Elbert 01 stratigraphic test well, Milne Point Unit, North Slope, Alaska, in International Conference on Gas Hydrates (ICGH 2008), 6th, Vancouver, British Columbia, Canada, 6–10 July 2008, Proceedings, International Conference on Gas Hydrates, 10 p.

ANWR Assessment Team, U.S. Geological Survey, 1999, The oil and gas resource potential of the Arctic National Wildlife Refuge 1002 Area, Alaska: U.S. Geological Survey Open-File Report 98–34, 12 p.

Archie, G.E., 1942, The electrical resistivity log as an aid in determining some reservoir characteristics: Journal of Petroleum Technology, v. 1, p. 55-62.

Arp, J. J., 1953, The effect of temperature on the density and electrical resistivity of sodium chloride solutions: Trans. Am. Inst. Min. Metall. Pet. Eng., 198, p. 327-330.

Ashford, D.I., Mizuta, T., Dallimore, S.R., Yamamoto, K., Nixon, F.M., Imasato, Y., Wright, J.F., Taylor, A.E., Applejohn, A., 2012, Overview of engineering and operations activities conducted as part of the JOGMEC/NRCan/Aurora Mallik 2007-2008 Gas hydrate Production Research Well Program, Part A: 2007 field program, in Scientific Results from the JOGMEC/NRCan/Aurora Mallik 2007-2008 Gas hydrate Production Research Well Program, Mackenzie Delta, Northwest Territories, Canada. Geological Survey of Canada Bulletin 601, p. 25-51.

Asquith, G.B., and Krygowski, D., 2004, Basic well log analysis, American Association of Petroleum Geologists, Tulsa, Oklahoma, 244 pp.

Bard, H.B., and Fairbanks, R.G., 1990, U-Th ages obtained by mass spectrometry in corals from Barbados, sea level during the past 130,000 years: Nature, v. 346, p. 456–458.

Bird, K.J., 1998, Geographic and geologic setting, Chapter GG, in The Oil and Gas Resource Potential of the Arctic National Wildlife Refuge 1002 Area, Alaska, by ANWR Assessment Team: U.S. Geological Survey Open-File Report 98-34, Version 1.0, p. GG1-GG51, CD-ROM. http://pubs.usgs.gov/of/1998/ofr-98-0034/GG.pdf

Bird, K.J., and Houseknecht, D.W., 2002, U.S. Geological Survey 2002 petroleum resource assessment of the National Petroleum Reserve in Alaska (NPRA)—Play maps and technically recoverable resource estimates: U.S. Geological Survey, Open-File Report 02–207, 201 p.

Bird, K.J., and Magoon, L.B., 1987, Petroleum geology of the northern part of the Arctic National Wildlife Refuge, northeastern Alaska: U.S. Geological Survey Bulletin 1778, 324 p.

Boswell, R., and Collett T. S., 2011, Current perspective on gas hydrate resources: Energy Environ. Sci., 4, 1206-1215 pp. DOI:10.1039/C0EE00203H

Boswell, R., Collett, T.S., Anderson B., and Hunter R., eds., 2011a, Thematic set on scientific results of the Mount Elbert Gas Hydrate Stratigraphic Test Well, Alaska North Slope: Marine and Petroleum Geology, v. 28, no. 2, p. 279-608.

Boswell, R., Collett, T.S., Suzuki, K., Yoneda, J., Haines, S., Okinaka, N., Tamaki, M., Crumley, S., Itter, D., and Hunter, R., 2020b, Alaska North Slope 2018 Hydrate-01 Stratigraphic Test Well: Technical results: Proceedings of the 10th International Conference on Gas Hydrates (ICGH10), Singapore, June 21-26, 2020, 6 p. Posted on the DOE National Energy Technology Laboratory website https://www.netl.doe.gov/node/10037.

Boswell, R., Hancock, S., Yamamoto, K., Collett, T.S., Pratap, M., Lee, S.-R., 2020a, Chapter 6 Natural Gas Hydrates: Status of potential as an energy resource: Future Energy 3rd edition - Book Chapter, Elsevier's Book, 36 p.

Boswell, R., Marsteller, S., Okinaka, N., Wakatsuki, M., Collett, T.S., Hunter, R., Walsh, T., Minge, D., Itter, D., and Crumley, S., 2019, Viable long-term gas hydrate testing site confirmed on the Alaska North Slope: Fire-in-the-ice, DOE-NETL Methane Hydrate News Letter, v. 19, Issue 1, p. 1-5.

Boswell, R., Rose, K., Collett, T.S., Lee, M.W., Winters, W.F., Lewis, K., and Agena, W.F., 2011b, Geologic controls on gas hydrate occurrence in the Mount Elbert prospect: Milne Point Unit: Journal of Marine and Petroleum Geology, v. 28, no. 2, p. 589–607.

Boswell, R., Schoderbek, D., Collett, T.S., Ohtsuki, S., White, M., and Anderson, B.J., 2017, The Iġnik Sikumi Field Experiment, Alaska North Slope: Design, operations, and implications for CO2−CH4 exchange in gas hydrate reservoirs: Energy Fuels, v. 31, no.1, p. 140-153.

Boswell R., Yamamoto K., Lee S.-R., Collett T., Kumar P., and Dallimore S., 2014, Methane Hydrates, chapter 8 *in* Letcher T.M. (Editor) Future Energy, Second Edition: Improved, Sustainable and Clean Options for our Planet, p.159-178. DOI: http://dx.doi.org/10.1016/B978-0-08-099424-6.00008-9

Boswell, R., Yoneda, J., Waite, and W.F., 2019, India National Gas Hydrate Program Expedition 02 summary of scientific results: Evaluation of natural gas-hydrate-bearing pressure cores: Journal of Marine and Petroleum Geology, v. 108, p. 143–153.

Brothers, L. L., Hart P. E., and Ruppel C. D., 2012, Minimum distribution of subsea ice-bearing permafrost on the U.S. Beaufort Sea continental shelf: Geophysical Research Letters, v. 39, L15501, 6 p. DOI: 10.1029/2012GL052222.
Brothers, L., Herman, B., Hart, P., and Ruppel, C., 2016, Subsea ice-bearing permafrost on the U.S. Beaufort Margin: (1) Minimum seaward extent defined from multichannel seismic reflection data: Journal of Geochemistry, Geophysics, Geosystems, v. 17, issue 11, p. 4354-4365.
Carman, G.J., and Hardwick, Peter, 1983, Geology and regional setting of the Kuparuk oil field, Alaska: American Association of Petroleum Geologists Bulletin, v. 67, no. 6, p. 1014–1031.
Chaouachi, M., Falenty, A., Sell, K., Enzmann, F., Kersten, M., Haberthur, D., and Kuhs, W.F., 2015, Microstructural evolution of gas hydrates in sedimentary matrices observed with synchrotron X-ray computed tomographic microscopy: Geochemistry, Geophysics, Geosystems, v. 16, p. 1711–1722. doi:10.1002/2015GC005811.
Chatterton, C.V., 1983, Statistical report, Alaska Oil and Gas Conservation Commission, 208 p. http://doa.alaska.gov/ogc/annual/annindex.html
Collett, T.S., 1992, Well log evaluation of natural gas hydrates: U.S. Geological Survey, Open-File Report 92-381, 28 p.
Collett, T.S., 1993, Natural gas hydrates of the Prudhoe Bay and Kuparuk River area, North Slope, Alaska: American Association of Petroleum Geologists Bulletin, v. 77, no. 5, p. 793-812.
Collett, T.S., 1995, Gas hydrate resources of the United States, *in* Gautier, D.L., Dolton, G.L., Takahashi, K.I., and Varnes, K.L., eds., 1995 National assessment of United States oil and gas resources on CD-ROM: U.S. Geological Survey Digital Data Series 30.
Collett, T.S., 2001, A review of well-log analysis techniques used to assess gas-hydrate-bearing reservoirs: Natural Gas Hydrates: Occurrence, Distribution, and Detection, American Geophysical Union: Geophysical Monograph 124, p. 189-210.
Collett, T.S., 2002, Energy resource potential of natural gas hydrates: American Association of Petroleum Geologists, v. 86, no. 11, p. 1971-1992.
Collett, T.S., Agena, W.F., Lee, M.W., Zyrianova, M.V., Bird, K.J., Charpentier, T.C., Houseknecht, D.W., Klett, T.R., Pollastro, R.M., and Schenk, C.J., 2008a, Assessment of gas hydrate resources on the North Slope, Alaska, 2008: U.S. Geological Survey Fact Sheet 2008–3073, 4 p. (Also available at http://pubs.usgs.gov/fs/2008/3073/.)
Collett T., Bahk, J.J., Baker, R., Boswell, R., Divins, D., Frye, M., Goldberg, D., Husebø, J., Koh, C., Malone, M., Morell, M., Myers, G., Shipp, C., and Torres, M., 2015, Methane hydrates in nature-current knowledge and challenges: Journal of Chemical Engineering Data, v. 60, p. 319–329.
Collett, T.S., Bird, K.J., Kvenvolden, K.A., and Magoon, L.B., 1988, Geologic interrelations relative to gas hydrates within the North Slope of Alaska: U.S. Geological Survey Open-File Report 88–389, 150 p.
Collett, T.S., Bird, K.J., and Magoon, L.B., 1993, Subsurface temperatures and geothermal gradients on the North Slope, Alaska: Cold Regions Science and Technology, v. 21, p. 275-293.
Collett, T., Boswell, R., Cochran, J., Kumar, P., Lall, M., Mazumdar, A., Ramana, M., Ramprasad, T., Riedel, M., Sain, K., Sathe, A., and Vishwanath, K., 2014, Geologic implications of gas hydrates in the offshore of India: Results of the National Gas

Hydrate Program Expedition 01: Journal of Marine and Petroleum Geology, v. 58, p. 1-28.
Collett, T.S., Boswell, R., Lee, M.W., Anderson, B.J., Rose, K., and Lewis, K.A., 2012, Evaluation of long-term gas hydrate-production testing locations on the Alaska North Slope: Society of Petroleum Engineers, Reservoir Evaluation and Engineering, v. 15, no. 2, p. 243-264.
Collett, T.S., Boswell, R., Waite, W.F., Kumar, P., Roy, S.K., Chopra, K., Singh, Sunil K., Yamada, Y., Tenma, N., Pohlman, J., Zyrianova, M., and NGHP Expedition 02 Scientific Party, 2019c, India National Gas Hydrate Program Expedition 02 summary of scientific results: Gas hydrate systems along the eastern continental margin of India: Journal of Marine and Petroleum Geology, v. 108, p. 39-142.
Collett, T.S., and Dallimore, S.R., 2002, Detailed analysis of gas hydrate induced drilling and production hazards: Proceedings of the Fourth International Conference on Gas Hydrates, Yokohama, Japan, May 19–23, p. 47–52.
Collett, T.S., Johnson, A.H., Knapp C.C., and Boswell, R., 2009, Natural Gas Hydrates: A Review, *in* Collett T., Johnson A., Knapp C., Boswell R., eds., Natural gas hydrates—Energy resource potential and associated geologic hazards: American Association of Petroleum Geologists Memoir 89, p. 146-219.
Collett, T.S., and Lee, M.W., 2012, Well log characterization of natural gas hydrates: Petrophysics, v. 53, no. 5 (October 2012), p. 348-367.
Collett, T., Lee, M., Agena, W., Miller, J., Lewis, K., Zyrianova, M., Boswell, R., and Inks, T., 2011a, Permafrost-associated natural gas hydrate occurrences on the Alaska North Slope: Journal of Marine and Petroleum Geology, v. 28, no. 2, p. 279-294.
Collett, T.S., Lewis, R.E., Winters, W.F., Lee, M.W., Rose, K.K., and Boswell, R.M., 2011b, Downhole well log and core montages from the Mount Elbert Gas Hydrate Stratigraphic Test Well, Alaska North Slope: Journal of Marine and Petroleum Geology v. 28, no. 2, p. 561-577.
Collett, T.S., Lewis, K.A., Zyrianova, M.V., Haines, S.S., Schenk, C.J., Mercier, T.J., Brownfield, M.E., Gaswirth, S.B., Marra, K.R., Leathers-Miller, H.M., Pitman, J.K., Tennyson, M.E., Woodall, C.A., and Houseknecht, D.W., 2019a, Assessment of undiscovered gas hydrate resources in the North Slope of Alaska, 2018: U.S. Geological Survey Fact Sheet 2019–3037, 4 p. https://doi.org/10.3133/fs20193037.
Collett, T.S., Okinaka, N., Wakatsuki, M., Boswell, R., Marsteller, S., Minge, D., Crumley, S., Itter, D., and Hunter, R., 2019b, Alaska North Slope 2018 Hydrate 01 Stratigraphic Test Well: Design and operations: Proceedings of the American Geophysical Union 2019 Fall Meeting, San Francisco, California, December 9-13, 2019, OS33A-01, 1 p. https://agu.confex.com/agu/fm19/meetingapp.cgi/Paper/510043
Collett, T., Okinaka, N., Wakatsuki, M., Boswell, R., Marsteller, S., Minge, D., Crumley, S., Itter, D., Hunter, R., 2020, Design and operations of the Hydrate-01 Stratigraphic Test Well, Alaska North Slope: Proceedings of the 10th International Conference on Gas Hydrates (ICGH10), Singapore, June 21-26, 2020, 6 p. Posted on the DOE National Energy Technology Laboratory website https://www.netl.doe.gov/node/10037
Collett, T.S., Riedel, M., Cochran, J.R., Boswell, R., Kumar, P., Sathe, A.V., and the NGHP Expedition 01 Scientific Party, 2008b, Indian continental margin gas hydrate prospects—Results of the Indian National Gas Hydrate Program (NGHP) Expedition 01: Proceedings of the 6th International Conference on Gas Hydrates (ICGH 2008), 6th, Vancouver, British Columbia, Canada, 6–10 July 2008, Proceedings: International Conference on Gas Hydrates, 10 p., http://hdl.handle.net/2429/1035

Crain, E.R., 1986, The log analysis handbook: Published by PennWell Publishing Company, Tulsa, Oklahoma, 95 p.
Dallimore, S.R., and Collett, T.S., eds., 2005, Scientific results from the Mallik 2002 gas hydrate production research well program, Mackenzie Delta, Northwest Territories, Canada: Geological Survey of Canada Bulletin 585, 2 CD-ROM set.
Dallimore, S.R., Wright, J.F., Nixon, F.M., Kurihara, M., Yamamoto, K., Fujii, T., Fujii, K., Numasawa, M., Yasuda, M., and Imasato, Y., 2008a, Geologic and porous media factors affecting the 2007 production response characteristics of the JOGMEC/NRCAN/AURORA Mallik Gas Hydrate Production Research Well: Proceedings of the 6th International Conference on Gas Hydrates (ICGH 2008), July 6-10, 2008, Vancouver, British Columbia, Canada, 10 p.
Dallimore, S. R., Wright, J.F., and Yamamoto, K., 2008b, Appendix D: Update on Mallik, in Energy from gas hydrates: Assessing the opportunities and challenges for Canada: Ottawa, Canada, Council of Canadian Academies, p. 196-200. http://www.scienceadvice.ca/documents/(2008-11-05)%20Report%20on%20GH.pdf
Dallimore, S.R., Yamamoto, K., Wright, J.F., and Bellefleur, G., eds., 2012, Scientific results from the JOGMEC/NRCan/Aurora Mallik 2007-2008 gas hydrate production research well program, Mackenzie Delta, Northwest Territories, Canada: Geological Survey of Canada Bulletin 601, 291 p. DOI:10.4095/291751
Decker, P.L., 2007, Brookian sequence stratigraphic correlations, Umiat Field to Milne Point Field, west-central North Slope, Alaska: Alaska Division of Geological and Geophysical Surveys Preliminary Interpretive Report 2007-2, 19 p., 1 sheet.
Farrell, H., Boswell, R., Howard, J., and Baker, R., 2010, CO2-CH4 exchange in natural gas hydrate reservoirs: potential and challenges: Fire-In-The-Ice, The National Energy Technology Laboratory Methane Hydrate Newsletter, v. 10, no. 1, p. 19-21.
Frye, M., 2008, Preliminary evaluation of in-place gas hydrate resources: Gulf of Mexico Outer Continental Shelf: Minerals Management Service Report 2008-004, 136 p.
Fujii, T., Namikawa, T., Okui, T., Kawasaki, M., Ochiai, K., Nakamizu, M., Nishimura, M., Takano, O., and Tsuji, Y., 2009, Methane hydrate occurrence and saturation confirmed from core samples, eastern Nankai Trough, Japan, *in* Collett, T., Johnson, A., Knapp, C., Boswell, R., eds., Natural Gas Hydrates -- Energy Resource Potential and Associated Geologic Hazards: American Association of Petroleum Geologists Memoir 89, p. 385-400.
Garrity, C.P., Houseknecht, D.W., Bird, K.J., Potter, C.J., Moore, T.E., Nelson, P.H., and Schenk, C.J., 2005, U.S. Geological Survey 2005 oil and gas resource assessment of the Central North Slope, Alaska—Play maps and results: U.S. Geological Survey Open-File Report 02–439 35 p.
Grantz, Arthur, Holmes, M.L., and Kososki, B.A., 1975, Geologic framework of the Alaskan continental terrace in the Chukchi and Beaufort Seas, *in* Yorath, C.J., Parker, E.R., and Glass, D.J., eds., Canada's continental margins and offshore petroleum exploration: Canadian Society of Petroleum Geologists Memoir 4, p. 669–700.
Gryc, George, 1988, Geology and exploration of the National Petroleum Reserve in Alaska, 1974 to 1982: U.S. Geological Survey Professional Paper 1399, 940 p.
Gryc, George, Patton, W.W., Jr., and Payne, T.G., 1951, Present Cretaceous stratigraphic nomenclature of northern Alaska: Washington Academy of Sciences Journal, v. 41, no. 5, p. 159–167.

Haines, S., Collett, T., Boswell, R., Lim, T-K., Okinaka, N., Suzuki, K., Fujimoto, A., 2020, Gas hydrate saturation estimation from acoustic log data in the 2018 Alaska North Slope Hydrate-01 Stratigraphic Test Well: Technical results: Proceedings of the 10th International Conference on Gas Hydrates (ICGH10), Singapore, June 21-26, 2020, 5 p. Posted on the DOE National Energy Technology Laboratory website https://www.netl.doe.gov/node/10037.

Helgerud, M.B., Dvorkin, J., Nur, A., Sakai, A., and Collett, T., 1999, Elastic-wave velocity in marine sediments with gas hydrates: Effective medium modeling: Geophysical Research Letters, v. 26, p. 2021-2024.

Hilchie, D.W., 1982, Applied Openhole Log Interpretation for Geologists and Engineers: Published by Douglas W. Hilchie Inc., Colorado School of Mines, Golden, Colorado, 243 p.

Holder, G.D., Malone, R.D., and Lawson, W.F., 1987, Effects of gas composition and geothermal properties on the thickness and depth of natural-gas-hydrate zone: Journal of Petroleum Technology, September, p. 1147–1152.

Hubbard, R.J., Edrich, S.P., and Rattey, R.P., 1987, Geologic evolution and hydrocarbon habitat of the 'Arctic Alaska Microplate,' in Tailleur, I., and Weimer, P., eds., Alaskan North Slope geology: Bakersfield, Calif., and Anchorage, Alaska, Pacific Section, Society of Economic Paleontologists and Mineralogists and Alaska Geological Society, p. 797–830.

Hunt, J.M., 1979, Petroleum geology and geochemistry: San Francisco, Calif., W.H. Freeman Publisher, 716 p.

Hunter, R., Collett, T., Boswell, R., Anderson, B., Digert, S., Pospisil, G., Baker, R., and Weeks, M., 2011, Mount Elbert gas hydrate stratigraphic test well, Alaska North Slope: Overview of scientific and technical program: Journal of Marine and Petroleum Geology, v. 28, no. 2, p. 295-310.

Inks, T.L., Lee, M.W., Agena, W.F., Taylor, D.J., Collett, T.S., Hunter, R.B., and Zyrianova, M.V., 2009, Seismic prospecting for gas hydrate and associated free-gas prospects in the Milne Point area of northern Alaska, *in* Collett, T., Johnson, A., Knapp, C., and Boswell, R., eds, Natural Gas Hydrates -- Energy Resource Potential and Associated Geologic Hazards: American Association of Petroleum Geologists Memoir 89, p. 541-554.

Judge, A.S., Smith, S.L., and Majorowicz, J., 1994, The current distribution and thermal stability of natural gas hydrates in the Canadian Polar Regions: Proceedings of the Fourth International Offshore and Polar Engineering Conference, Osaka, Japan, p. 307-313.

Kadhim, F.S., Samsuria, A., and Kamal, A., 2013, A Review in correlations between cementation factor and carbonate rocks properties: Life Science Journal, v. 10, no. 4, p. 2451-2458.

Kleinberg, R.L., Flaum, C., and Collett, T.S., 2005, Magnetic resonance log of JAPEX/JNOC/GSC et al. Mallik 5L-38 gas hydrate production research well: Gas hydrate saturation, growth habit, relative permeability, *in* Dallimore, S.R., Collett, T.S. (Eds.), Scientific Results from the Mallik 2000 Gas Hydrate Production Research Well Program: Geological Survey of Canada Bulletin, v. 585, p. 10.

Konno, Y., Fujii, T., Sato, A., Akamine, K., Naiki, M., Masuda, Y., Yamamoto, K., Nagao, J., 2017, Key findings of the world's first offshore methane hydrate production test off the coast of Japan: Toward future commercial production: Energy & Fuels, v. 31, no. 3, p. 2607-2616.

Konno, Y., Yoneda, J., Egawa, K., Ito, T., Jin, Y., Kida, M., Suzuki, K., Fujii, T., Nagao, J., 2015, Permeability of sediment cores from methane hydrate deposit in the Eastern Nankai Trough: Journal of Marine and Petroleum Geology, v. 66, no. 2, p. 487–495.
Kumar, P., Collett, T., Yadav, U., Boswell, R., Cochran, J., Lall, M., Mazumdar, A., Ramana, M., Ramprasad, T., Riedel, M., Sain, K., Sathe, A., and Vishwanath, K., 2014, Geologic implications of gas hydrates in the offshore of India: Krishna-Godovari Basin, Mahanadi Basin, Andaman Sea, and Kerala-Konkan Basin: Journal of Marine and Petroleum Geology, v. 58, p. 29-98.
Kvenvolden, K.A., 1988, Methane hydrate--A major reservoir of carbon in the shallow geosphere: Chemical Geology, v. 71, p. 41-51.
Kvenvolden, K.A., 1993, A primer in gas hydrates, *in* Howell, D.G., ed., The Future of Energy Gases: U.S. Geological Survey Professional Paper 1570, p. 279-292.
Lachenbruch, A.H., Galanis, S.P., and Moses, T.H., 1987b, A thermal cross section for the permafrost and hydrate stability zones in the Kuparuk and Prudhoe Bay Oil Fields, *in* Galloway, J.P., and Hamilton, T.D., eds., Geological Studies in Alaska by the U.S. Geological Survey during 1987: USGS Circular 1017, 4 p.
Lachenbruch, A.H., Sass, J.H., Lawver, L.A., Brewer, M.C., Marshall, B.V., Munroe, R.J., Kennelly, J.P., Jr., Galanis, S.P., Jr., and Moses, T.H., Jr., 1987a, Temperature and depth of permafrost on the Alaskan North Slope, *in* Tailleur, I.L., and Weimer, Paul, eds., Alaskan North Slope Geology: Bakersfield, Calif., Pacific Section, Society of Economic Paleontologists and Mineralogists and the Alaska Geological Society, Book 50, v. 2, p. 545–558.
Lee, M.W., 2005, Proposed moduli of dry rock and their application to predicting elastic velocities of sandstones: U. S. Geological Survey Scientific Investigation Report 2005-5119, 14 p.
Lee, M.W., 2007, Velocities and attenuations of gas hydrate-bearing sediments: U.S. Geological Survey Scientific Investigations Report 2007-5264, 11 p.
Lee, M.W., 2008, Models for gas hydrate-bearing sediments inferred from hydraulic permeability and elastic velocities: U.S. Geological Survey Scientific Investigations Report 2008-5219, 15 p.
Lee, M.W., Agena, W.F., Collett, T.S., and Inks, T.L., 2011, Pre- and post-drill comparison of the Mount Elbert gas hydrate prospect, Alaska North Slope: Journal of Marine and Petroleum Geology, v. 28, no. 2, p. 578–588.
Lee, M.W., and Collett, T.S., 2005, Assessments of gas hydrate concentrations estimated from sonic logs in the Mallik 5L-38 Well, N. W. T., Canada, in Dallimore, S.R., and Collett, T.S., (eds.), Scientific results for Mallik 2002 gas hydrate production research well program, Mackenzie Delta, Northwest Territories, Canada: Geological Survey of Canada Bulletin 585, 10 p.
Lee, M.W., and Collett, T.S., 2006, A method of shaly sand correction for estimating gas-hydrate saturations using downhole electrical resistivity log data: U.S. Geological Survey Scientific Investigation Report 2006-5121, 10 p.
Lee, M.W., and Collett, T.S., 2011, In-situ gas hydrate saturation estimated from various well logs at the Mount Elbert Gas Hydrate Stratigraphic Test Well, Alaska North Slope: Journal of Marine and Petroleum Geology, v. 28, no. 2, p. 439-449.
Lee, M.W., Collett, T.S., and Agena, W.F., 2008, Assessing gas-hydrate prospects on the North Slope of Alaska—Theoretical considerations: U.S. Geological Survey, Scientific Investigations Report 2008–5175, 28 p.

Lee, M.W., Collett, T.S., and Inks, T.L., 2009, Seismic attribute analysis for gas-hydrate and free-gas prospects on the North Slope of Alaska, *in* Collett, T., Johnson, A., Knapp, C., Boswell, R., eds., Natural Gas Hydrates -- Energy Resource Potential and Associated Geologic Hazards: American Association of Petroleum Geologists Memoir 89, p. 525–540.
Lee, M.W., and Waite, W.F., 2008, Estimating pore-space gas hydrate saturations from well-log acoustic data: Geochemistry, Geophysics, Geosystems, v. 9, Q07008, doi:10,1029/2008GC002081, 8 p.
Lee, Sung-Rock, and UBGH2 Science Party, 2011, 2nd Ulleung Basin Gas Hydrate Expedition (UBGH2): findings and implications, in DOE-NETL Fire In the Ice Methane Hydrate Newsletter, Summer, 2011, v. 11, issue 1, p. 6-9.
Lerand, M., 1973, Beaufort Sea, *in* McCrossan, R.G., ed., Future petroleum provinces of Canada--Their geology and potential: Canadian Society of Petroleum Geologists Memoir 1, p. 315-386.
Lewis, K.A., and Collett, T.S., 2013, Brookian sequence well log correlation sections and occurrence of gas hydrates, north-central North Slope, Alaska: U.S. Geological Survey Scientific Investigations Report 2013–5050, 23 p. http://pubs.usgs.gov/sir/2013/5050/.
Lim, T.K., Fujimoto, A., Kobayashi, T., 2020, DAS-3DVSP data acquisition at 2018 Stratigraphic Test Well (Hydrate-01): Proceedings of the 10th International Conference on Gas Hydrates (ICGH10), Singapore, June 21-26, 2020, 6 p. Posted on the DOE National Energy Technology Laboratory website https://www.netl.doe.gov/node/10037.
Lorenson, T.D., and Collett, T.S., 2011, Gas hydrate prospecting using well cuttings and mud gas geochemistry from 35 wells, Alaska North Slope: U.S. Geological Survey Scientific Investigations Report 2011–5195, 27 p.
Lorenson, T.D., and Collett, T.S., 2018, National Gas Hydrate Program Expedition 01 offshore India; gas hydrate systems as revealed by hydrocarbon gas geochemistry: Journal of Marine and Petroleum Geology, v. 92, p. 477-492.
Lorenson, T.D., Collett, T.S., and Hunter, R.B., 2011, Gas geochemistry of the Mount Elbert Gas Hydrate Stratigraphic Test Well, Alaska North Slope—Implications for gas hydrate exploration in the Arctic, *in* Boswell, R., Collett, T., Anderson, B., and Hunter, R., eds., Scientific results of the Mount Elbert gas hydrate stratigraphic test well, Alaska North Slope: Journal of Marine and Petroleum Geology, v. 28, no. 2, p. 343–360.
Makogon, Y. F., 1981, Hydrates of natural gas: Tulsa, Oklahoma, U.S.A., Penn Well, 237 p.
Masterson, D., Dzou, L., Holba, A., Fincannon, A., and Ellis, L., 2001, Evidence for biodegradation and evaporative fractionation in West Sak, Kuparuk, and Prudhoe Bay field areas, North Slope, Alaska: Organic Geochemistry, v. 32, no. 3, p. 411–441.
Maute, R.E., Lyle, W.D. and Sprunt Eve, 1992, Improved Data- Analysis Method Determines Archie Parameters From Core Data," JPT, January 1992, p. 103-107.
Miller, J.J., Agena, W.F., Lee, M.W., Zihlman, F.N., Grow, J.A., Taylor, D.J., Killgore, Michele, and Oliver, H.L., 2000, Regional seismic lines reprocessed using post-stack processing techniques—National Petroleum Reserve, Alaska: U.S. Geological Survey Open-File Report 00–286. [1 CD-ROM disk]
Miller, J.J., Agena, W.F., Lee, M.W., Zihlman, F.N., Grow, J.A., Taylor, D.J., Killgore, Michele, and Oliver, H.L., 2001, Four regional seismic lines—National Petroleum

Reserve, Alaska (supplement to U. S. Geological Survey Open-File Report 00–286): U.S. Geological Survey Open File Report Open-File Report 01–337. [1 CD-ROM disk]
Molenaar, C.M., Bird, K.J., and Collett, T.S., 1987a, Regional correlation sections across the North Slope of Alaska: U.S. Geological Survey Miscellaneous Field Investigations Map, Scale1:200000, MF-1907, 1 plate.
Molenaar, C.M., Bird, K.J., and Kirk, A.R., 1987b, Cretaceous and Tertiary stratigraphy of northeastern Alaska, *in* Tailleur, I., and Weimer, P., eds., Alaskan North Slope Geology, v. 1: Bakersfield, California, Pacific Section, Society of Economic Paleontologists and Mineralogists and Alaska Geological Society, p. 513–528.
Molochushkin, E.N., 1978, The effect of thermal abrasion on the temperature of the permafrost in the coastal zone of the Laptev Sea: Proceedings of the Second International Conference on Permafrost, Yakutsk, USSR, July 13-28, 1973: National Academy of Sciences, Washington D.C., p. 90-93.
Moridis, G.J. and Sloan, E.D., 2007, Gas production potential of disperse low-saturation hydrate accumulations in oceanic sediments. Energy Conversion and Management, v. 48, no. 6, p. 834-1849 pp. DOI: 10.1016/j.enconman.2007.01.023.
Moridis, G.J., Collett, T.S., Boswell, R., Kurihara, M., Reagan, M.T., Koh, C., and Sloan, E.D., 2009, Toward production from gas hydrates: current status, assessment of resources, and simulation-based evaluation of technology and potential: SPE Reservoir Evaluation & Engineering, v. 12, no. 5, p. 745-771. (doi: 10.2118/114163-PA)
Moridis, G.J., Collett, T.S., Pooladi-Darvish, M., Hancock, S., Santamarina, C., Boswell, R. Kneafsey, T., Rutqvist, J., Kowalsky, M., Reagan, M.T., Sloan, E.D., Sum, A.K., and Koh, C., 2011a, Challenges, uncertainties and issues facing gas production from gas hydrate deposits: SPE Reservoir Evaluation & Engineering, v. 14, no. 1, p. 76-112. (doi: 10.2118/131792-PA)
Moridis, G.J., Reagan, M.T., Boyle, K., and Zhang, K., 2010, Evaluation of a deposit at the PBU-L106 Site, North Slope, Alaska, for a potential long-term test of gas production from hydrates, Paper SPE 133601: Proc. 2010 Western Regional Meeting, Anaheim, California, May 27-29, 2010, 28 p.
Moridis, G.J., Seol, Y., and Kneafsey, T., 2005, Studies of Reaction Kinetics of Methane Hydrate Dissociation in Porous Media, Paper 1004: Proceedings of the Fifth International Conference on Gas Hydrates, Trondheim, Norway, June 13-16, 2005, 18 p.
Moridis, G.J., Silpngarmlert, S., Reagan, M.T., Collett, T.S., and Zhang, K., 2011b, Gas Production From a cold, stratigraphically bounded hydrate deposit at the Mount Elbert Site, North Slope, Alaska: Journal of Marine and Petroleum Geology, v. 28, no. 2, p. 517-534.
Mull, C.G., Houseknecht, D.W. and Bird, K.J., 2003, Revised Cretaceous and Tertiary stratigraphic nomenclature in the Colville Basin, Northern Alaska: U.S. Geological Survey Professional Paper, v. 1673, 51 p.
Myshakin, E., Seol, Y., Gai, X., Collett, T.S., Boswell, R.., Kumagai, K., Ohtsuki, S., and Suzuki, K., 2020, Numerical simulations of gas production from gas hydrate reservoirs at the Prudhoe Bay Unit 7-11-12 pad on Alaska North Slope: Proceedings of the 10th International Conference on Gas Hydrates (ICGH10), Singapore, June 21-26, 2020, 6 p. Posted on the DOE National Energy Technology Laboratory website https://www.netl.doe.gov/node/10037
Okinaka, N., Boswell, R., Collett, T.S., Yamamoto, K., and Anderson, B., 2019, Progress toward the establishment of an extended-duration gas hydrate reservoir response

test on the Alaska North Slope: Proceedings of the American Geophysical Union 2019 Fall Meeting, San Francisco, California, December 9-13, 2019, OS33A-02, 1 p. https://agu.confex.com/agu/fm19/meetingapp.cgi/Paper/512560

Okinaka, N., Boswell, R., Collett, T., Yamamoto, K., Anderson, B., 2020, Progress toward the establishment of an extended duration gas hydrate reservoir response test on the Alaska North Slope: Proceedings of the 10th International Conference on Gas Hydrates (ICGH10), Singapore, June 21-26, 2020, 6 p. Posted on the DOE National Energy Technology Laboratory website https://www.netl.doe.gov/node/10037.

Osadetz, K.G. and Chen, Z., 2005, A re-examination of Beaufort Sea – Mackenzie Delta Basin gas hydrate resource potential using a petroleum system approach: Proceedings of the Fifth International Conference on Gas Hydrates, Trondheim, Norway, June 13-16, 2005, 11 p.

Osterkamp, T.E. and Fei, T., 1993, Potential occurrence of permafrost and gas hydrates in the continental shelf near Lonely, Alaska: Proceedings of the Sixth International Conference on Permafrost, Beijing, China, July 5-9, 1993: National Academy of Sciences, Washington D.C., p. 500-505.

Park, Kuen-Pil, 2008, Gas hydrate exploration activities in Korea: Proceedings of the 6th International Conference on Gas Hydrates (ICGH 2008), July 6-10, 2008, Vancouver, British Columbia, Canada, 10 p.

Pearson, C.F., Halleck, P.M., McGuire, P.L., Hermes, R., and Mathews, M., 1983, Natural gas hydrate deposit: a review of in-situ properties: Journal of Physical Chemistry, v. 97, p. 4180–4185.

Pickett, G. R., 1966, A review of current techniques for determination of water saturation from logs: Journal of Petroleum Technology, v. 18, no. 11, p. 1425-1433.

Riedel, M., Collett, T.S., Malone, M.J., and the Expedition 311 Scientists, 2006, Cascadia Margin Gas Hydrates, Expedition 311, Sites U1325 - U1329, 28 August - 28 October, 2005: Integrated Ocean Drilling Program Management International, Inc., for the Integrated Ocean Drilling Program, v. 311. http://iodp.tamu.edu/publications/exp311/311title.htm

Roberts, Stephen, 2008, Geologic assessment of undiscovered, technically recoverable coalbed-gas resources in Cretaceous and Tertiary rocks, North Slope, and adjacent State waters, Alaska: U.S. Geological Survey Digital Data Series DDS–69-S.

Rose, K., Boswell, R., and Collett, T., 2011, Mount Elbert Gas Hydrate Stratigraphic Test Well, Alaska North Slope: Coring operations, core sedimentology, and lithostratigraphy: Journal of Marine and Petroleum Geology, v. 28, no. 2, p. 311-331.

Ruppel, C., Herman, B., Brothers, L., and Hart, P., 2016, Subsea ice-bearing permafrost on the U.S. Beaufort Margin: (2) Borehole constraints: Journal of Geochemistry, Geophysics, Geosystems, v. 17, issue 11, p. 4333-4353.

Scheihing, M., 2010, ConocoPhillips Gas Hydrate Production Test, Appendix 3: Geocellular Model for Evaluation of Gas Hydrate Production Mechanism in Selected Sandstones of the Sagavanirktok Formation. Progress Report, First Half of 2010, DOE Award No.DE-NT0006553, US DOE/NETL, Washington, DC (26 August 2010), http://www.netl.doe.gov/technologies/oil-gas/publications/Hydrates/2010Reports/NT0006553_SemiAnnJan-Jul2010.pdf.

Schlumberger, 1998, Log Interpretation Charts: Sugar Land, Texas, Schlumberger Wireline and Testing, SMP-7006.

Schoderbek, D., Farrel, H., Hester, K., Howard, J., Raterman, K., Silpngarmlert, S., Martin, K. L., Smith, B. and Klein, P., 2013, ConocoPhillips Gas Hydrate Production Test Final

Technical Report, Prepared by ConocoPhillips Company for the United States Department of Energy, National Energy Technology Laboratory, 204 p. Available online at http://www.netl.doe.gov/File%20Library/Research/Oil-Gas/methane%20hydrates/nt0006553-final-report-hydrates.pdf.
Schoderbek, D., Martin, K., Howard, J., Silpngarmlert, S., and Hester, K., 2012, North Slope hydrate field trial: CO2/CH4 exchange: Proceedings Arctic Technology Conference, December 3-5, 2012, Houston, Texas, 17 p.
Serra, O., 1984, Fundamentals of Well-Log interpretation. Developments in Petroleum Science, v. 1, Elsevier Publishing, Amsterdam, The Netherlands.
Silpngarmlert, S., 2010, Appendix 2: Thermal effects of hot fluid production/injection in existing wells, *in* Schoderbek, D., 2010, Progress Report, First Half of 2010, National Energy Technology Laboratory. 46 p. http://www.netl.doe.gov/technologies/oil-gas/publications /Hydrates/2010Reports/NT0006553_SemiAnnJan-Jul2010.pdf
Simandoux, P., 1963, Dielectric measurements on porous media; Application to the measurement of water-saturations: Revue de l'Institut Franscais du Petrole 18, supplementary issue, p. 193-215. (Translated text in shaly sand reprint volume, Society of Professional Well Log Analysts, Houston, p. IV 97−124).
Sloan, E.D., and Koh, C.A., 2008, Clathrate hydrates of natural gases, Third Edition: CRC Press, Taylor and Francis Group, Publishers, New York, New York, 721 p.
Spangenberg, Erik, 2001, Modeling of the influence of gas hydrate content on the electrical properties of porous sediments: Journal of Geophysical Research: Solid Earth, v. 106, Issue B4, p. 6535-6548.
Suzuki, K., Collett, T., Boswell, R., Tamaki, M., Okinaka, N., Sato, D., 2019. Interpretation of logging data from the Hydrate-01 Stratigraphic Test Well drilled in the Prudhoe Bay Unit, Alaska North Slope. Proc. American Geophysical Union Fall Meeting, San Francisco, CA, Dec 10, 2019.
Torres, M., Collett, T., Rose, K., Sample, J., Agena, W., Rosenbaum, E., 2011, Pore Fluid Geochemistry from the Mount Elbert Gas Hydrate Stratigraphic Test Well, Alaska North Slope: Journal of Marine and Petroleum Geology, v. 28, no 2, p. 332-342.
Torres, M.E., Tréhu, A.M., Cespedes, N., Kastner, M., Wortmann, U.G., Kim, J.H., Long, P., Malinverno, A., Pohlman, J.W., Riedel, M., and Collett, T.S., 2008, Methane hydrate formation in turbidite sediments of northern Cascadia, IODP Expedition 311: Earth and Planetary Science Letters, v. 271, p. 170-180.
U.S. Geological Survey Alaska Gas Hydrate Assessment Team, 2013, National Assessment of Oil and Gas Project—Geologic assessment of undiscovered gas hydrate resources on the North Slope, Alaska: U.S. Geological Survey Digital Data Series 69–CC, 100 p., http://dx.doi.org/10.3133/ds69CC.
Werner, M.R., 1987, Tertiary and Upper Cretaceous heavy oil sands, Kuparuk River area, Alaskan North Slope, *in* Tailleur, I.L., Weimer, Paul (Eds.), Alaskan North Slope Geology: Pacific Section, Society of Economic Paleontologists and Mineralogists and the Alaska Geological Society, Book 50, vol. 1, p. 109-118.
Western Atlas International Inc., 1995, Introduction to wireline log analysis: Western Atlas International Inc., Chapter 4, 312 p.
Winters W., Walker M., Collett T., Boswell R., K., Waite W., Torres M. and Patil S., Dandekar A., 2011, Physical properties of sediment from the Mount Elbert Gas Hydrate Stratigraphic Test Well, Alaska North Slope: Journal of Marine and Petroleum Geology, v. 28, no. 2, p. 361-380.

Worthington, P.F., 1985, The evolution of shaly-sand concepts in reservoir evaluation: The Log Analyst, no. 1, p. 23-40.
Yamamoto, K., 2015, Overview and introduction: pressure core-sampling and analysis in the 2012-2013 MH21 offshore test of gas production from methane hydrates in the Nankai Trough: Journal of Marine and Petroleum Geology, v. 66, p. 296-309.
Yamamoto, K., and Dallimore, S., 2008, Aurora-JOGMEC-NRCan Mallik 2006-2008 Gas Hydrate Research Project progress, in DOE-NETL Fire in the Ice Methane Hydrate Newsletter, summer 2008, p. 1-5. http://www.netl.doe.gov/technologies/oil-gas/publications/ Hydrates/Newsletter/HMNewsSummer08.pdf#Page=1
Yamamoto, K., Terao, Y., Fujii, T., Terumichi, I., Seki, M., Matsuzawa, M., Kanno, T., 2014, Operational overview of the first offshore production test of methane hydrates in the Eastern Nankai Trough: Proceeding of the Offshore Technology Conference, OTC-25243, Houston, Texas, 15 p.
Yang, S., Zhang, H., Wu, N., Su, X., Schultheiss, P., Holland, M., Zhang, G., Liang, J., Lu, J., and Rose, K., 2008, High concentration hydrate in disseminated forms obtained in Shenhu area, North Slope of South China Sea: Proceedings of the 6th International Conference on Gas Hydrates (ICGH 2008), July 6-10, 2008, Vancouver, British Columbia, Canada, 10 p.
Yoneda, J., Jin, Y., Muraoka, M., Oshima, M., Suzuki, K., Walker, M., Westacott, D., Ohstuki, S., Kumagai, K., Collett, T., Boswell, R., and Okinaka, N., 2020a, Petrophysical and geomechanical properties of gas hydrate-bearing sediments recovered from Alaska North Slope 2018 Hydrate-01 Stratigraphic Test Well: Proceedings of the 10th International Conference on Gas Hydrates (ICGH10), Singapore, June 21-26, 2020, 6 p. Posted on the DOE National Energy Technology Laboratory website https://www.netl.doe.gov/node/10037
Yoneda, J., Jin, Y., Muraoka, M., Oshima, M., Suzuki, K., Walker, M., Westacott, D., Otsuki, S., Kumagai, K., Collett, T.S., Boswell, R., and Okinaka, N., 2020b, Multiple physical properties of gas hydrate-bearing sediments recovered from Alaska North Slope 2018 Hydrate-01 Stratigraphic Test Well: Journal of Marine and Petroleum Geology, v. 123, 43 p. https://doi.org/10.1016/j.marpetgeo.2020.104748
Yoneda, J., Oshima, M., Kida, M., Kato, A., Konno, Y., Jin, Y., Jang, J., Waite, W., Kumar, P., Tenma, N., 2019, Permeability Variation and Anisotropy of Gas Hydrate-bearing Pressure-core Sediments Recovered from the Krishna-Godavari Basin, Offshore India: Journal of Marine and Petroleum Geology, v. 108, p. 524–536.

List of Abbreviations and Symbols

Abbreviations

AFE	Authorization for expenditure
ANS	Alaska North Slope
ANWR	Alaska National Wildlife Refuge
AOGCC	Alaska Oil and Gas Conservation Commission
API	American Petroleum Institute
AT90	Electrical resistivity
Bbl	Barrels
BCF	Billion cubic feet
BGHS	Base of gas hydrate stability
BGHS	Base of gas hydrate stability zone
BHA	Bottom-hole assembly
BHP	Bottom-hole pressure
BHSZ	Base of gas hydrate stability zone
BIBPF	Base of ice-bearing permafrost
BPXA	BP Exploration Alaska Incorporated
BSL	Below sea level
CH_4	Methane
CO_2	Carbon dioxide
Csg	Casing
CMR	Nuclear magnetic resonance logging tool
DAS	Distributed acoustic system
DEN	Density
DOE	U.S. Department of Energy
DNR	Department of Natural Resources
DSS	Distributed shear system
DT	Acoustic transit time
DTS	Distributed temperature system
GDW	Geoscience Data Well
G&G	Geologic and Geophysical
GH	Gas hydrate
GHSZ	Gas hydrate stability zone
HCAL	Caliper
HSZ	Hydrate stability zone
IA	Interagency Agreement
IMT	Incident Management Team
JOGMEC	Japan Oil, Gas and Metals National Corporation
KRU	Kuparuk River Unit
LWD	Logging while drilling
MAD	Measurement-after-drilling
MD	Measured depth
MDT	Modular Dynamic Tool
MOBM	Mineral oil base mud
MPU	Milne Point Unit
MSL	Mean sea level

MWD	Measurement while drilling
NMR	Nuclear magnetic resonance
NPRA	National Petroleum Reserve in Alaska
NPT	Non-productive time
PBU	Prudhoe Bay Unit
POG	Alaska Project Owners Group
PRA	Petrotechnical Resources of Alaska
PT	Pressure transmitter
P/T	Pressure and temperature
PTW-1	Production Test Well Number 1
PTW-2	Production Test Well Number 2
P-wave	Compressional wave
R&D	Research and development
RHOBB	Bulk density
RSS	Rotary steerable system
SDR	NMR Schlumberger-Doll Research
sH	Structure H hydrate
sI	Structure I hydrate
sII	Structure I hydrate
SOA	State of Alaska
SOR	Statement of Requirements
STW	Stratigraphic Test Well (Hydrate-01)
S-wave	Shear wave
TAPS	Trans Alaska Pipeline System
TAS	Temperature Array Sensors
TD	Total depth of well
THSZ	Top gas hydrate stability zone
T2	NMR transverse relaxation
TWC	Two-way communication
TPE	Biot-type equation
TPO	Third Party Operator
3D	Three-dimensional
TVD	True vertical depth
TVDss	True vertical depth subsea
2D	Two-dimensional
USGS	U.S. Geological Survey
VSP	Vertical seismic profile
WIO	Working Interest Owners
WLL	Wireline logging
XPT	Pressure Express logging tool

Symbols

a	Archie tortuosity factor
C	Celsius
°	Degrees
ρ_h	Hydrate density
ρ_{ma}	Matrix density

ρ_w	Water density
F	Fahrenheit
FF	Formation factor
ft	Feet
GR	Gamma ray
GR_{cln}	Gamma-ray log value for clean sand
GR_{sh}	Gamma-ray log value for shale
I_{GR}	Gamma-ray index
g/cm^3	Grams per cubic centimeter
km/sec	Kilometers per second
kPa	kilopascals
kPa/m	kilopascals per meter
m	Meter
m	Archie cementation exponent
mD	Millidarcy
MPa	Megapascals
µsec/ft	Microseconds per foot
msec/ft	Milliseconds per foot
mscf	Thousand standard cubic feet
m/sec	Meters per second
m^3/d	Cubic meters per day
mi^2	Square miles
n	Archie saturation exponent
ohm-m	Ohm-meters
ppt	Parts per thousand
ϕ	Porosity
ϕ_{NMR}	NMR porosity
psi	Pounds per square inch
psi/ft	pounds per square inch per foot
R_t	Formation resistivity
R_w	Connate water resistivity
scf/D	Standard cubic feet per day
S_h	Gas hydrate saturation
S_w	Water saturation
Vgh	Gas hydrate saturation
Vp	Compressional velocity
Vs	Sheer velocity
V_{sh}	Sediment shale volumes
λ_h	NMR correction constant

Appendix: Project Publications

This section of the DOE-USGS IA Final Report contains a list of the research publications generated in support of the "Alaska Gas Hydrate Production Field Experiment" in chronological order.

Anderson, B., Boswell, R., Collett. T.S., Farrell, H., Ohtsuka, S., White, M., and Zyrianova, M., 2014, Review of the findings of the Iġnik-Sikumi CO2-CH4 gas hydrate exchange field test: Proceedings of the 8th International Conference on Gas Hydrates (ICGH8-2014), Beijing, China, 28 July - 1 August, 2014, 17 p.

Boswell, R., Saeki, T., Shipp, C., Frye, M., Shedd, B., Collett, T.S., Shelander, D., and McConnell, D., 2014, Prospecting for gas hydrate resources: DOE-NETL Fire in the Ice Newsletter, v. 14, Issue 2, 4 p.

Boswell, R., Yamamoto, K., Lee, S.R., Collett, T.S., Kumar, P., and Dallimore, S., 2014, Methane hydrates, *in* T.M. Letcher ed., Future of Energy - Improved, Sustainable and Clean Options for our Planet, Second Edition, Elsevier B.V. Publishing, p. 159-178.

Collett, T.S., 2014, Reservoir Controls on the Occurrence and Production of Gas Hydrates in Nature: Proceedings of the Offshore Technology Conference, Houston, Texas, 5–8 May 2014, OTC 25242, 12 p.

Collett, T.S., 2014, The gas hydrate petroleum system: Proceedings of the 8th International Conference on Gas Hydrates (ICGH8-2014), Beijing, China, 28-July to 1-August, 2014, 12 p.

Collett, T.S., 2014, Reservoir controls on the occurrence and production of gas hydrates in marine and Arctic permafrost settings: Proceedings of the 8th International Conference on Gas Hydrates (ICGH8-2014), Beijing, China, 28-July to 1-August, 2014, 14 p.

Collett, T., Bahk, J-J., Baker, R., Boswell, R., Divins, D., Frye, M., Goldberg, D., Husebo, J., Koh, C., Malone, M., Morell, M., Myers, G., Shipp, C., and Torres, M., 2015, Methane hydrates in nature – current knowledge and challenges: Journal Chemical Engineering Data, v. 60, no. 2, p. 319-329.

Boswell, R., Bünz, S., Collett, T.S., Frye, M., Fujii, T., McConnell, D., Meinery, J., Pecher, I., Reichel, T., Ryu, B.-J., Shelander, D., and Shin, K.-S., 2016, Introduction to special section: Exploration and characterization of gas hydrates: Interpretation Journal, v. 4, Issue 1, 21 p.

Boswell, R., and Collett, T.S., 2016, Emerging Issues in the Development of Geologic Models for Gas Hydrate Numerical Simulation: Fire in the Ice U.S. Department of Energy Newsletter, v. 16, p. 19-22.

Myshakin, E., Ajayi, Taiwo, Anderson, B.J., Seol, Y., and Boswell, R., 2016, Numerical simulations of depressurization-induced gas production from gas hydrates using 3-D heterogeneous models of L-Pad, Prudhoe Bay Unit, North Slope Alaska: Journal of Natural Gas Science and Engineering, v. 35, p. 1336-1352.

Nandanwar, M., Anderson, B., Ajayi, T., Collett, T.S., and Zyrianova, M., 2016, Evaluation of gas production potential from gas hydrate deposits in the National Petroleum Reserve Alaska using numerical simulations: Journal of Natural Gas Science and Engineering, v. 30, p. 760-772.

Boswell, R., Collett, T.S., Myshakin, E., Ajayi, T., and Seol, Y., 2017, The increasingly complex challenge of gas hydrate reservoir simulation: Proceeding of the 9th International Conference on Gas Hydrates; June 25-30, 2017; Denver, Colorado, USA, 10 p.

Boswell, R., Schoderbek, D., Collett, T.S., Ohtsuki, S., White, M., and Anderson, B., 2017, The Iġnik Sikumi Field Experiment, Alaska North Slope: Design, operations, and implications for CO2−CH4 exchange in gas hydrate reservoirs: Journal Energy and Fuels, v. 31, p. 140-153.

Demas, A., 2017, Exploring Gas Hydrates as a Future Energy Source: U.S. Geological Survey Transition Information, November-2016, 2 p. https://www.usgs.gov/center-news/exploring-gas-hydrates-a-future-energy-source

Lewis, K., and Collett, T.S., 2017, Brookian Sequence Well Log Correlation Sections and the Occurrence of Gas Hydrates along the North-Central North Slope of Alaska: Proceeding of the 9th International Conference on Gas Hydrates; June 25-30, 2017; Denver, Colorado, USA, 2 p.

Riedel, M., and Collett, T.S., 2017, Observed correlation between the depth to base and top of gas hydrate occurrence from review of global drilling data: Journal of Geochem. Geophys. Geosyst., v. 18, 19 p. doi:10.1002/ 2017GC006805.

Uchida, S., Lin, J.S., Myshakin, E.M., Seol, Y., Collett, T.S., and Boswell, R., 2017, Numerical simulations of sand production in interbedded hydrate-bearing sediments during depressurization: Proceeding of the 9th International Conference on Gas Hydrates; June 25-30, 2017; Denver, Colorado, USA, 10 p.

Zyrianova, M.V., Collett, T.S., and Boswell, R., 2017, Characterization of the structural-stratigraphic and reservoir controls on the occurrence of gas hydrate in the Eileen Gas Hydrate Trend, Alaska North Slope: Proceeding of the 9th International Conference on Gas Hydrates; June 25-30, 2017; Denver, Colorado, USA, 2 p.

Boswell, R., Marsteller, S., Okinaka, N., Wakatsuki, M., Collett, T.S., Hunter, R., Walsh, T., Minge, D., Itter, D., and Crumley, S., 2019, Viable long-term gas hydrate testing site confirmed on the Alaska North Slope: Fire-in-the-ice, DOE-NETL Methane Hydrate Newsletter, v. 19, Issue 1, p. 1-5.

Collett, T.S., 2019, Gas hydrate production testing – knowledge gained: Proceedings of the Offshore Technology Conference, Houston, Texas, USA, May 6-9, OTC-29516-MS, 16 p.

Collett, T.S., 2019, USGS National and Global Oil and Gas Assessment Project-Northern Alaska Province, Gas Hydrate Assessment Unit Boundaries and Assessment Input Data Forms: U.S. Geological Survey data release, 12 p. https://doi.org/10.5066/P9HSWE98

Collett, T.S., Lewis, K.A., Zyrianova, M.V., Haines, S.S., Schenk, C.J., Mercier, T.J., Brownfield, M.E., Gaswirth, S.B., Marra, K.R., Leathers-Miller, H.M., Pitman, J.K., Tennyson, M.E., Woodall, C.A., and Houseknecht, D.W., 2019, Assessment of undiscovered gas hydrate resources in the North Slope of Alaska, 2018: U.S. Geological Survey Fact Sheet 2019–3037, 4 p. https://doi.org/10.3133/fs20193037

Collett, T.S., Okinaka, N., Wakatsuki, M., Boswell, R., Marsteller, S., Minge, D., Crumley, S., Itter, D., and Hunter, R., 2019, Alaska North Slope 2018 Hydrate 01 Stratigraphic Test Well: Design and operations: Proceedings of the American Geophysical Union 2019 Fall Meeting, San Francisco, California, December 9-13, 2019, OS33A-01, 1 p. https://agu.confex.com/agu/fm19/meetingapp.cgi/Paper/510043.

Haines, S., Collett, T.S., Boswell, R., Lim, T.K., Okinaka, N., Suzuki, K., and Fujimoto, A., 2019, Gas hydrate saturation estimation from acoustic log data in the 2018 Alaska North Slope Hydrate-01 stratigraphic test well: Proceedings of the American Geophysical Union 2019 Fall Meeting, San Francisco, California, December 9-13, 2019, OS33A-03, 1 p. https://agu.confex.com/agu/fm19/meetingapp.cgi/Paper/491035.

Hancock, S., Boswell, R., and Collett, T.S., 2019, Development of deepwater natural gas hydrates: Proceedings of the Offshore Technology Conference, Houston, Texas, USA, May 6-9, OTC-29374-MS, 16 p.

Okinaka, N., Boswell, R., Collett, T.S., Yamamoto, K., and Anderson, B., 2019, Progress toward the establishment of an extended-duration gas hydrate reservoir response test on the Alaska North Slope: Proceedings of the American Geophysical Union 2019 Fall Meeting, San Francisco, California, December 9-13, 2019, OS33A-02, 1 p. https://agu.confex.com/agu/fm19/meetingapp.cgi/Paper/512560

Suzuki, K., Collett, T.S., Boswell, R., Tamaki, M., Okinaka, N., and Sato, D., 2019, Interpretation of logging data from the Hydrate-01 Stratigraphic Test Well drilled in the Prudhoe Bay Unit, Alaska North Slope: Proceedings of the American Geophysical Union 2019 Fall Meeting, San Francisco, California, December 9-13, 2019, OS41C-1688, 1 p. https://agu.confex.com/agu/fm19/meetingapp.cgi/Paper/526858

Yoneda, J., Jin, Y., Muraoka, M., Oshima, M., Suzuki, K., Walker, M., Westacott, D., Otsuki, S., Kumagai, K., Collett, T.S., Boswell, R., and Okinaka, N., 2019, Petrophysical and geomechanical properties of gas hydrate-bearing sediments recovered by a side-wall pressure corer: Proceedings of the American Geophysical Union 2019 Fall Meeting, San Francisco, California, December 9-13, 2019, OS41C-1692, 1 p. https://agu.confex.com/agu/fm19/meetingapp.cgi/Paper/505153

You, K., Flemings, P.B., Malinverno, A., Collett, T.S., and Darnell, K., 2019, Mechanisms of methane hydrate formation in geological systems: Reviews of Geophysics, v. 57, p. 1146-1196. https://doi.org/10.1029/2018RG000638

Boswell, R., Collett, T.S., Suzuki, K., Yoneda, J., Haines, S., Okinaka, N., Tamaki, M., Crumley, S., Itter, D., and Hunter, R., 2020, Alaska North Slope 2018 Hydrate-01 Stratigraphic Test Well: Technical results: Proceedings of the 10th International Conference on Gas Hydrates (ICGH10), Singapore, June 21-26, 2020, 6 p. Posted on the DOE National Energy Technology Laboratory website https://www.netl.doe.gov/node/10037

Boswell, R., Hancock, S., Yamamoto, K., Collett, T.S., Pratap, M., Lee, S.-R., 2020, Chapter 6 Natural Gas Hydrates: Status of potential as an energy resource: In Future Energy 3rd edition - Book Chapter, Elsevier's Book, 36 p.

Collett, T.S., 2020, American Association of Petroleum Geologists, Energy Minerals Division Gas Hydrates Committee Annual Report: American Association of Petroleum Geologists, Energy Minerals Division Gas Hydrates Committee web site, 18 p.

Collett, T., Okinaka, N., Wakatsuki, M., Boswell, R., Marsteller, S., Minge, D., Crumley, S., Itter, D., Hunter, R., 2020, Design and operations of the Hydrate-01 Stratigraphic Test Well, Alaska North Slope: Proceedings of the 10th International Conference on Gas Hydrates (ICGH10), Singapore, June 21-26, 2020, 6 p. Posted on the DOE National Energy Technology Laboratory website https://www.netl.doe.gov/node/10037

Gai, X., Myshakin, E., Uchida, S., Lin, J., and Seol, Y., 2020, Fully Thermal-Hydro-Chemo-Mechanical (THCM) Coupled Numerical Simulations of Gas Production from Gas Hydrate Reservoirs at Alaska North Slope: Proceedings of the 10th International Conference on Gas Hydrates (ICGH10), Singapore, June 21-26, 2020, 1 p. Posted on the DOE National Energy Technology Laboratory website https://www.netl.doe.gov/node/10037

Haines, S., Collett, T., Boswell, R., Lim, T-K., Okinaka, N., Suzuki, K., and Fujimoto, A., 2020, Gas hydrate saturation estimation from acoustic log data in the 2018 Alaska North Slope Hydrate-01 Stratigraphic Test Well: Proceedings of the 10th International Conference on Gas Hydrates (ICGH10), Singapore, June 21-26, 2020, 6 p. Posted on the DOE National Energy Technology Laboratory website https://www.netl.doe.gov/node/10037

Kurvits, T., et al., 2020, Northern issues, science gaps and recommendations: UNEP ArcGIS Story Map Series, 18 p. https://storymaps.arcgis.com/stories/74bf8d1540c542b7a444a5a2ba1559e2

Myshakin, E., Seol, Y., Gai, X., Collett, T.S., Boswell, R.., Kumagai, K., Ohtsuki, S., and Suzuki, K., 2020, Numerical simulations of gas production from gas hydrate reservoirs at the Prudhoe Bay Unit 7-11-12 pad on Alaska North Slope: Proceedings of the 10th International Conference on Gas Hydrates (ICGH10), Singapore, June 21-26, 2020, 6 p.

Posted on the DOE National Energy Technology Laboratory website https://www.netl.doe.gov/node/10037

Okinaka, N., Boswell, R., Collett, T., Yamamoto, K., and Anderson, B., 2020, Progress toward the establishment of an extended duration gas hydrate reservoir response test on the Alaska North Slope: Proceedings of the 10th International Conference on Gas Hydrates (ICGH10), Singapore, June 21-26, 2020, 6 p. Posted on the DOE National Energy Technology Laboratory website https://www.netl.doe.gov/node/10037

Uchida, S., Seol, Y., and Yamamoto, K., 2020, Numerical modeling of sand migration during gas production from gas hydrate reservoir in the Prudhoe Bay Unit on the Alaska North Slope: Proceedings of the 10th International Conference on Gas Hydrates (ICGH10), Singapore, June 21-26, 2020, 6 p. Posted on the DOE National Energy Technology Laboratory website https://www.netl.doe.gov/node/10037

White, M.D., Kneafsey, T.J., Seol, Y., Waite, William F., Uchida, S., Lin, J.S., Myshakin, E.M., Gai, X., Gupta, S., Reagan, M.T., Queiruga, A.F., and Kimoto, S., 2020, An international code comparison study on coupled thermal, hydrologic and geomechanical processes of natural gas hydrate-bearing sediments: Journal of Marine and Petroleum Geology, v. 120 (Article 104566), 55 p. https://www.sciencedirect.com/journal/marine-and-petroleum-geology/vol/120/suppl/C

Yoneda, J., Jin, Y., Muraoka, M., Oshima, M., Suzuki, K., Walker, M., Westacott, D., Ohstuki, S., Kumagai, K., Collett, T., Boswell, R., and Okinaka, N., 2020a, Petrophysical and geomechanical properties of gas hydrate-bearing sediments recovered from Alaska North Slope 2018 Hydrate-01 Stratigraphic Test Well: Proceedings of the 10th International Conference on Gas Hydrates (ICGH10), Singapore, June 21-26, 2020, 6 p. Posted on the DOE National Energy Technology Laboratory website https://www.netl.doe.gov/node/10037

Yoneda, J., Jin, Y., Muraoka, M., Oshima, M., Suzuki, K., Walker, M., Westacott, D., Otsuki, S., Kumagai, K., Collett, T.S., Boswell, R., and Okinaka, N., 2020b, Multiple physical properties of gas hydrate-bearing sediments recovered from Alaska North Slope 2018 Hydrate-01 Stratigraphic Test Well: Journal of Marine and Petroleum Geology, v. 123, 43 p. https://doi.org/10.1016/j.marpetgeo.2020.104748

Collett, T.S., Boswell, R., and Zyrianova, M., (in press), Alaska North Slope terrestrial gas hydrate systems: Insights from Scientific Drilling: Springer World Atlas of Submarine Gas Hydrates in Continental Margins, 21 p.

Garapati, N., Zyrianova, M.V., and Collett, T.S., (in press), Economic and life cycle assessment of gas production from gas hydrate prospects on Alaska North Slope: Proceedings of the 10th International Conference on Gas Hydrates (ICGH10), Singapore, June 2023, 6 p.

National Energy Technology Laboratory

626 Cochrans Mill Road
P.O. Box 10940
Pittsburgh, PA 15236-0940

3610 Collins Ferry Road
P.O. Box 880
Morgantown, WV 26507-0880

13131 Dairy Ashford Road, Suite 225
Sugar Land, TX 77478

1450 Queen Avenue SW
Albany, OR 97321-2198

Arctic Energy Office
420 L Street, Suite 305
Anchorage, AK 99501

Visit the NETL website at:
www.netl.doe.gov

Customer Service Line:
1-800-553-7681

U.S. DEPARTMENT OF ENERGY | NATIONAL ENERGY TECHNOLOGY LABORATORY